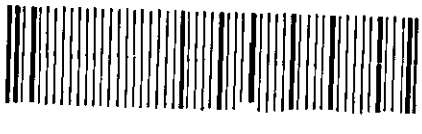

LOUGHBOROUGH UNIVERSITY OF TECHNOLOGY

The Effect of Space Charges on the Conductivity of Dielectrics under Medium Direct Voltage Stress Conditions

by

WILLIAM SAM, B.Sc(Eng)Lond., M.Phil.Lond.

Thesis submitted for Ph.D. degree in Electrical Engineering of Loughborough University of Technology.

Supervisor: H. Barber.

August 1969

This thesis is Dedicated to

Pa (my father) and sister Victoria both of whom died whilst I was away from home

and

Diane

Acknowledgements:

The author wishes to express his thanks to Professor H. Buckingham for facilities provided and to Mr. H. Barber and Dr. J.M. Ivison for most helpful discussions.

The author would also like to thank Messrs. Green and Topley who helped in various ways in the laboratory and with the photography.

The author is also grateful to ICI Limited, CIBA Limited and Pilkingtons for supplying the test samples and to the former AEI cables division at Woolwich, London for providing the equipment for the cable tests.

CONTENTS

SUMMARY:

Conduction and space charge theories in dielectrics under direct voltage conditions are reviewed and analysed.

Published information on gas discharge processes in insulation, conductivity, discharge detection and measuring methods are also summarised.

A combined technique whereby both discharges and current can be studied simultaneously is employed in the investigation of non-ohmic conduction in solid dielectrics at moderate d.c. stresses.

Experimental evidence suggests that none of the conventional laws of conduction adequately explains the observed phenomena e.g. the thickness dependence of conductivity; and that the operating stress 'E' calculated as the ratio of the externally applied voltage to the thickness of the dielectric may not be the actual resultant stress.

Some anomalies are explained on the basis of a new dielectric equivalent circuit, a modified Maxwellian 'n' strata dielectric and induced interfacial or space charges.

The discharge behaviour of gaseous voids in dielectrics is analysed using an equivalent circuit incorporating the resistivity of the void gas. Extinction is explained partly by an extended Maxwellian polarisation phenomena.

It is postulated that the empirical relation of the form

$$J_{vol} = K_o E \exp (\alpha_L + \beta_L E + \gamma_L E^2)$$

$$\alpha_L >> \beta_L >> \gamma_L$$

(where J_{vol} = volumetric (bulk) current density instead of the normal definition obtained as current per unit area E defined as above K_o α_L, β_L, γ_L are constants for a particular thickness of dieelectric), defines more accurately the conductivity stress relationship.

Stress distributions in a polythene cable are analysed using an ICL IBM 1905 computer and assuming an approximate logarithmic current stress relationship.

List of principal symbols

P	=	pressure
$\bar{P}$	=	polarization vector
ω	=	some function of frequency
M	=	dipole moment
W	=	potential barrier to be overcome or ionization energy
R	=	gas constant
ϵ	=	exponential
E_i	=	discharge inception stress
τ	=	time constant factor
1	=	subscript relating to a particular portion of media as described in text
2	=	subscript relating to a particular portion of media as described in text
J	=	current density
J_o	=	current density under ohmic conditions
σ	=	conductivity
σ_o	=	conductivity under low field conditions
e	=	electronic charge magnitude
μ	=	charge carrier mobility
v	=	drift velocity
ρ	=	total net charge per unit volume of dielectric
D	=	vectorial charge density (electric field displacement)
ϵ_o	=	permittivity of free space
ϵ_r	=	relative permittivity
ϵ_f	=	relative permittivity at high frequencies
ϵ	=	absolute permittivity
ϵ_Q	=	equivalent absolute permittivity
k	=	Boltzmann's constant
D_i	=	diffusion constant
T	=	absolute temperature

$1(t)$ = unit step function

V = $V(x)$ voltage at x

V_A = externally applied voltage

$V_o.1(t)$ = step voltage of steady state value V_o

E = electric field strength

= voltage applied to thickness of dielectric: ratio only under ohmic conditions in a uniform field.

$E_o.1(t)$ = electric stress in the dielectric due to an applied voltage of $V = V_o.1(t)$

E_x = E stress at any point x within the dielectric

$f(\varepsilon.e)$ = function of permittivity and electronic charge

$F\{\exp\{(E,T)\}$ = exponential function of temperature and stress

P.I. = particular integral

C.F. = complementary function

a = subscript relating to void

i = subscript relating to insulation

i.c.p. = initial charging phase

e.p.p. = eventual polarization phase

i.d.c.p. = initial discharging phase

s.s.i.v. = steady state inception voltage

t.i.v. = transient inception voltage

Other constants and symbols are as defined in the relevant part of the text.

A definition of terms is also provided in appendix 1.

CHAPTER 1

Introduction.

The conventional method for transmitting electrical power is by employing alternating voltage techniques. This is primarily due to the ease with which alternating voltages can be transformed from a lower level to a higher level and vice versa. Hence the theories and design information in connection concerning a.c. transmission are abundant.

When transmission of electrical power is required at high voltages and over long distances, the use of alternating voltages becomes very inefficient and costly.

One of the reasons for this is the high dielectric hysteresis losses which increase as the square of the voltage and to high corona losses causing power losses and radio interference in the popular amplitude modulated wavebands employed by several radio and wireless broadcasting stations.

The above mentioned effects are believed to be greatly reduced under direct voltage conditions. Apart from this direct voltage transmission has these other advantages.: The peak voltage on a direct voltage line (unlike that on an alternating voltage line) is the same as the rated voltage, thus the former can carry more power than the latter for a given maximum voltage between conductors. Also a direct voltage transmission line needs only two conductors instead of the three required for the three phase alternating voltage system.

Another aspect which is different from alternating voltage transmission is that continuity of transmission can be maintained with one line out of service in a two conductor direct voltage line by using the earth as a return line. Consequently a direct voltage line costs about twenty five per cent less than a three phase alternating voltage line of the same capacity. Moreover due to difficulties over frequency and phase matching, direct voltage transmission is preferable where there is an interchange of power between two countries.

These above advantages and relative cost must be matched against the high expense of terminal equipment such as rectifiers, inverters etc., needed for conversion and inversion in the case of direct voltage transmission.

Hence a direct voltage line is usually more efficient and economic when power must be transferred at high voltages over long distances by land or by cable under water between two systems or two countries.

As a result of the above advantages however there has been a great increase lately in the demand for high voltage direct current transmission for the various equipments which provide this, and in the design and working knowledge of these pieces of equipment.

1.1 Voltage and stress distribution.

Theoretical and empirical information acquired over the years of alternating voltage transmission firmly establishes that at working voltages the stress distribution in a dielectric (insulation) largely depends on the permittivity and obeys Ohm's law.

On the other hand theoretical considerations predict that under direct voltage conditions the voltage distribution in the dielectric depends on the resistivity and should obey Ohm's law up to stresses at which field emission from the electrodes may be expected to occur. This means that at working voltages, well below the accepted field emission stresses (with respect to information gathered in experiments with vacuum) the stress distribution should be ohmic. Some experiments have established that non-ohmic characteristics could occur at these working voltages.

Information on this line of research has been rather conflicting and scattered. Nevertheless one fact stands out above all: that the major problem lies in the mode of conduction in dielectric under direct voltage conditions for this will determine the stress distribution. This conduction has in the past been measured at very low or very high electrical stresses and information on the medium stresses working range

is scanty hence there has been a tendency to attribute any non-ohmicity to field emission from the electrodes.

1.2 Electrode material and screens

As a result of the theories of field emission the effect of electrode materials has been greatly emphasized. For example, it is reported that for some dielectrics evaporated carbon films are superior to evaporated noble metal electrodes and to the widely used colloidal graphite and silver paint electrodes. It has been mentioned that the latter two give rise to thermal hysteresis and possibly deviations in measurements. This would seem to be in direct contradiction with Baarden's theory of surface states according to which within the limits the electrode surface is immaterial. The relevance of this in connection with direct voltage equipment design cannot be over-stressed since as, for example, in the case with a.c. cables, carbon impregnated (semi-conductor) materials are used extensively to serve as screens or electrodes. Obviously this situation needs classification.

1.3 Surface and internal discharges.

As mentioned earlier one of the hazards of high voltage work even with d.c. is that at high stresses air trapped in cavities in the insulation or at the interface between insulation and electrode or conductor tends to ionise causing discharge[2] and consequent energy loss and in some cases breakdown of the dielectrics[3,4]. Even though the unsteady nature of conduction current (in dielectrics under direct voltage conditions) after the initial transient has disappeared and other anomalies like non-ohmic behaviour have been attributed in some cases to microdischarge within the dielectric, there appears to be very little published information relating the effects of discharge on the conduction process in dielectrics. It is apparent that the study of discharges is relevant to the general study of

conduction in dielectrics since the decay of surface discharges under direct voltage conditions appears to exhibit similar time constant characteristics to the decay of current through the dielectrics[5].

Moreover it appears that discharges tend to increase the intrinsic conductivity since they invariably lead to breakdown at which the conductivity is infinite.

1.4 Space charges

Some workers have attributed the causes of non-ohmic conduction in dielectrics to space charge formation occuring as a result of non-uniformities and inhomogeneities within the material and at the electrode/material interface. Experimental evidence of this in connection with high resistivity solid dielectrics has been rather limited.

1.5 Equivalent circuits

Engineers generally prefer the use of equivalent circuits but it appears that due to lack of information at medium direct voltages, high voltage engineers invariably fall back on simple equivalent circuits of perfect and imperfect characteristics derived at low stresses.

These equivalent circuits are insufficient if not misleading. Moreover if the claims of non-ohmicity and space charges at these working stresses, apparently before the onset of field emission, are true, then new equivalent circuits to simulate conduction, discharge performance and behaviour[6,7] correctly are badly needed.

In short there is a need to draw up a more comprehensive theory to include conduction and discharge characteristics of dielectrics under direct voltage conditions.

It is hoped that this work will make a constribution in this direction. It is based on an investigation into the effect of space charges on the conductivity, equivalent circuits and discharge behaviour of perfect and imperfect dielectrics. It is therefore appropriate to start by reviewing the general processes of conduction in dielectrics.

CHAPTER 2

Conduction Processes in Dielectrics

General macroscopic measureable conduction can be caused by any one of the following effects: chemical, electrical, mechanical and thermal.

Chemical conduction which is caused by a concentration gradient can be observed as a matter current, levelling the concentration (diffusion). An electric field causes an electrical conduction which is characterised as ionic current, ionic conductivity or dielectric loss mechanism. Mechanical stress fields and the vibrations of sound field cause mechanical movement which is characterised as an elastic deformation or diffusion creep (piezoelectric effect) and thermal conduction is generated by a temperature gradient the observed effects of which are the concentration gradient (Ludwig-Sonet effect) and an ionic e.m.f. (Seebeck effect).

Usually the observed macroscopic effect depends on a number of atomic variables, such as the concentration, mobilities and relaxation of the ions and the general behaviour of migrating charged and uncharged defects. These in turn are functions of external parameters depending on experimental conditions, these include temperature, pressure, frequency, doping species, concentration etc., and an adequate analysis requires an investigation into the effect of each of these.

In general, however, these conditions are inter-related and it is worth noting that the general conduction processes governed by irradiation, presence of dislocation and/or colour centres, and boundary effects, polarization capacity, reorientation of substituted molecular ions like OH^- could be included in the above considerations.

2.1 Electrical processes

The basic concepts of defect movement in crystals have been covered in detail by Frenkel, Schottky and others[8,9] but it is relevant to mention the motion of a defect from one equilibrium portion in the

lattice to the next since this constitutes a fundamental conduction process. Some defect dipoles have no total charge and therefore take no part in electric conductivity, but can be very effective for diffusion. They can reorientate into geometrically allowed directions (hindered rotation) and thus cause relaxation phenomena in 'time' dependent electric or mechanical fields.

It has been postulated that diffusion of defects results from the statistical succession of a large number of jumps with a jump defined as a movement of an ion or charged defect from a lower energy state to a higher one and described by

$$\omega_m = \Omega \exp -\frac{G_m}{kT} = \Omega \exp \frac{S_m}{k} \exp -\frac{H_m}{kT} \quad \ldots \quad \ldots \quad \ldots \quad \ldots \quad (2.1)$$

where ω_m is a mean jump frequency to a particular neighbouring site, S_m and H_m are activation entropy and enthalpy respectively. G_m is the Gibb's free energy of activation and Ω a vibration frequency of the order of the Debye limiting frequency ($10^{12}S^{-1}$). This leads to a net current of defects down a concentration gradient (grad. x). Any class 'i' of parallel jump paths of length r, forming an angle θ_i with the direction of the gradient ($0 < \theta_i < \frac{\pi}{2}$) contributes an amount $-(\Delta x_i/\Omega)\omega_m r\mathrm{Cos}\theta_i$ to the current where $\Delta x_i = |\mathrm{grad}x|r\mathrm{Cos}\theta_i$. The total current is $-\omega_m r^2 |\mathrm{grad}x/\Omega| \Sigma\mathrm{Cos}^2\theta_i$. Considering a particular case: for a cubic lattice $\Sigma\mathrm{Cos}^2\theta_i = \frac{1}{2}n\mathrm{Cos}^2\theta = n/6$ (n = number of attainable neighbouring sites), the diffusion coefficient (factor of $-|\mathrm{grad}x/\Omega|$)

$$D = 1/6\ n\omega_m r^2 = g\omega_m a^2 \quad \ldots \quad \ldots \quad \ldots \quad \ldots \quad \ldots \quad \ldots \quad \ldots \quad (2.2)$$

where 'a' is the lattice parameter, and 'g' includes a geometric factor characteristic of the jump geometry, e.g. g = 1 for shortest jumps in a cation sublattice of say the Nacl Structure when 'a' is taken as the large cube edge.

With regard to ionic conductivity, from equation (2.1) an applied electric field E modifies the activation enthalpy H_m of singly charged defects by amounts $\pm \frac{1}{2}$ $eEr\mathrm{Cos}\theta_i$ where $\frac{1}{2}r$ is the distance between the

saddle point and the equilibrium position of the defect and θ_i is the angle between the jump and field directions. Hence every pair of opposite jump direction yields an excess probability.

$\Delta\omega_m = 2\omega_m \sinh\left(\frac{1}{2} erE \frac{\cos\theta_i}{kT}\right)$ for jumps with a component in the field direction. The resulting contribution to the current density J is $\Delta J = \frac{x}{\Omega} er\, \Delta\omega_m \cos\theta_i$ assuming that the neighbouring site is reached on a rectilinear path. For 1/2 erE << kT, linear expansion of $\Delta\omega_m$ gives a field-dependent conductivity $\frac{J}{E} = \sigma = xe\mu/\Omega$ with a mobility

$$\mu = gea^2 \omega_m/kT \quad \ldots \quad \ldots \quad \ldots \quad \ldots \quad \ldots \quad \ldots \quad \ldots \quad \ldots \quad \ldots \quad \ldots \quad (2.3)$$

where $g = nr^2\cos^2\theta/2\, a^2$ as in equation 2.2. Expansion of $\Delta\omega_m$ to the third order introduces a non-ohmic correction factor $(1 + g_1 e^2a^2E^2/k^2T^2)$ on the right-hand side of equation (2.3) with $g_1 = nr^4 \cos^4\theta/48ga^4$.

Conductivity and self-diffusion are of course related by the well known Nernst - Einstein relation $\frac{D}{\mu} = \frac{kT}{e}$ as is evident from equation (2.2) and (2.3).

2.1.1 Dielectric relaxation

Dielectric relaxation may be viewed as a distinct phenomenon separate from the contribution of ionic conductivity to dielectric loss. This phenomenon is of special importance in cases where the migration of a charged point defect is restricted totally to a few jumps, therefore being detectable only in a varying electric field.

The simplest example is given by tightly bound defect dipoles. In a time-dependent field they orientate with a relaxation time τ, that is, the distribution of the dipoles over the energetically different orientations relative to the external field follows its variation with τ, τ is given by the frequencies of the individual jumps contributing to reorientation and therefore depends on the jump geometry.

According to this theory let M be the absolute value of the effective dipole moment of the pair in the special case of ME << kT, constant field E and cubic symmetry ($\cos^2\theta = 1/3$) then polarization

$\vec{P} = \frac{M^2 x_d E}{3vkT}$ where x_d is the mole fraction of the dipoles. This means a Δe - fold increase of the original (defect free) polarization with the dimensionless relaxation strength $\Delta e = \vec{P}/\epsilon_o (\epsilon-1)E$. $\vec{P}$ lags behind the time-dependent field by τ, causing dielectric loss. For instance after switch off E at t=o, the relaxation current density is given as $J = (\vec{P}/t) \exp(-t/\tau)$, for Ohmic conduction. The above theories explain non-ohmic conduction at stresses 100 kV/cm for Kcl, KB and Nacl on the basis of conduction mechanism by electrons emitted by the cathodic electrode due to a locally high field in front of it or by the possibility of ionic space charge limited processes. - 100 kV/cm for KCl etc.

Most of these processes are however grouped under the emission and conduction laws:

2.1.2 Laws of electronic emission and conduction

Several laws of emission have been postulated to be due to [illegible] the following mechanisms.

Thermionic emission	Richardson-Dushman
Pure Schottky emission	Schottky emission
Field assisted thermionic emission ...	T-F composite Schottky/FN
Pure field or cold emission	Fowler-Nordheim-Tunneling[10]
Photo-electric emission -	
Secondary emission caused by electron bombardment	
Emission caused by metastable atoms.	

Almost all the emission processes listed above are known to be connected with electron emission from metallic surfaces. The first five being the most common. Of these the least relevant to the present investigations is the pure thermionic emission, (the experimental work was conducted at room temperature) where current density J_o is given by

$$J_o = AT^2 \exp\left(\frac{-e\phi}{kT}\right)$$

where A = constant

The field emission laws which are dependent on some function of the field are the relevant ones, it is therefore desirable to study the background to these laws since much work has been done to evaluate the various factors which influence them.

2.1.3 Image laws and electronic field emission

Consider the following:

The diagram on figs. 1a, 1b, 1c illustrate the effect of an applied field.

Once an electron has escaped from the metal into either a vacuum, gaseous or a solid dielectric, it is attracted back to the metal due to the charge induced on the metal surface. From the theory of electrical images the force on an electron having a charge -e is given by $-e^2/4\epsilon_T K_T x^2$, where x is the distance from the metal surface (for large x) and ϵ_T is the permittivity for the dielectric region, ϵ_T equals unity for gases and vacua. K_T is a constant equals 1 (in C.G.S. units) equals 4π (in M.K.S. units).

The energy of the electron at x is $e^2/4\epsilon_T K_T x$.

For an applied field E, the field E provides a contribution -eEx to the potential of the electron. Therefore the potential of the electron V(x) from the interface is given by $V(x) = -eEx - \frac{e^2}{4\epsilon_T K_T x}$ $(x > o)$. Thus the electric field reduces the height of the barrier and the maximum height of the barrier is given by the value of x when

$$\frac{dV(x)}{dx} = -eE + \frac{e^2}{4\epsilon_T K_T x^2}$$

$$= o$$

$$\text{i.e. } x_o = \tfrac{1}{2}\sqrt{\frac{e}{EK_T\epsilon_T}}$$

$$\text{and } V(x) \text{ maximum} = e\sqrt{\frac{eE}{\epsilon_T K_T}}$$

This gives the maximum value of the potential barrier to be over-

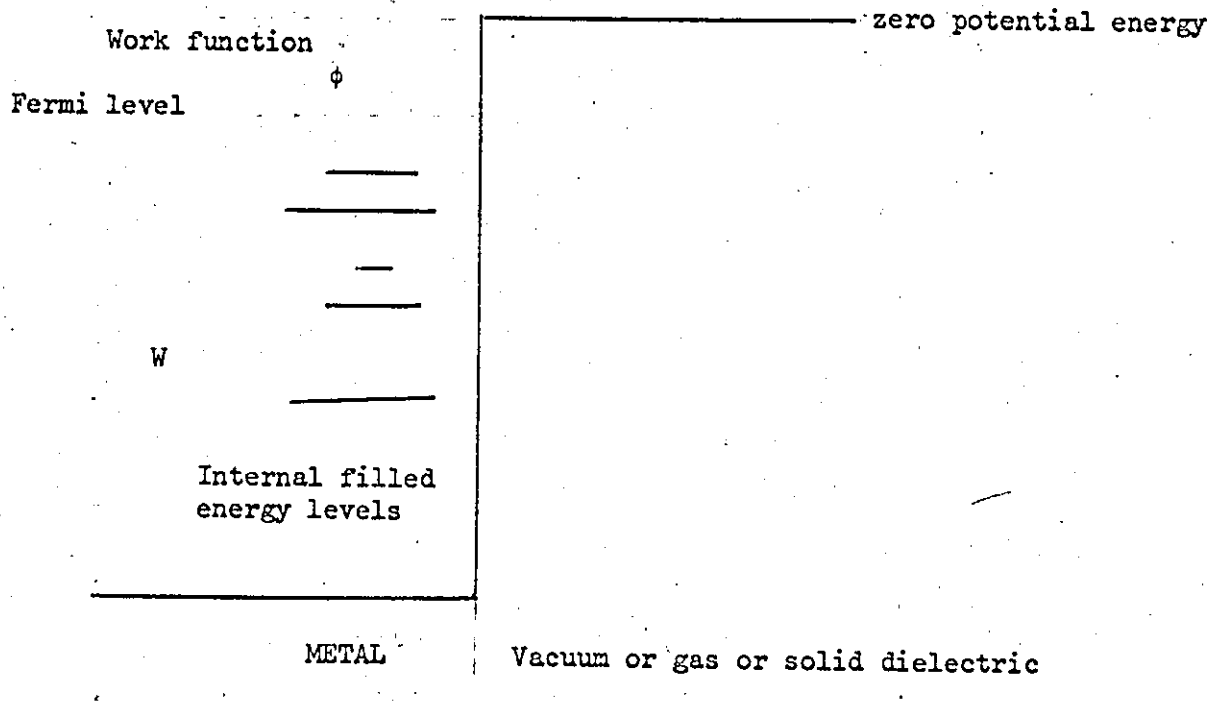

Fig. 1a

Energy distribution at a metal/vacuum interface.
dielectric

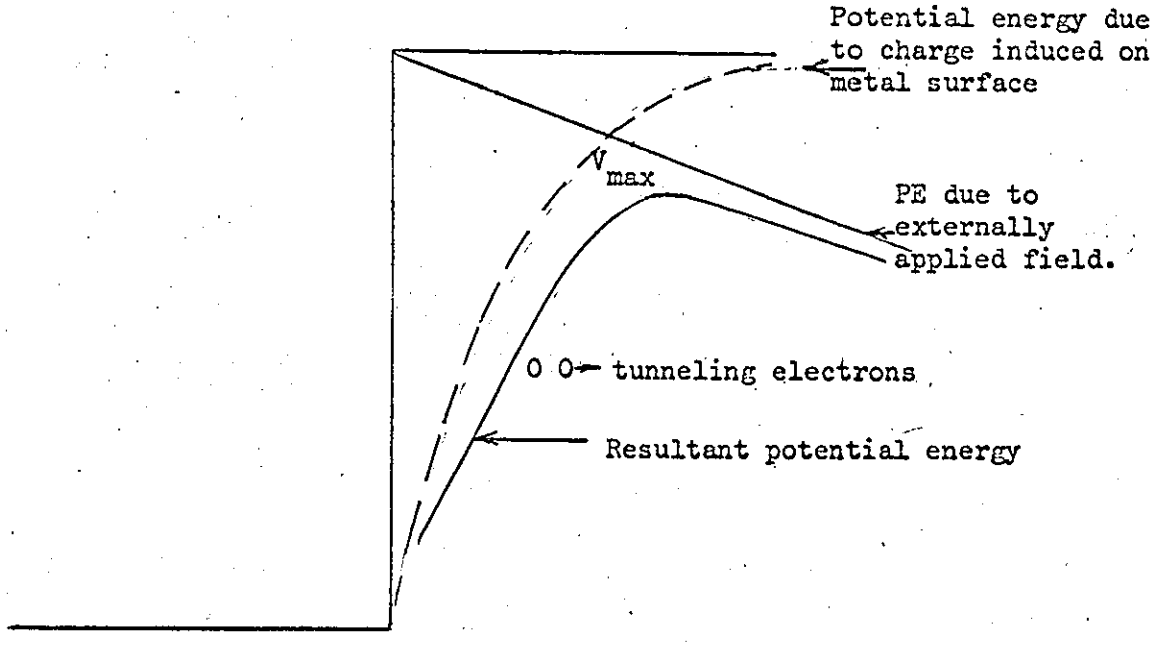

Fig. 1b

Potential distribution due to various fields

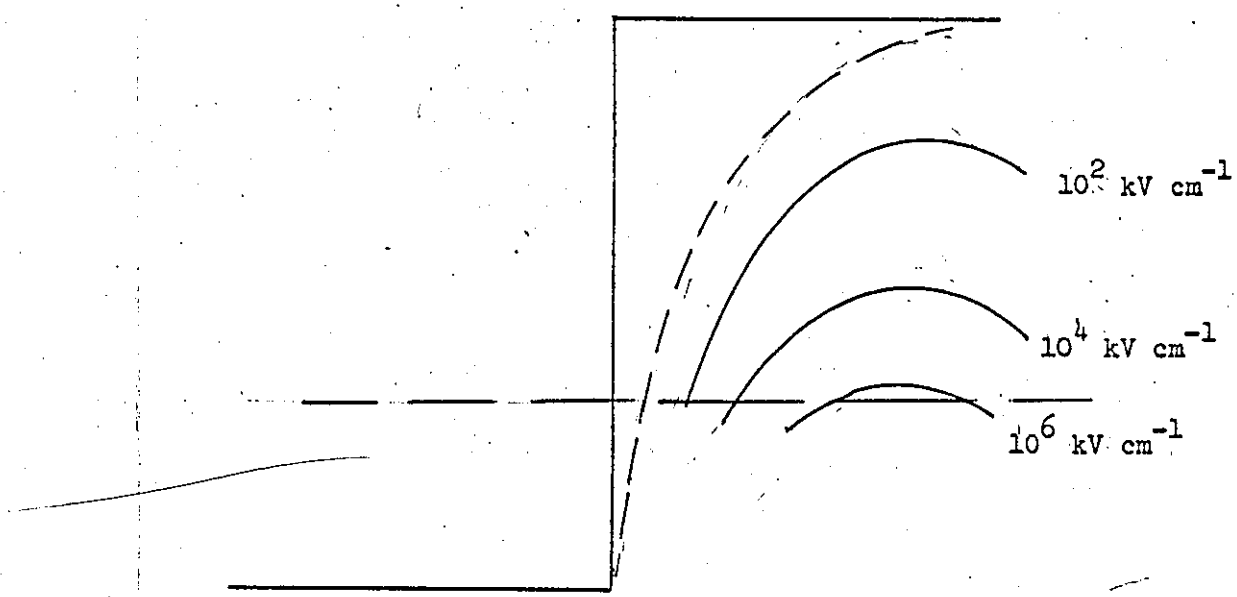

Fig. 1c

Influence of high stresses on potential to be overcome before emission

come by any electron (Fig. 1b).

The basis of Poole's and Frenkel's theories are very similar to the above considerations but it will be more instructive to treat them separately.

2.1.4 Poole's Conduction theory

Poole's[11] conduction law might be explained as follows: According to Maxwell's law for the electron distribution the number of electrons possessing a given energy u should be proportioned to $\exp(3U/2U_m)$ where U_m is the mean electronic energy. As regards insulators in a very strong field, sufficient energy may be contributed by the field to enable some with high energies to escape into the conduction band. For this to be possible the electron energy should not be less than $U_1 - U_2$ where U_1 is the minimum energy required to move into the conduction band and U_2 is the energy to be contributed by the electric field. U_2 may be expressed as $U_2 = Eed$.

d = some atomic distance

Hence the number of available electrons and so the current might be expected to contain $\exp(3Ede/2U_m)$ as a factor.

Poole's equation in its current form is explained as follows. If the diagram in fig. 2 represents an insulator with traps or energy barriers then in the absence of an applied field the probability for a jump is $p_o \propto \exp(-W/kT)$ in all directions. When a field is applied the probability of a jump in the field direction $p_1 \propto \exp -(W-\frac{1}{2}Ed)/kT$ and against the field $p_2 \propto \exp -(W+\frac{1}{2}Ed)/kT$. Therefore the resultant current flow is given by $p_1 - p_2 \propto \sinh eEd/2kT$ this reduces to $p \propto eEd/2kT$ when E is large i.e. at high stresses.

Thus the final equation obtained is of the form $\sigma = \sigma_o \exp bE$ at constant temperature.

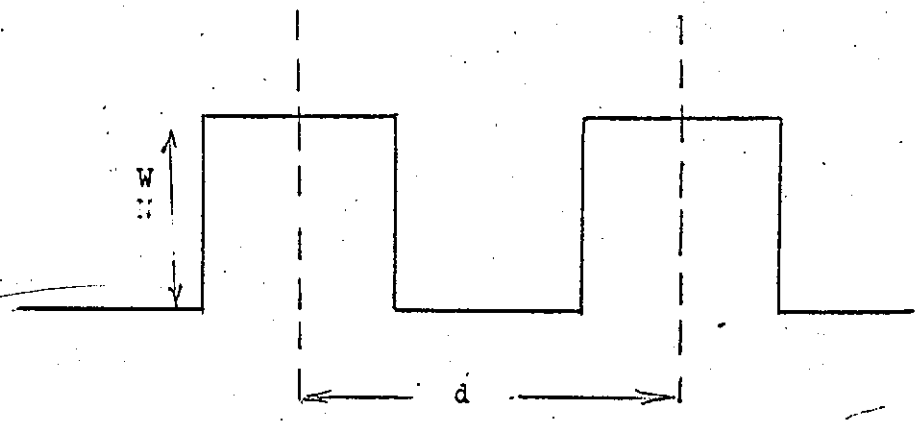

Potential well, No applied field

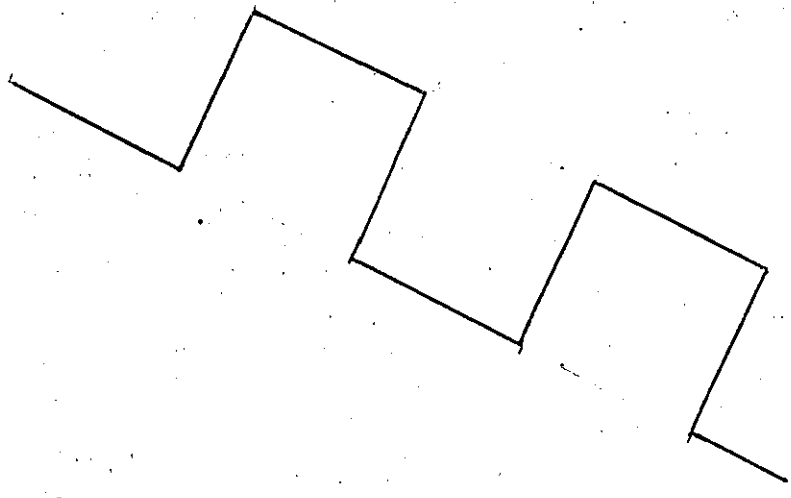

Influence of an applied field

Fig. 2
Illustration of Poole's Law.

2.1.5 Frenkel's conduction theory

Frenkel[8] in his approach points out that because the illumination of an electronic semi-conductor or dielectric results in an additional increase of the conductivity independent of E, this shows that the increase of electrical conductivity at high fields is due to an increase of the number of free electrons and not of their mobility.

The dielectric (or semi-conductor) is then described not as a system of free electrons moving in a self-consistent periodic field of force, but simply as a system of neutral atoms. This refers to the normal state in which there are no free electrons.

After ionization of an atom, the electron is then described as free moving in the surrounding medium of neutral polarization atoms and the field of the remaining positive ion.

Since this field is screened by the polarization of the surrounding atoms, the ionization energy must be decreased in the ratio $\epsilon:1$ where ϵ is the electronic component of the dielectric constant.

In an applied field E, this energy is further reduced by a mechanism similar to that of Schottky effect in the thermoelectronic emission from metals. In fig. 3, the full line represents the normal potential energy of the electron as a function of the distance from the positive ion while the dotted line represents the same quantity in the presence of the field. The height of the potential barrier is lowered in the field by the amount.

$$\Delta W = eEr_o + \frac{e^2}{\epsilon r_o}$$

where r_o, the distance to the maximum from the ion is given by

$$e^2/\epsilon r_o^2 = eE, \text{ thus } r_o = (e/\epsilon E)^{\frac{1}{2}} \text{ and}$$

$$\Delta W = 2eEr_o = 2e(eE/\epsilon)^{\frac{1}{2}}$$

Now if, in the absence of the electric field, the number of free electrons due to thermal ionization of the atoms is proportional to

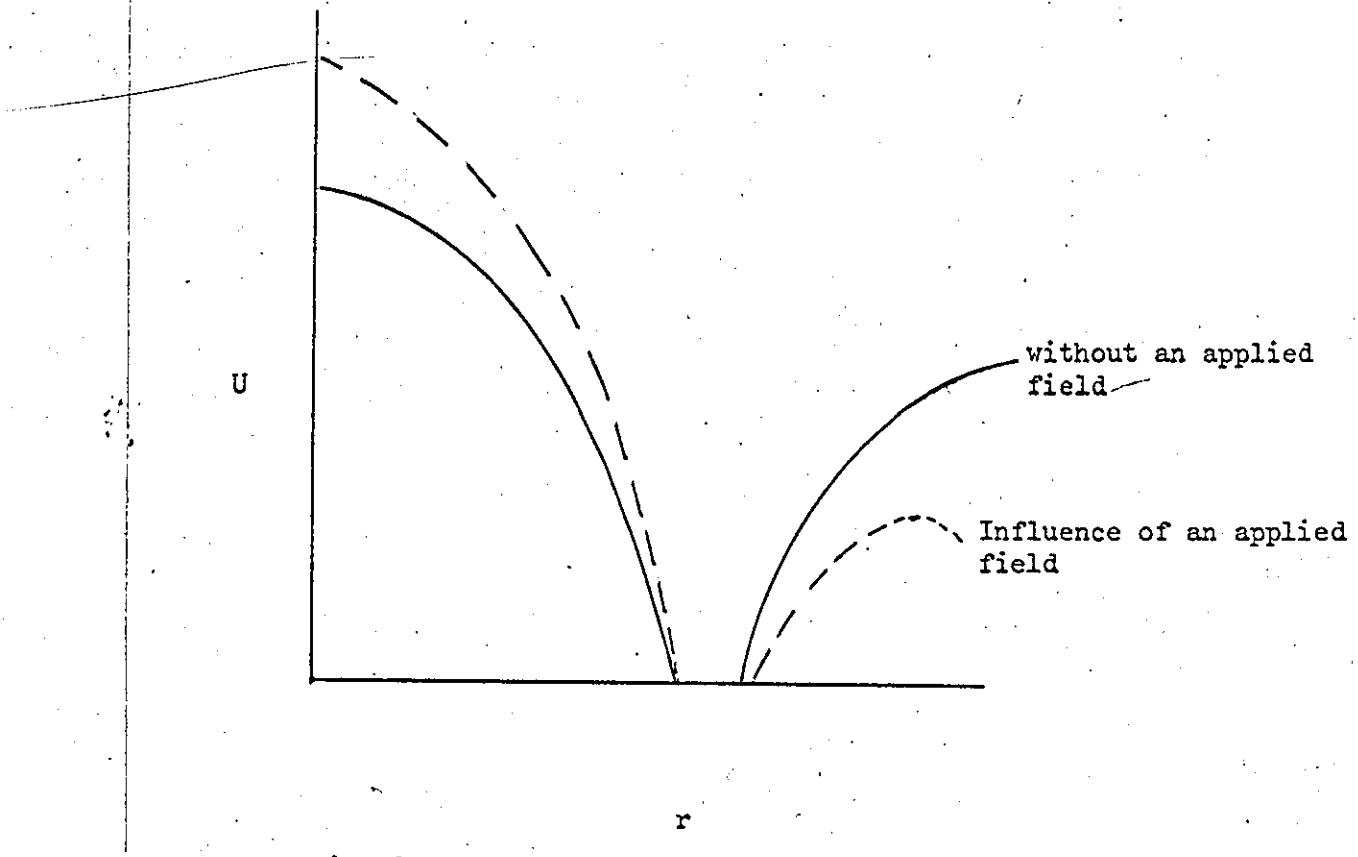

Fig. 3
Potential distribution,
Illustration of Frenkel's Law

$\exp(-W_o/2kT)$, where W_o is the ionization energy (decreased in the ratio ε:1) compared to an isolated atom, the electrical conductivity in the presence of the field will be proportional to

$$\exp -(W_o - \Delta W)/2kT$$

thus $\sigma = \sigma_o \exp (e^3E/\epsilon)^{\frac{1}{2}}/kT$

differing from Poole's law by the substitution of $E^{\frac{1}{2}}$ for E.

Most of the laws arising from the above survey and claimed to govern conduction are as follows.

2.1.6 Gas and vacuum conduction

For pure Schottky emission, J the current density per unit emitting area is given by

$$J = J_o \exp e\left(\frac{e}{4\pi\epsilon_o}\right)^{\frac{1}{2}} \frac{E^{\frac{1}{2}}}{AT}$$

or at constant temperature

$$J = BT^2 \exp (\delta E^{\frac{1}{2}}/T)$$

where B = constant

δ is a function of electronic charge and permittivity

For pure field or cold emission, a Fowler-Nordheim emission or for Tunneling.

$$J = A_1E^2 \exp (-\alpha/E)$$

where A_1 is a constant and α depend on the metal to vacuum work function and mass and charge of an electron.

For field assisted thermionic emission known as composite Schottky/Fowler/Nordheim or T-F emission, J is given by a mixture of the Schottky and Fowler-Nordheim equations given above.

2.1.7 Solid dielectric conduction

The process of emission and conduction in metal/dielectric/metal systems as opposed to metal/vacuum/metal system are not very clear.

Although it is held by some theories that because of contamination, induced dipoles etc., the stress E (defined earlier) is no longer uniform hence the laws of emission should be different; others believe that the introduction of the dielectric merely affects the work function and absolute permittivity in the Schottky and Fowler Nordheim laws listed earlier and may make emission start at lower stresses. Still others believe that because of possible traps present in the dielectric a hooked in space charge is produced which alters the potential barrier and hence potential barrier and emission laws.

It has been generally recognised however that solid dielectrics exhibit two main steady state forms of conduction when subjected to direct voltage stresses, these may be classified as ohmic and non-ohmic.

Ohmic conduction is characterised by an equation of the form:

$$J_o = \sigma E \qquad 2.4$$

and non-ohmic conduction by:

$$J = J_o . f(\epsilon,e) . F\{\exp(E,T)\} \qquad 2.5$$

At low stresses the conduction is ohmic, the process changing to non-ohmic as the stress is increased. The precise value of stress at which non-ohmic conduction starts is not clearly defined for a particular dielectric although it has been stated[12] that for polythene the transition takes place at stresses above 40 kV/cm.

Equation (2.5) is open to several different variations according to whether most of the electrons for conduction are obtained as:

(a) a result of field emission at high fields and low temperature,

(b) a result of thermal emission at high temperatures and low fields.

(c) a result of both field and thermal emission at medium temperatures and moderate fields.

Thus for Fowler-Nordheim (or Zener) emission the expressions for the current density is of the form:

$$J = AE^2 \exp(-\alpha/E)$$

and for the Schottky emission

$$J = B. \exp (\delta E^{\frac{1}{2}}/T)$$

where A and α depend on the electron mass and the metal to dielectric work function and where B and δ depend on the permittivity and ohmic properties of the dielectric.

The type of conduction described as being due to the Richardson-Schottky[13] effect gives an expression of the form:

$$\sigma = \sigma_o . \exp \left(\frac{\beta_s E^{\frac{1}{2}}}{kT}\right)$$

which may be modified to take into account the Poole-Frenkel effect as follows:

$$\sigma = \sigma_o . \exp \left(\frac{\beta_{pF} E^{\frac{1}{2}}}{kT}\right)$$

$$\text{where } \beta_{pF} = 2\beta_s = \left(\frac{e^3}{\pi \epsilon_o \epsilon_F}\right)^{\frac{1}{2}}$$

The Poole-Frenkel relationship is claimed to be effective when the conduction process is bulk limited and the Richardson-Schottky type when conduction is electrode limited.

In addition to the above expressions the Poole conduction process leads to the following expression for conductivity:

$$\sigma = \sigma_o E \exp bE$$

where b is a constant.

It is believed by some authors that at very low field the only conduction under steady state conditions that can occur is of the Richardson-Dushman type at very high temperature ~ 3000°K, that at medium fields ~ 100 kv/cm, no Fowler-Nordheim conduction can occur and that conduction at medium temperatures (1000 K) with these fields are of the Schottky type, and of the T-F type at very high temperatures. It is suggested that Fowler-Nordheim conduction can occur at around room temperature only at high fields (~1000 kv/cm) but some workers[14] have pointed out that in presence of various dielectrics and as explained earlier conduction may occur at much lower fields.

There is no doubt however that there is conduction at moderate fields 30 - . 100 kv/cm and several attempts have been made to explain this on the basis of the existing laws listed above. It is found however that experimental current densities measured are not compatible with the calculated quantities predicted by the various laws.

Some other explanations have been offered on the basis of patch fields, particles on electrode surface, and different surface condition but although these may explain some of the abnormalities obtained they do not by any means explain the conduction in dielectrics.

It is believed that the above anomalies could be explained on space charge basis.

CHAPTER 3

Space Charges in Gaseous Dielectrics

The concept of space charges has been in use for a long time. The most prominent area of its usage has been in connection with gas conduction, corona and breakdown theories[15,16,17].

The application of space charge theories to insulator or dielectric conduction has been rather limited because of the lack of consensus as to whether space charges can be claimed to exist in insulators at all. Only in the field of semi-conductors are space charge theories as applicable to dielectrics accepted[18].

This survey therefore begins with the review of a general space charge theory for all poor conductors and then continues with accepted forms of space charge as obtains in air/gases.

3.1 Space charges in poor conductors.

In order to appreciate the concept of space charge in this connection, consider this approach by Herzefeld[19] which involves two distinct possibilites: (i) space charge due to electrons between parallel plates and (ii) space charge in an ionized medium between two plates.

3.1.1 Space charge due to electrons between parallel plates.

For the first type he quotes the results of an earlier worker where ρ the charge density and V_x the potential are given respectively by

$$\rho = \frac{RT}{F} \frac{2A^2}{\cos^2 Ax}$$

$$V = \frac{RT}{F} \log \cos^2 Ax + B$$

Here the point of origin from which x is measured is between two plates. F is the Faraday equivalent i.e. F = ionic charge multiplied by number of molecules per mol, and A and B are constants. From further

calculation it is concluded that the number of electrons which would be present in the centre of the plates should be high enough to give measureable electron conductivity, if this number were limited by space charge and not by the surface forces. Accordingly, he concluded that surface forces are responsible for the absence of these electrons.

3.1.2 Space charge in an ionized medium between two plates.

In this case he assumes a uniform generation of q pairs of ions and a recombination of α (n+) (n-) per second per cubic centimetre, where the number of positive and negative ions present per cubic centimetre are n+ and n- respectively, and α is a constant.

The diffusion of the positive and negative ions are D+ and D- respectively.

Let E be the electric field and V the potential and y = VF/RT. Assuming that both ions have the same charge, ~~Which~~ this later might be a multiple of the charge of the electron, in which case F must be taken as a multiple of the Faraday equivalent.

All quantities referring to the left plate (X = -L) are designated by the subscript 1 and all those to the right plate (X = +L) by subscript 2 where 2L is the distance between the plates with the origin of coordinates at the middle of the plates and the potential at this point assumed to be zero. Let the current density be J. Then using the expression

$$\frac{\mu}{D} = \frac{e^2\epsilon}{kT} = \frac{F^2\epsilon}{NRT}$$

where

k = R/N the Boltzmann's constant

= gas constant R divided by number of molecules per mol. N.

and e = the Faraday equivalent divided by N.

The equations of motion for the ion were then written as

$$D+ \left\{\frac{d^2(n+)}{dx^2} - \frac{F}{RT}\frac{d}{dx}E(n+)\right\} = (\alpha n+)(n-) - q$$

$$D- \left\{\frac{d^2(n-)}{dx^2} + \frac{F}{RT}\frac{d}{dx}E(n-)\right\} = (\alpha n+)(n-) - q$$

and Poisson's equation gives

$$\frac{dE}{dx} = \frac{4\pi F}{\epsilon N}(n+) - (n-)$$

From further analysis and approximation a very complicated expression for the potential V is obtained: viz Langevin's approximation.

$$V = \frac{V_1 x}{L} + \frac{4\pi FL^2}{\epsilon N y_1^2}\frac{\exp.-y_1}{1-\exp.-2y_1}\left\{\left[(n+)_2 - (n+)_1 - \frac{2yq}{\alpha+}\right](1-\exp.\ y_1 x/L)\right.$$

$$\left. - \left[(n-)_1 - (n-)_2 - \frac{2y_1 q}{\alpha-}\right](1-\exp -y_1 x/L)\right\} + \frac{2\pi F}{3\epsilon N} L y_1 q \left(\frac{1}{\alpha+} + \frac{1}{\alpha-}\right)\left(\frac{x^2}{L^2} - 1\right)x$$

$$\frac{+2\pi F}{\epsilon N}\frac{1}{1-\exp 2y_1}\left\{(n+)_1 - (n+)_2 \exp(-2y_1) - (n-)_2 + (n-)_1 \exp(-2y_1) + y_1 q\right.$$

$$\left.(1+\exp -2y_1)\left(\frac{1}{\alpha+} + \frac{1}{\alpha-}\right)\right\} x(x-L)$$

$$+ \frac{4\pi FL}{\epsilon N y_1^2}\left\{(n+)_2 - (n+)_1 - \frac{2y_1 q}{\alpha+} + \left[(n-)_1 - (n-)_2 - \frac{2y_1 q}{\alpha-}\right]\exp.-y_1\right\} x$$

If it is further assumed that all ions are discharged immediately upon reaching the electrodes as in the case of gases. This means $(n+)_1 = (n+)_2 = (n-)_2 = (n-)_1 = (n-)_2 = 0$ and the expression for the potential is reduced to:

$$V = \frac{V_1 x}{L} - \frac{8\pi FL^2}{\epsilon N y_1}\frac{\exp.-y_1}{q\ 1-\exp -2y_1}\left(\frac{1-\exp\ y_1 x/L}{\alpha+} - \frac{1-\exp -y_1\ x/L}{\alpha-}\right)$$

$$+ \frac{4\pi FL^2}{6\epsilon N} y_1 q \left(\frac{1}{\alpha+} + \frac{1}{\alpha-}\right)\frac{x}{L}\left(\frac{x^2}{L^2} - 1\right)$$

$$+\frac{2\pi F}{\epsilon N}\ y_1 q\ \frac{1+\exp -2y_1}{1+\exp -2y_1}\ x(x-L)\left(\frac{1}{\alpha+}-\frac{1}{\alpha-}\right)-\frac{8\pi FL}{\epsilon N y_1}\ q\ \left(\frac{1}{\alpha+}+\frac{\exp -y_1}{\alpha-}\right)\ x.$$

Another approximation is then considered which gives for the potential an expression

$$V = 3/2\ \frac{RT}{FqL^2}\ Jx\ \left\{G+\frac{A}{6}\ \frac{x^2}{L^2}\ (G-2/3)-\frac{A}{60}\ \frac{x^4}{L^4}\ \left(G-\frac{AG}{2}+\frac{A}{3}\right)\right.$$

$$\left.-\frac{A}{360}\ \frac{x^6}{L^6}\ \left(G-\frac{AG}{14}-\frac{4}{7}+\frac{A}{21}\right)+\frac{A^2}{6048}\ \frac{x^8}{L^8}\ \left(G-\frac{11}{15}\ AG+\frac{7A}{15}+\frac{A^2G}{60}\quad\frac{-A^2}{90}\right)\right\}$$

where

$$A=\frac{4\pi F^2}{\epsilon RTN}\ \frac{q}{D}\ L^4$$

$$\text{and } G = 1+\frac{A}{360}\ \frac{7-(A^2/16)}{1+29A/320+A^2/960+A^2/3840}$$

Making a further assumption that no ions are discharged on the plates under normal conditions without field and that the number of ions without field is uniformly the equilibrium number throughout space. It is concluded that

$$E=\frac{JNRT}{2F^2n_oD}\ -A\delta\cosh\delta x$$

$$\text{where } \delta^2=\frac{8\pi F^2n_o}{\epsilon NRT}$$

$$\text{and } n_o\ =\ \left(\frac{q}{\alpha}\right)^{\frac{1}{2}}=n^1{}_+=n^1{}_-$$

This finally gives V as

$$V=V_1{}^1\frac{x}{L}+(V_1-V_1{}^1)\ \frac{\sinh\ \delta x-\delta x}{\sinh\ \delta L-\delta L}$$

$$\text{where } V_1{}^1\ =\ E_oL$$

$$-E_o=\frac{JNRT}{2F^2N_oD}\ +\ A\delta\quad\text{(the electric field at the origin)}$$

and $V_1 - V_1^1 = A (\sinh \delta L - \delta L)$ - the excess potential

Other cases are considered which first takes into account diffusion and then neglects it for comparison. The conclusion is that since if one considers the relative importance of the current due to diffusion and that due to the electric field in the equation for the stream of ions passing a certain cross section

$$D \left(\frac{dn}{dx} - \frac{F}{RT} nE\right) = Dn \left(\frac{d\log n}{dx} - \frac{FE}{RT}\right)$$

$$= Dn \frac{1}{\Delta x} \left(\Delta \log n + \frac{F}{RT} \Delta V\right)$$

and because n within the brackets is a log function, except for a potential drop of the order of a few volts, the effect of diffusion can be neglected.

3.2 Space charges in gases.

3.2.1 Child's analysis.

The most prominent amongst space charge theories is Child/Langmuir's three half power law for gas conduction in vacuum tubes.

In order to appreciate its similarity with the semi conductor/ insulator theory given elsewhere consider the following analysis.

In this analysis it is assumed that the currents are predominantly carried by charges of only one sign and that the net charge is not zero. It is assumed that the motion of the charges are sufficiently slow so that electrostatics formulae are valid and Poisson's equation holds.

Thus $\nabla^2 V = - \frac{\rho}{\epsilon_v}$ ... ... (3.1)

where V is the potential. The charges are supposed to be similar and associated with a mass m and to acquire their energy entirely from a superimposed field. Thus if their velocity is v and charge e, their

energy at a point where the potential is V will be

$$mv^2 = 2e\,(V_o - V) \quad \ldots \quad (3.2)$$

where V_o is their potential of origin. The current density at any point is given by

$$J = \rho v \quad \ldots \quad (3.3)$$

The simplest case is the one in which the charges are freed in unlimited quantity at the plane x = o and accelerated with a total potential V to a plane x = b. At the surface x = o charges will be freed until there is no longer an electric field to move them away so that the boundary condition at that point

$$\left(\frac{dv}{dx}\right)_{x = o} = o \quad \ldots \quad (3.4)$$

Here all the velocities are in the x- direction so that eliminating ρ and v from equation 3.1 by means of equations 2.2 and 3.3 we have

$$\frac{\partial^2 V}{\partial x^2} = \frac{J}{\epsilon_v}\left[\frac{m}{2e(V_o - V)}\right]^{\frac{1}{2}} \quad \ldots \quad (3.5)$$

Multiplying through by dV/dx and integrating from $V = V_o$ and $\frac{dV}{dx} = o$ to V and $\frac{dV}{dx}$

we have $\left(\frac{dV}{dx}\right)^2 = \frac{4J}{\epsilon_v}\left[\frac{m\,(V_o - V)}{2e}\right]^{\frac{1}{2}}$

Taking the square roots of both sides, integrating from $V = V_o$, x = o to V = o and x = b and solving for J,

$$J = \frac{4\epsilon_v}{9}\left(\frac{2e}{m}\right)^{\frac{1}{2}}\frac{V_o^{3/2}}{b^2} \quad \ldots \quad (3.6)$$

This is known as Child's equation. It shows that with an unlimited supply of charges at one plate, the current between the plates varies as the three halves power of the potential. Such a current is said to be space-charge limited. It can be seen from

equation 3.6 that the space-charge limitation is much more serious for charged atoms than for electrons because of their greater mass.

3.2.2 Cylindrical co-ordinate system.

In practice the emitter frequently takes the form of a small circular cylinder with the charges being accelerated to a larger concentric cylinder. In this case, using cylindrical co-ordinates and if I is the total current per unit length of cylinders equation (3.3) becomes

$$I = 2\pi r\rho v \quad \ldots \quad \ldots \quad \ldots \quad \ldots \quad \ldots \quad \ldots \quad \ldots \quad \ldots \quad \ldots \quad (3.7)$$

Writing equation (3.1) in cylindrical co-ordinates, eliminating ρ and v by equation (3.2) and (3.7) and writing V for $V_o - V$,

$$r\frac{d^2V}{dr^2} + \frac{dV}{dr} = \frac{-I}{2\pi\epsilon_v}\left(\frac{m}{2qV}\right)^{\frac{1}{2}} \quad \ldots \quad \ldots \quad \ldots \quad \ldots \quad \ldots \quad \ldots \quad (3.8)$$

The direct solution of this equation in finite terms is difficult, if not impossible.

One may however obtain a solution in series as follows:

Assume that q,m and V enter into this solution in the same way as into equation (3.6) leading to a solution of equation (3.8).

Try the solution:

$$-I = \frac{8\pi\epsilon_v}{9}\left(\frac{2q}{m}\right)^{\frac{1}{2}}\frac{V^{3/2}}{r\beta^2} \quad \ldots \quad \ldots \quad \ldots \quad \ldots \quad \ldots \quad \ldots \quad (3.9)$$

and check if β^2 can be determined to satisfy equation (3.8).

Substituting 3.9 in equation 3.8 gives the equation.

$$3\beta\frac{d^2\beta}{d\gamma^2} + \left(\frac{d\beta}{d\gamma}\right)^2 + 4\beta\frac{d\beta}{d\gamma} + \beta^2 - 1 = 0$$

where $\gamma = \log\left(\frac{r}{a}\right)$

This equation can be solved in the regular way in series which

gives

$$\beta = \gamma - 2/5\gamma^2 + \frac{11}{120}\ \gamma^3 - \frac{47\gamma^4}{3300}$$

$$\text{i.e.}\quad \beta = \log\left(\frac{r}{a}\right) - \frac{2}{5}\left(\log\frac{r}{a}\right)^2 + \frac{11}{120}\ \left(\log\frac{r}{a}\right)^3$$

Here a is the radius of the inner cylinder. Tables of β as a function of r/a have been published by Langmuir.

3.2.3 Space charges and Townsend's gas conduction theories.

In order to evaluate the anomalies in the results obtained using Townsend's electron avalanche theories[20,21] the workers concerned assumed that space charges occurred (A phenomena neglected by Townsend). The following analysis was presented[22].

Consider two parallel plate electrodes enclosing a gap L. Assume that the potentials at the terminals are zero and V_A respectively, also that a current of electrons i_o is released at one electrode. According to Townsend (section 5.1) these will travel through the gas towards the anode producing by ionization collisions further electrons and associated positive ions.

At any point in the gap at a distance x from the electron releasing electrode, the electron current $i_x = i_o \exp.\alpha x$ where α is Townsend's first ionization coefficient. The current arriving at the receiving electrode is thus given by $i_L = i_o \exp.\ \alpha L$.

From the condition of continuity, the total current crossing any plane parallel to the electrodes must be a constant. Let there be another charge carrier of mobility i_M

$\therefore\ i = i_L + i_M$ (assuming that i_M is of similar form to i_L).

To determine the effect of space charge, Poisson's equation must be solved

$$\text{i.e.}\quad \nabla^2 V = -\rho_{ML}$$

$$\frac{d^2V}{dx^2} = -\rho_{ML}$$

By using the equations

$$J = \rho v$$

and $v = \mu E$

μ = mobility

by writing $E = \frac{dV}{dx}$ and inserting the values of i_M and i_L assuming that at the receiving electrode $i_M = o$ (This last assumption is made to simplify the analysis but the generality of the analysis is not lost)

Then $i_M = i_o$ (exp αL - exp αx)

$$\text{Hence } \frac{d(dV/dx)}{dx} = \frac{-J_o}{dV/dx} \left[\frac{\exp(\alpha L) - \exp - \alpha x}{\mu_M} - \frac{\exp \alpha x}{\mu_L} \right]$$

where J_o is the electron current density at the releasing electrode.

If it is assumed that

$$\mu_L >> \mu_M$$

$$\text{Then } \frac{dV}{dx}\,\frac{d}{dx}\,(dV/dx) = \frac{-J_o}{\mu_M} \left[\exp(\alpha L) - \exp \alpha x \right]$$

$$E\frac{dE}{dx} = \frac{-J_o}{\mu_M} \left[\exp(\alpha L) - \exp \alpha x \right]$$

Now $\frac{\alpha}{p} = f\left(\frac{E}{p}\right)$ or at constant pressure

$$\alpha = f(E)$$

Now for Townsend's equation to hold the stress in the gap E must be uniform. If space charge is present and the field is not uniform then

$$i_x = i_o \exp \int_o^x \alpha dx$$

The equation to be solved then becomes

$$E\,\frac{dE}{dx} = \left[\frac{-J_o}{\mu_L}\right] \left[\exp \left(\int_o^d \alpha dx\right) - \exp \left(\int_o^x \alpha dx\right)\right]$$

This equation with certain assumptions is solved in the above reference for selected values of J_o in air.

CHAPTER 4.

Space Charges in Solid Dielectrics

Space charges and their effect on the conductivity in solid dielectrics under direct voltage conditions however has not been very clear. Whereas some authors[23] ignore its effect at operating voltages, others[24,25,26] stress its influence.

The former assume that (in the absence of field emission) the initial current density at switch-on, (J(t)), is given by:

$$J(t) = \epsilon E_o.V(t) + \sum_{1=1}^{n} X_i(t).E_o 1(t) + J_o \quad \ldots \quad \ldots \quad \ldots \quad 4.1$$

where $X_i(t) = \sigma_i . \exp(-t/t_i)$

σ_i depends on the conductivity of the dielectric and t_i depends on the polarization time.

The final steady-state current density is governed solely by the applied voltage across the specimen and its thickness. Hence the conductivity in the steady-state condition may be expressed as:

$$\sigma = \sigma_o . \exp(K_1 E_x + K_2 T) \quad \ldots \quad \ldots \quad \ldots \quad \ldots \quad \ldots \quad 4.2$$

where E_x depends on the externally applied stress and K_1, K_2 are constants.

In the case of a parallel plate capacitor in which the dielectric is held at a constant and uniform temperature, an application of the above argument results in the following expression for the stress, (E_x) at a point within the dielectric;

$$E_x = \frac{V_A}{L}$$

Other writers[25,26,27] argue that space charge within the dielectric will effect the stress distribution and, as a result of this together with the consequent interfacial polarization, Poisson's equation will

hold, i.e. under steady-state conditions

$$\text{div } D = \rho \quad \ldots \quad \ldots \quad \ldots \quad \ldots \quad \ldots \quad \ldots \quad \ldots \quad \ldots \quad 4.3$$

$$J = ne\mu . \text{ grad } V - \mu kT . \text{ grad } n \quad \ldots \quad \ldots \quad \ldots \quad 4.4$$

$$\mu/D_i = e/kT \text{ (Einstein's equation)} \quad \ldots \quad \ldots \quad \ldots \quad 4.5$$

Solution of the above equations hsows that, for example, the stress distribution in a parallel plate capacitor will no longer be linear[23] but will be of the form:

$$S(x) = E(x) + G(x) \quad \ldots \quad \ldots \quad \ldots \quad \ldots \quad \ldots \quad \ldots \quad 4.6$$

In other words the stress distribution, S(x), is made up of two components, one, E(x), being the distribution when space charges are assumed to be absent and the other, G(x), the distribution due to the space charge.

4.1.1 Current density (approximate solution)

In order to obtain a solution to the above set of equations, 4.3, 4.4 and 4.5, it may be assumed that diffusion is negligible and that

$$\text{div } J = 0$$

$$J = \rho v$$

$$ne = \rho$$

$$\text{then, } D_i = o$$

also

$$ne = \rho \text{ under steady state conditions}$$

$$\text{hence } J = ne\mu E$$

This simplification of the equation for J assumes that the mean thermal energy of the space charge is greater than the energy gained from the electric field, (since continuous collisions with the lattice tend to dissipate the latter). Hence an expression is obtained for the drift velocity v in terms of the applied stress and the current

carrier mobility in semiconductors viz $v = \mu E$. This should be contrasted with the case of the vacuum diode (analysed earlier) where the relationship between velocity v and stress $\frac{V}{L}$ is obtained by equating the kinetic energy of the electrons to the accelerating force ($\frac{1}{2} m v^2 = Ve$) neglecting the thermal velocities of the emitted electrons.

Now solving the equations

$$J = ne\mu E$$

then from $\frac{d^2V}{dx^2} = -\frac{\rho}{\epsilon}$,

and $\rho = ne$

$$= \frac{J}{\mu E}$$

$$\frac{d^2V}{dx^2} = \frac{J}{\mu \epsilon E}$$

Then $\frac{d^2V}{dx^2} \frac{dV}{dx} = \frac{J}{\epsilon\mu}$,

$$\therefore \frac{\epsilon\mu}{J} \frac{d^2V}{dx^2} \frac{dV}{dx} = 1$$

$$\therefore \frac{\epsilon\mu}{2J} \left(\frac{dV}{dx}\right) = x + C_1$$

$$\left(\frac{\epsilon\mu}{2J}\right)^{\frac{1}{2}} \frac{dV}{dx} = (x + C_1)^{\frac{1}{2}}$$

$$\left(\frac{\epsilon\mu}{2J}\right)^{\frac{1}{2}} V = \frac{2}{3} (x + C_1)^{3/2} + C_2$$

if $V = o$ at $x = o$ - first boundary condition $C_2 = -\frac{2}{3} C_1^{3/2}$

$$\therefore \left(\frac{\epsilon\mu}{2J}\right)^{\frac{1}{2}} V = \frac{2}{3} (x + C_1)^{3/2} - \frac{2}{3} C_1^{3/2}$$

and for an applied voltage V_A and thickness of dielectric L, that is for $V = V_A$ at $x = L$ - second boundary condition

$$\left(\frac{\epsilon\mu}{2J}\right)^{\frac{1}{2}} \quad V_A = \frac{2}{3}(L + C_1)^{3/2} - \frac{2}{3} C_1^{3/2}$$

The above equation reduces to the familiar $J = \frac{9}{8} \epsilon\mu \frac{V_A^2}{L^3}$ when one assumes that at x = o (electrode dielectric interface) $\frac{dV}{dx} = o$.

Notice that in this case J is proportioned to L^{-3}.

Current density - series solution

The other method assumes a series for G(x) or ρ - (e.g. Taylor's series[28].) The equation being solved by applying the appropriate boundary conditions.

In this case it is more instructive to separate the charge carriers into positive and negative charge carriers and the equations become:-

$$\nabla^2 V = \frac{-e}{\epsilon} (p-n) \quad \ldots \quad \ldots \quad \ldots \quad \ldots \quad \ldots \quad \ldots \quad \ldots \quad \ldots \quad \ldots \quad 4.7$$

$$J = -e \text{ grad } V (\mu_p p + \mu_n n) - kT (\mu_p \text{ grad } p - \mu_n \text{ grad } n) \ldots \quad \ldots \quad 4.8$$

$$\text{div } J = eK - \frac{e^2}{\epsilon} (\mu_p + \mu_n) pn = \frac{\partial \rho}{\partial t} \quad \ldots \quad \ldots \quad \ldots \quad \ldots \quad \ldots \quad \ldots \quad 4.9$$

$$(p-n)e = p$$

where K = number of pairs of charge carriers generated per unit volume per unit by dissociation, where p and n are positive and negative charge carrier densities respectively μ_p, μ_n are the mobilities of positive and negative charge carrier densities.

$$\text{and } \frac{e^2}{\epsilon} (\mu_p + \mu_n) pn = \text{recombination factor}$$

The rest of the symbols are defined as before.

Now assuming that $\mu_p = \mu_n = \mu$ and writing

$$A = p + n = A^1(x) \text{ where } p = p^1(x) \text{ and } n = n^1(x) \quad \ldots \quad \ldots \quad \ldots \quad \ldots \quad 4.10$$

$$B = p-n = B^1(x)$$

The equations 4.7, 4.8, for the one dimensional case can be written as

$$\frac{\partial^2 V}{\partial x^2} = \frac{-e}{\epsilon} B \quad \ldots \quad \ldots \quad \ldots \quad \ldots \quad \ldots \quad \ldots \quad \ldots \quad \ldots \quad \ldots \quad 4.11$$

$$J = -e \frac{\partial V}{\partial x} A - kT\mu \frac{\partial B}{\partial x} \quad \ldots \quad \ldots \quad \ldots \quad \ldots \quad \ldots \quad \ldots \quad \ldots \quad 4.12$$

Differentiating 4.11 with respect to x:

$$\frac{\partial J}{\partial x} = -e\mu A \frac{\partial^2 V}{\partial x^2} - e\mu \frac{\partial V}{\partial x} \frac{\partial A}{\partial x} - kT\mu \frac{\partial^2 B}{\partial x^2}$$

From equations 4.9 and 4.10 $\frac{\partial J}{\partial x} = eK - \frac{e^2}{2\epsilon} \mu (A^2 - B^2)$ $\ldots \quad \ldots \quad \ldots \quad \ldots \quad \ldots \quad 4.13$

Assuming that $p(x)$ and $n^1(x)$ across the dielectric are as shown in Fig. 4a, then $A(x)$ and $B^1(x)$ are as shown in Fig. 4b .

Now let $B^1(x) = \alpha_1 + \beta_1 x + \gamma_1 x^2$

Assuming symmetrical charge distribution systems as in diagrams for $p^1(x)$ and $n^1(x)$.

$\therefore \quad B^1(o) = p^1(o) - n^1(o) = o.$

and since $B^1(x)$ is symmetrical about the origin.

$$\left(\frac{\partial^2 B}{\partial x^2}\right)_{x=o} = o$$

$\therefore \quad \alpha_1 = \gamma_1 = o$

$\therefore \quad B^1(x) = \beta_1 x$

Substituting $\beta_1 x$ into 4.11 and integrating

$$\frac{\partial V}{\partial x} = \frac{-e}{\epsilon} \frac{\beta_1 x^2}{2} + \left(\frac{\partial V}{\partial x}\right)_{x=o} \quad \ldots \quad \ldots \quad \ldots \quad \ldots \quad \ldots \quad \ldots \quad \ldots \quad 4.14$$

Therefore $V = \frac{-e}{\epsilon} \frac{\beta x^3}{6} + \left(\frac{\partial V}{\partial x}\right)_{x=o} . x + \frac{V_A}{2}$ $\ldots \quad \ldots \quad \ldots \quad \ldots \quad 4.15$

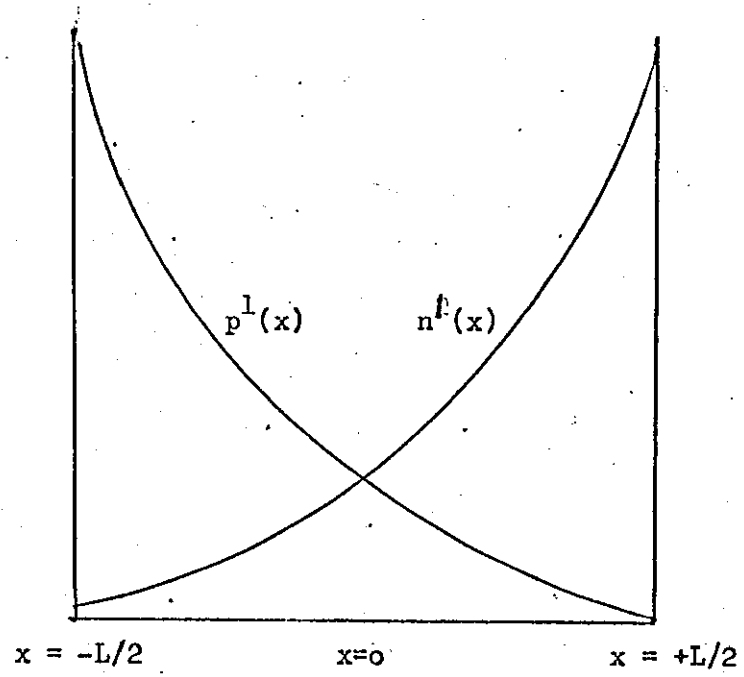

Fig. 4a

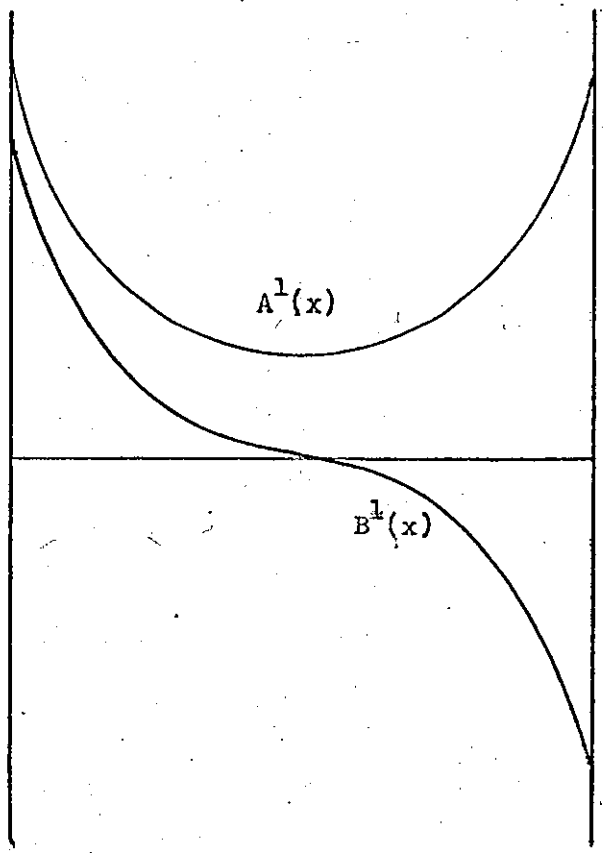

Fig. 4b

Assumed charge carrier distribution in a dielectric in a parallel plate Capaicitor configuration.

where V_A is the voltage applied and $\frac{V_A}{2}$ is the consequent voltage at x=o in the absence of space charge.

If boundary conditions are such that

at $x = -L/2$, $\frac{\partial V}{\partial x} = S$ and $V = 0$

Equations 4.14 and 4.15 give

$$\beta_1 = \frac{-12\epsilon}{eL^2} \left(S - \frac{V_A}{L}\right) \quad \ldots \quad 4.16$$

$$\left(\frac{\partial V}{\partial x}\right)_{x=o} = \frac{3}{2} \frac{V_A}{L} - \frac{S}{2} \quad \ldots \quad 4.17$$

From the continuity equation

$$J(0) = J\left(-\frac{L}{2}\right)$$

Also from equation 4.12

$$J(0) = -e\mu \left(\frac{\partial V}{\partial x}\right)_{x=o} A^1(0) - \mu kT\beta_1 \quad \ldots \quad 4.18$$

Considering Fig. 4B and from equation 4.13 at x=o

$$B^1(0) = \left(\frac{\partial^2 B}{\partial x^2}\right)_{x=o} = \left(\frac{\partial A}{\partial x}\right)_{x=o} = 0$$

also under steady state

$$\frac{\partial J}{\partial x} = 0$$

$$\therefore \quad eK - \frac{e^2}{2\epsilon} \mu A(0)^2 = 0 \quad \ldots \quad 4.19$$

$$\therefore \quad A_o = \sqrt{\frac{2\epsilon}{e\mu}}$$

$\therefore$ From equations 4.18 and 4.19

$$-J(0) = J = \sqrt{e\mu} \left(\frac{\partial V}{\partial x}\right)_{x=o} \cdot \sqrt{2\epsilon K} + \mu kT\beta_1 \quad \ldots \quad 4.20$$

By substituting equations 4.16 and 4.17 in equation 4.20 the total current J may be obtained assuming that

$$\left|\frac{\partial V}{\partial x}\right|_{x=-\frac{1}{2}} \ll \frac{V_A}{L}$$

Then substituting for β_1 and $\left|\frac{\partial V}{\partial x}\right|_{x=o}$ i.e. equations 4.16 and 4.17 in equation 4.20

$$J = \sqrt{e\mu}\ \frac{3}{2}\ \frac{V_A}{L}\ \sqrt{2\epsilon K} + \mu kT\ \frac{12\epsilon V_A}{eL^3}$$

and $K = K_o \exp(-W/kT)$

where W is the ionization energy.

4.2 Space charge formation.

Most other papers on the subject[14,29,30] recognise the effect of space charges when there is field emission but apparently not before though this is not made very clear. Others even explain the decay of durrent in dielectrics in response to a d.c. stress as a result of space charge accumulation due to electrical inhomogeneities within the dielectric.

The question is whether there is space charge at both low and high stresses with and without emission and if so at what stresses is its effect felt most. The case for space charge in presence of field emission seems well established[29,30,31] but so far experiments carried out to investigate stress distribution in other cases have not been widely accepted because of the claim that the insertion of probes within the dielectric to measure the stress may in itself effect the stress pattern[25,27,32,33]. Another uncertainty is whether deviations from Ohm's law are necessarily due to field emission[34].

CHAPTER 5

Gas Discharge Processes in Insulation

Serious and systematic study of discharges in insulation began with the work of Gemant and Phillipoff[35]. Since that time this type of investigation has become a major part of the study of electrical insulation breakdown. The background of the work however dates back to the work by Townsend on electron avalanche supplemented in some respect by the work of Peek.[16]

5.1 Townsend's theories.

Townsend[20,21] postulated that if n negative ions are moving in a gas between two parallel plates at a distance d apart, also if E is the ohmic electric stress given by $\frac{V_1-V_2}{d}$ where V_1 and V_2 are the potentials of the two electrodes respectively and P, the gas pressure of the gas inbetween the plates, then in covering a distance dx the n ions produce $\alpha n\, dx$ others where α (known as Townsend's first ionization coefficient) is a constant dependent on E and P and temperature. (The coefficient α is practically zero for small values of E unless P is also small, i.e. $\frac{\alpha}{P} = F(\frac{E}{P})$. In the absence of space charge this has been shown to be of the form $\frac{\alpha}{P} = A\exp(\frac{BP}{E})$ thus $dn = \alpha n\, dx$ ... 5.1

and $n = n_o \exp \alpha x$ 5.2

Hence n_o ion starting at a distance x from one of the plates will give rise to $n_o(\exp \alpha x - 1)$ others. When the ions arrive at the plate the formation of new ions ceases and the current stops. Let n_o be the number of ions produced per unit volume. The total number of ions produced per unit area will therefore be

$$\int_o^d n_o \exp \alpha x\, dx = \frac{n_o}{\alpha}(\exp \alpha d - 1)$$

where, $n_o d$ is the number produced by the rays per unit area hence

$$\frac{i}{i_o} = \frac{i}{\alpha d}(\exp \alpha d - 1)$$

where i is the current for a large intensity E and i_o the current composed of the ions produced.

Townsend's second ionization coefficient γ is introduced by assuming that there are other mechanisms solely or partly responsible for the production of secondary ions. Consider first the case where secondary electrons are produced at the cathode by positive ion bombardment.

Let n = number of electrons reaching the anode per sec.

n_o = number of electrons released by external radiation.

n+ = number of electrons released from the cathode by positive ion bombardment.

γ = number of electrons released from the cathode per incident positive ion.

Then $n = (n_o + n_+) \exp\alpha d$

$$n_+ = \gamma[n - (n_o + n_+)]$$

Eliminating n_+,

$$n = n_o \frac{\exp\alpha d}{1-\gamma(\exp\alpha d-1)} \quad \ldots \quad 5.3$$

or $$i = i_o \frac{\exp\alpha d}{1-\gamma(\exp\alpha d-1)} \quad \ldots \quad 5.4$$

Note the similarity between equations 5.2 and 5.3 when $\gamma = o$.

From equation 5.4 breakdown is deemed to occur when

$$\gamma(\exp\alpha d-1) = 1 \quad \ldots \quad 5.5$$

Here γ is taken to represent the number of secondary electrons per positive ion, noting that this may represent one or more of several mechanisms. The value of $\gamma(\exp\alpha d-1)$ is zero at low voltage gradients but increases as the voltage gradient is raised until equation 5.5 is satisfied. In general at the value of α corresponding to breakdown $\exp\alpha d \gg 1$ and therefore equation 5.5 can be written in the form $\gamma \cdot \exp\alpha d = 1$.

5.2 Streamer theories.

The other notable gas breakdown theory apart from Townsend's theory is the Streamer Theory.[36,37]. This was enunciated because the very short time lags of breakdown recorded when uniform gaps were overstressed were not consistent with Townsend's theories. The very irregular nature of breakdowns in long but supposedly uniform gaps also did not conform to the known theories. Thus as a result of experiments by Raether and Meek and Loeb, the streamer theory was postulated. The theory is centred around the space charge properties of the medium, which is claimed to transform the single Townsend avalanche into a plasma streamer, after this there is a sharp increase in conductivity and there is breakdown in the channel of this avalanche.

For a streamer to cause breakdown apart from the first Townsend avalanche there must be a large amount of photoionization of gas molecules in the space -head of the streamer and a rapid increase of the spatial stress by the ion space charge at the tip of the streamer. Obviously there must occur a distortion of this spatial stress pattern due to the space charges. This space charge is claimed to be formed by the large difference in mobility between positive ions and electrons, as a result the avalanche formed by the electrons leaves behind this positive space charge.

If the stress due to the space charge is designated as some function $E_r = KE$ where K is a constant and E the externally applied stress calculated on an ohmic basis then at the head of the avalanche where the ion density reaches its maximum value, the stress at this point will be $(1 + K)E$.

It is further postulated that when the avalanche has crossed the gap, the electrons at the head of the first avalanche are swept into the anode, the positive ions remaining in a cone-shaped volume. Further auxiliary avalanches are formed as a result of photo-electron ionization and the streamer proceeds across the gap to form a conducting

channel.

An avalanche is considered to be able to develop into a streamer when $E_r \sim E$. In order to calculate the approximate value of E_r assume that the positive ions of charge Q, are contained in a spherical volume of radius r at the head of the avalanche. Therefore E_r at radius r is given by

$$E_r = \frac{Q}{4\pi\epsilon_o r^2} = \frac{\frac{4}{3}\pi r^3 ne}{4\pi\epsilon_o r^2} = \frac{rne}{3\epsilon_o} \quad v/m$$

In a distance dx at the end of a path x the number of ions mass produced is $\alpha e^{\alpha x} dx$ and therefore

$$n = \frac{\alpha e^{\alpha x}}{\pi r^2} \cdot \frac{dx}{dx}$$

$$= \frac{\alpha e^{\alpha x}}{\pi r^2}$$

Therefore $E_r = \frac{e\alpha e^{\alpha x}}{3\epsilon_o \pi r}$ volts/metre

$$= \frac{e\alpha e^{\alpha x}}{3r\epsilon_o \pi}$$

The radius r is that of the avalanche after it has travelled a distance x and is given by the diffusion expression $r = \sqrt{(2Dt)}$

$$t = \frac{x}{v-}$$

where D is the diffusion coefficient and v- is the velocity of the avalanche and therefore of electrons in the applied field hence $v- = \mu E$ where μ is mobility.

Thus substituting for r in the expression and assuming that permittivity $\epsilon_o = 1$ for E_r, $E_r = \frac{e\alpha e^{\alpha x}}{\pi 3\sqrt{\{2D(x/v)}}$

Now $v = \mu E$

$$\therefore \quad E_r = \frac{e\alpha e^{\alpha x}}{\pi 3\sqrt{\{(2D/\mu)(x/E)}} \quad v/m.$$

From further consideration of the value of $\frac{D}{\mu}$ for electrons the expression

was reduced to

$$E_r = 5.27 \times 10^{-7} \frac{\alpha \exp \alpha x}{(x/\rho)^{\frac{1}{2}}} \text{ v/cm}$$

The condition for the propogation of a streamer is $E_r = KE$ where $K \sim 1$.

Raethers criterion for anode directed streamers is similar and is given as when the applied stress $\approx \frac{e\alpha \exp \alpha x}{4\pi r^2 \epsilon_o}$ where r is the avalanche radius.

It has been established by several workers that for a value of Pd much less than 6,000 mm Hg cm where P is pressure in millimeters of mercury and d is electrode distance Townsend's mechanisms are the main causes of breakdown of gases though it must be remembered that the transition is also affected by the ratio $\frac{E}{p}$ where E is stress in volts per centimetre. However for very small gaps breakdown could be assumed to be Townsendic.

5.3. Breakdown of air voids in insulation.

Breakdown of air voids in insulation is considered to be similar to Townsend's theories of electron avalanches between plane metal electrodes and several workers have established this. Mason[38] showed that though the discharge-inception stress in non-ventilated voids in polythene is in fair agreement with the mean of collected results for the breakdown stress between plane parallel metal electrodes the values for the former were 10;20% lower than the latter. He also established that if the void was adjacent to a metal electrode, the deterioration is more rapid than is with the void totally enclosed in the dielectric though no explanation was offered* he also explained discharge extinction as being due to excessive carbonization. Mason also obtained the stress E_v in a void enclosed in a dielectric as approximately given by

$$E_V = E_o \frac{\epsilon}{\epsilon - (\epsilon-1)F} \left[1 - \frac{(\epsilon-1)t_1}{t+(\epsilon-1)t_1} \frac{d}{d+t} \right] \quad \ldots \quad \ldots \quad \ldots \quad 5.6$$

*(see chapter 9)

where E_o is the initial stress in the dielectric (=V/t)

ϵ_1 = permittivity of the void material (=1)

t = thickness of the dielectric slab

t_1 = depth of void

d = diameter of the void

When $d > t_1$, the function F is defined by

$$F = x^2/(x^2-1)\left[1 - (x^2-1)^{-\frac{1}{2}} \text{ arc Cos } x^{-1}\right]$$

and when $d < t_1$ is given by

$$F = \frac{x^2}{x^2-1}\left[\frac{\text{arc Cosh} x^{-1}}{(1-x^2)^{\frac{1}{2}}} - 1\right]$$

where $x = \frac{d}{t_1}$

The above equations apply to voids cylindrical in shape, with a thickness always less than their diameter, within a plane slab of dielectric always much thicker than the void but not thick compared with the diameter of the void.

When d is much greater than t, E is given by

$$E = E_o \epsilon/\left[1+(\epsilon-1)\, t/t_1\right] \text{ and for } t_1 << d < t$$

$$E = E_o \epsilon/\left[\epsilon - (\epsilon-1)\, F\right] \quad \ldots \quad \ldots \quad \ldots \quad \ldots \quad \ldots \quad \ldots \quad \ldots \quad 5.7$$

Other expressions are derived for the field strength at the inception voltage of voids in metal electrodes, at the end of a carbonized pit which forms a conducting extension of one electrode and at the end of a conducting pit which is close to an electrode. Expressions are also given for the voltage distribution when a conducting pit is enclosed asymmetrically in a dielectric slab between parallel electrodes and for the magnitude and energy of discharges.

5.4 Direct voltage discharge theories.

5.4.1 Rogers and Skipper.

The development of discharge theories under direct voltage conditions is also modelled and given treatment similar to that under a.c. conditions - a practice which has been criticised by some workers. The literature on d.c. work is scanty but Rogers and Skipper[39] analysed the stresses in cavities and the discharges repetition rate under direct-voltage conditions and showed that the time between successive discharges, τ, in an oblate spheroidal cavity located in a uniformily stressed, infinite dielectric medium is given by

$$\tau_o = -\tau \log_{\epsilon} \left(1 - \frac{E_i}{\lambda E^1}\right)$$

where E_i = discharge inception stress in the cavity

E^1 = uniform stress applied to the dielectric

$$\frac{1}{\lambda} = 1-\left(\frac{1}{\sigma_2}\right)(\alpha \text{arc cot}\alpha - 1)\left[\sigma_{so}\alpha/c)+(\sigma_1-\sigma_2)(1+\alpha^2)\right]$$

a = semi minor axis
b = semi major axis } of the oblate spheroidal cavity
$2c$ = focal length

σ_{so} = the surface conductivity of the cavity boundary at the poles of the cavity

σ_1, σ_2 = conductivities of the media inside and outside the cavity respectively

$\alpha = \frac{a}{c}$, (not in this case the 1st Townsend coefficient)

$$\tau = \frac{\epsilon_o(\epsilon_1-\epsilon_2)(1+\alpha^2)(\alpha \text{arc cot}\alpha - 1) - \epsilon_o\epsilon_2}{\left[\sigma_{so}\alpha/c)+(\sigma_1-\sigma_2)(1+\alpha^2)\right]\left[(\alpha \text{arc cot}\alpha - 1\right]-\sigma_2} \quad \ldots \quad \ldots \quad 5.8$$

and ϵ_1, ϵ_2 = relative permitivities of the media inside and outside the cavity.

The expression for τ is simplified further when minimum

$\tau_m \approx 8.85 \times 10^{-12} \frac{\lambda^1+\epsilon_2-1}{1\sigma_2}$ is considered. (where λ^1 is the value of λ when $\sigma_{so} = o$) (see appendix 7)

Hence it was concluded that the maximum discharge repetition rate which occurs when the surface conductivity $\sigma_{so} = o$ depends on the permittivity and volume conductivity of the dielectric, the ratio $\frac{E^1}{E_i}$ and the shape of the cavity. Thus for a laminar cavity the maximum discharge repetition frequency, f_1 is given by $f_1 \approx 1.13 \times 10^{11} \sigma_2 \frac{E^1}{E_i}$.

5.4.2 Salvage.

Salvage[40] analysing the stresses in cavities assumed that the gaseous cavity had zero conductivity and that the electric stress in direct voltage conditions is equal to that obtained in alternating voltage conditions when the permittivity of the solid tends to infinity. Thus for a cavity located in an infinite dielectric which is subjected to an electric stress E that is uniform at very large distances from the cavity, E^1 - the electric stress in the cavity for an elliptical cylindrical cavity under direct voltage conditions is given.

The stresses in a circular cylindrical cavity and an oblate spheroidal cavity are also given. For the case of two infinite plane parallel electrodes whose distance apart 't' is not great compared with the dimensions of the cavity, the electric stress for a laminar cavity is obtained as $E^1_1 = \frac{tE}{2n}$. (where 2n is the thickness of the cavity). In conclusion he points out that the volume and surface conductivities of the cavities which have been neglected in the above analysis may be appreciable and significantly alter the electric stresses in the cavity. (see chapter 9 appendix 6 and 7).

CHAPTER 6

Current and Discharge Measurement Techniques.

It is convenient to start the review of dielectric current measurement with dielectric relaxation measurement techniques since every steady state condition for dielectrics under direct voltage conditions is preceeded by some form of relaxation[41-44].

6.1 Relaxation current measurement.

(i) The first experimental approach to dielectric relaxation was the work on 'defect dipoles', alternating voltages in the commonly studied audio frequency range were used in conjunction with a.c. bridges. The average detection limit was about 10^{-5} molar fractions of dipoles.

For long relaxation times however (of the order of one second or more) direct voltage methods are usually employed[43,45,46]. The techniques rely on the fact that when a static electric field is suddenly applied or removed the time-dependent charging or discharging current display the relaxation of reorientating dipoles. With sensitive vacuum tube electrometers, the effect could be measured and recorded. These currents may be conveniently observed at temperatures (-80 to 25°C) and at low stresses where the normal steady state conduction is negligible.

Plots of log I versus time are made and the linear regions with different slopes taken to correspond to various relaxation mechanisms. Their activation enthalpy H_d is taken from measurements at different temperatures and the concentration of dipole evaluated from the initial current.

(ii) A recent d.c. method[46,47] makes use of the depolarization current released by slowly warming up a crystal from a temperature T_o where I (relaxation time) is of the order of several hours. Previously the dipoles were assumed to be polarized to saturation at a high temperature T_p by a field E_p acting for an interval of time $t_p >> \tau_p$, followed by

cooling down to T_o and turning off E_p. A linear rate of warming up (dT/dt = const) makes the evaluation of the ionic thermo currents (ITC) versus T plots very lucid. From them T_o and H_d can be obtained in two different ways and the area delimited by the ITC band being proportional to E_p/T_p gives the initial number of dipoles. Overlapping ITC bands corresponding to several relaxation mechanisms can be distinguished by repeating the cycle with a modified temperature programme and possible pseudo-relaxation ITC bands originating from space charges or electrode effects can be easily identified. In the various experiments ITC's down to 10^{-16} amperes have been measured as a difference of potential across a resistor with a vibrating grid electrometer (vibron). The response time does not reach 10 seconds and the rate of warming up is about $0.1\,^{o}Ks^{-1}$. The detection limit of the method approaches 10^{-7} molar fraction of dipoles.

6.2.1 Steady state conductivity (Low resistivity dielectrics)

Resistivities of up to 10^{8} Ω-cm are sometimes measured using conventional a.c. bridge methods. Difficulties arise however due to polarization effects located at the crystal-electrode interface. They are normally overcome by using unpolarizable electrodes consisting of a cation metal if possible (especially when operating in the high stress, high temperature region). Silver and copper halides are sometimes employed. A possible solution is to apply alternating or pulsed currents thus recording the initial current before the build up of interfacial space charge. The frequency or reciprocal pulse time should not be too high in order to avoid contributions by reorientating defect dipoles and by other possible relaxation mechanisms e.g. by dislocation. In KCl it is claimed that up to 250°C polarization effects of this kind play an important role but it is thought that the Joffe type space-charge polarization is still present too. Both types of polarization appear to have been emphasized alternatively in the past.

A possible third kind of polarization is claimed to operate from a high resistive surface layer.

It is obvious that the above method of measurement is suitable for dielectrics with little or no polarizability and low resistivities. For dielectrics with very high resistivities different methods are employed.

6.2.2 Steady state conductivity (high resistivity dielectrics).

Direct voltage methods which are more suitable for high resistivity dielectrics (e.g. polythene) are widely used (especially in the low temperature medium to low stress region).

The method employed is essentially a voltage divider method. This enables a reasonable d.c. load (10^{-6} to 10^{-14} amps) on the dielectric obtained as a result of d.c. stressing to be measured directly by measuring the potential drop across standard resistors connected in series with the sample by means of high sensitivity electrometers especially of the vibrating reed or capacitor type (vibron). The limit of the response is set by the input impedance of the valves which appears to be of the order of 10^{16} Ω.

The steady state value of current after the initial decay is the relevant value. Temperature, visible light and ultraviolet light etc., are also known to affect the steady state conditions.

One method which involves both a.c. and d.c. measurement is the one which makes use of the fact that upon applying a sinusoidal voltage together with its first harmonic any non-ohmic term gives rise to a direct current. This is of course only applicable when one is operating in the non-ohmic region.

6.3 Discharge detection and measurement.

6.3.1 Non electrical methods.

Different methods have been used in the detection of discharges in

dielectrics[48]. Those dependent on the human senses of hearing (hissing) and seeing (corona glow) have been tried. Chemical deterioration of the dielectric and changes in temperature and pressure have been presented as a means of discharge detection. These methods give little or no indication of the magnitude and number of discharges and their sensitivity is very poor.

6.3.2 Electrical principles and methods.

Some attempt has been made to improve the above methods of the senses by employing electrical equipment[49-51] but most modern methods have been developed along different lines.

Most of the work in this field has been carried out with alternating voltages and even where direct voltages have been used, they have been mostly connected with simple tests to predict alternating voltage performance[52-54], a practice which has received considerable criticism[55-57].

Thus the following review of discharge detection and measurement is made for both alternating and d.c. testing techniques since it is from the a.c. techniques that most of the direct voltage work has emerged.

The main electrical methods employed in the detection and measurement of discharges are

(a) Bridge methods

(b) Photomultiplier method

(c) Methods involving the measurement of voltage or current pulses produced by discharges - High frequency discharge detector.

The principles involved in (a) and (c) have been aimed at either detecting the changes or phenomena caused by the appearance at the terminals of the specimen of a sudden change of voltage of the form of a unit function following a Townsend discharge (discussed earlier see chapter 5).

6.3.2.1 Bridge methods.

The bridge methods[58,59] may be subdivided into two

(i) The power factor method[60].

This involves measuring the contribution by discharges to both the in and out-of-phase components of voltage at the fundamental frequency. Thus assuming that the power factor of a discharge free specimen is constant at increasing voltage the smallest detectable increase of power factor may be judged as the onset of discharges.

(ii) Lissajous figure or oscillographic bridge method.

The set up of the equipment is such that the test specimen and a discharge free capacitor form the high voltage branches of a Schering bridge. The signal from the detector branch is fed to the horizontal plates of an oscilloscope whose vertical plates are supplied with a voltage 90^{o} out of phase with the bridge supply voltage. An ellipse is then obtained with its major axis vertical and the discharge voltage superimposed on this.

6.3.2.2 Photomultiplier methods.

In the photomultiplier method, the light accompanying the discharge actuates a photomultiplier. This method can also be used for both a.c. and d.c. discharge detection with only minor alterations though it has the major disadvantage that it can only be used with translucent dielectrics e.g. polythene. Nevertheless several workers[61,62] adopted the method.

6.3.2.3 The high frequency discharge detector method.

The circuits usually employed are derived from Fig. 5 where C_x is the test object capacitance and C_b the high voltage coupling capacitance. L_d, R_d and C_d are the elements across which the high frequency voltage is produced. C_d is the effective detector capacitance. This basic

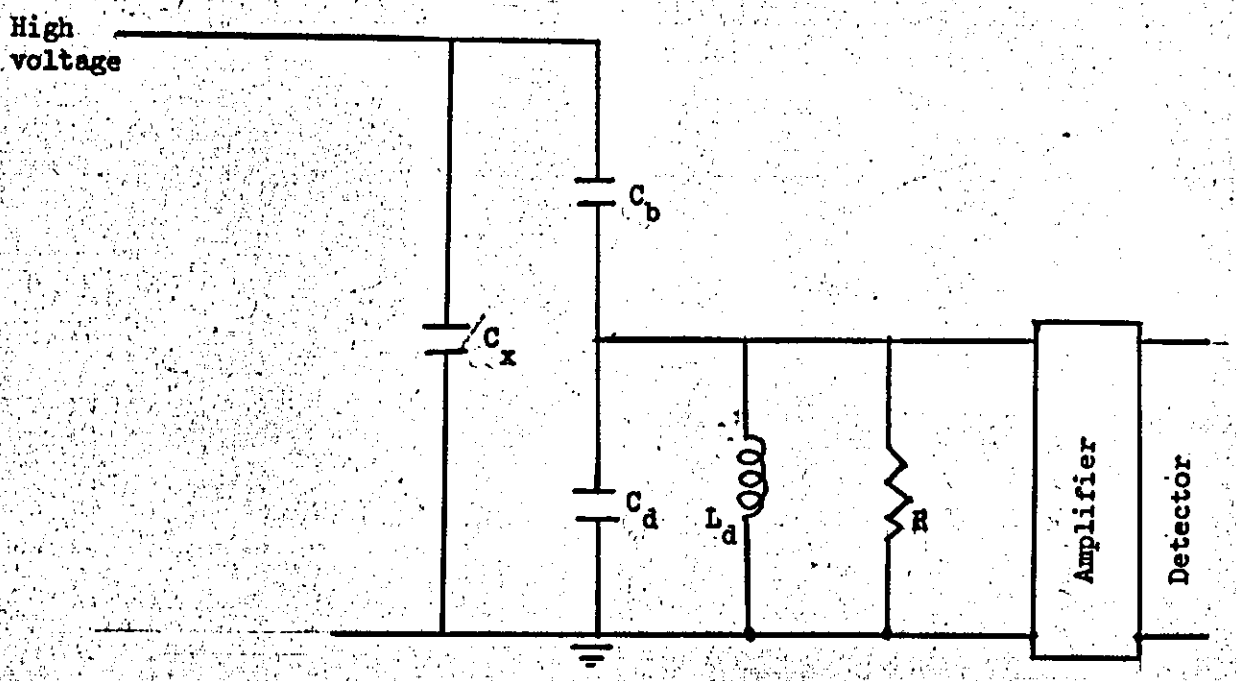

(i)

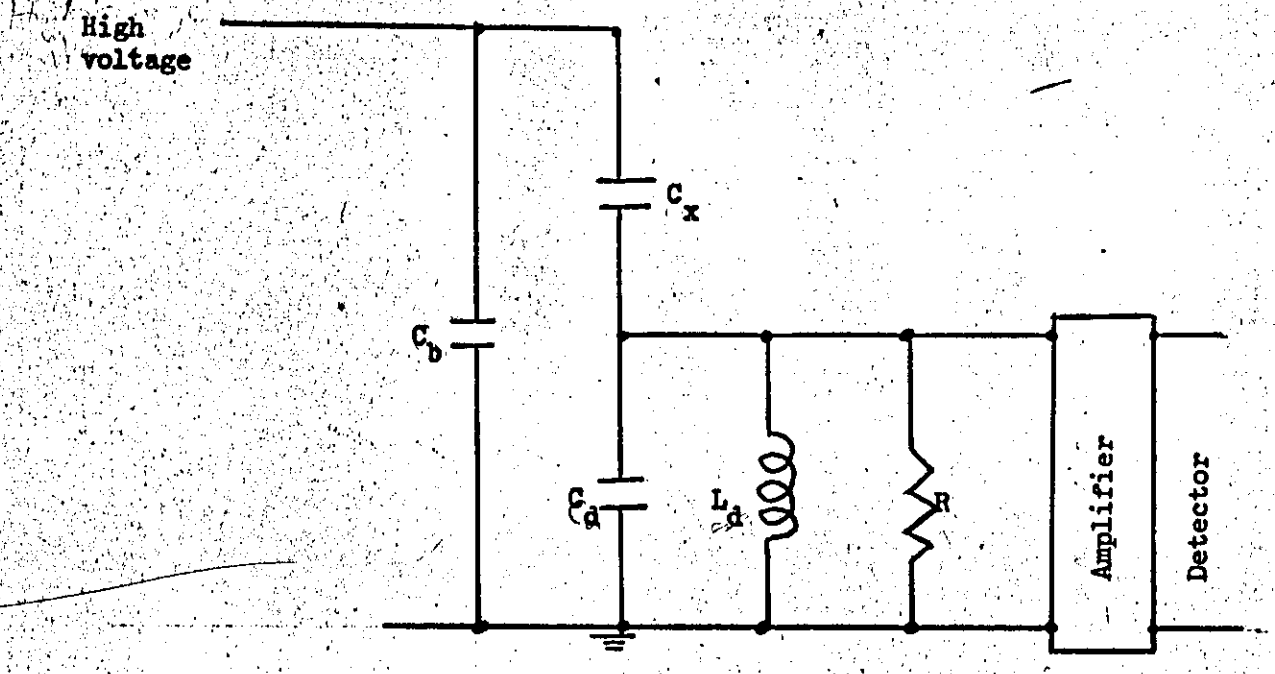

(ii)

Fig. 5
High frequency discharge detector circuits

circuit can be formed into a bridge in which case it is a bridge method (high frequency type) or can be used singly.

This method can be and has been used for both A.C. and D.C. discharge detection by appropriate modification of the detector impedance. The signal across the detector impedance is usually amplified and detected by one or more of the following oscilloscopes, peak, r.m.s. or average reading meters pulse and signal counting devices such as the conventional scalers or in the d.c. case a more appropriate detector may be a tape recorder or an ultraviolet recorder.

6.3.4 Discharge detector response.

In order to show that the high frequency discharge detector circuit measures the magnitude of the discharge, consider a brief mathematical analysis of the circuit (which is the same for both a.c. and d.c. discharges once they he·e occurred since the discharge itself is a high frequency phenomenon).

Assuming that a discharge of initial magnitude Q occurs in the test object C_x, then if the output impedance of the high voltage source and associated filtering or limiting circuits is assumed as infinite.

Let q(t) be the charge on and i(t) be the current from C_x at time t.

Therefore $\frac{dq(t)}{dt} + i(t) = o$ (see fig. 5 (ii))

Thus in Laplace transforms

$$p\bar{q} = -\bar{i} + Q \quad \ldots \quad \ldots \quad \ldots \quad \ldots \quad \ldots \quad \ldots \quad \ldots \quad \ldots \quad \ldots \quad 6.1$$

$$\text{also } \frac{\bar{q}}{C_x} = \bar{i}\left\{ \frac{1}{pC_b} + \frac{pRL}{p^2RLC_d + pL + R} \right\} \quad \ldots \quad \ldots \quad \ldots \quad \ldots \quad \ldots \quad 6.2$$

where p is the Laplace operator but definable in transformations as $p = j$ multiplied by angular frequency. and $\bar{q}$ and $\bar{i}$ are the Laplace transformations of q(t) and i(t) respectively.

From equations 6.1 and 6.2

$$\frac{-\bar{i}+Q}{pC_x} = \bar{i}\left\{\frac{1}{pC_b} + \frac{pRL}{p^2RLC_d + pL+R}\right\} \quad \ldots\ \ldots\ \ldots\ \ldots\ \ldots\ \ldots \quad 6.3$$

Rearranging equation 6.3.

$$\frac{Q}{pC_x} = \bar{i}\left\{\frac{C_x(p^2RLC_d + pL + R) + p^2RLC_xC_b + C_b(p^2RLC_d + pL + R)}{pC_xC_b(p^2RLC_d + pL + R)}\right\}$$

$$= \bar{i}\left\{\frac{p^2\left[RL(C_xC_d + C_xC_b + C_dC_b)\right] + pL(C_b + C_x) + R(C_b + C_x)}{pC_xC_b(p^2RLC_d + pL + R)}\right\}$$

$$\bar{i} = \frac{QC_b(p^2RLC_d + pL + R)}{\{C_xC_d + C_xC_b + C_dC_b\}\ \{p^2RL + \frac{pL}{m} + \frac{R}{m}\}}$$

where $m = C_d + \frac{C_bC_x}{C_b+C_x}$

But $\bar{V} = \frac{\bar{i}pRL}{p^2RLC_d + pL + R}$

Therefore $\bar{V} = \frac{pQRLC_b}{RL(C_xC_d + C_xC_b + C_dC_b)(p^2 + \frac{p}{mR} + \frac{1}{mL})}$

$$= \left\{\frac{QC_b}{\bar{C}_b(C_x + C_d) + C_xC_d}\right\} \quad \frac{(p + \frac{1}{2mR}) - \frac{1}{2mR}}{(p + \frac{1}{2mR})^2 + \beta^2}$$

where $\beta^2 = \frac{1}{Lm} - \frac{1}{4m^2R^2}$

Hence

$$V(t) = \frac{Q}{C_x(1 + C_d/C_b) + C_d}\left[\text{Cos}\beta t.\exp(-t/2mR) - \frac{\sin\beta t.\exp(-t/2mR)}{2mR\beta}\right]$$

Therefore $V(t) = \frac{Q.\exp(-t/2mR)}{C_x(1+C_d/C_b)+C_d}\left[\text{Cos}\beta t - \text{Sin}\beta t/2mR\beta\right]$

In practical cases the values of C_x, C_b, C_d, and R are such that the coefficient of Sinβt is much less than the coefficient of Cosβt.

Hence $V(t) \doteq \frac{Q.\exp(-t/2mR)}{C_x(1+C_d/C_b)+C_d} \quad \cos\beta t.$

$$\doteq \frac{Q.\exp(-t/2mR)}{C_E} \quad \cos\beta t \quad \ldots \quad \ldots \quad \ldots \quad \ldots \quad \ldots \quad \ldots \quad 6.4$$

where C_E = equivalent capacitance

$= C_x(1+C_d/C_b) + C_d.$

For an inductive-capacitive detector impedance, that is, with R open circuited.

$$V(t) = \frac{Q}{C_E} \cos\beta^1 t \quad \ldots \quad \ldots \quad \ldots \quad \ldots \quad \ldots \quad \ldots \quad \ldots \quad \ldots \quad 6.5$$

where $(\beta^1)^2 = 1/Lm.$

For a resistive-capacitive detector impedance

$$V(t) = \frac{Q}{C_E} \exp(-t/Rm) \quad \ldots \quad \ldots \quad \ldots \quad \ldots \quad \ldots \quad \ldots \quad \ldots \quad \ldots \quad 6.6$$

Equations 6.4, 6.5 and 6.6 mean that the peak value of the voltage developed across the detector impedance for the three possible cases is always equal to Q/C_E.

Hence the voltage developed across the detector is directly proportional to the magnitude of the discharge occurring in the test object.

6.3.5 Calibration of the detector.

The calibration of this type of detector is usually obtained by injecting a pulse of known magnitudes V_q in series with a known magnitude C_q at the appropriate terminals e.g. Fig. 6a. The discharge magnitude will in the following analysis be shown to be given by the product V_qC_q modified by a function $F(C_b,C_x)$ and independent of the detector impedance.

In the circuit of Fig. 6b let the capacitance of the cable and the

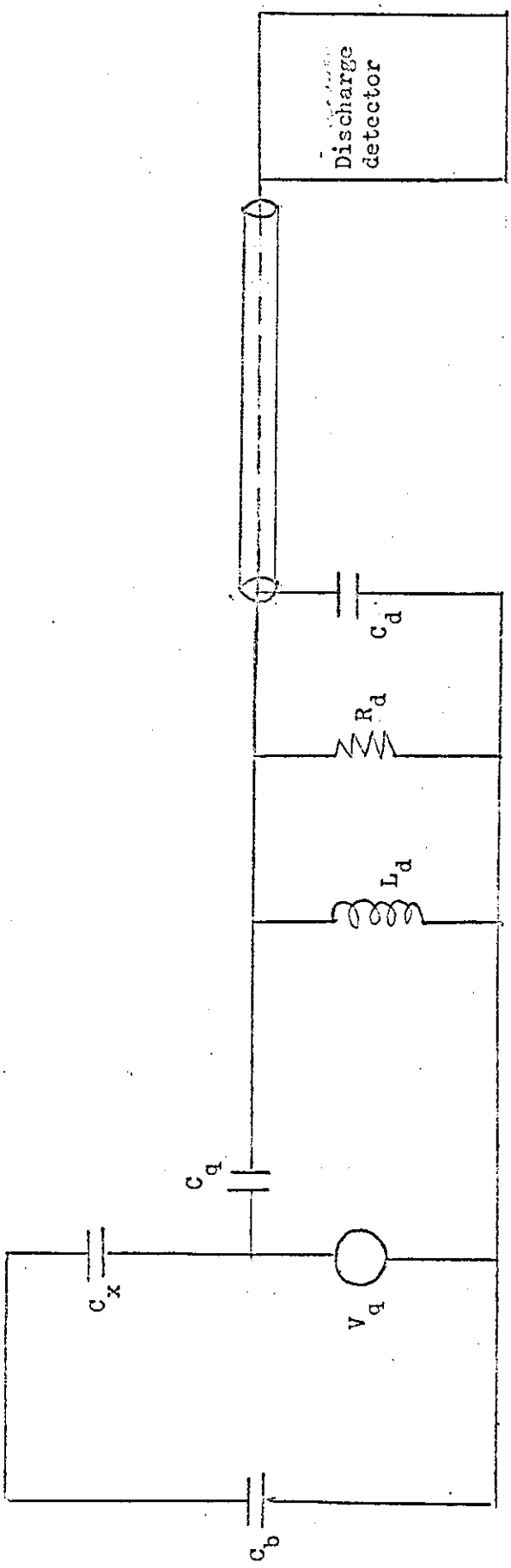

Fig. 6a
Circuit for Calibration of the discharge detector

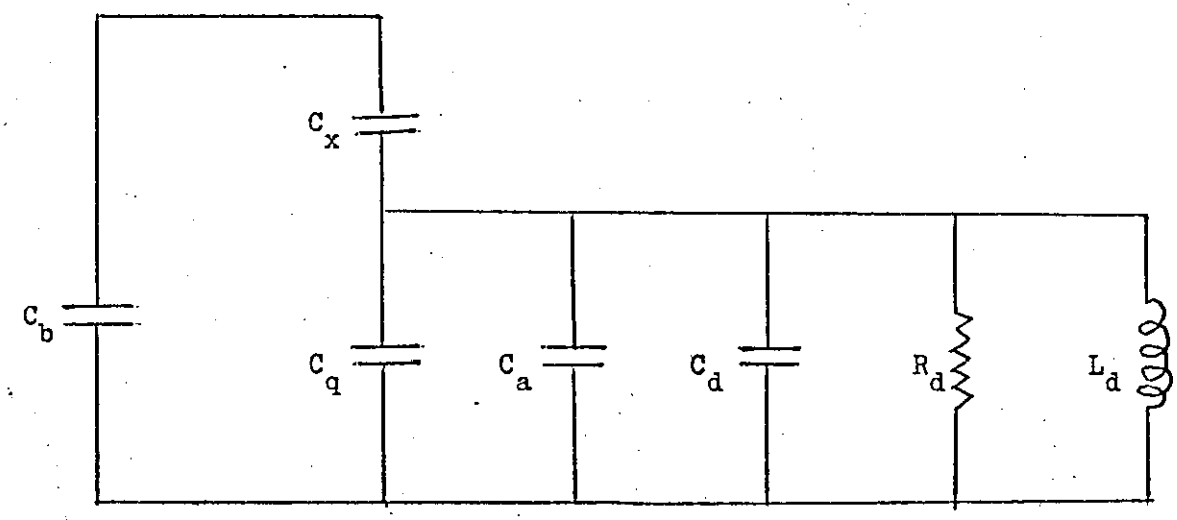

Fig. 6b
Equivalent circuit for the calibration of the discharge detector

self capacitance of the system to ground be C_a. Assume that the generator is of zero impedance. Now let, C_a, C_d, L_d, R_d be replaced by an impedance Z. (Fig. 6c).

If a voltage V_x appears in series with C_x the voltage across C_d

$$= \frac{V_x \, 1/(C_q+Z)}{1/(C_q+Z) + 1/C_b + 1/C_x}$$

If a voltage V_q is supplied by the calibrating pulse generator G, the voltage across

$$C_d = V_q \quad \frac{C_q}{C_q + Z + C_b C_x/(C_b+C_x)}$$

If these two voltage are equal

$$\frac{V_x}{1 + (C_q+Z)(C_b+C_x)/C_b C_x} = \frac{V_q C_q}{(C_q+Z + C_b C_x/(C_b+C_x)}$$

$$\therefore \quad V_x C_x = V_q C_q \left[C_x + \frac{(C_q + Z)(C_b + C_x)}{C_b} \right] \Bigg/ \frac{(C_b+C_x)(C_q+C_z) + C_b C_x}{C_b+C_x}$$

$$= V_q C_q \quad \left(\frac{C_b+C_x}{C_b}\right)$$

$$= V_q C_q \quad \left(1 + \frac{C_x}{C_b}\right)$$

The above expression is independent of Z hence the detector may be calibrated by injecting pulses of known magnitude from a reliable stable pulse generator. In fact in a commercial discharge detector[63] (ERA Model 3) this is an incorporated feature.

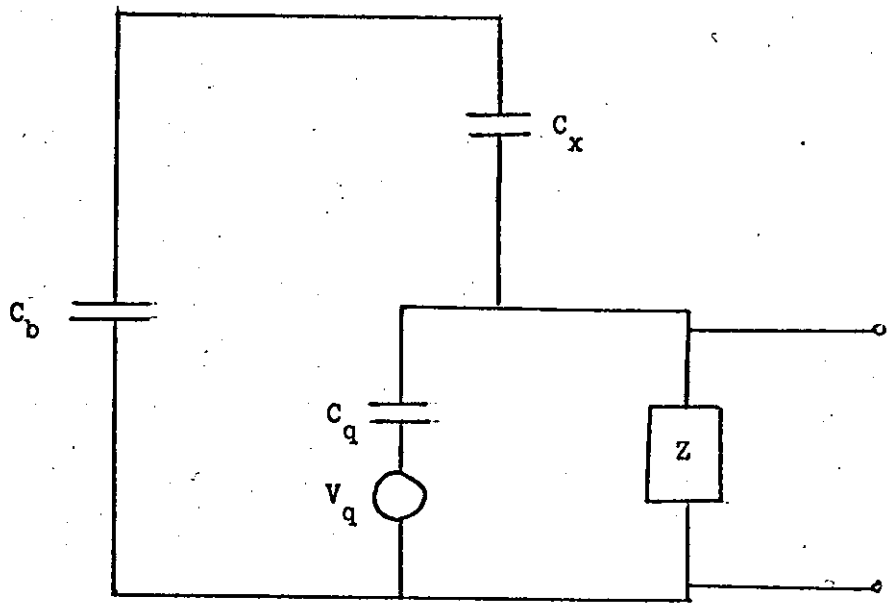

Fig. 6c
Reduced equivalent circuit for the calibration of the discharge detector

CHAPTER 7

Experimental Investigation of Conductivity and Discharge Phenomena

The set up for this investigation was a combination of one of the current measuring techniques with the high frequency discharge detection method. The current measuring part was the voltage divider method where the voltage across a standard resistor in series with the test object was measured by a vibrating capacitor method in this case an EIL vibron[64] electrometer commercially available (Model 33C, capable of measuring currents down to 10^{-14} amperes). The two circuits were connected by means of a by-pass capacitor. The choice of this capacitor was crucial because its dielectric resistance had to be higher than that of the vibron input resistor and had to be lower than the dielectric resistance of the test object in order for it not to affect the results.

7.1 Equipments

The complete set up of any particular test was as shown in the diagram (Fig. 7, plate 1) where the signal from the detector impedance was fed to the detector amplifier (forming part of a ERA discharge detector model 3)[65] part of the output from the amplifier to the discharge detector oscilloscope screen was fed to a high speed peak voltmeter, the circuit diagram of which is shown in Fig. 8a. The peak voltmeter was provided with fast diodes (1GP7) with very high cut off frequencies and the signal was then passed on to an EKCO automatic scaler[66] (type N530G capable of counting above set levels) to be counted, or to a fast bridge diode rectifier circuit provided with the appropriate time constants by means of C and R (see Fig. 8b) then passed on to a twelve channel ultraviolet recorder[67]. The above processes could be carried out simultaneously, thus at any time it was possible to observe, count record or photograph the discharge pulses. The current from the vibron was also fed to one channel of the ultraviolet recorder

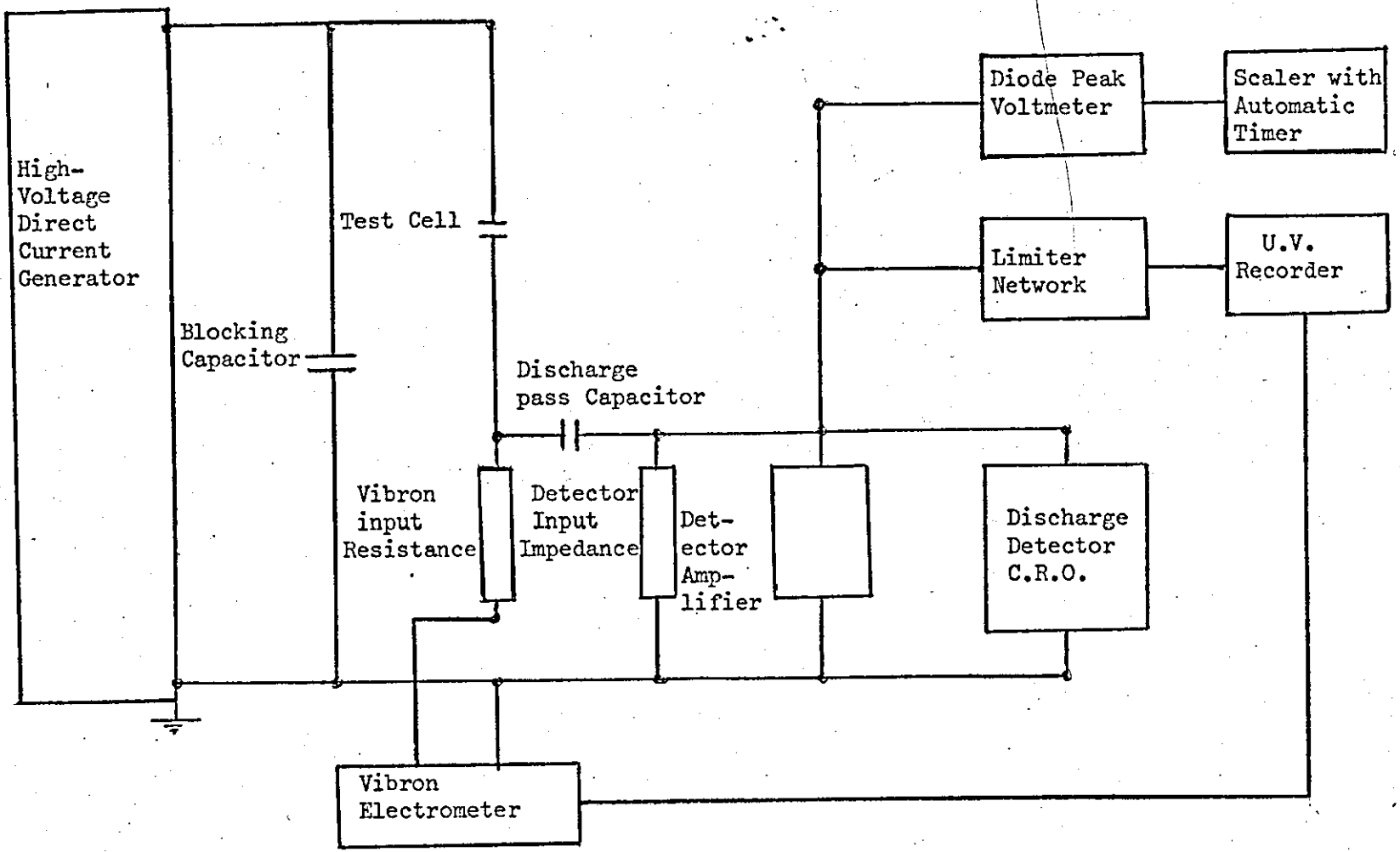

Schematic of discharge detection and current measuring circuit.

Fig. 7.

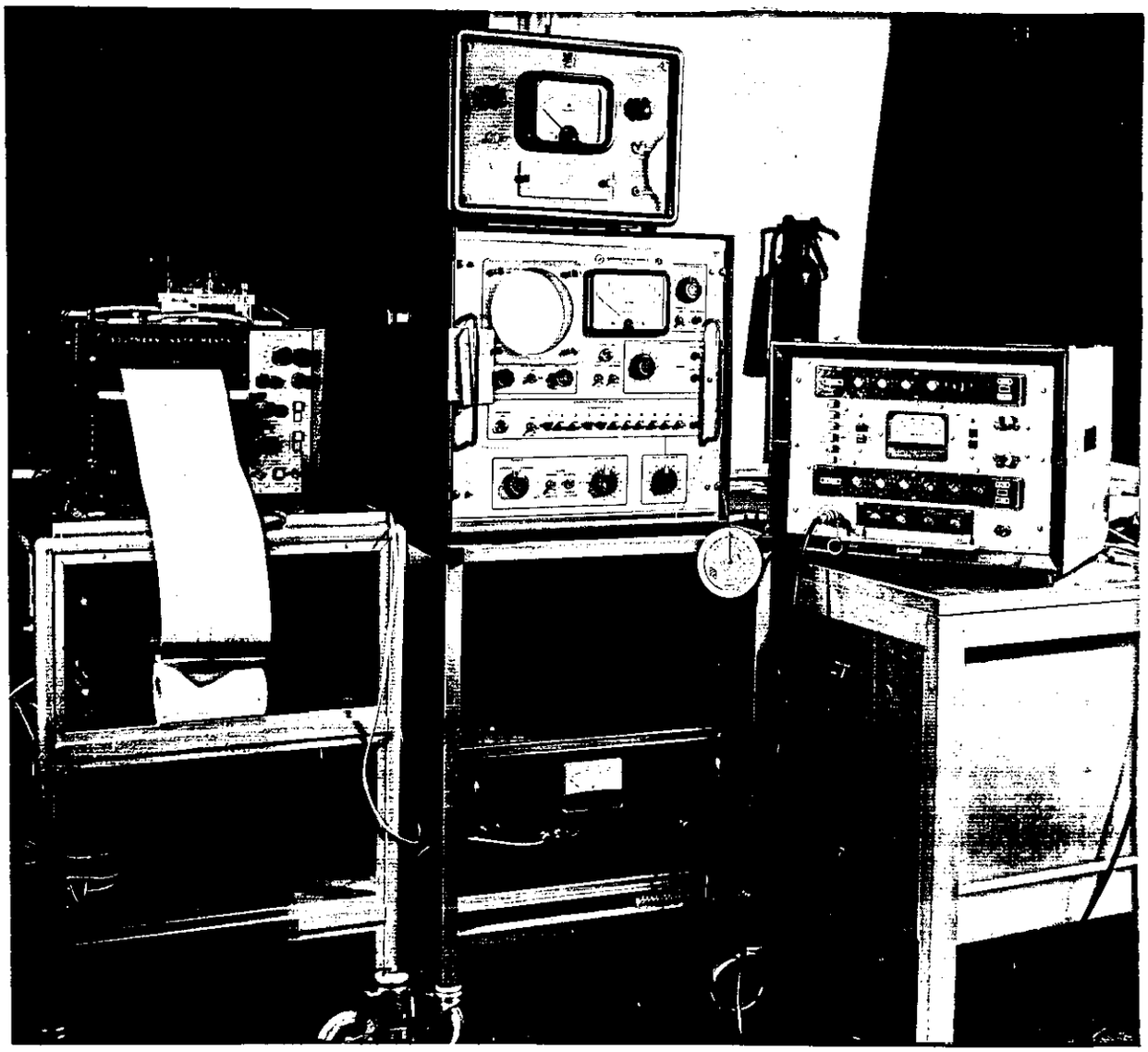

PLATE I.

Equipment for current and discharge measurement.
Left of picture - U.V. recorder.
Right of picture - Automatic Counter (scaler)

Middle of picture) top - part of vibron measuring equipment.
) centre - discharge detector.
) bottom - discharge peak voltmeter.

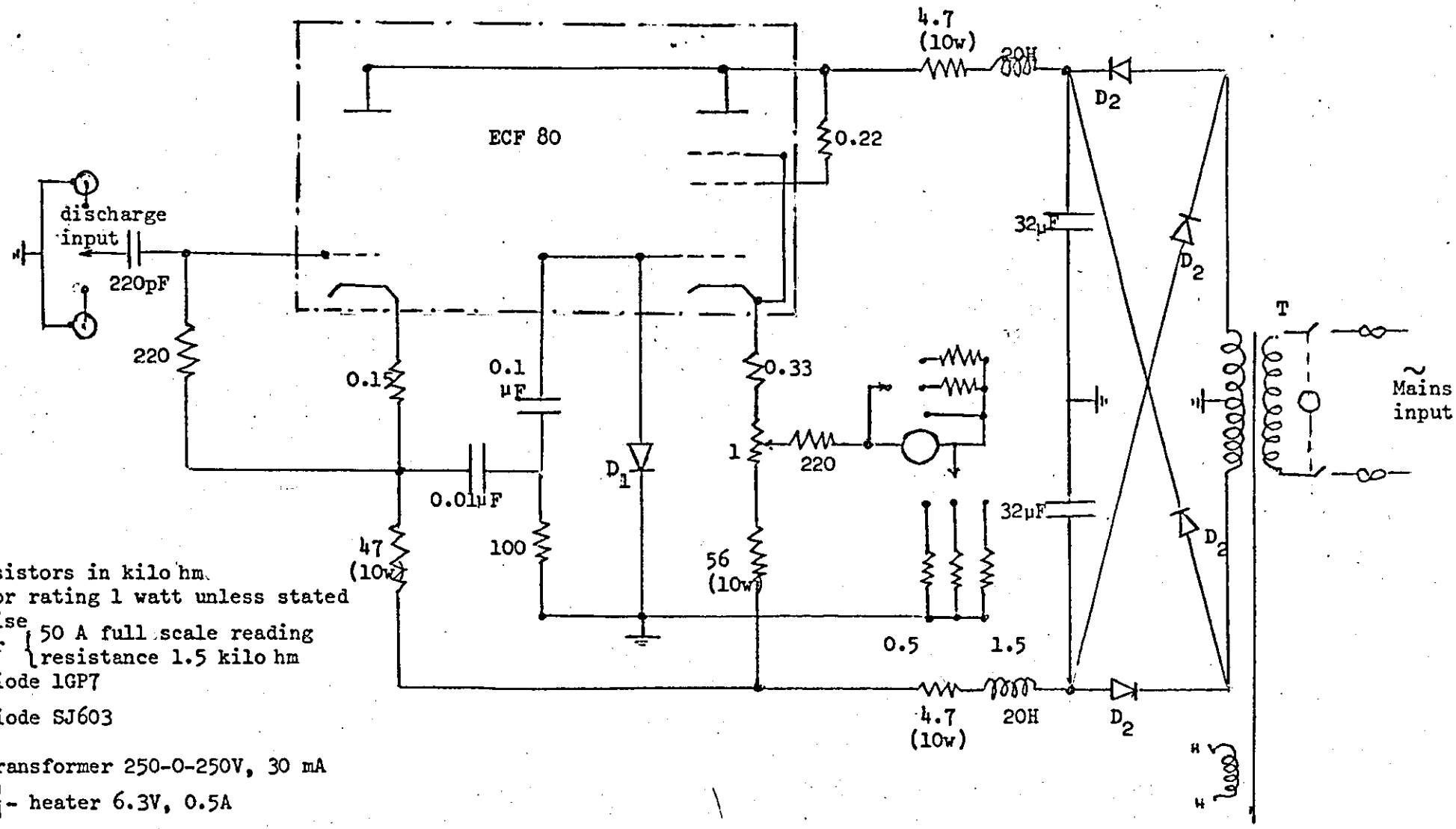

1. All resistors in kilo hm.
2. Resistor rating 1 watt unless stated otherwise
3. M-Meter { 50 A full scale reading / resistance 1.5 kilo hm
4. D_1 - Diode 1GP7
5. D_2 - Diode SJ603
6. T - Transformer 250-0-250V, 30 mA
   H, H - heater 6.3V, 0.5A

Fig. 8a
Circuit diagram of discharge peak voltmeter

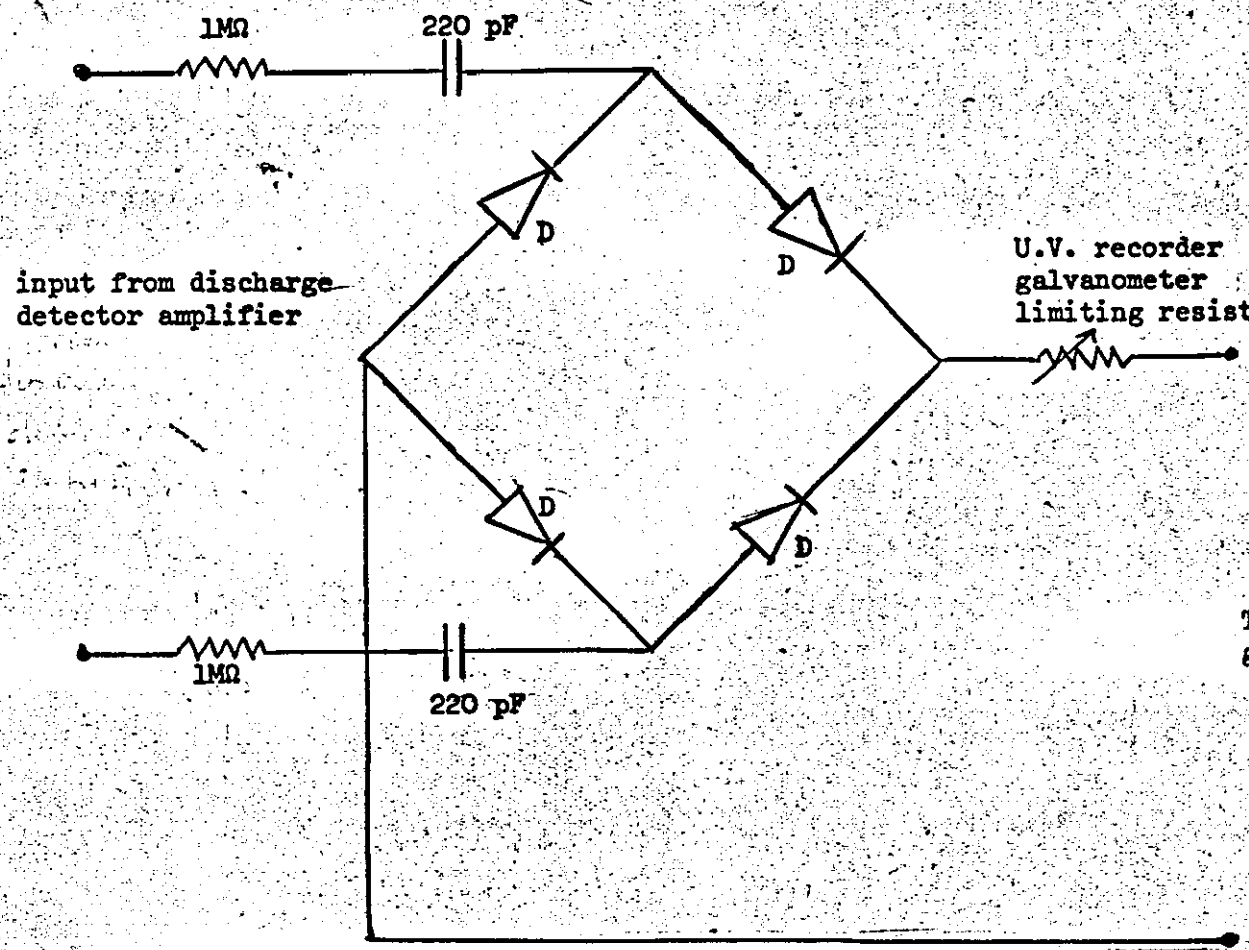

D - 1GP7

Fig. 8b

Bridge rectifying circuit for discharges

provided with suitable galvanometers. Thus the current through the test object and its discharge characteristics could be studied and recorded simultaneously.

7.1.1 High voltage direct current sources

Two high voltage, direct current sources were used for the conductivity and discharge experiments. One source was provided by a portable high voltage generator[68], type MR30/R capable of a discharge free output of up to 30 kV, of reversible polarity at 2 mA. It had a ripple of less than 0.1 per cent at full output and a stability of better than 0.5 per cent. It was provided with a trip mechanism to switch off the high voltage supply whenever the current exceeded the maximum value or as a result of breakdown etc. (plate 2).

The other h.v d.c. supply for higher voltage and larger current drains (as for example in the equivalent circuit experiments) was derived from a Cockcroft-Walton d.c. generator set designed by the author. (see plate 3). It was capable of an output of 130 kV d.c., of reversible polarity at 20 mA. Its transient d.c. discharge inception voltage was better than 100 kV d.c..

Voltage measurement was by means of a high voltage resistor (1000 megohm) and a 100 kilohm resistor forming a voltage divider (see fig. 9a) the output from the voltage divider being fed to a Marconi valve voltmeter. The voltage control was by means of an air cooled regulator (Gresham) and the rate of voltage application could be better than 10 kV dc per second. On bringing the regulator to its minimum setting, the decay of voltage across the test sample to zero could be observed by means of the valve voltmeter mentioned above. Fig. 9b.

7.1.2 High alternating voltage source

For comparative alternating voltage tests, the high voltage was derived from a small English Electric high voltage transformer rated at

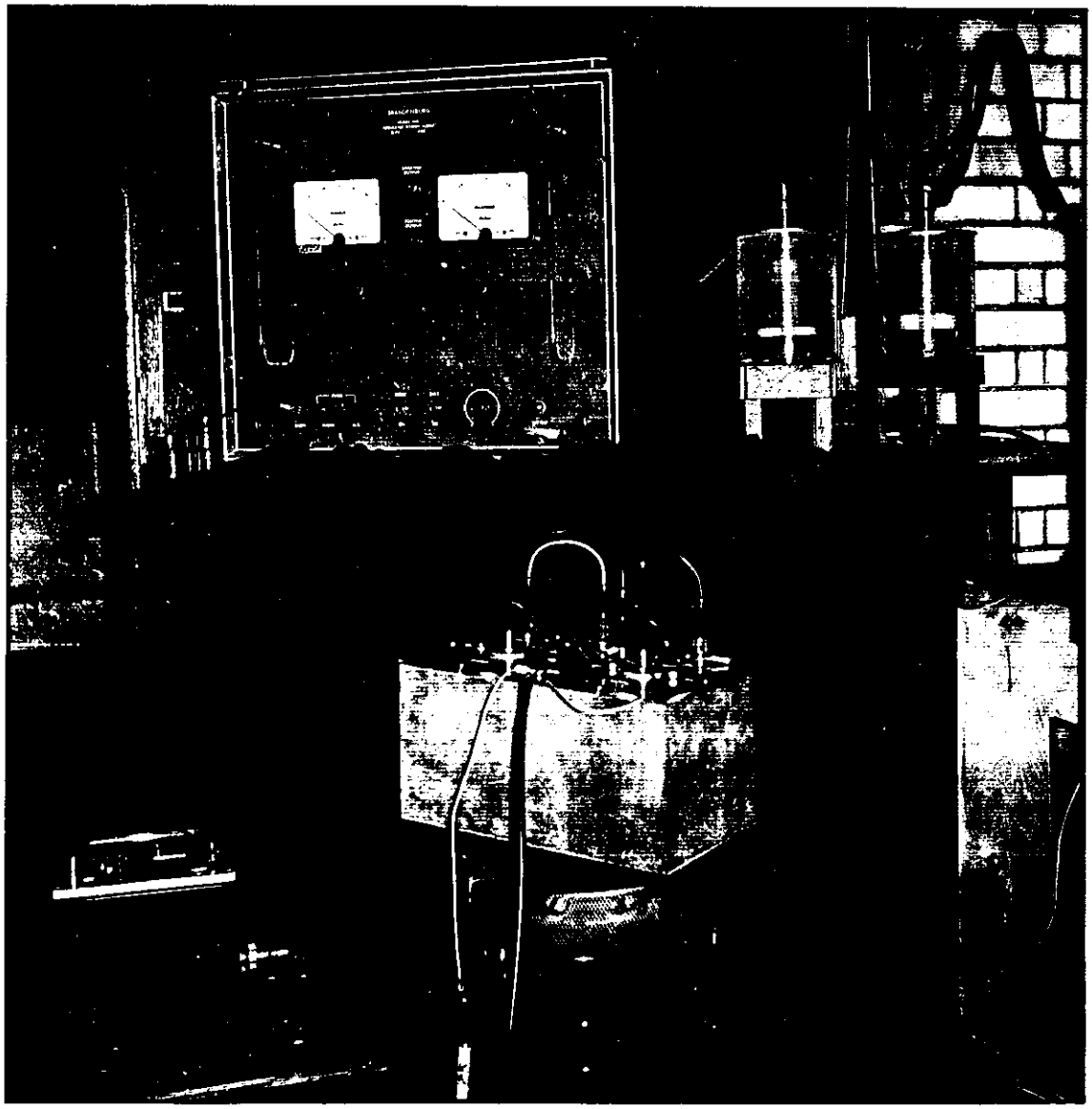

PLATE 2.
Equipment for stressing solid dielectrics.
Top left - Brandenburg generator.
Top right - transparent perspex coils.
centre - switching box.
bottom left - part of vibron measuring equipment.

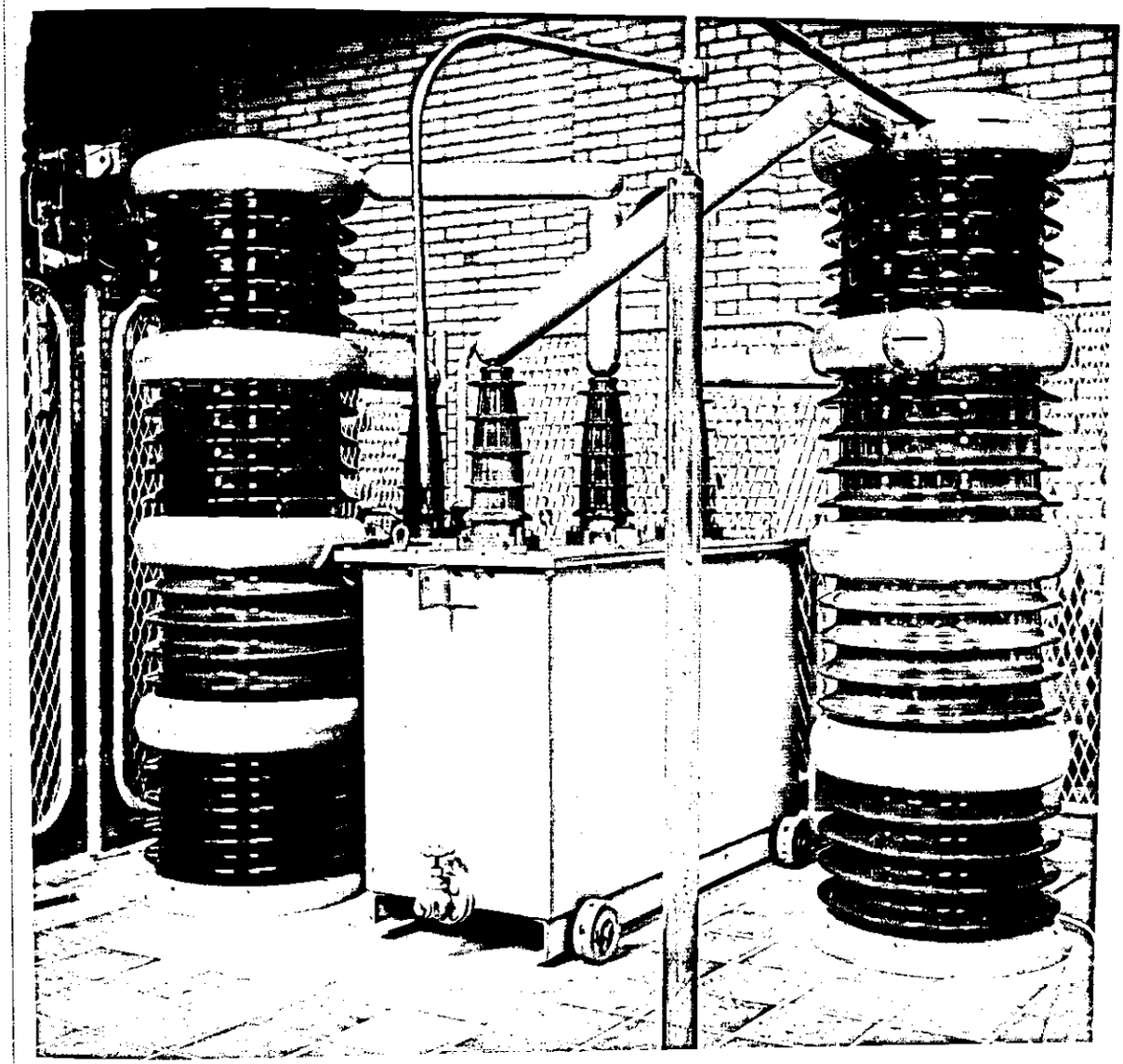

PLATE 3.
Cockcroft - Walton d.c. generator - a source for discharge tests.

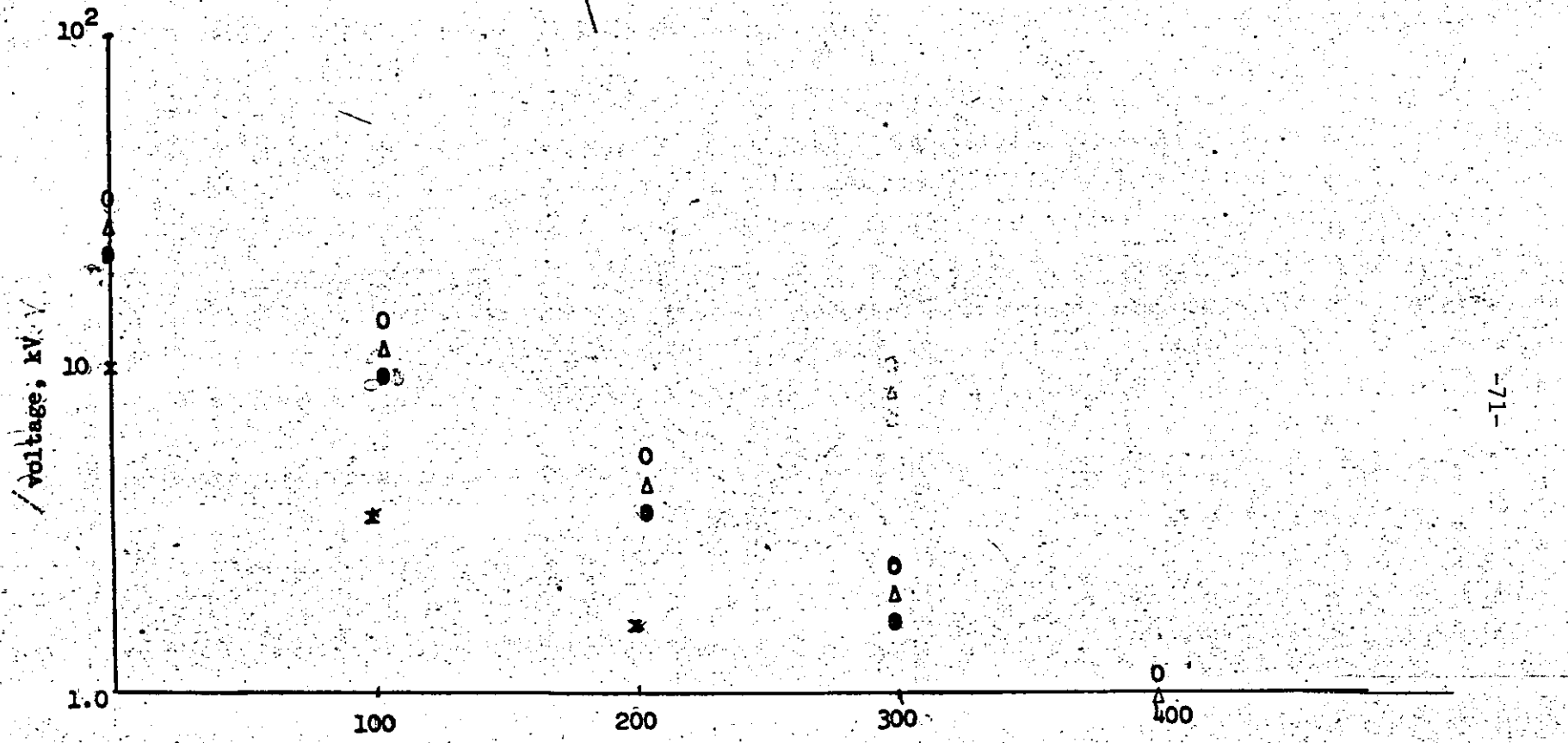

Fig. 9b

Voltage decay against time after input reduction to zero

o - 40 kV

Δ - 20 kV/voltage applied before input was reduced to zero

● - 245 kV

x - 10 kV

50 VA, with a maximum output of 20 kV. Voltage control was by means of a variac at the low voltage side of the transformer. Voltage measurement was by means of an ERA Robinson high voltage resistor divider and its associated meters.

7.1.3 Test cell and electrodes

The test cell was of cylindrical form, manufactured from thin walled perspex, 10" tall with a diameter of 6". It was sealed at the lower end to which was rigidly attached an electrode support fitted with a thread to which could be screwed electrodes of different materials and shapes. The top electrode was screwed on to a threaded brass rod to which was connected the high voltage supply. Pressure on the top electrode was provided by means of lead weights (see fig. 10, and plate 4).

Parallel plane electrodes were employed (plate 5A) the edges of some of the electrodes being machined to follow a Rogowski profile in order to reduce edge effects (plate 5B). The above system was used both with and without guarded electrodes in order to obtain comparative results. The guarded electrodes were manufactured by surrounding the central circular electrode with a shell of approximately twice the electrode diameter, filling the annular volume with resin and allowing the resin to set. (plate 6) The allowable radial resistance of the annular guard gap was fixed by the input resistance of the electrometer (see Fig 7) since the guard gap resistance effectively shunts the electrometer. The electrodes were kept clean by constant polishing and buffing when not in use.

7.1.4 Test samples

Three types of polythene were used in the test:

Type X - commercially available polythene sheet manufactured to B.S. 3012 (1958).

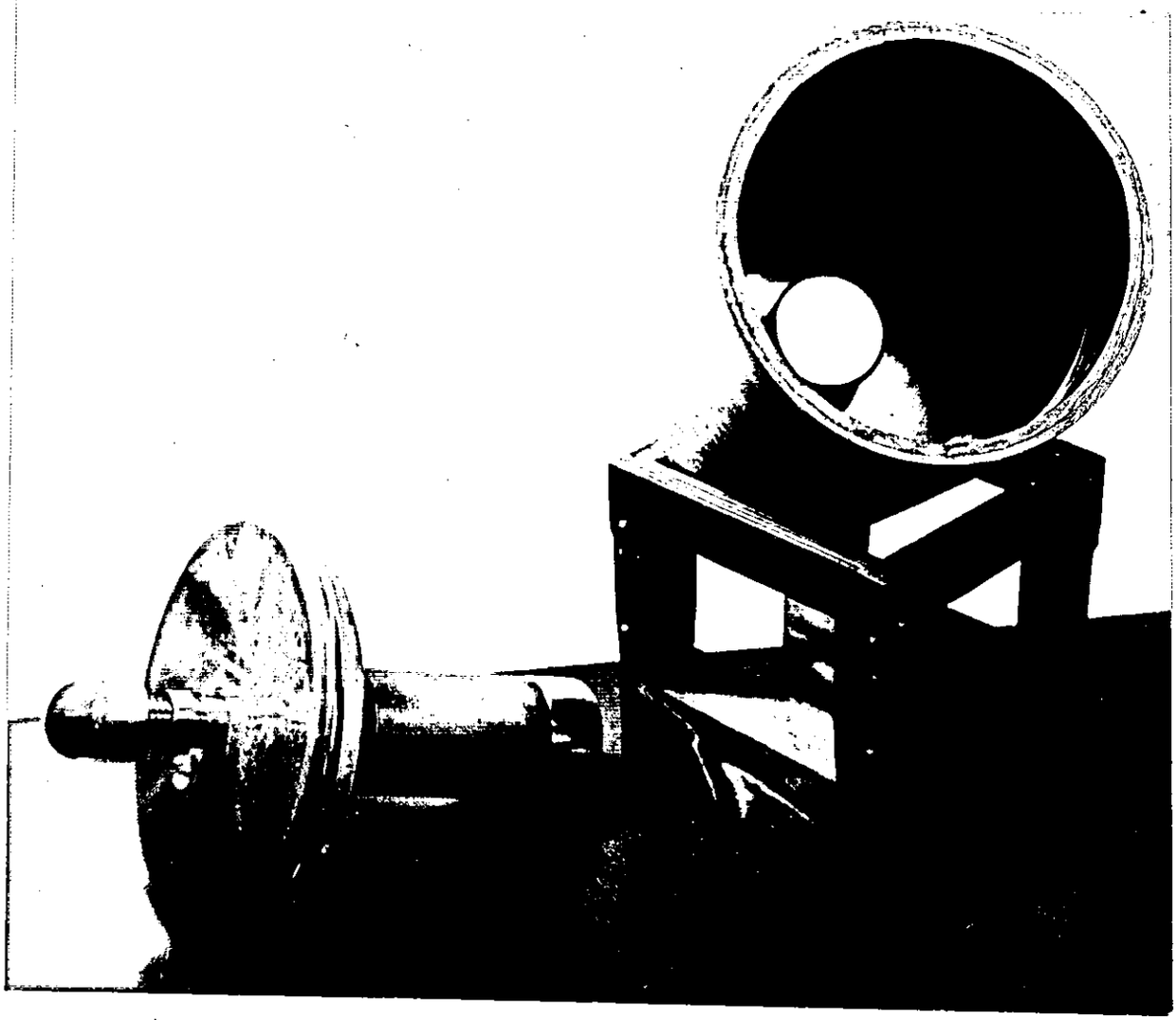

PLATE 4.
Test cell - proof to visible light, for solid dielectric samples, with small diameters.

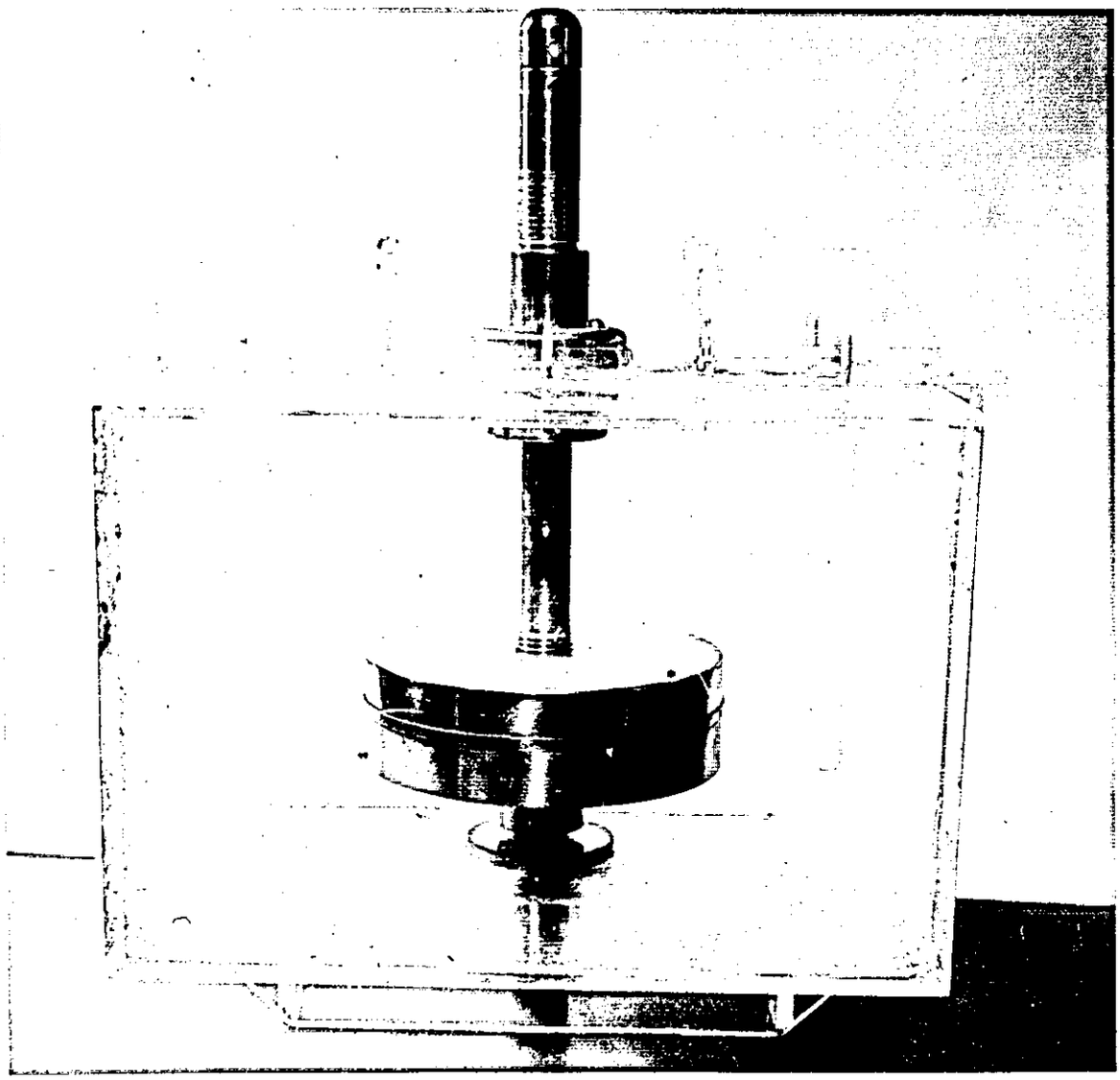

PLATE 5A.
Test Cell for solid dielectric samples with large diameters.

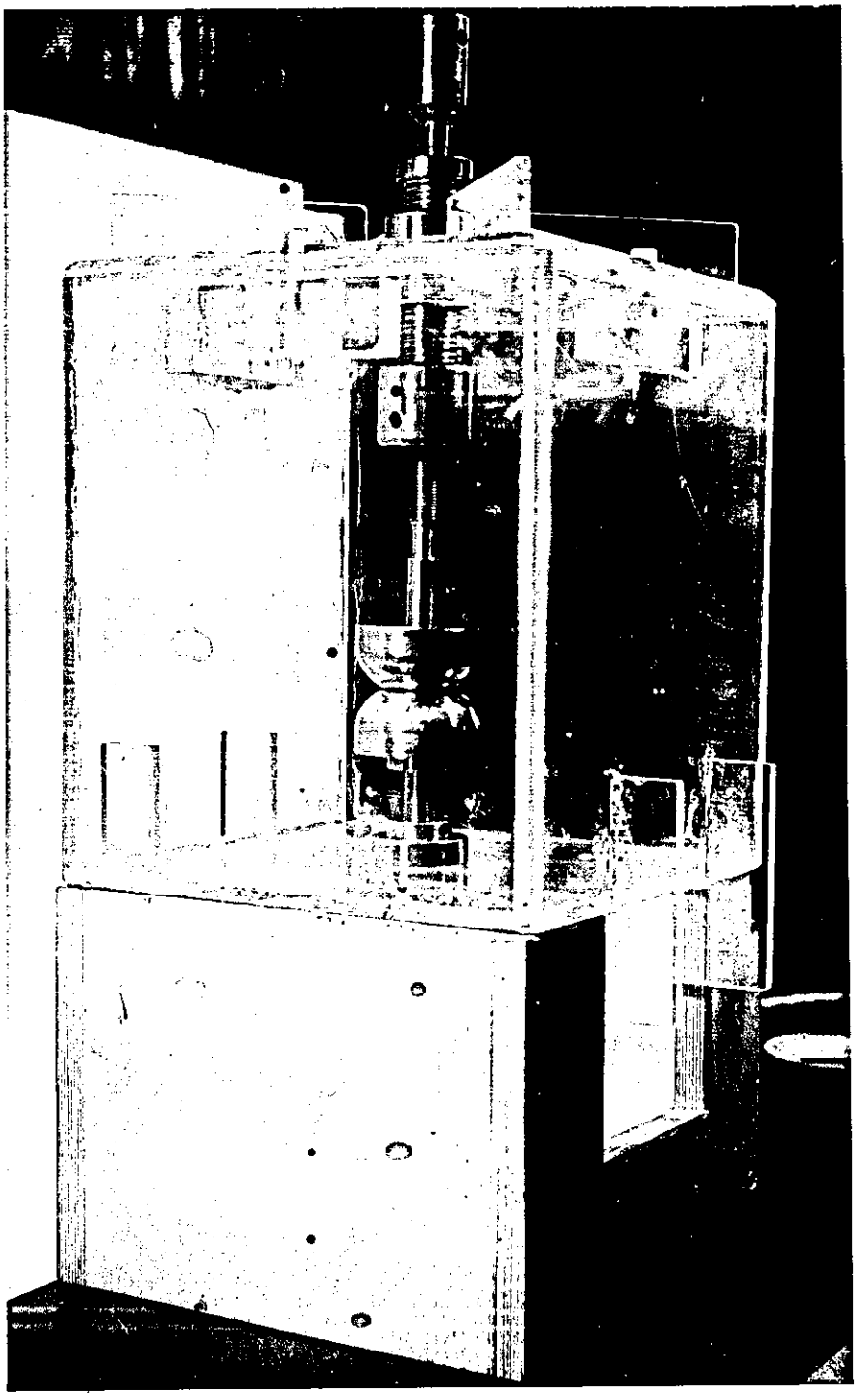

PLATE 5B.
Test Cell - for air gap tests, (also shows the Rogowski profile of the electrodes.

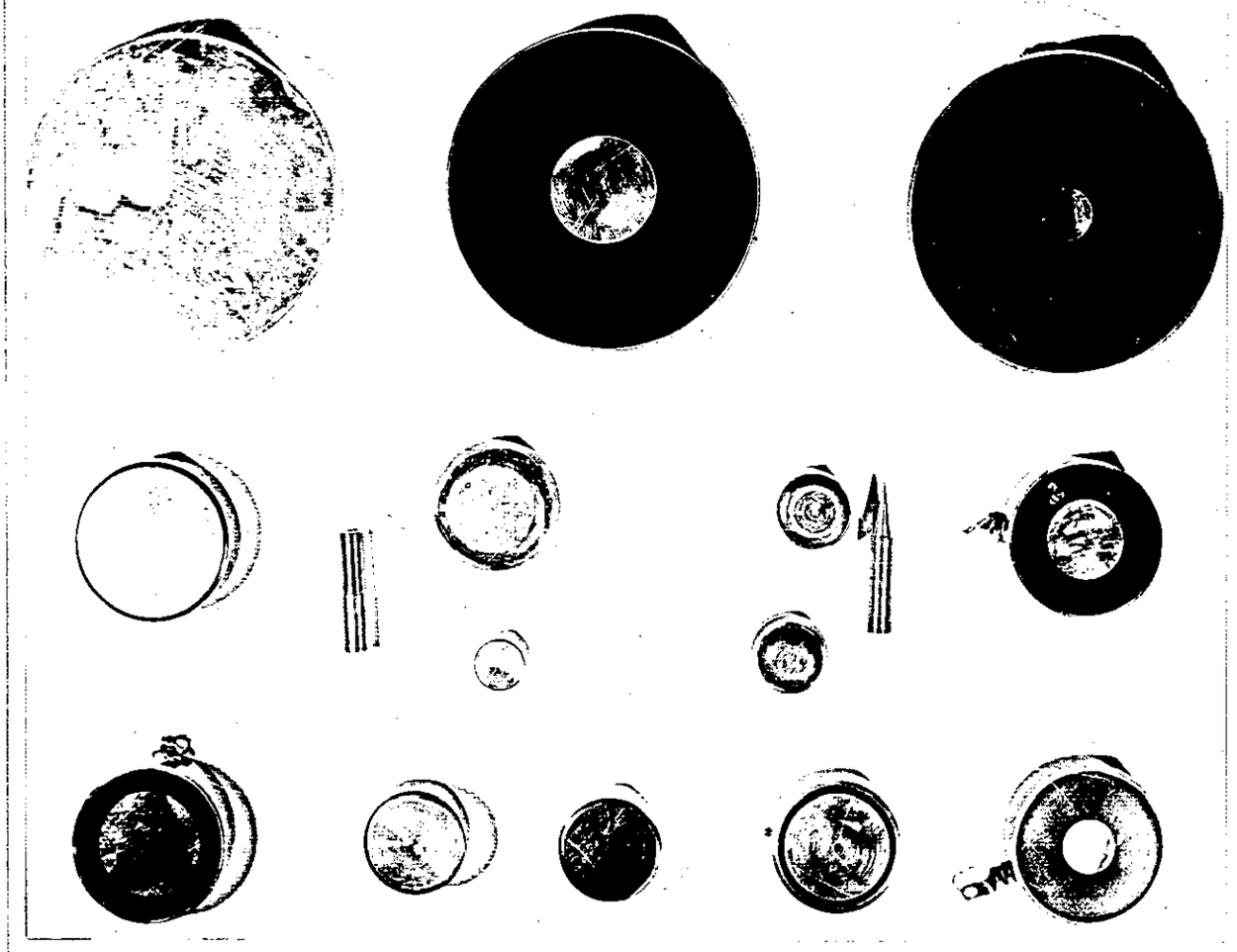

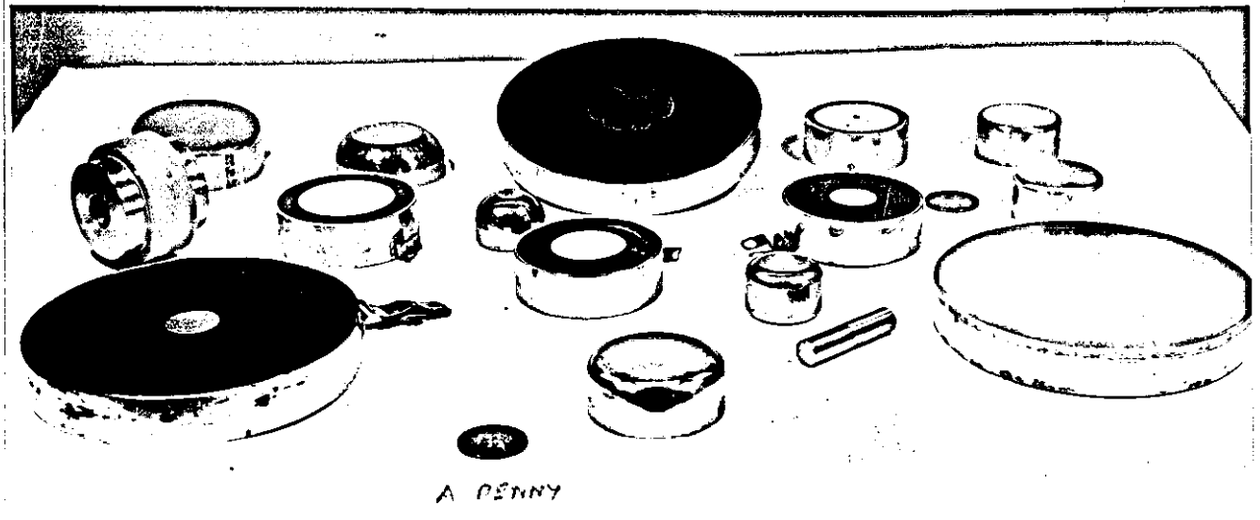

PLATE 6.
Various electrodes.

Type Y_1 - polythene (Alkathene), Q1388 - manufactured especially for the tests and containing no anti-oxidant.

Type Y_2 - as type Y_1 but with the addition of 0.07% Santonox R anti-oxidant.

Type Y_3 - as type Y_1 but with the addition of 0.14% of Santonox R anti-oxidant.

The samples were obtained in different thicknesses ranging from 0.02" to 0.06" for type X and from 0.001" to 0.03" for type Y. Some of the epoxy resin samples were cast between parallel plane electrodes, they were of thicknesses up to 0.02", different types were used both with and without fillers.

For the internal discharge and breakdown tests artificial voids within and at the interface of dielectrics were prepared by first moulding a hole in a thin disc of polythene. The sample containing the void was then attached to one or more other void free samples of polythene by heat treatment (fig. 11a).

Other samples of dielectrics were specially machined to simulate a partially enclosed void (fig. 11b).

7.2 Methods

7.2.1 Calibration

With regard to the current measuring part of the circuit one method of calibration was by injecting a known voltage (millivolts) from a standard cell and comparing this with the voltage reading registered on the vibron indicating meter. (A comparative check was also made with a Keightley electrometer[69]).

Another, performed and periodically checked in the standards laboratory (of the department) was by putting across any of the input resistors a known voltage and comparing the calculated current with current registered on a sensitive meter. Most of the resistors calibrated in this way were within 1 per cent of their nominal values.

The calibration of the discharge detector was as described in the

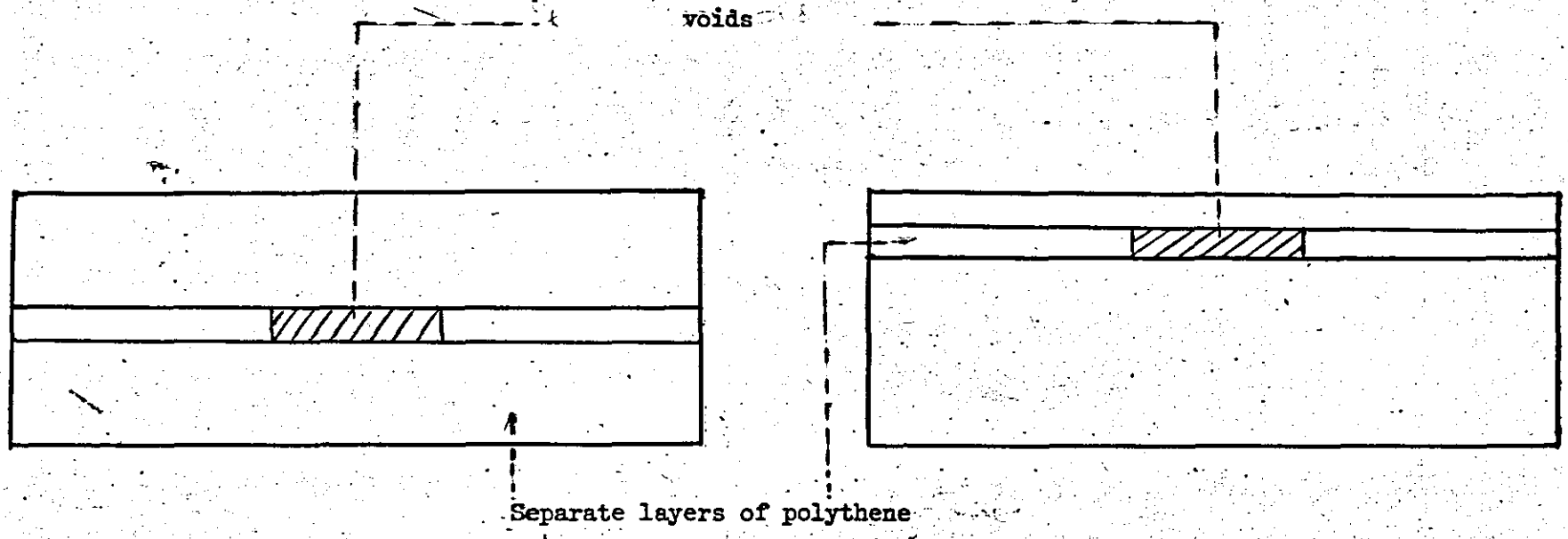

Fig. 11a
Artificial void in polythene

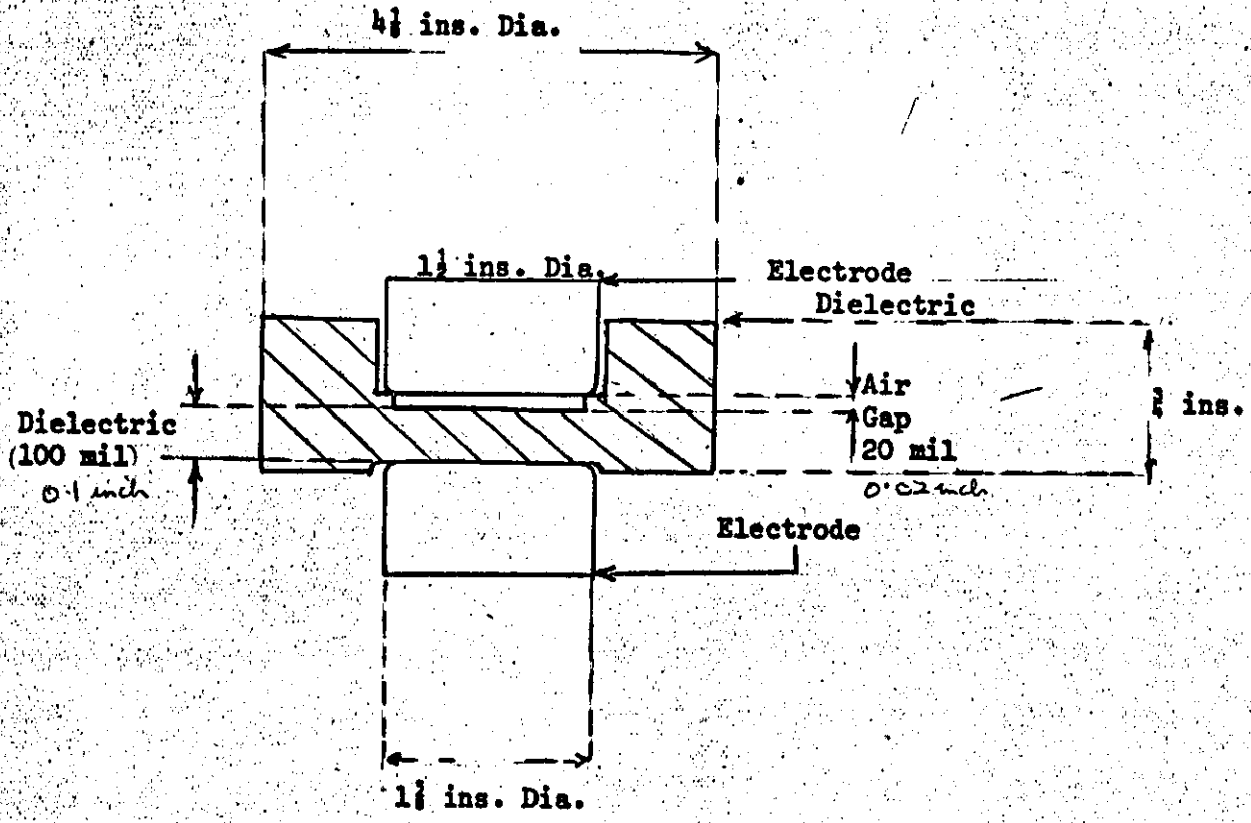

Polythene dielectric machined to contain artificial void

Fig. 11b

previous chapter. In order to assess the level of pulses being counted by the scaler, calibration pulses of known magnitude were fed to the scaler at a fixed repetition rate. The levels of the calibrating pulses were adjusted till the rate counts registered on the scaler matched those produced by the calibrating source. The ultra violet recorder could be calibrated in a similar way. The sensitivity of discharge detection was better than 0.3 picocoulombs.

The effect of the by-pass capacitor (where used) on the conduction current in the main test sample could be ascertained by connecting, then disconnecting the capacitor from the circuit, taking a set of results in either case then comparing them. There was no measurable difference in the two sets of results.

7.2.2 Conduction and surface discharge tests

(i) The first set of experiments were designed to evaluate the effect of stress on steady state conductivity. In pursuance of steady state conditions the following procedure was followed. The current and surface discharge variation with time were observed and measured almost continuously for the first 6-8 hours and thereafter at 24 hourly intervals. These 24 hourly readings were continued till conditions were attained where any sets of readings separated by a 48 hour interval did not exhibit an appreciable change. This condition which in some cases was obtained after a period of continuous stressing lasting more than two weeks (336 hours) is termed steady state.

Later, in order to investigate some of the laws listed in Chapter 2, tests were carried out using brass, copper, aluminium, silver and graphite electrodes. In the case of silver and graphite, solutions of these materials were brushed on to give thin coatings. A special switching arrangement (fig. 12, plate 7) was designed for the purpose of these tests in order to facilitate the simultaneous observation of discharge and current patterns in identical test cells with similar dielectrics but different electrode materials.

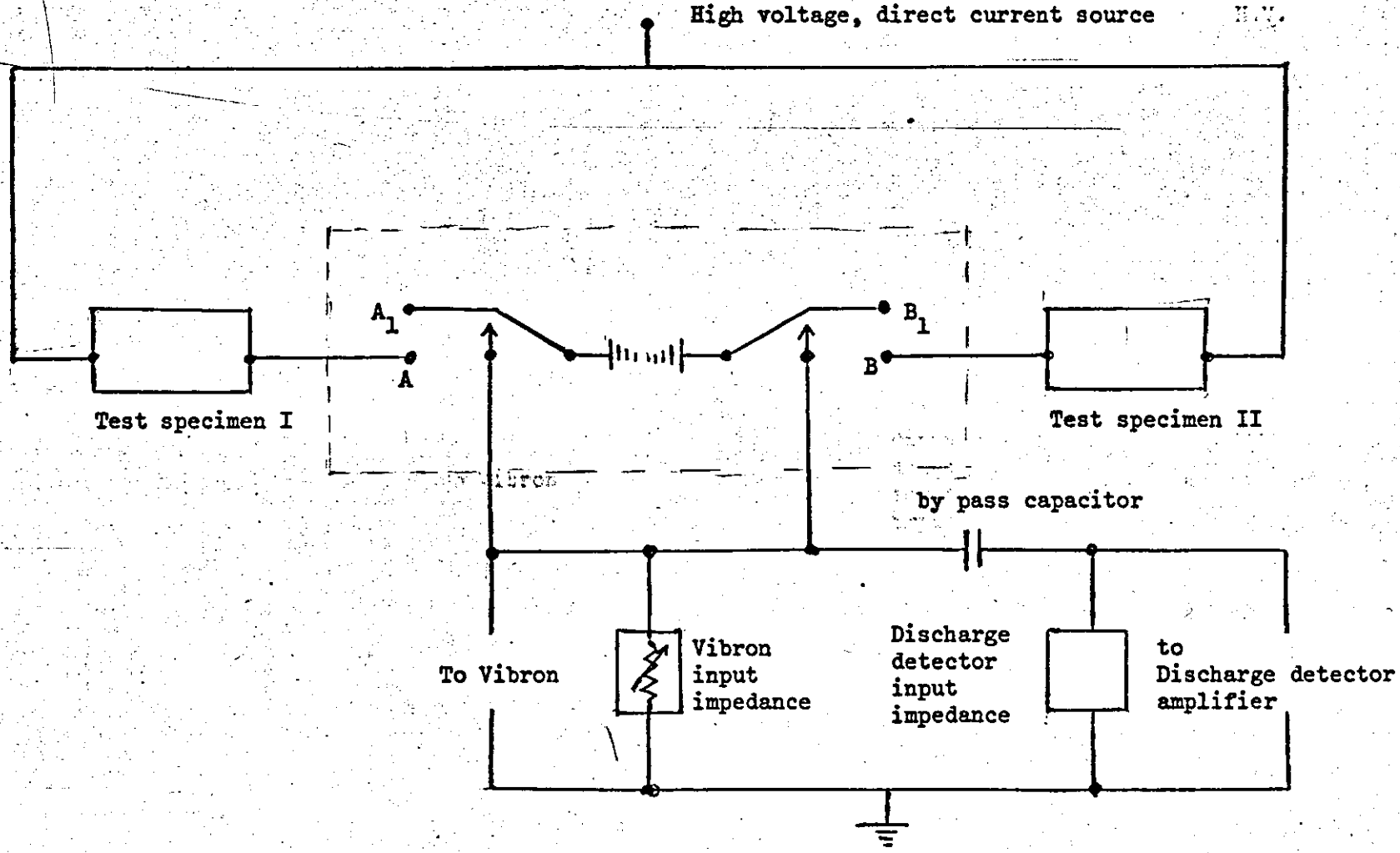

H_1, BB_1 are joined when necessary to earth either specimen

Fig. 12

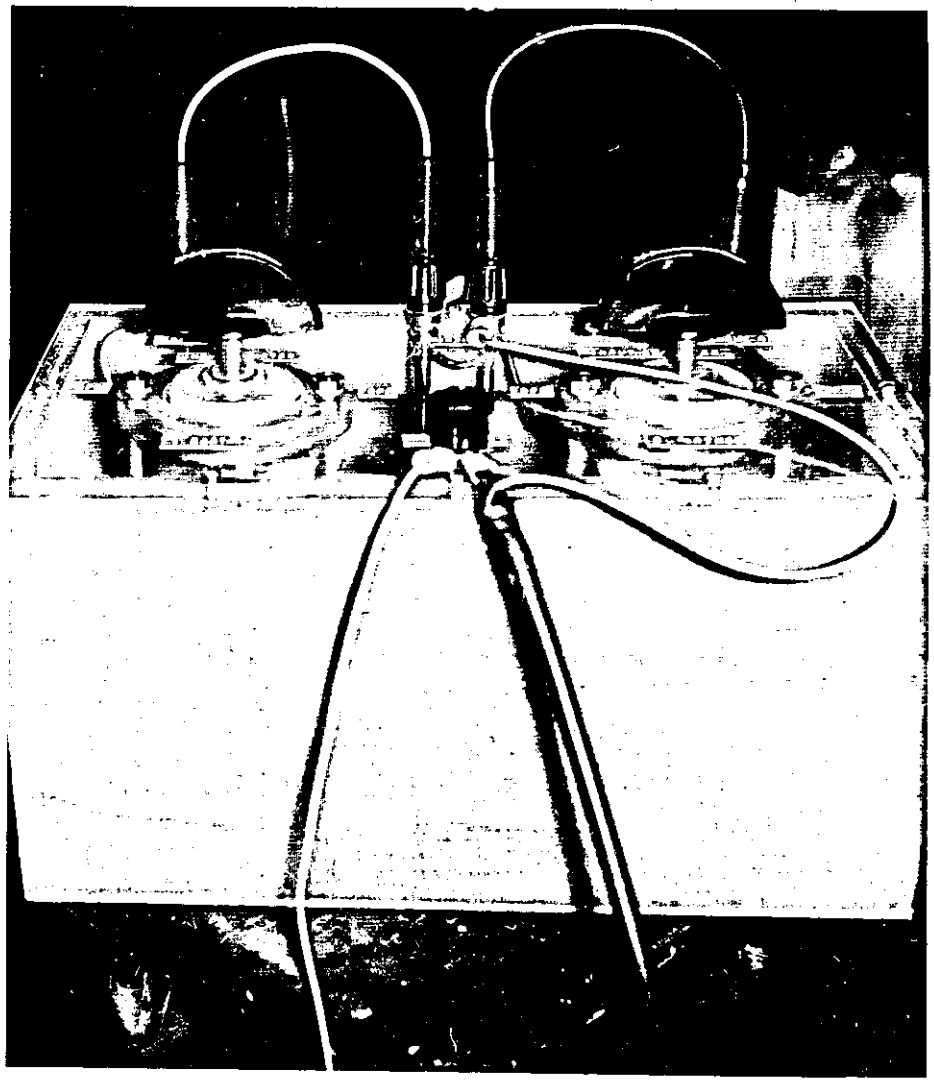

PLATE 7.
Switching box.

Further experiments were performed in an attempt to discover the stresses above which ohmic conduction did not apply using the different dielectrics available, these tests were repeated for various thicknesses of the same dielectric.

The conductivity of the various samples of polythene was measured at a fixed stress for sample thicknesses down to 0.001", the diameters of the test samples ranging from 2" to 4".

Surface discharge counts and ultra-violet recording of results were made during the conduction current tests, these were prolonged until the current recorded on the electrometer reached a steady state value.

The stresses used were mainly in the range 10-600 kV/cm, this being in accordance with the aim of the tests in attempting to obtain information at moderate stresses. A few results were obtained outside the range for comparison purposes.

(ii) Anomalies observed in the first test were studied in detail. Different parts of the first method were repeated for different dielectric samples and for different polarities.

In order to assess the effect of visible light(70, 71, 72) the transparent perspex cell was in some cases replaced by a visible-light proof cell for some of the tests.

7.2.3 Internal discharge and breakdown tests.

In order to test the validity of conventional discharge and equivalent circuit theories and the influence of internal or space charges various circuits were set up in order to study discharge inception voltage and discharge behaviour together with the polarization phenomena in air gaps by themselves, and

in air gaps in various configurations with solid dielectrics.

Some partially or totally enclosed voids in layers of thin samples of polythene were also tested in a cell under oil (Silicone oil) for discharges. Other samples as shown in Fig. 11b were tested in air. The position of these voids and air gaps in relation to the high voltage source or earth were reversed in some cases so that any influence on the discharge performance (if any) due to the relative void position could be assessed.

Some cable discharge tests were also made. (See appendix).

7.2.4 Comparative a.c. tests.

For comparative purposes some of the void gap breakdown and discharge tests were repeated under alternating voltage conditions.

All the tests were carried out at a thermostatically controlled room temperature, it is expected that under these conditions any variations in characteristics due to changes in temperature would be negligible.

7.3 Experimental results

The values of steady state conductivity obtained at various applied voltages were plotted against corresponding functions of stress (Figs. 13-17) in accordance with the various laws stated in Section 2. The points on the graphs are not joined since it would appear that different regions on some of the graphs could be interpreted as either straight lines or curves each of which appears to be valid over a part of the range considered. If straight lines are used then once again the slopes are difficult to determine, they appear to be complex functions of the variables, i.e. temperature, stress, low frequency or high frequency of permittivity and electrode to dielectric work function.

Some of the laws however clearly imply that widely different electrode materials should not give the same results. The validity of these concepts, which depend upon the presence of electronic field emission, was tested by plotting graphs corresponding to the different electrode materials (Fig. 18).

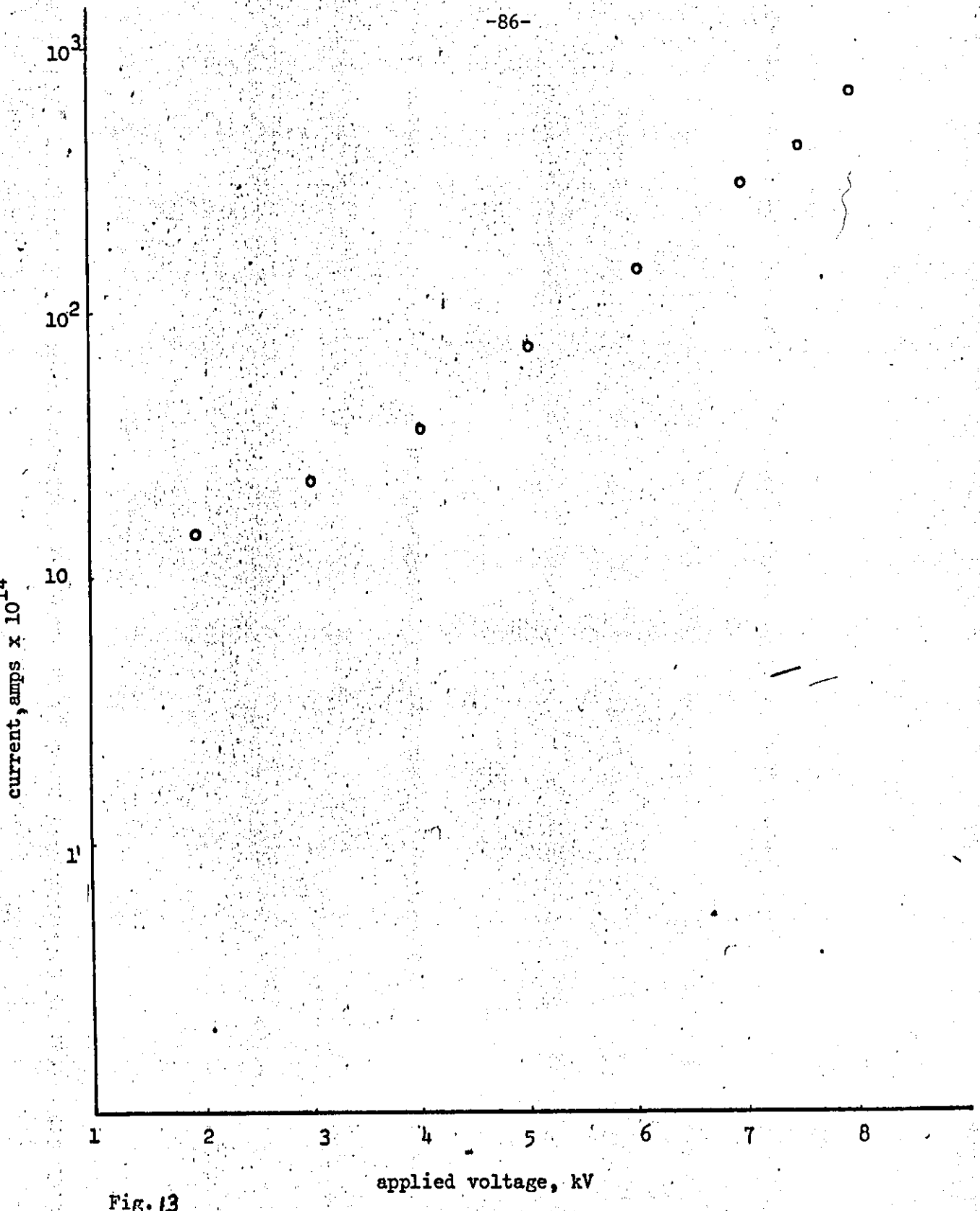

Fig. 13

Log current against voltage
Sample Y, thickness of dielectric 0.01 inch *

* The electrode diameter and thickness are to be taken as 2 inch and 0.02 inch respectively unless specified otherwise.

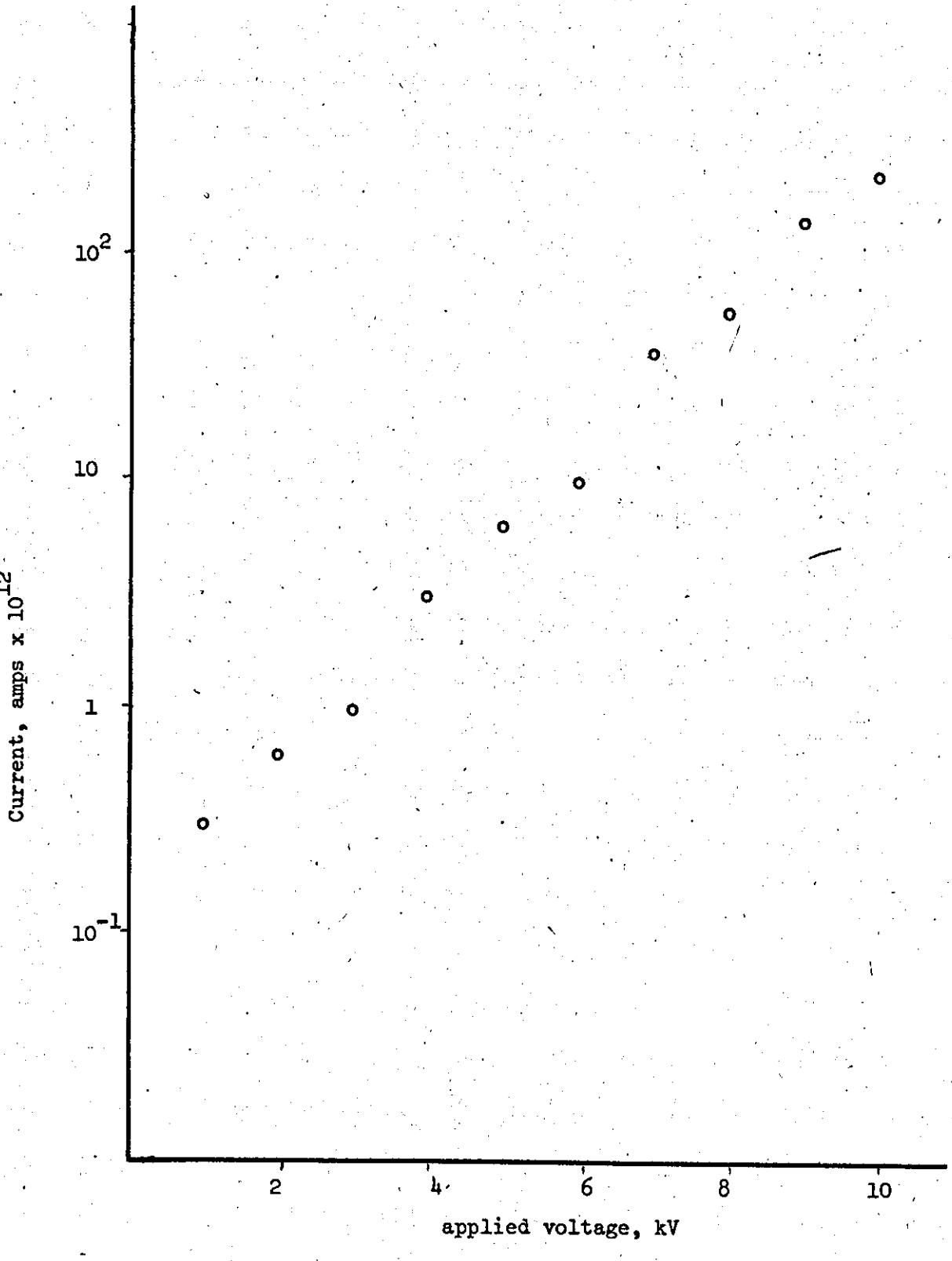

Fig. 14

Log current versus voltage
Sample X.

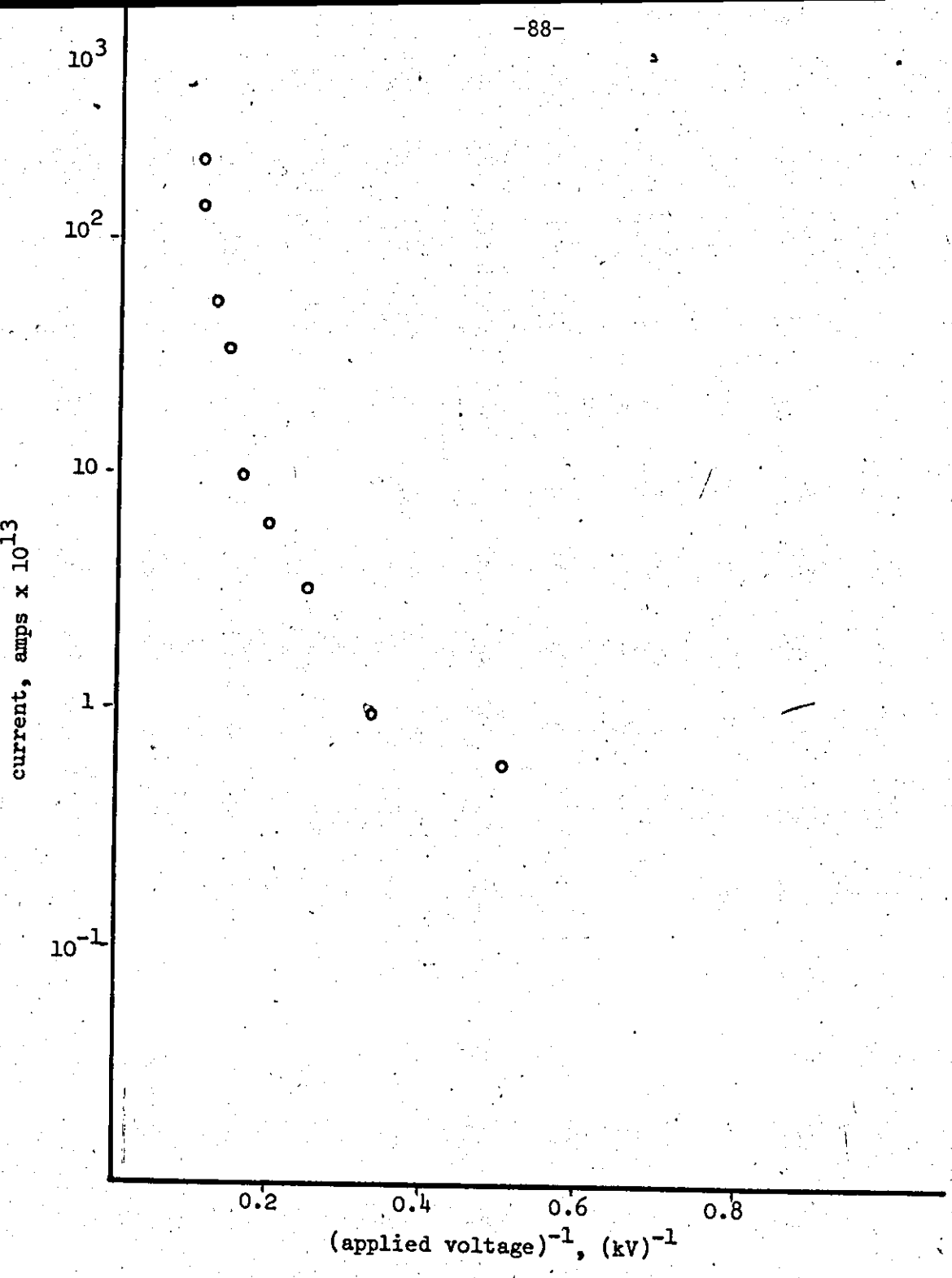

Fig. 15

Fowler-Norheim basis, Log current versus (voltage)$^{-1}$
Sample X.

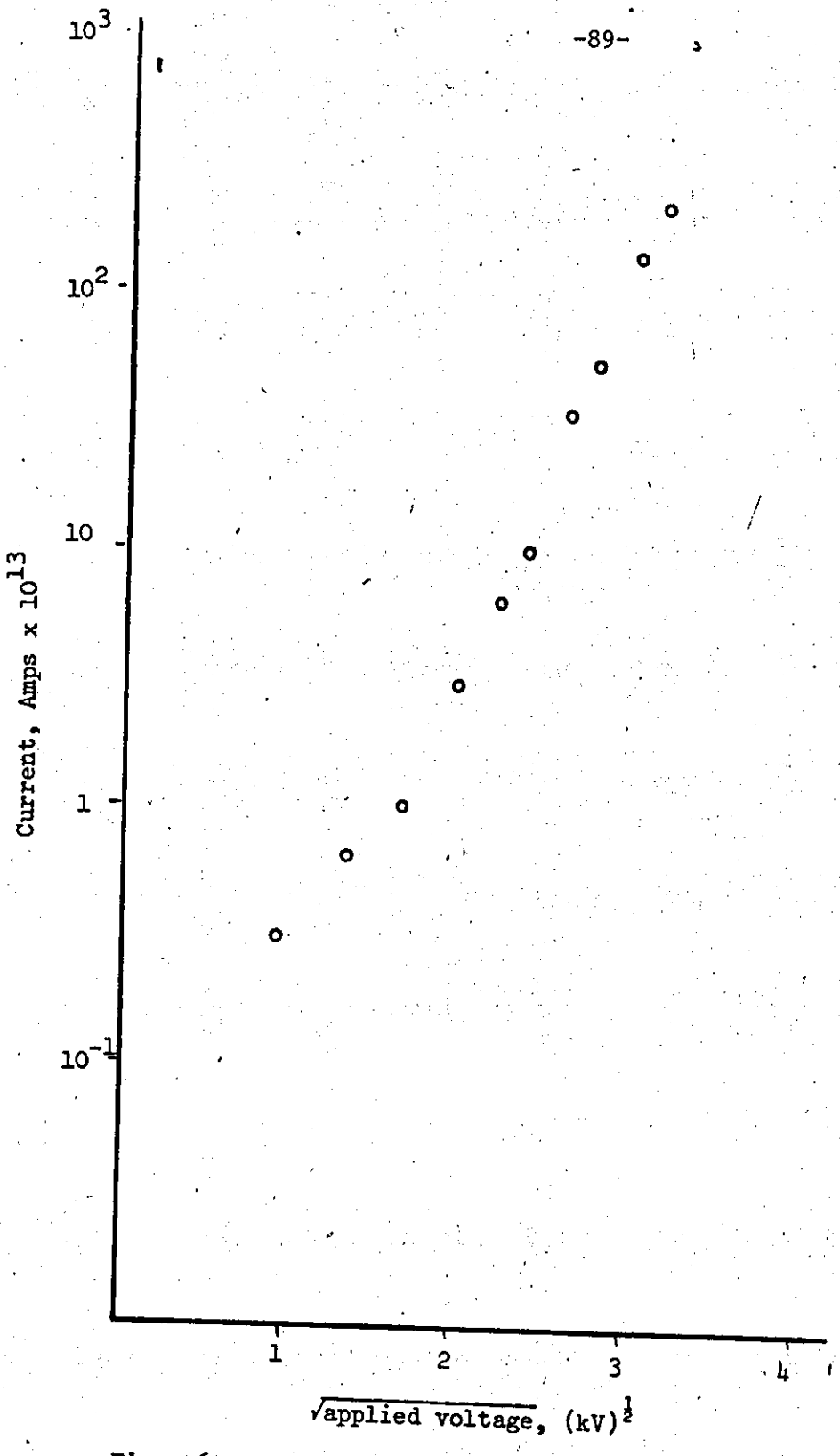

Fig. 16

Poole-Frenkel, Richardson-Schottky basis, log current against $(\text{voltage})^{\frac{1}{2}}$
Sample X,

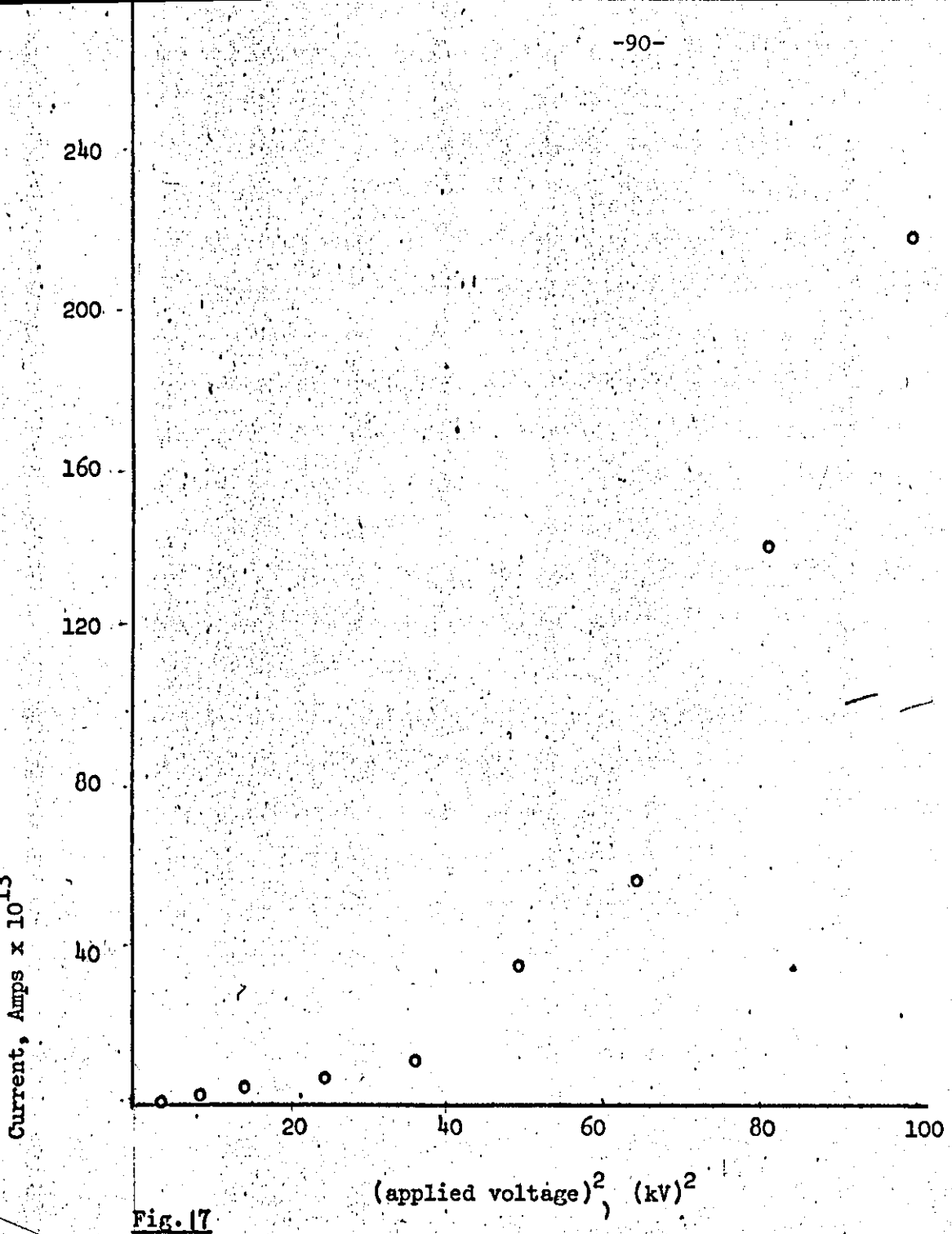

Fig. 17

Log current against square of voltage
Sample X

silica glass - (for comparison with polythene)

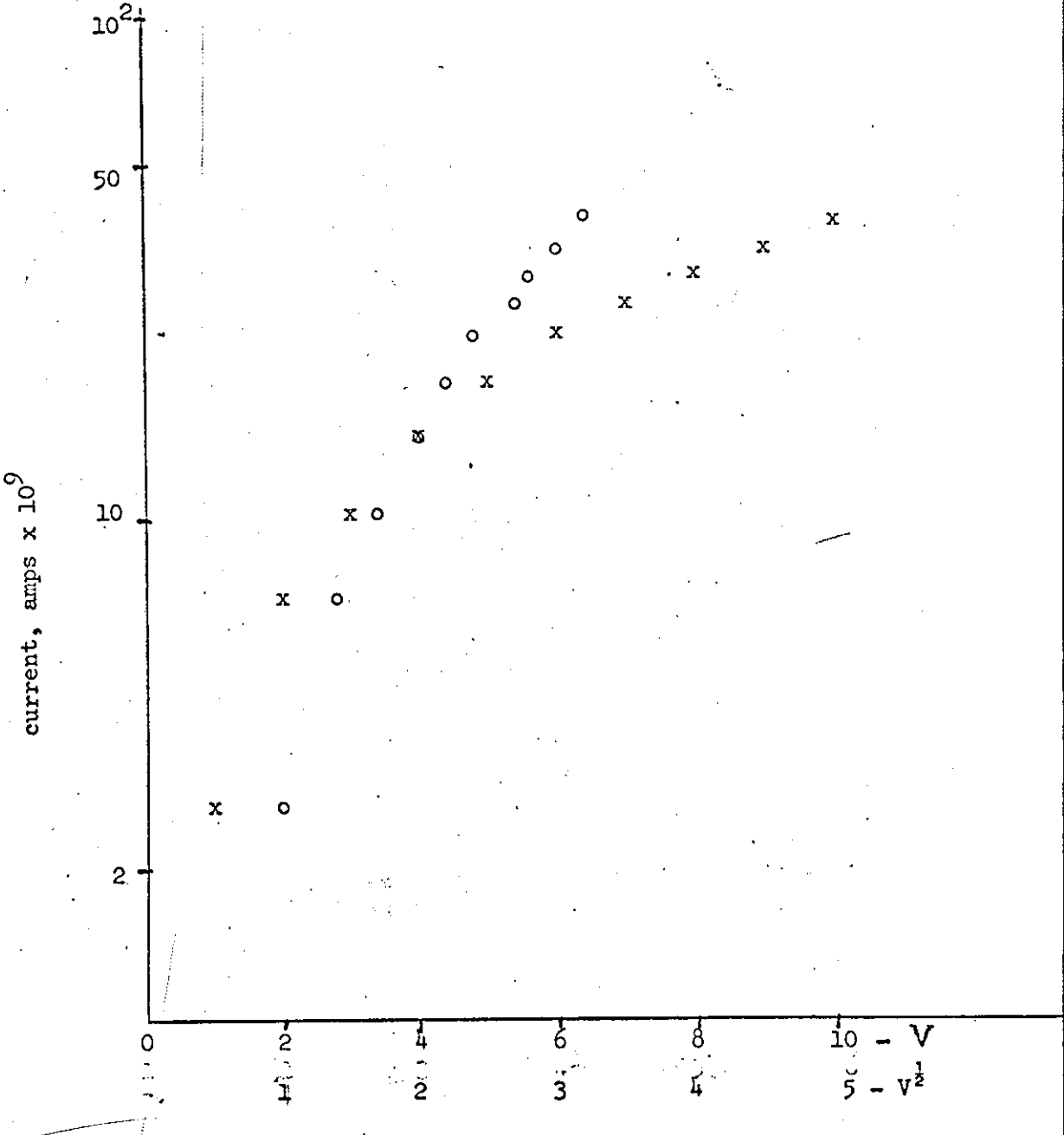

Fig. 17b

x - current versus voltage
o - current versus $(\text{voltage})^{\frac{1}{2}}$
thickness of dielectric 2.8 mm
electrode diameter 2 inches

Soda-glass (for comparison with polythene)

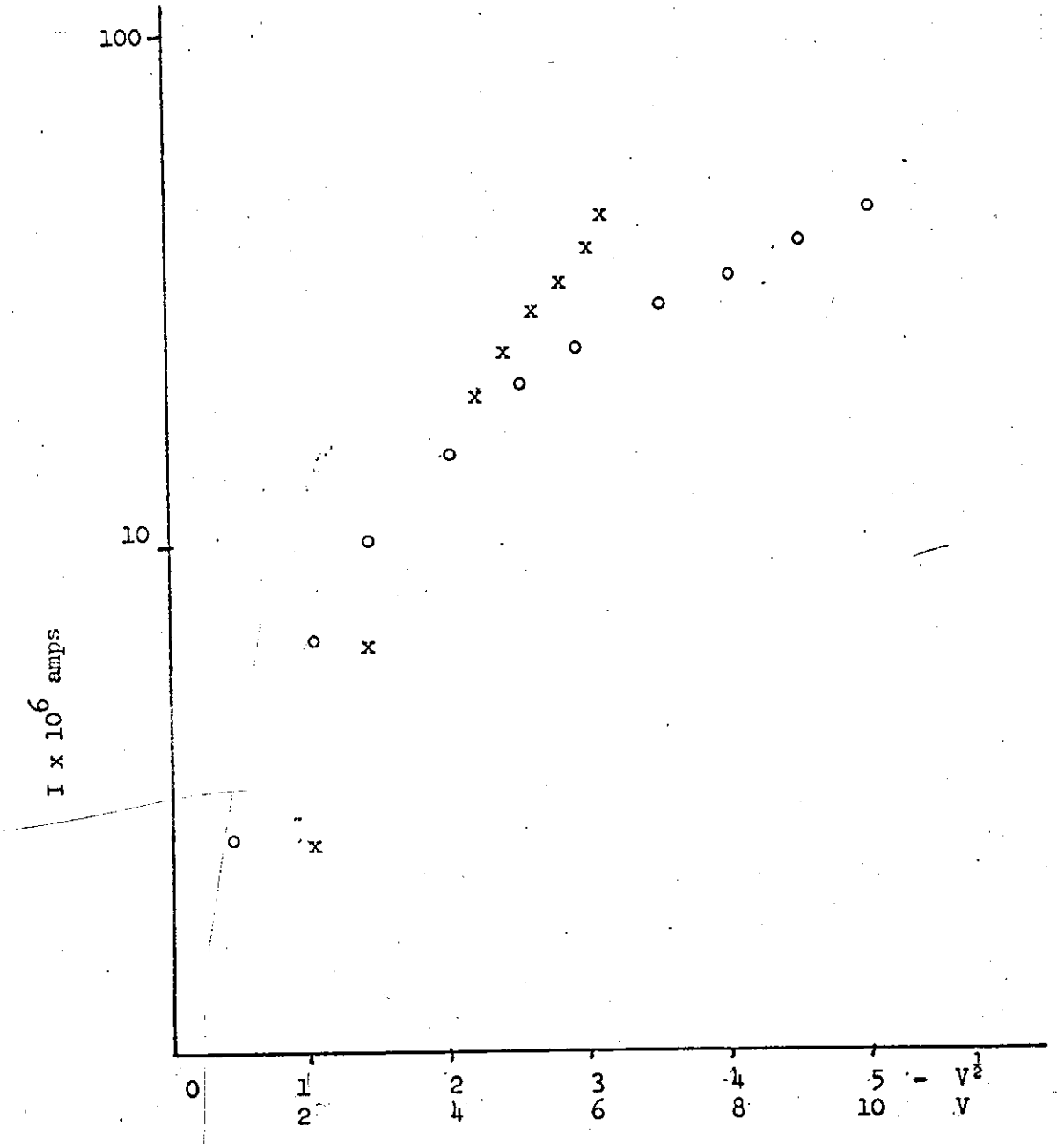

Fig. 17c

o - current versus voltage
x - current versus (voltage)$^{\frac{1}{2}}$
thickness of dielectric 2 mm
electrode diameter 2 inches

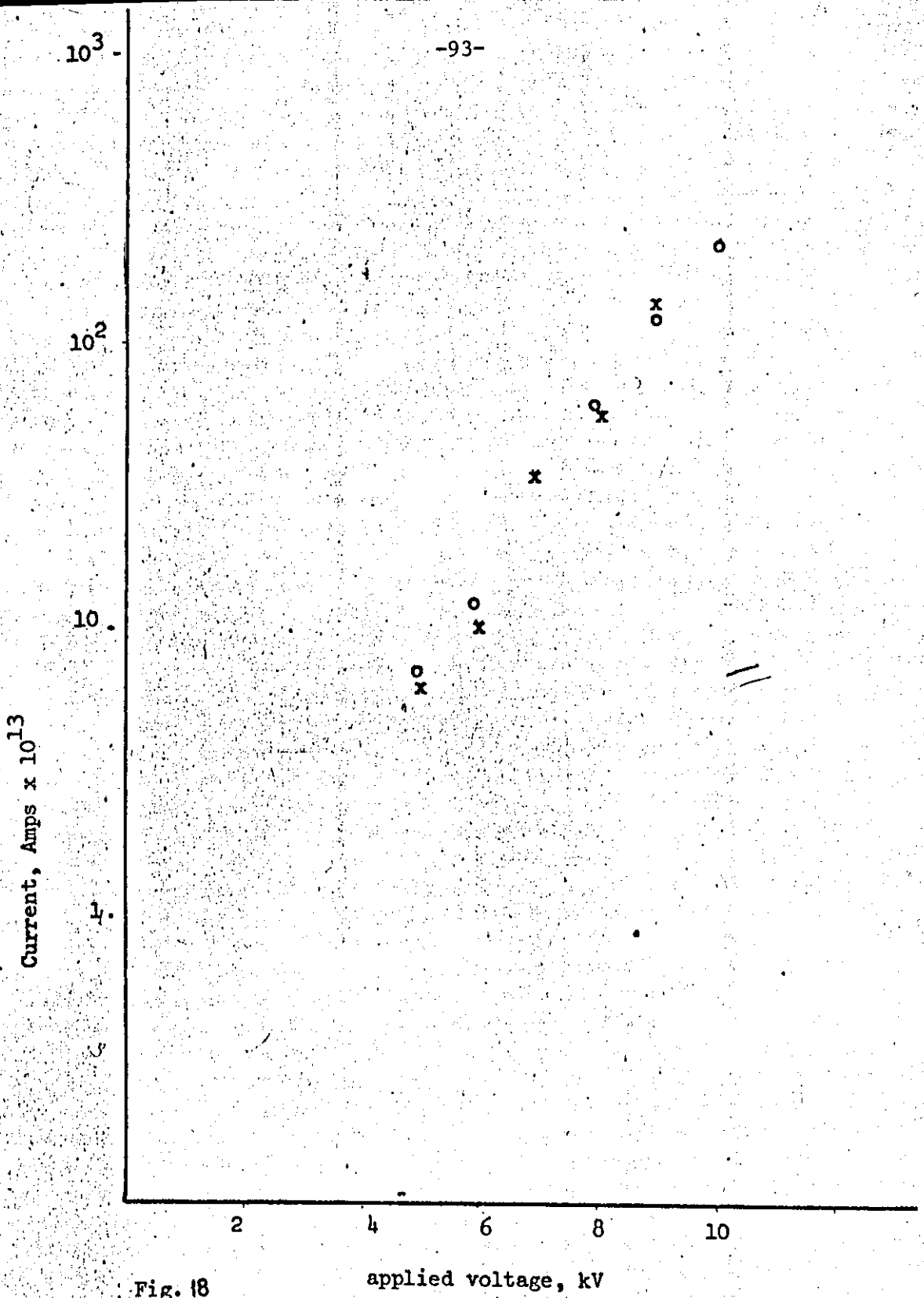

Fig. 18

Comparison of effect of electrode materials
o Graphite Coated electrodes
x Silver coated electrodes
Sample X

Plots of the variation of current and surface discharge with time (Figs. 19-21) were also made, in this connection the behaviour of the type X polythene (Fig. 21) should be noted in particular since this appears to present a different pattern compared with the others. Plots of current through different dielectric samples placed in the transparent cell in some cases and in the visible light proof cell in other cases, with time were made. Surface discharge/time plots were also made.

Results of equivalent circuit tests are also presented in Chapter 9. More results discussion and conclusions are presented in the succeeding chapters.

7.4 Observations and comments.

7.4.1 Nature of 'transient' current

It was observed that the current response to a step voltage change had two distinct time decay processes. A short fast decay and much longer decay which took hours. At low stresses the latter was too small to be measured.

It was also observed that, above stresses of about 220 kV/cm, the conduction current of one of the samples of polythene tended to decay with time until a point was reached at which the current began to increase again (Fig. 21 and U.V. record 1A). This is in contradiction to the normally expected pattern of behaviour in which the decay is permanent. This phenomenon which has previously been observed in some semiconductors[73-77] is treated in more detail in the next section. The results also show that the current decay rate is faster for the samples Y_2, Y_3 than for the sample Y_1. This is probably because of the various dosages of anti-oxidant sample Y_1 seemed to have the highest initial charging current Above stresses of about 500 kV cm^{-1} the transient current of Y_3 tended to exhibit peculiarities similar to that of sample X above about 250 kV cm^{-1} (see fig. 22).

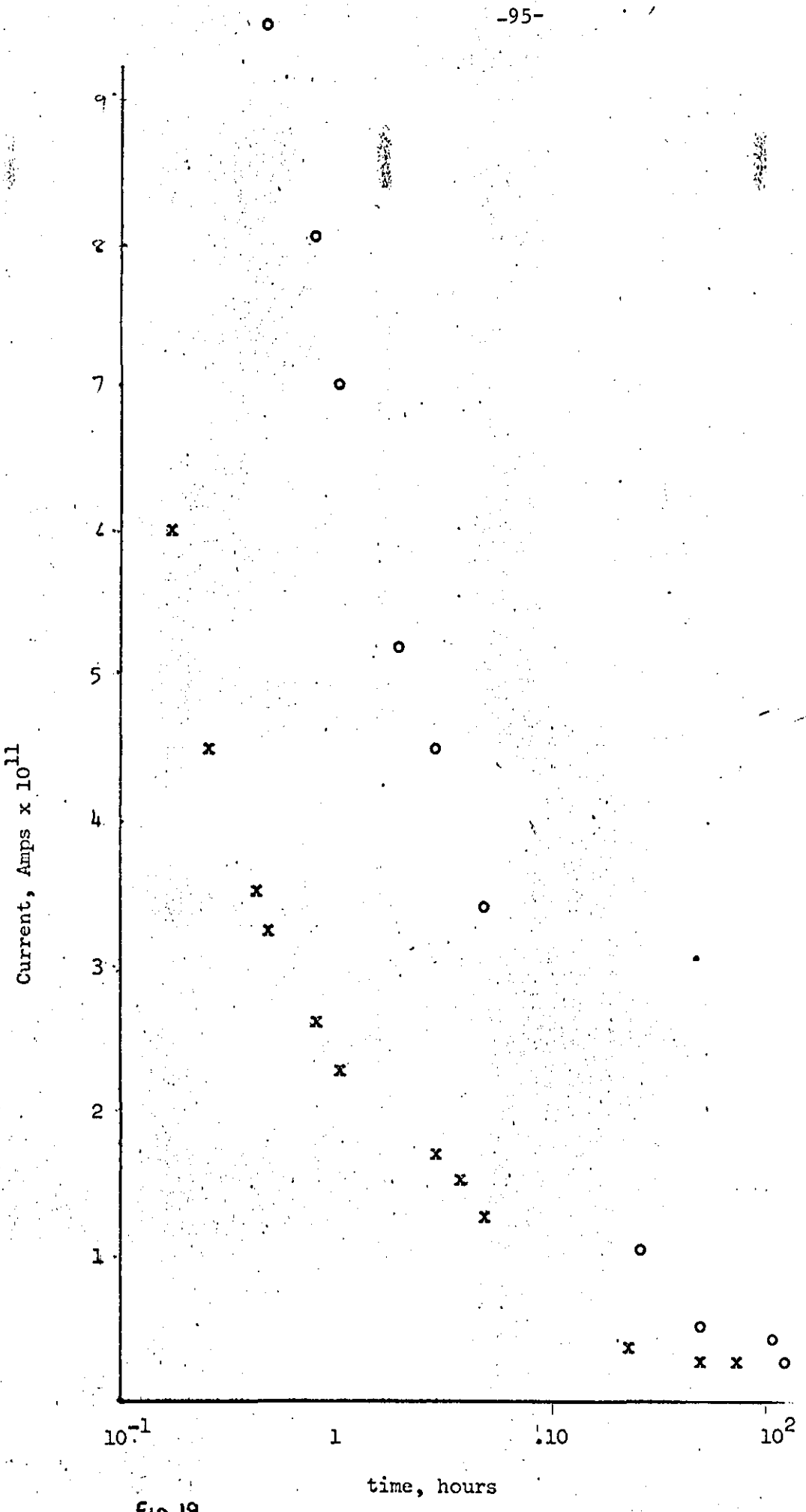

Fig 19

Current against time (X - with antioxidant)
X - Sample Y_2 O - Sample Y_1
Applied Stress - 395 kV cm^{-1}

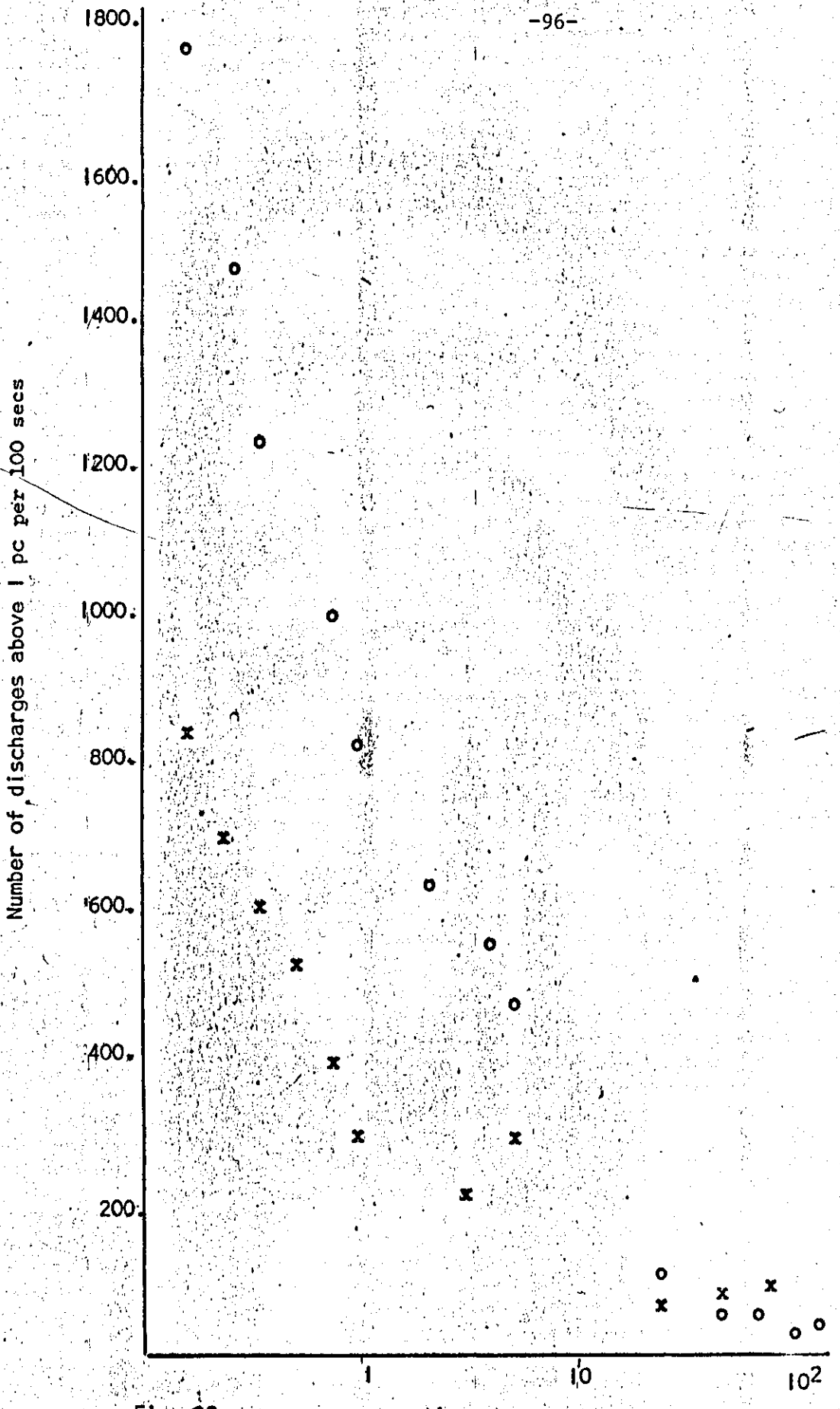

Fig. 20

Surface discharges versus time

x - sample Y_2 o - sample Y_1

Applied stress - 395 kV cm^{-1}

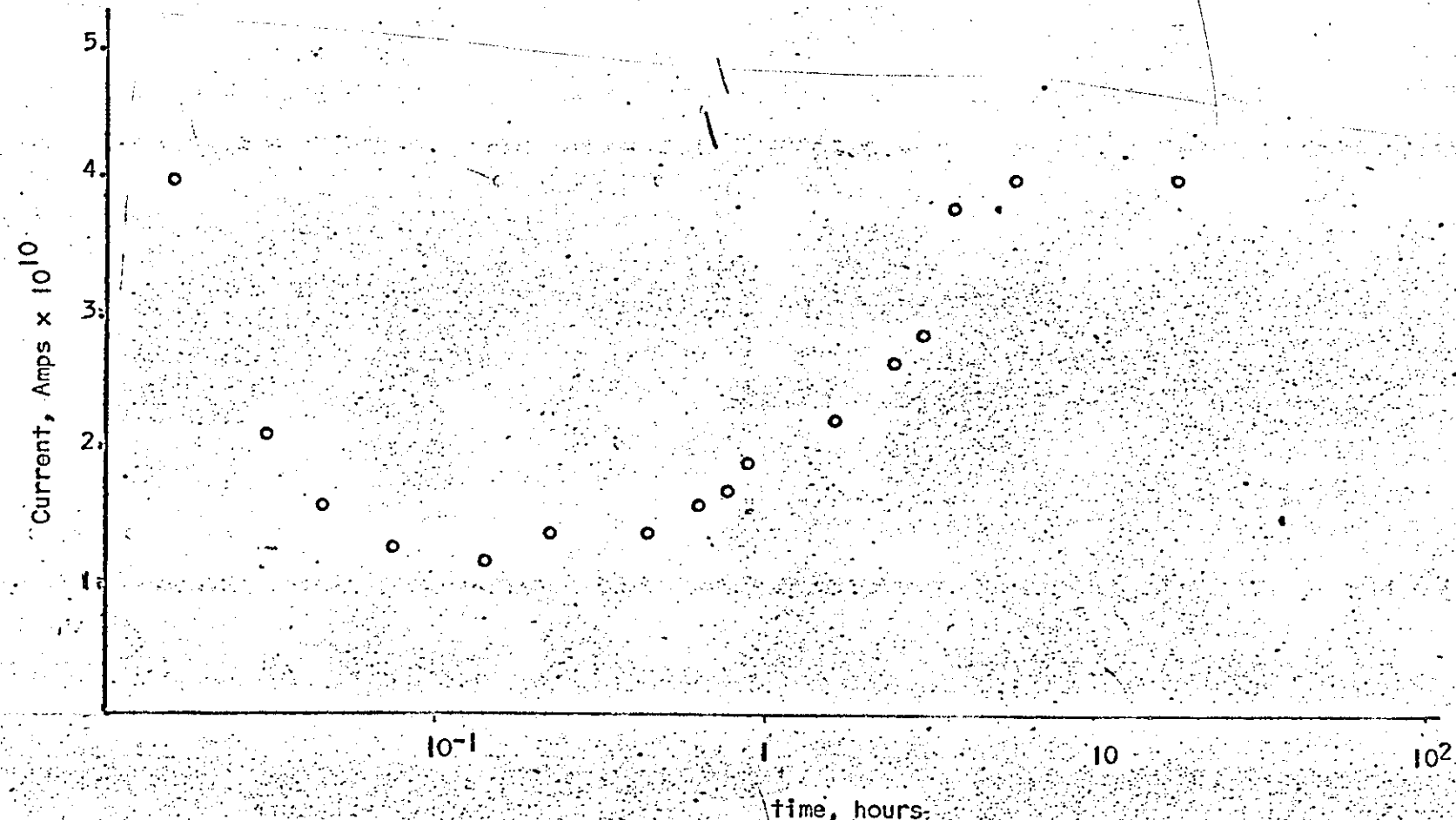

Fig. 21

Current against time

Sample X,

Applied stress 300 kV cm^{-1}

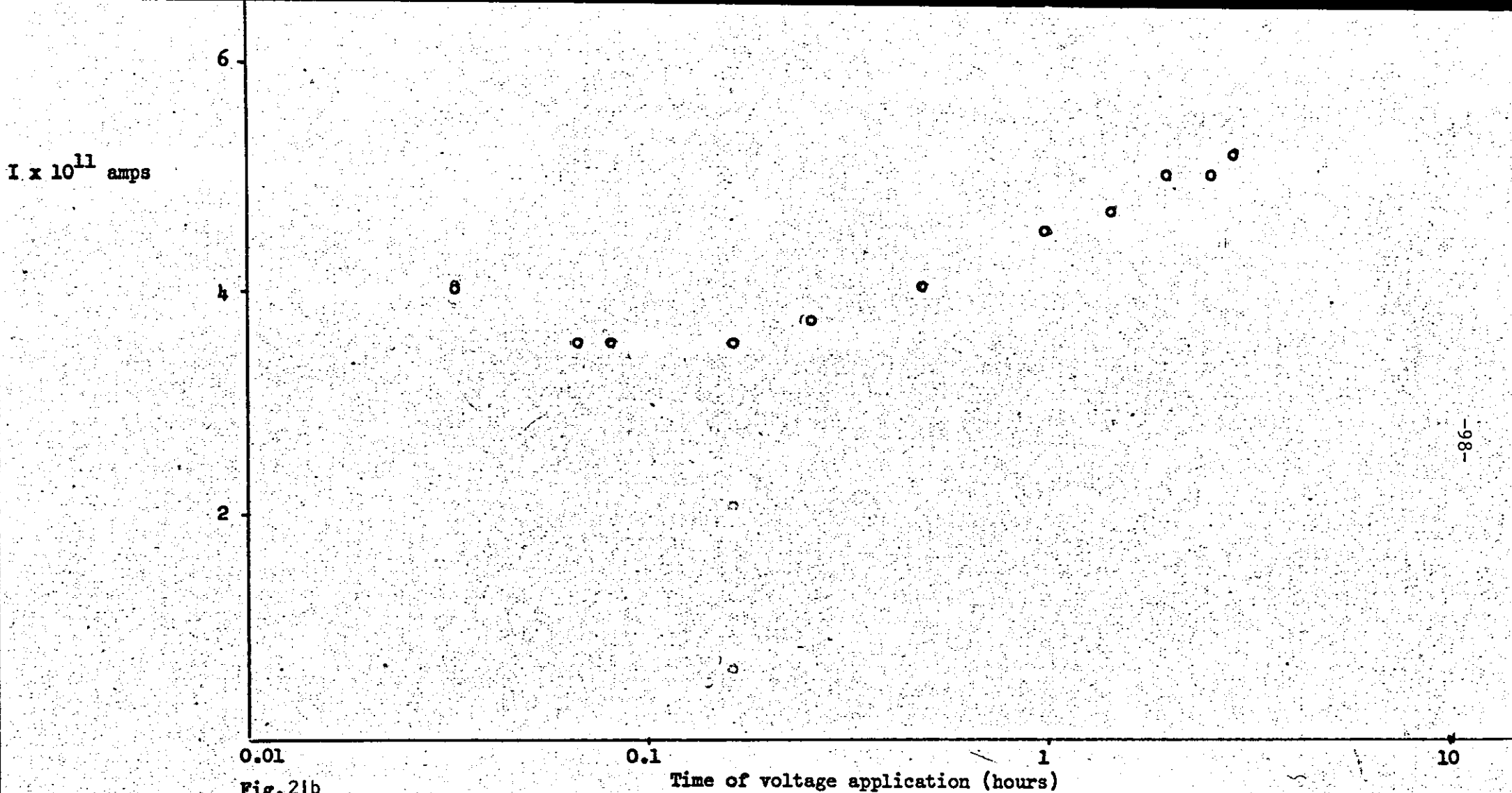

Fig. 21b
Graph of ~~voltage~~ current against time of voltage application
20 mil (Bloore) polythene at 15kV
½" Brass Electrodes (no guards)

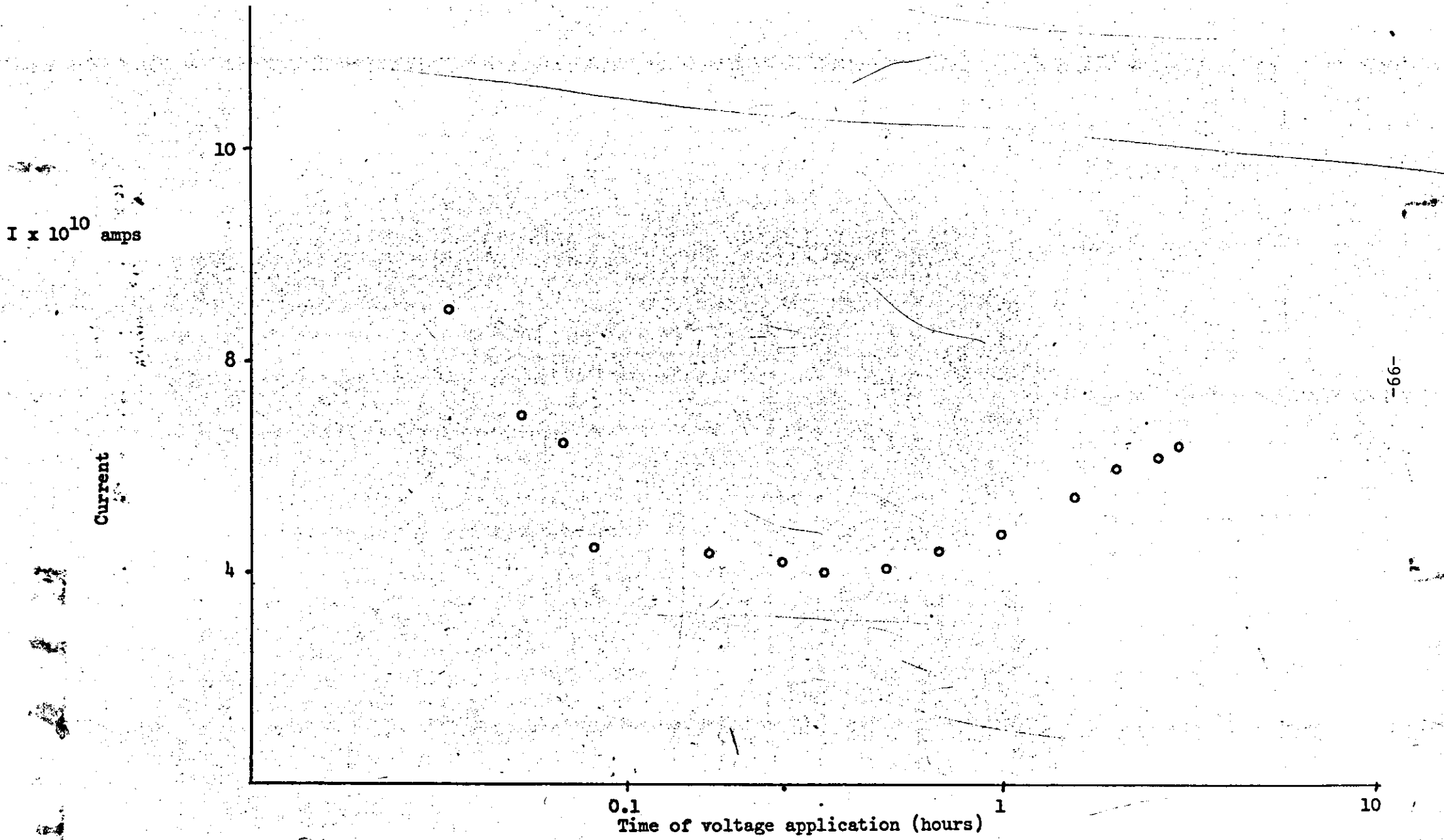

Fig. 21c
Graph of current against time after voltage application
20 mil (Bloore) Polythene at 15kV
2½" Brass Electrodes (No guards)

U.V. record IB
d.c. discharges - behaviour of discharges with time with increase of stress (compare with U.V. record IA(a)).
Sample as in fig. IIb , paper speed - 0.02 ins.sec^{-1}.

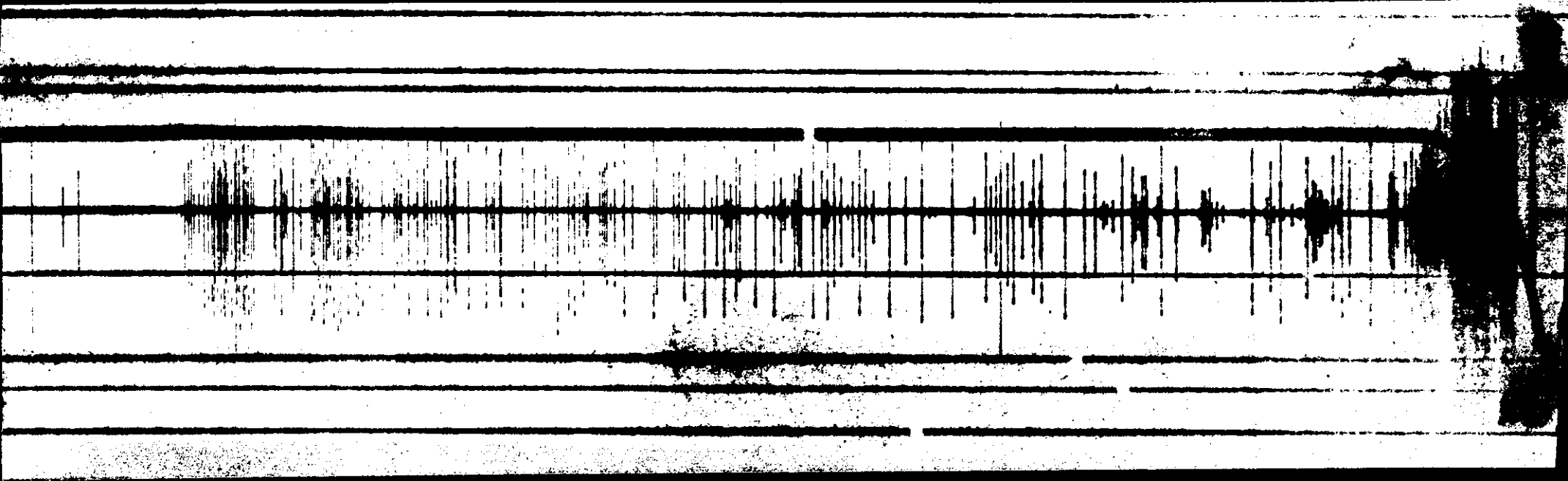

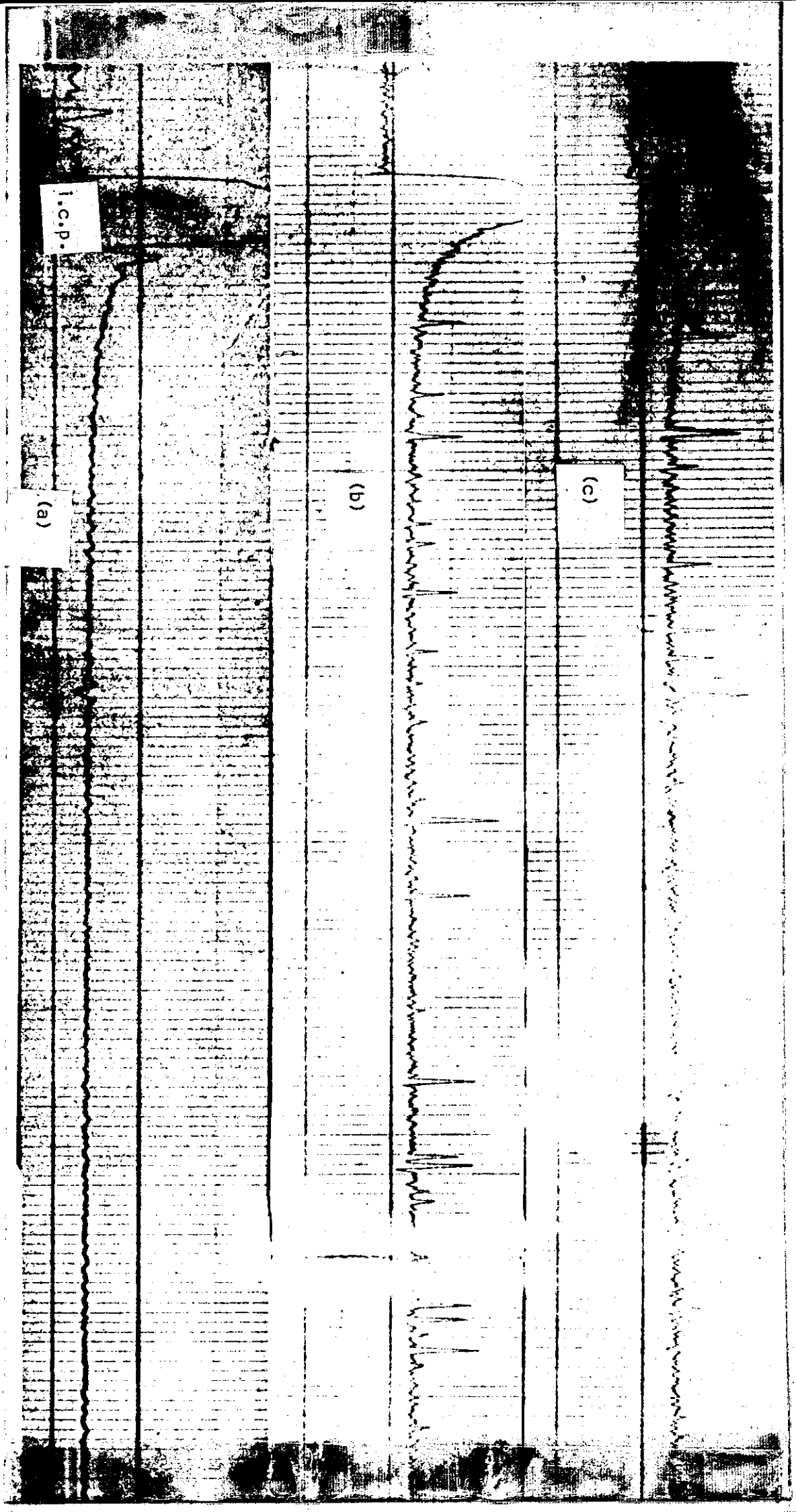
(a)
(b)
(c)

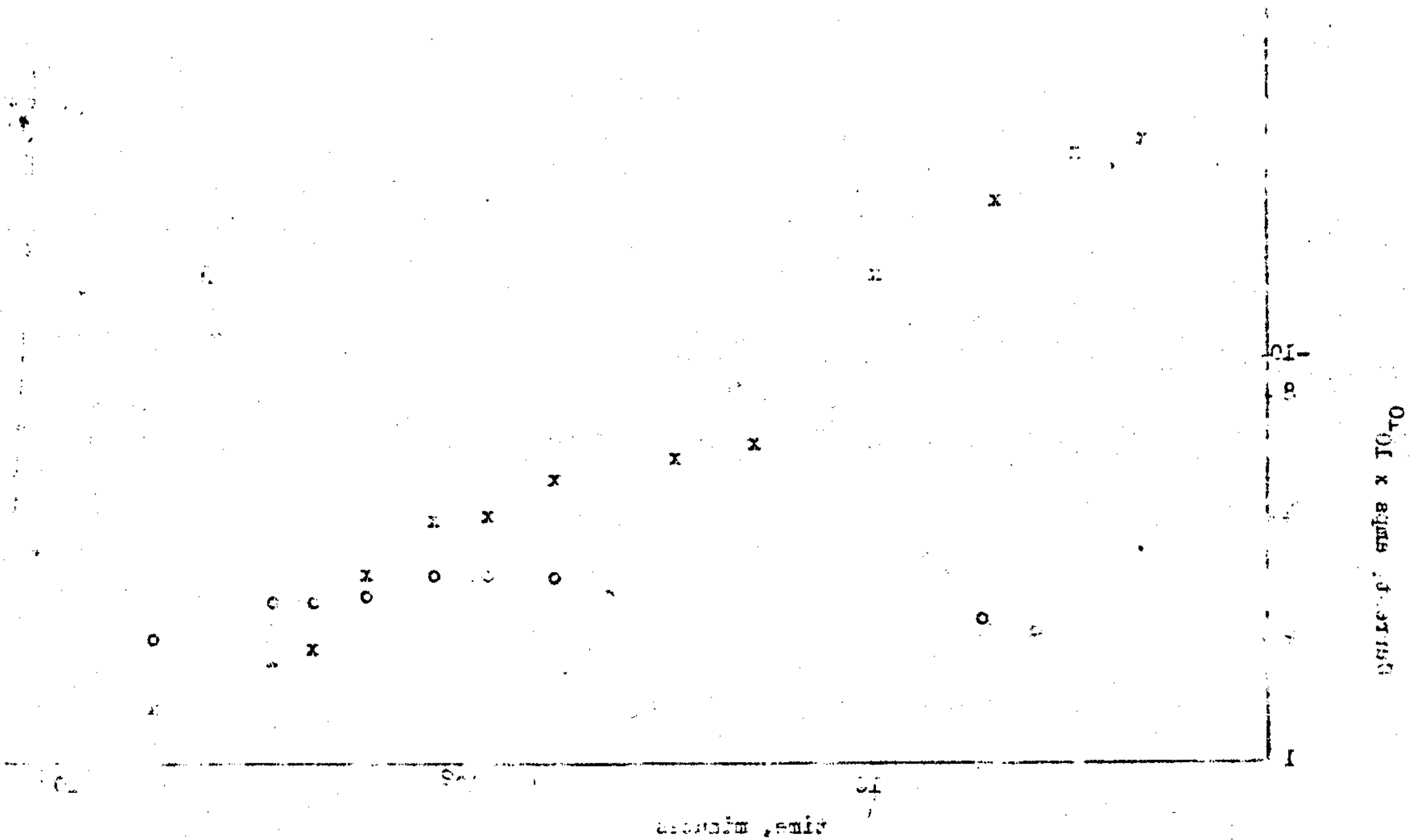

Fig. 22

Circuit against time of voltage application

x - sample Y_1

o - sample Y_2

electrode diameter - 1½ inches

electrode thickness - 0.025 inches

Applied voltage - 25 kV

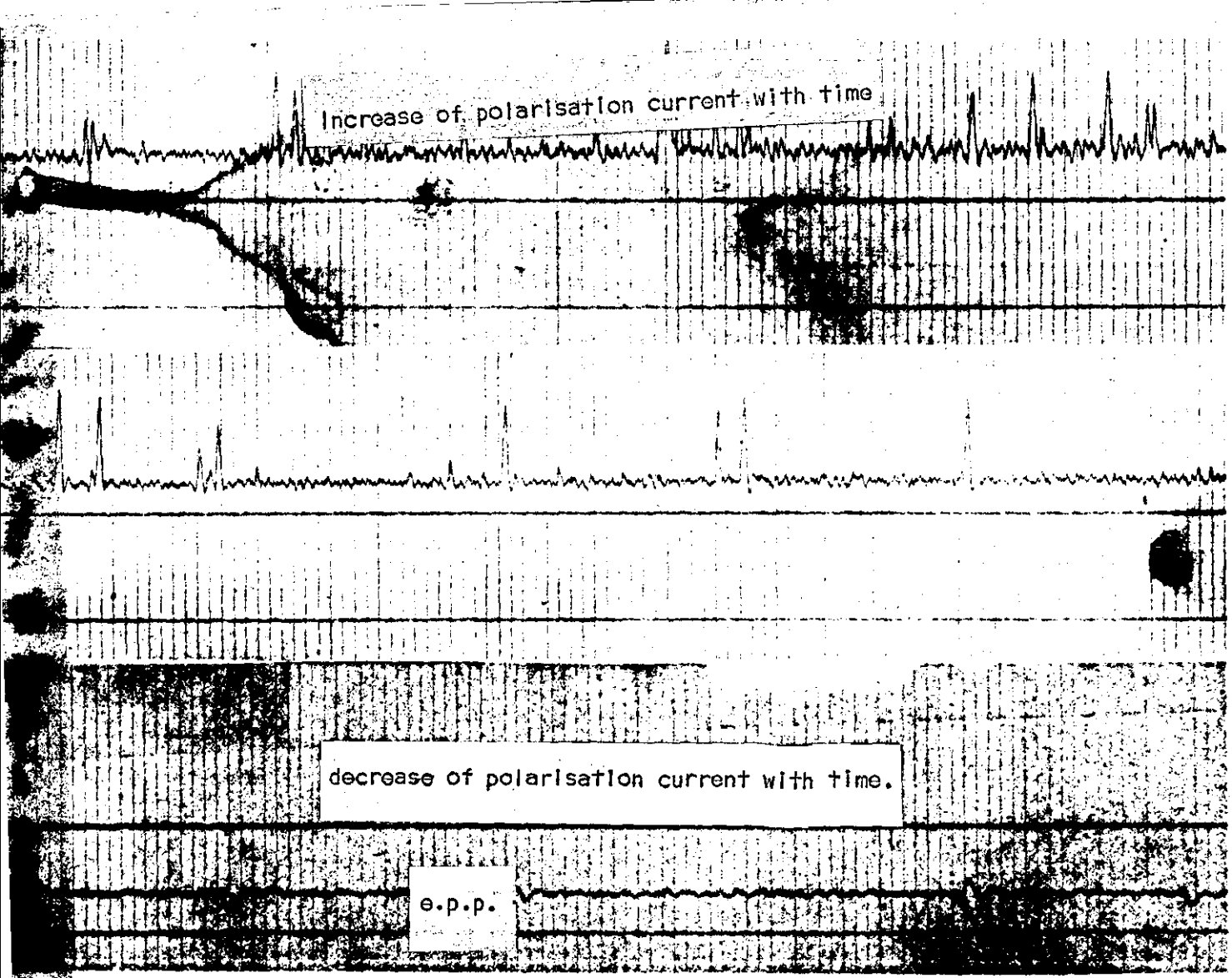
Increase of polarisation current with time
decrease of polarisation current with time.
e.p.p.

U.V. record 1A
Polarisation current traces - (a) current at 200 $kV.cm^{-1}$ stress
(b) current at 400 $kV.cm^{-1}$ stress
(c) current at 600 $kV.cm^{-1}$ stress
Sample X, paper speed - 0.02 $ins.sec^{-1}$.

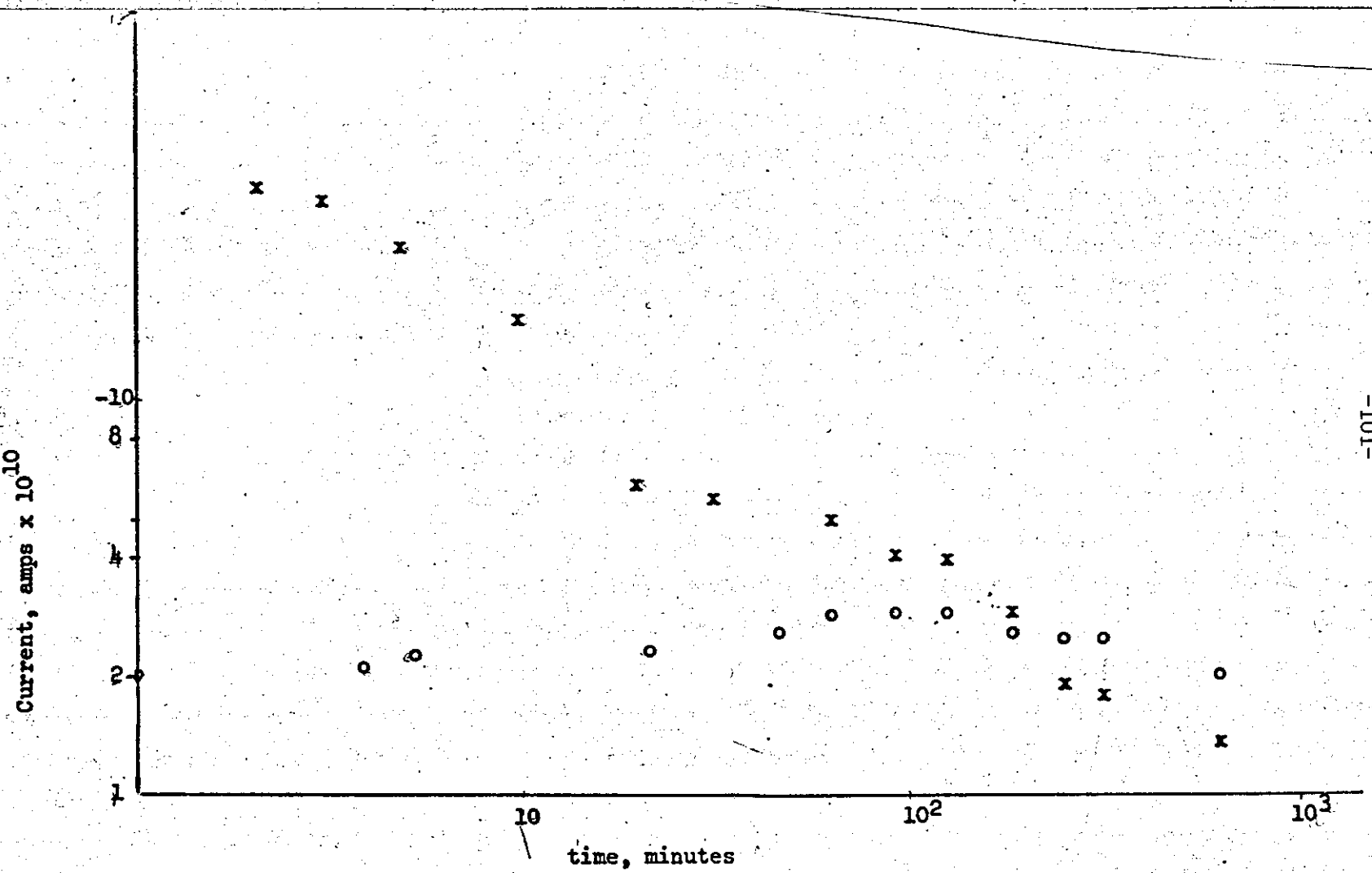

Fig. 22
Current ~~Circuit~~ against time of voltage application
x - sample Y_2
o - sample Y_3
electrode diameter - $1\frac{3}{4}$ inches
dielectric ~~electrode~~ thickness - 0.025 inches
Applied voltage - 25 kV

For stresses up to the value at which polarization current anomalies occurred in sample X, sample X had the highest initial current and decay rate. (see figs. 23a, 23b).

The effect of visible light was not investigated in great detail but it seemed as if it affected the rate of transient current decay (see figs. 24a-24c).

Oscillations of current through the dielectric in the absence of discharges were observed, these became more pronounced at the lowest stresses. Various explanations have been offered[78,79] for this effect when noticed in other dielectrics and the possibility that it may be due to the interaction of two types of charge carrier cannot be dismissed.

7.4.2 Steady state conductivity

It was apparent from the measurements that, in the absence of surface discharges, the steady-state conductivity was not influenced by the use of a guard electrode system. All the graphs indicate that the current through the dielectric is a logarithmic exponential (non-ohmic) function of the applied stress although it is impossible to conclude, so far as the stress range considered is concerned, which of the precise laws listed earlier the curves can be said to obey.

The tests on sample X of the polythene with different electrode materials and at stresses between 30 and 300 kV/cm show that, whilst conductivity still appears to be a logarithmic function of stress, it is independent of the electrode material and hence there is no evidence that field emission from the electrodes plays a significant part. Therefore it would appear that the non-ohmic logarithmic conductivity is an intrinsic property of the dielectric material.

It may be seen from Figs. 25-26 that the effect of reducing the thickness of the samples whilst maintaining the stress constant was to reduce the non-ohmic conductivity of the dielectric. This effect has been observed previously[80] and has been interpreted as a relative

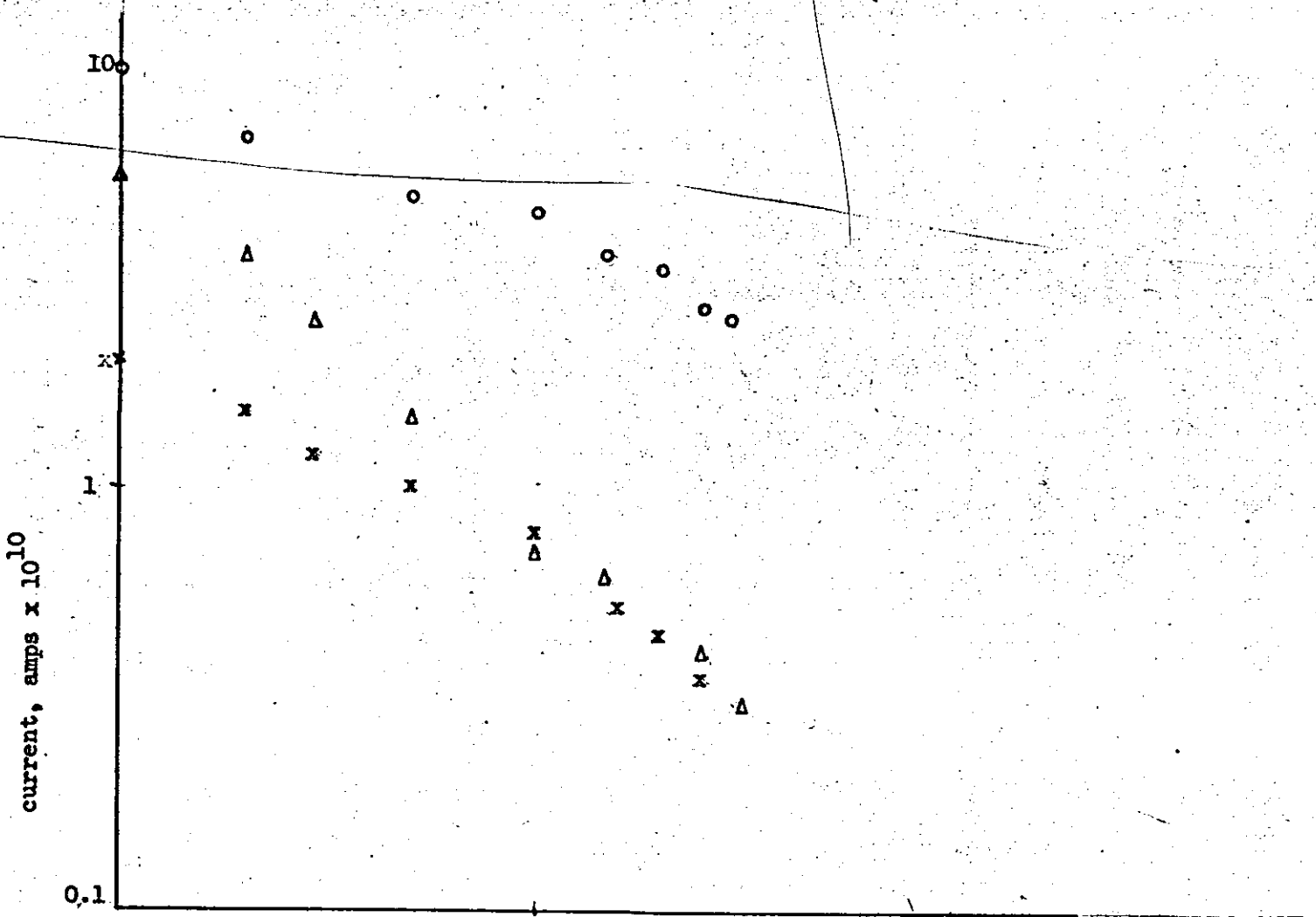

Fig. 23a
Current versus time after voltage application, negative polarity
Electrode diameter 1½ inch guarded electrode
Applied voltage 16½ kV
Dielectric thickness 0.02 inch
O - sample Y_1
Δ - sample Y_2
x - sample Y_3

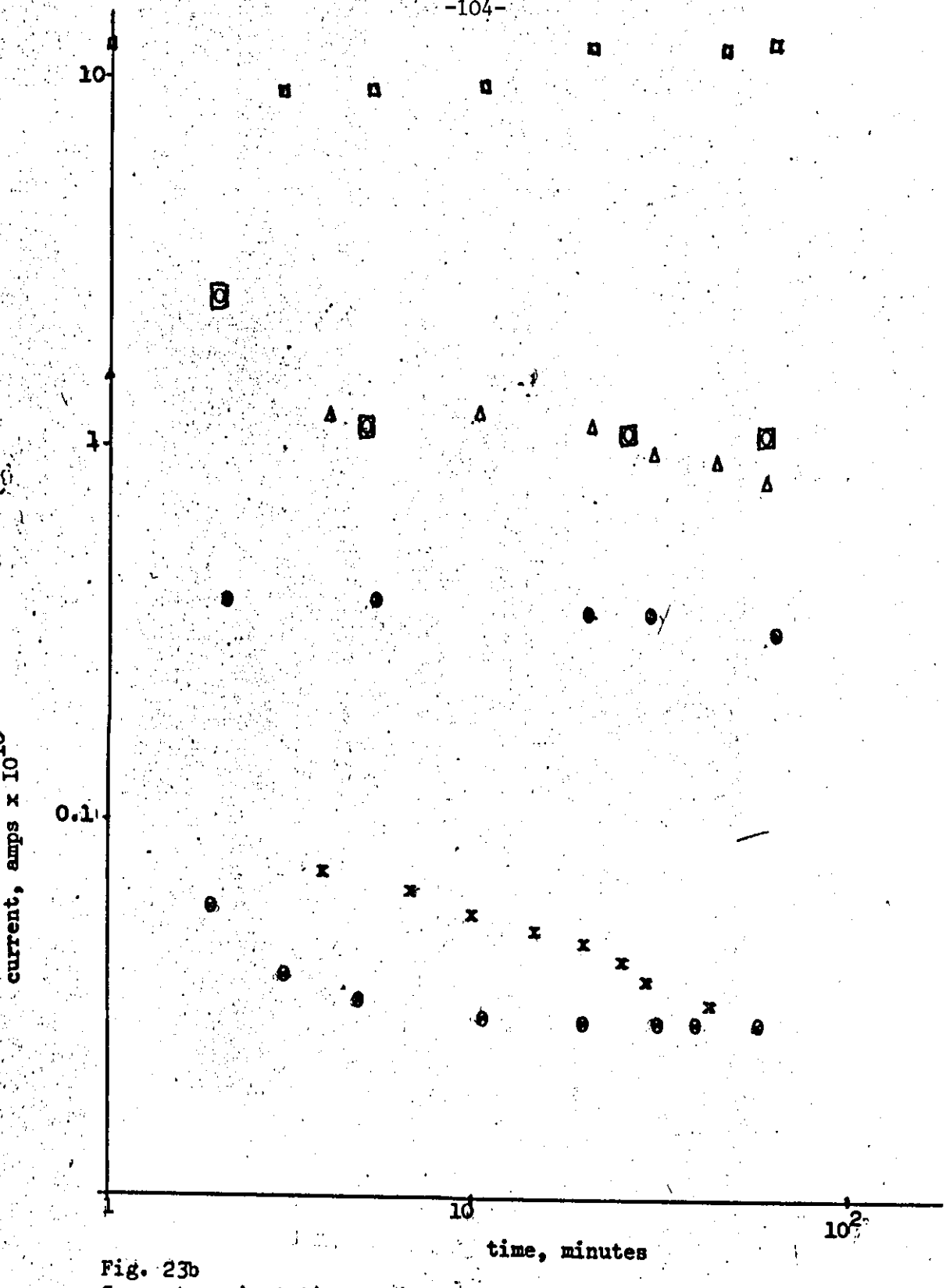

Fig. 23b
Current against time after stress application
electrode diameter 2½ inch

x, Δ, □ } sample X

θ, θ, □ } sample Y_2

⊗ } Applied stress 100 kV cm^{-1} (applied voltage 5 kV)
Δ, ⊙ } Applied stress 200 kV cm^{-1} (applied voltage 10 kV)
□, ⊡ } Applied stress 400 kV cm^{-1} (applied voltage 20 kV)

Dielectric thickness 20 mil

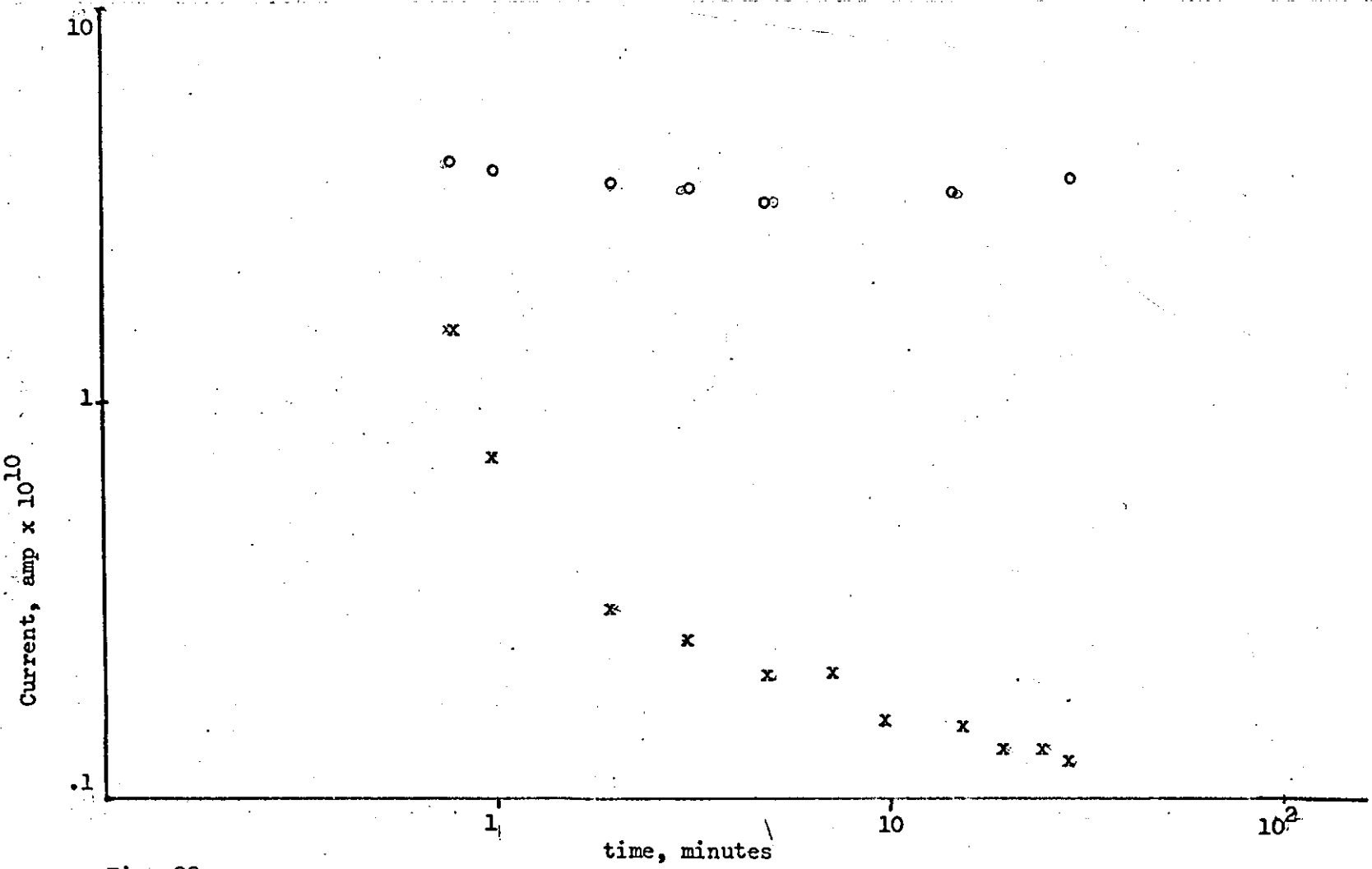

Fig. 23c
Circuit versus time after voltage application, positive polarity
Sample x
Electrode diameter 2¼ inch
x - applied voltage 5 kV
o - applied voltage 12 kV
Dielectric thickness 0.02 inch

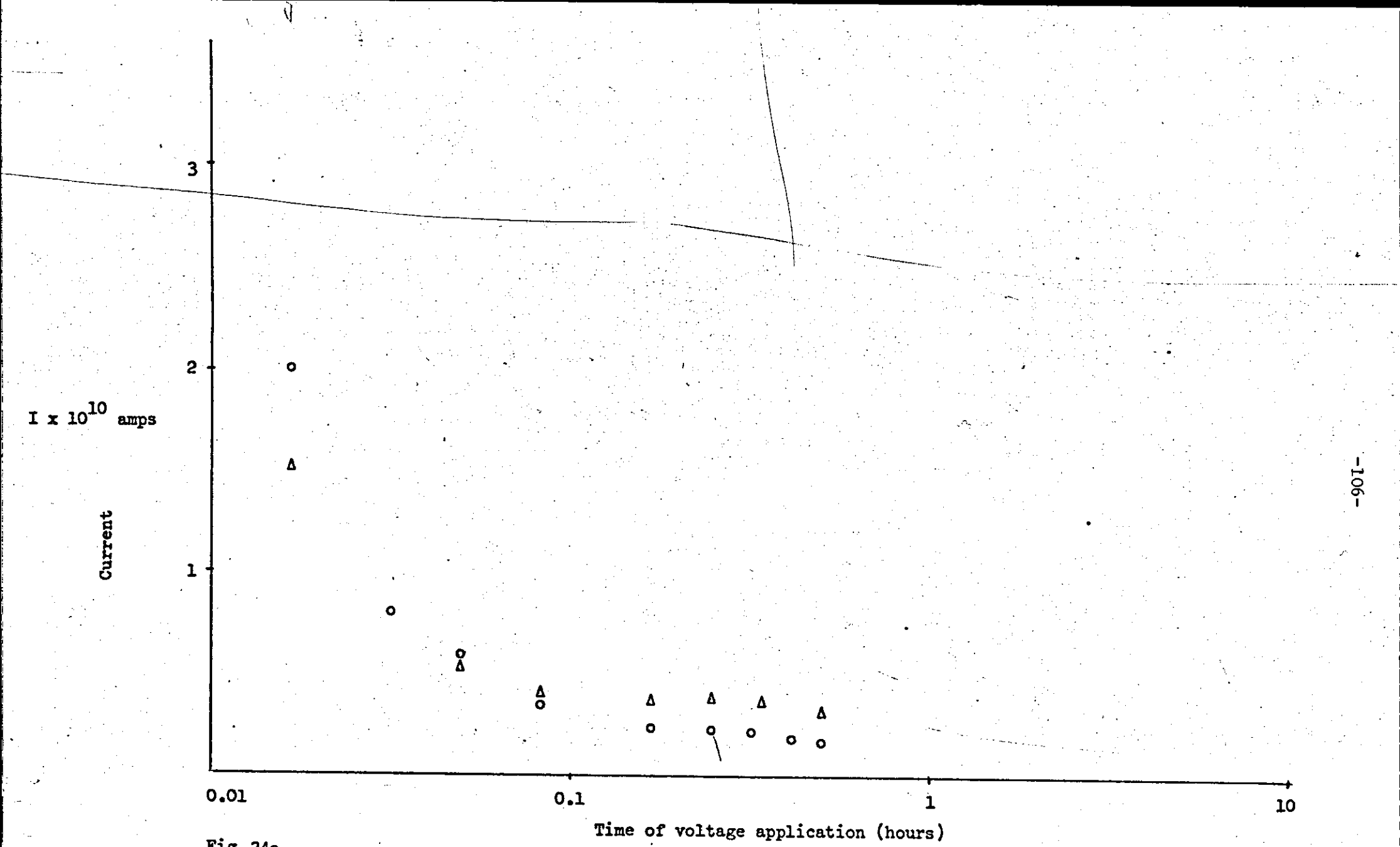

Fig. 24a
Graph of current against time of voltage application (hours)
20 mil (Bloore) Polythene
Δ light proof o Transparent From 1 to 5kV

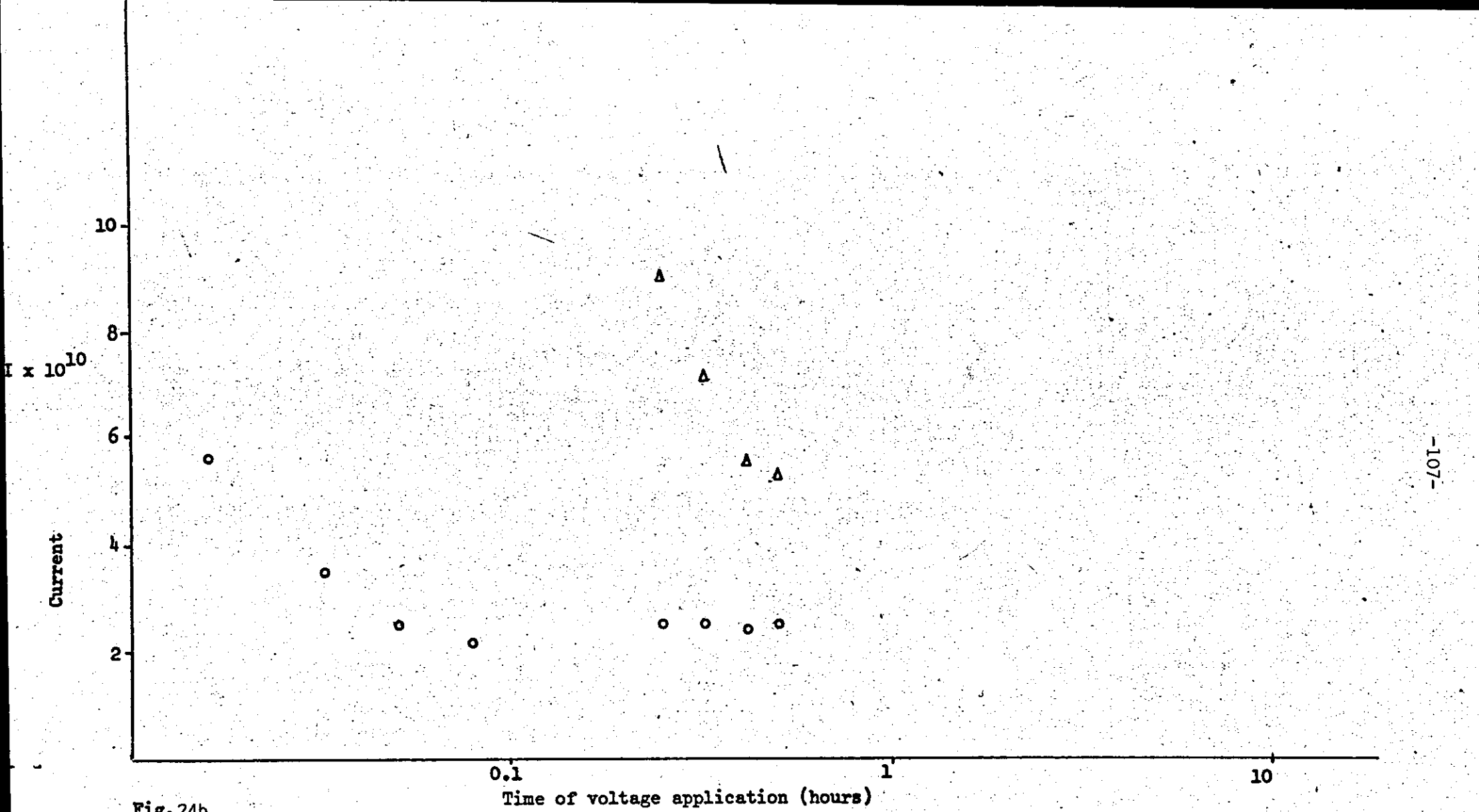

Fig. 24b
Graph of current against time of voltage application (hours)
20 mil (Bloore) Polythene - 2¼" electrodes
From 5-10 kV Δ - light proof cell
o - Transparent cell

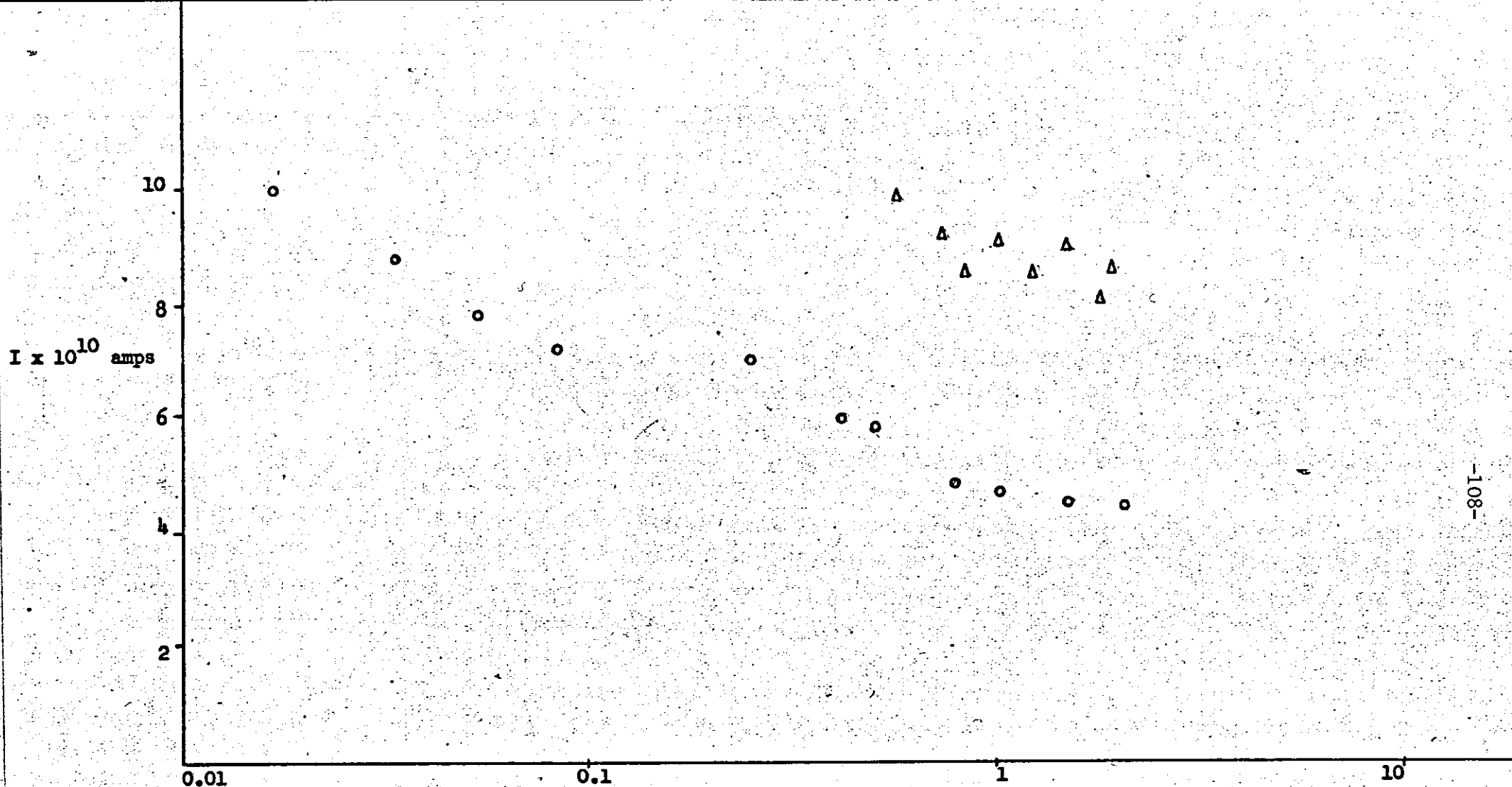

Fig. 24C
Graph of voltage against time — Bloore Polythene 20 mil @ 12kV
Δ light proof cell
o transparent cell
12kV (graphite painted electrodes)

increase of dielectric or electric strength, other explanations have also been offered[31]. Non-ohmic conduction begins at different stresses for different thicknesses of the same dielectric, the general tendency being for this to begin in thicker dielectrics at lower stress. With the polythene samples tested there was very little difference in this critical value of stress up to 0.01" but for thicknesses greater than 0.02" the changes were quite obvious. (Figs. 25-26). The results indicated that non-linearity started at much lower stresses in the resin samples compared with those manufactured from polythene (Fig. 27). The steady state current results also showed that, for the different polythene samples (X, Y_1, Y_2, Y_3), up to thicknesses of about 0.01" the conductivity for samples Y_1 and Y_2 were practically the same, however for thicknesses greater than 0.01" the steady state conductivity of sample Y_1 was more than that of sample Y_2. On the whole the steady state conductivity for the sample X was the highest for the four types of polythene. The steady state conductivity for Y_3 was more than that of either Y_1 or Y_2. It must be noted in connection with this that up to steady state conditions the transient conductivity of Y_2 was usually more than that of Y_3. The eventual polarization times for the samples Y_1 and Y_2 were the longest, and the sample X ~~with~~ had the shortest polarization time.

7.4.3 Surface and internal discharges

The magnitude and number of discharges over the surface of the insulation decayed over long periods (Fig. 19-20). This period of decay seemed to be of the same order as the time it took the current to decay to a steady state value. (This appears to bear out the work of Davies[5]). This 'time constant' however was in some cases more than just a few hours. This order of time constant is far higher (hours) than the normal polarization time constants (seconds) predicted by dielectric theory.

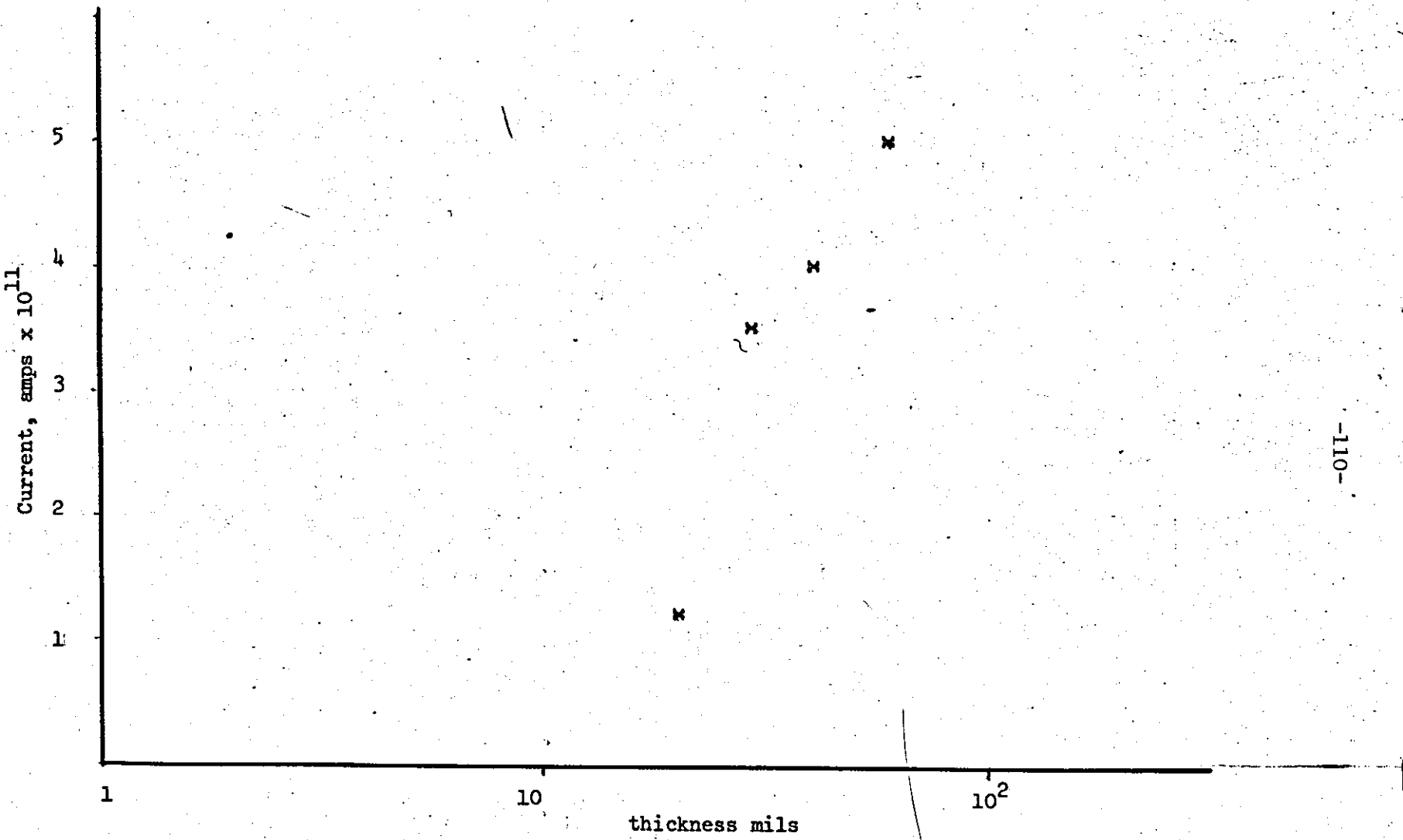

Fig. 25
Current against thickness
Epoxy resin sample
Fixed stress - 198 kV cm^{-1}

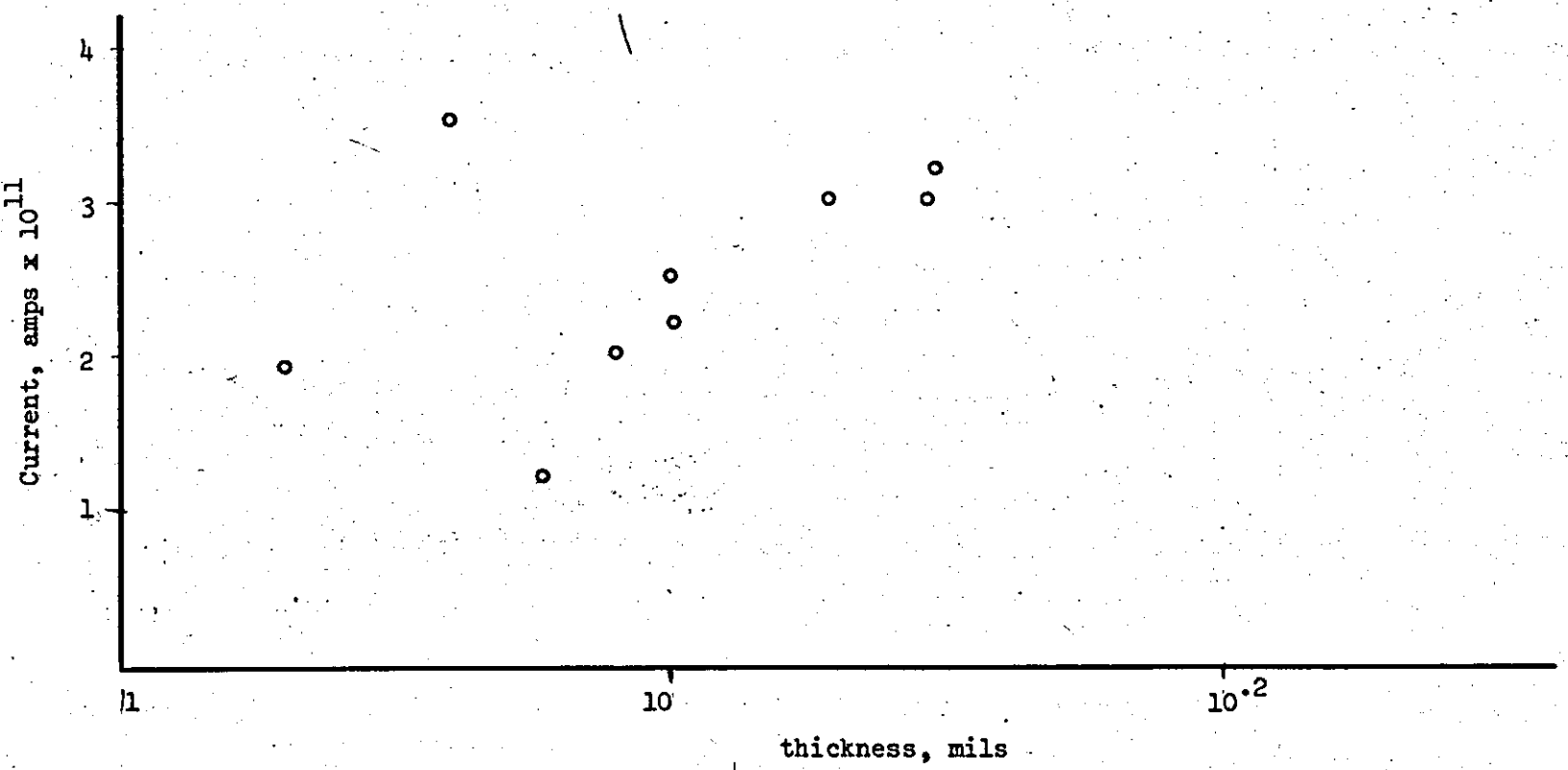

Fig. 26
Current against thickness
Sample Y_2
Fixed stress 395 kV cm^{-1}

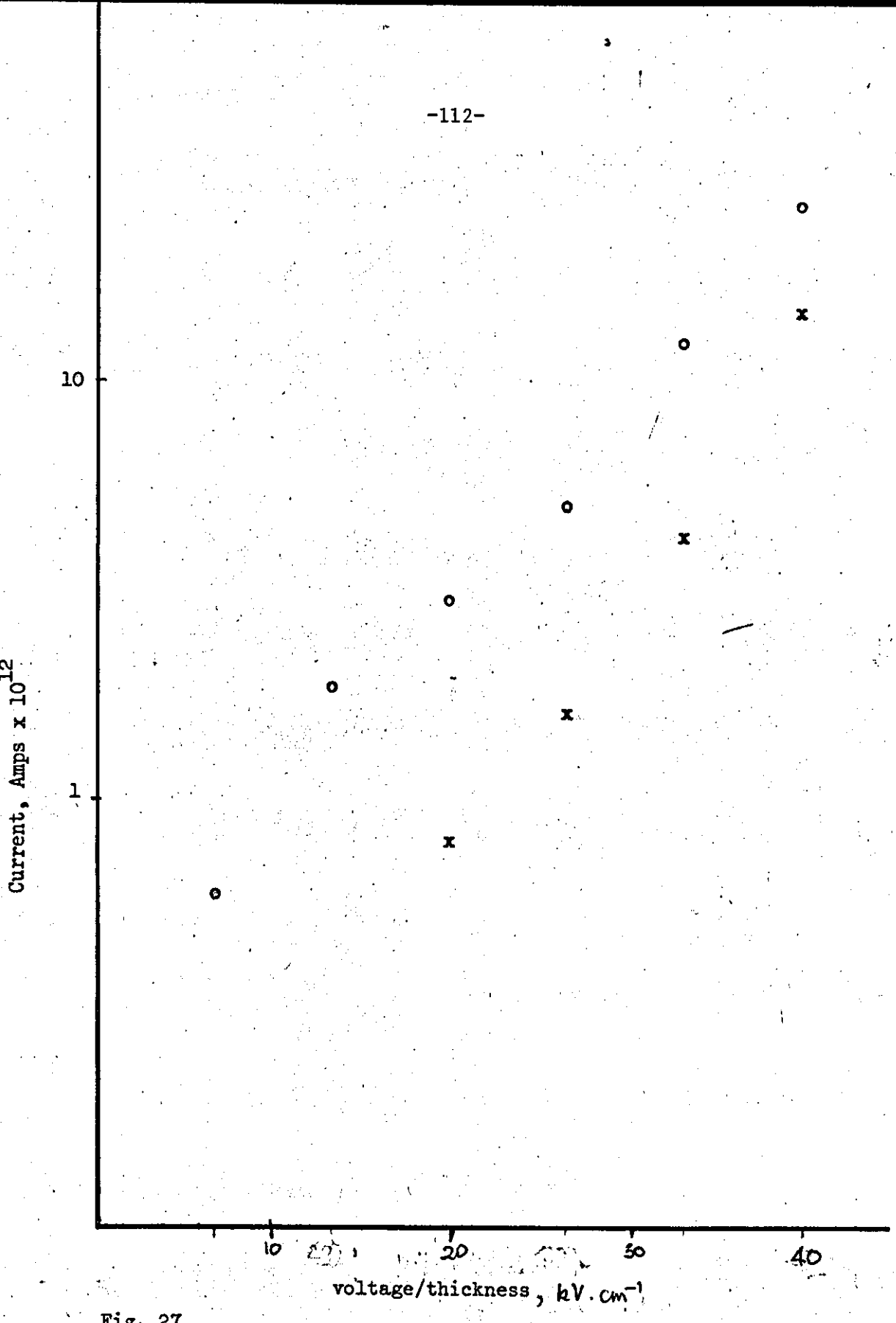

Fig. 27
x - thickness of dielectric 0.02 inch
o - thickness of dielectric 0.03 inch
Electrode diameter - 1.5 inch
Epoxy resin sample

These graphs also show that the decay rate of the surface discharge for the sample Y_2 was faster than for the sample Y_1.

It was also observed that the behaviour of internal discharges in response to a step voltage change was very similar to the current response (U.V. record 1B). There was an initial burst of discharges which rapidly reduced and a much slower decay which took a considerable time (Fig. 29). The former is the effect which is normally recognised as being due to a charging polarization process. However this initial burst of discharges occurred above a certain voltage. Below this voltage (termed the transient d.c. inception voltage) there were no discharges at all on increasing or decreasing the voltage (see U.V. record 2A). Above this voltage (V_i) and below a second voltage (V_2) this initial burst of discharges occurred on a step change but rapidly decayed to zero. Above V_2 discharges occur on a change which take a much longer time to decay to zero. (Compare with the a.c. case, U.V. record 2B).

If however the voltage is decreased some discharges start in the opposite direction (after a short time lag). These discharges could be very severe and cause a breakdown even though no d.c. steady state discharges occur with the voltage fully on. (Fig. 30 U.V. record 3A).

On still increasing the voltage above V_2 one arrives at the d.c. steady state inception voltage, where the discharges decay to a steady state value with a fairly regular repetition rate, Fig. 31. This repetition rate increases with stress (see Rogers and Skippers work)[39] so did the discharge magnitude to a lesser extent.

If at this point the voltage is reduced these steady state discharges decay fairly rapidly to zero. As they approach zero, reverse discharges (with direction opposite to the steady state ones) take over, increase in repetition rate and magnitude to a maximum and then decrease to zero eventually.

With regard to the discharge and gas breakdown tests, the following

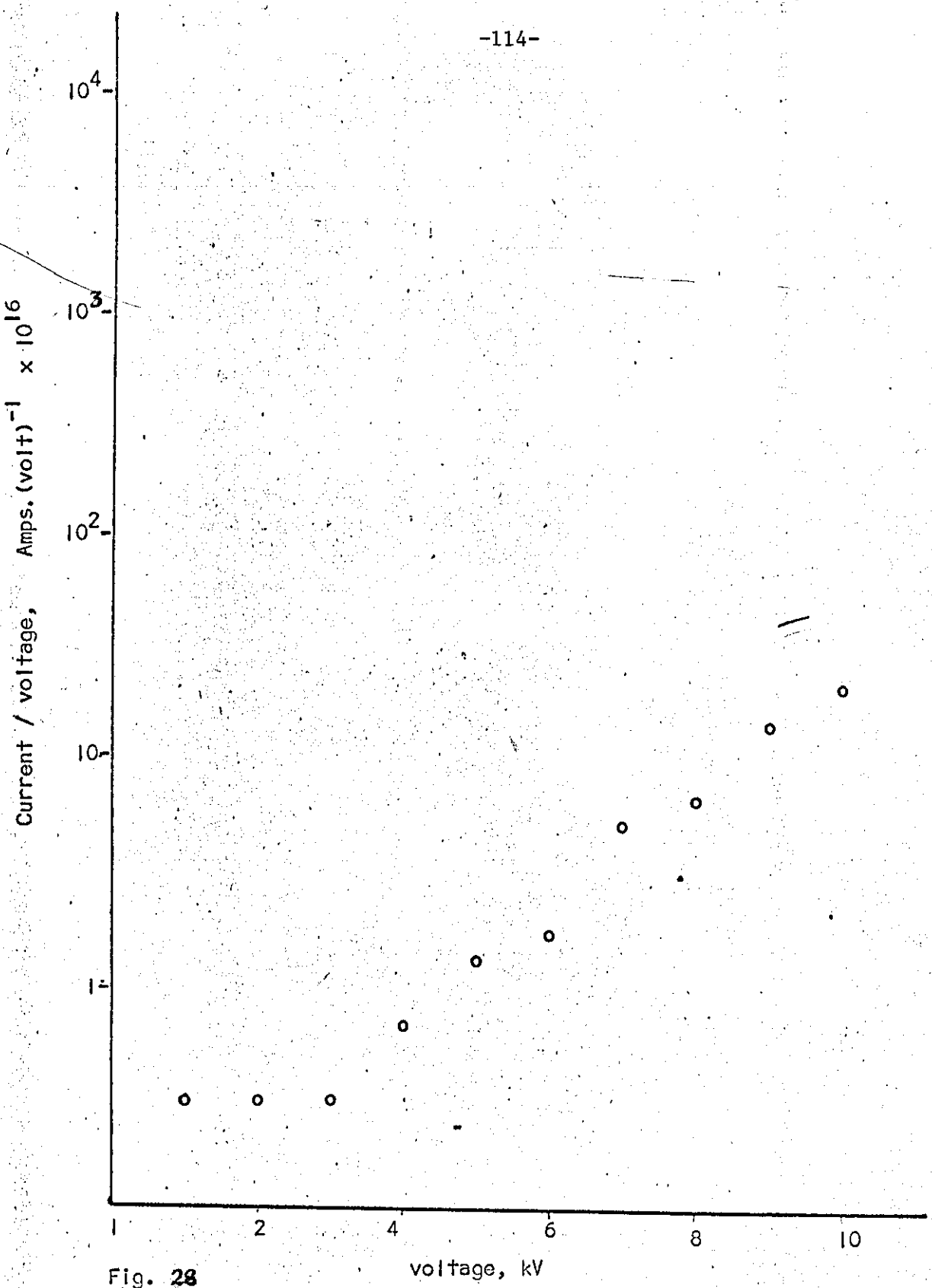

Fig. 28

Empirical law, log (current/voltage) versus voltage

Sample X,

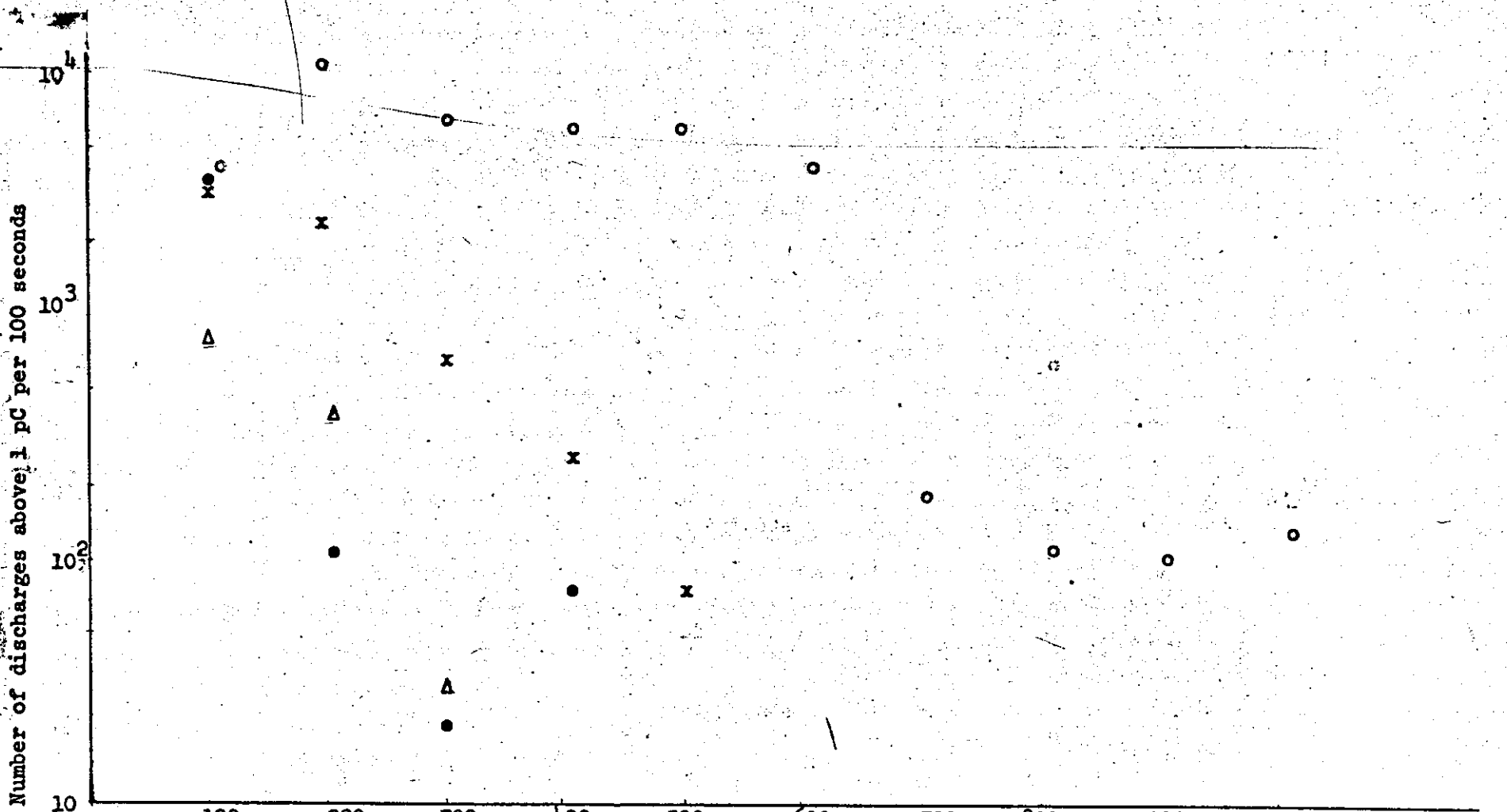

Fig. 29

O H.V voltage applied
Δ H.V. removed — air gap facing high voltage electrode
● H.V. applied
x H.V. removed — specimen portion removed

U.V. record 2A

(a) d.c. discharges - d.c. transient inception, d.c. steady state inception and decay of discharges.
(compare with U.V. records 2B)
sample as in fig.11b.

(b) Applied voltage trace
paper speed - 0.02 ins.sec^{-1}

U.V. record 2B

(a) a.c. discharges - inception and extinction. (Compare with U.V. record 2A) Sample as in Fig.11b.

(b) Applied voltage trace.
paper speed - 0.02 ins.sec^{-1}

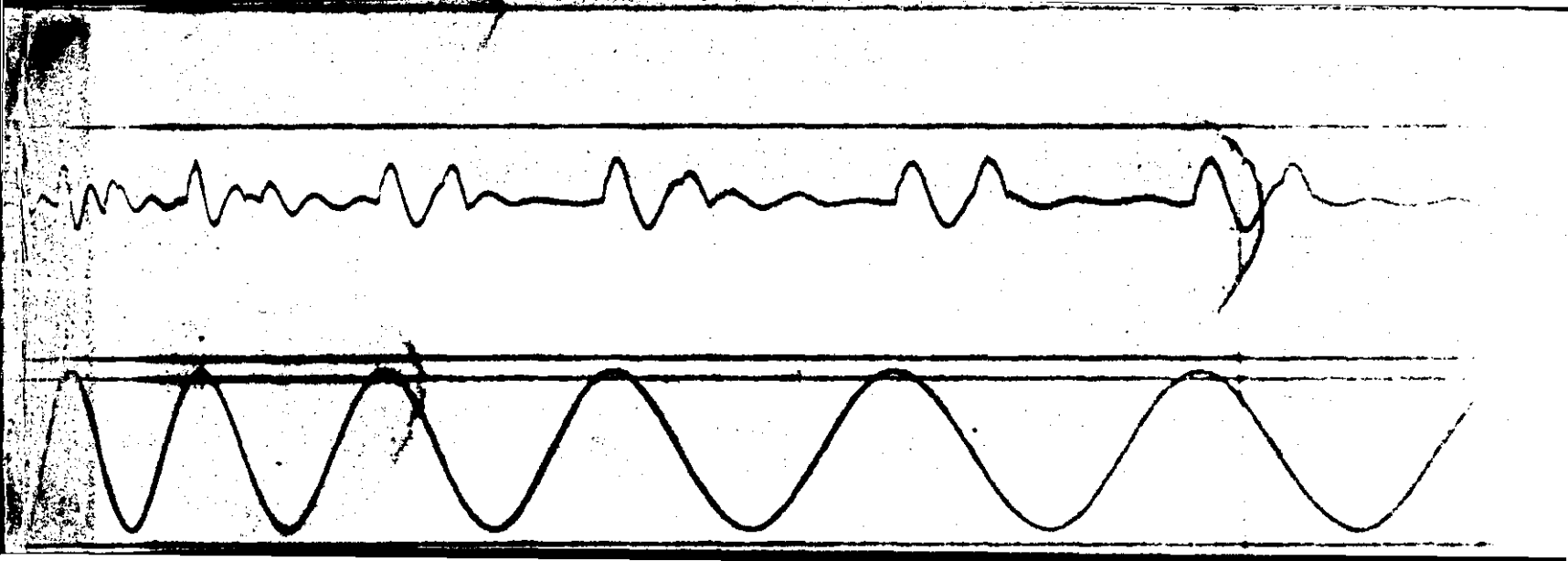


Above t.l.v.

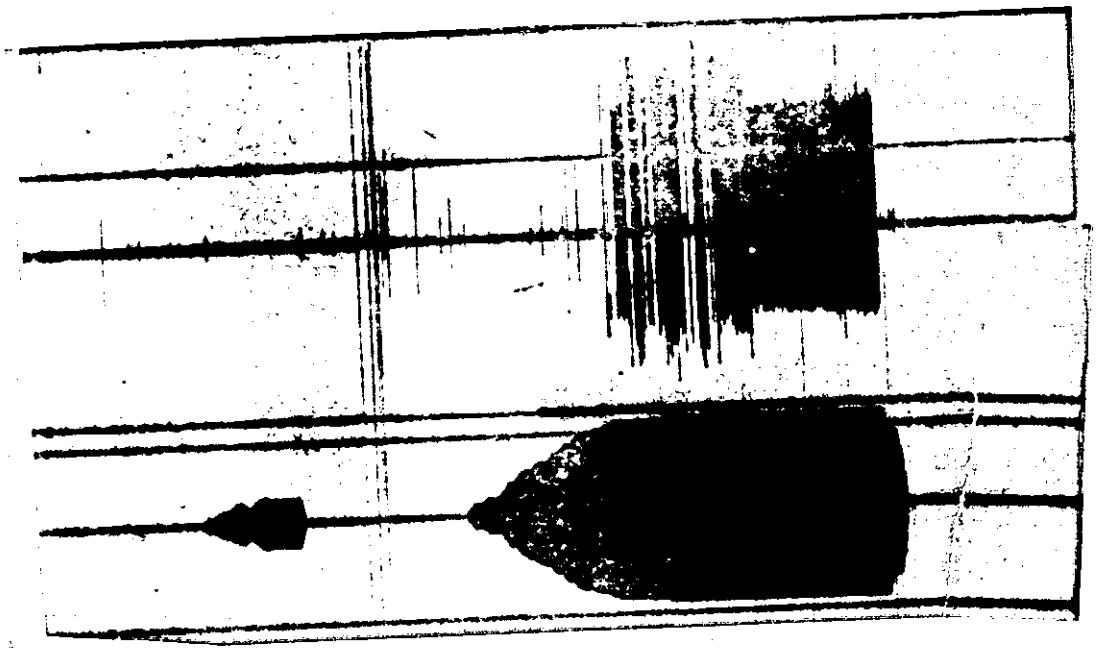

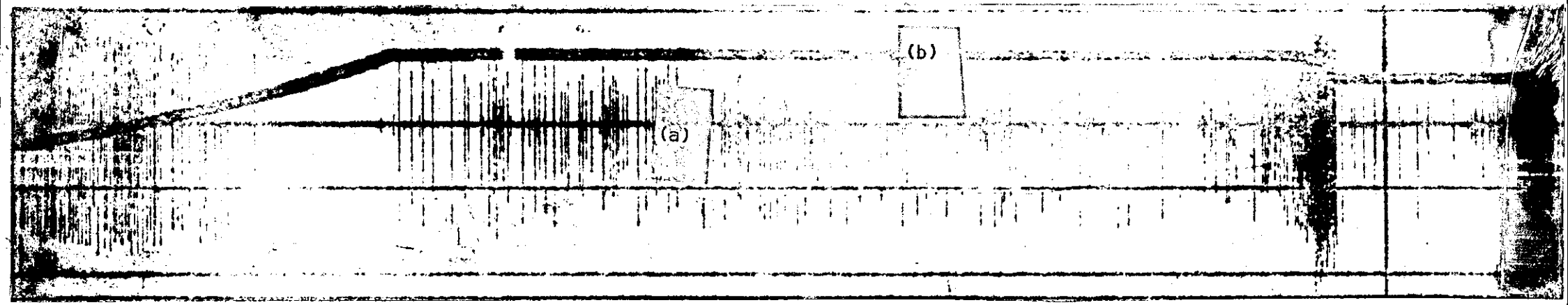
(b)
(a)

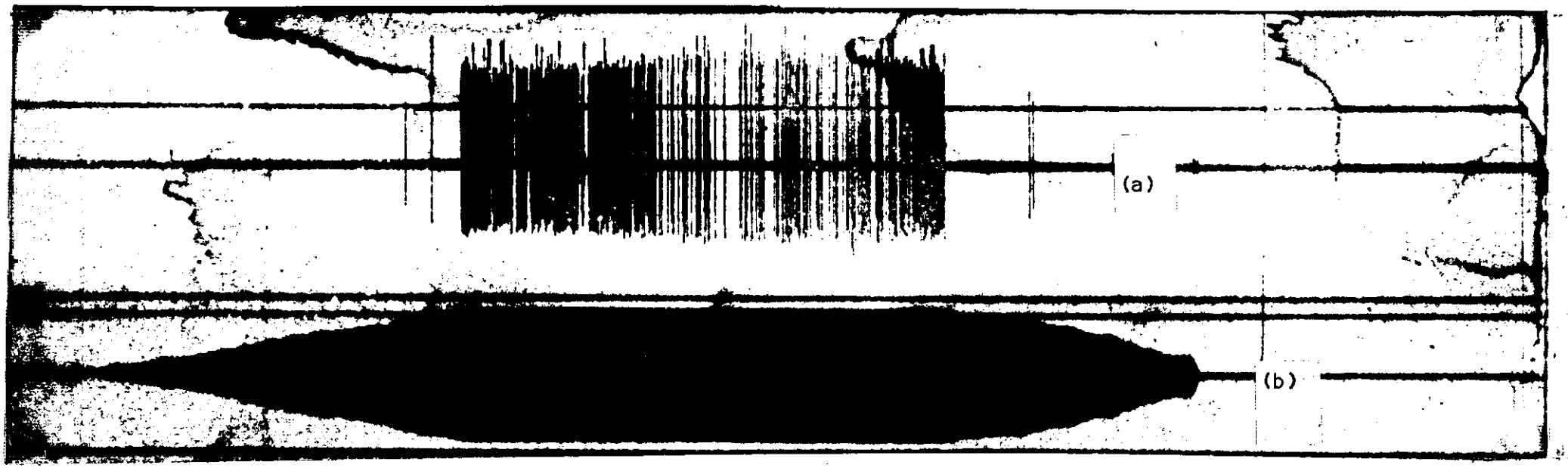
(a)
(b)

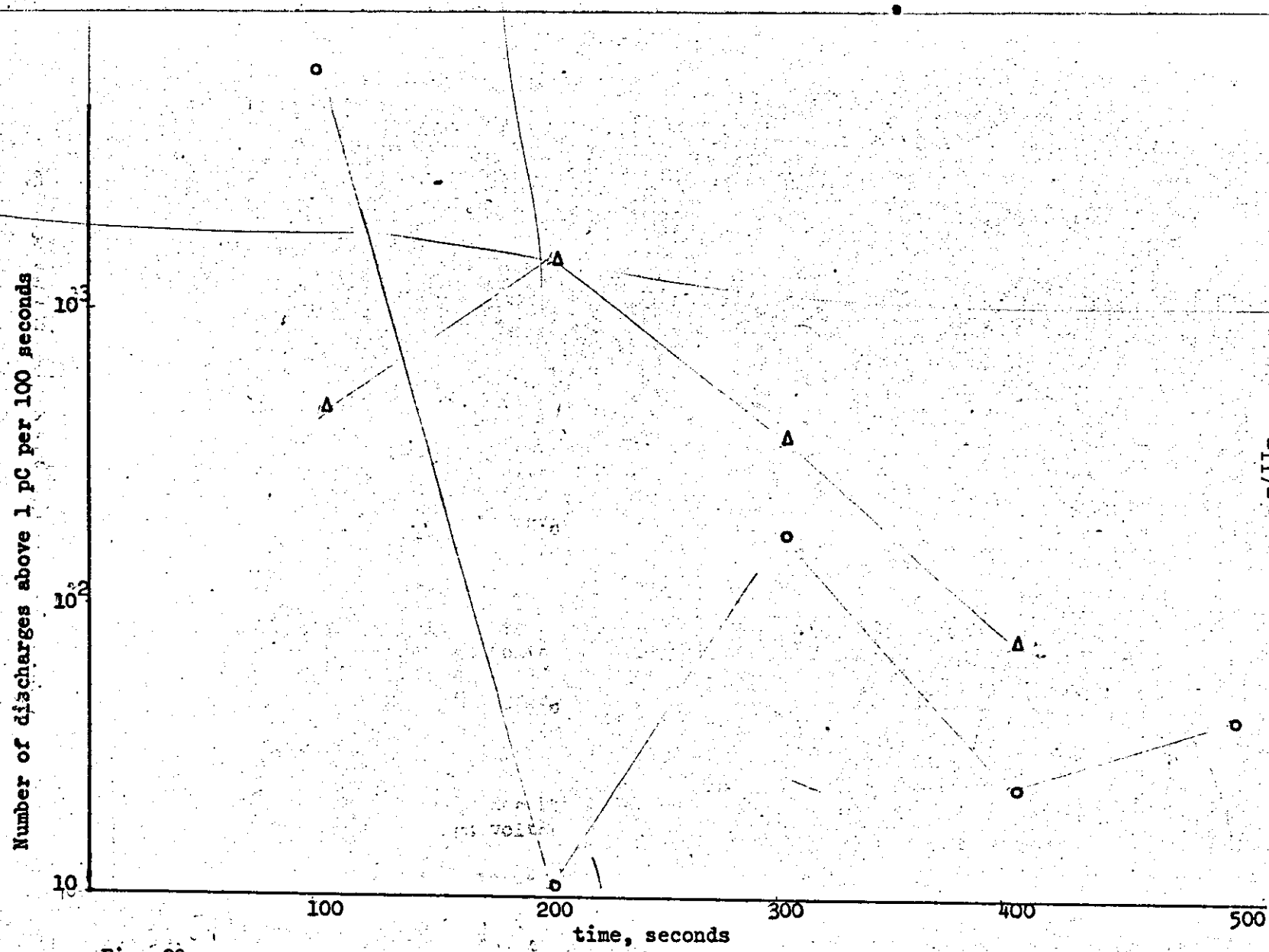

Fig. 30
Number of discharges above 1 pC per 100 sec against time
The air gap is nearest the high voltage electrode
O - high voltage fully applied
Δ - high voltage input reduced to zero

anomalies were observed: the breakdown voltage to gap length ratio decreased with gap length, Fig. 32. Also whereas under ohmic conditions the discharge inception voltage was independent of the axial gap void position (in a parallel plate configuration) for an air gap and dielectric in series. Under non-ohmic conditions the position of the gap/void influenced the inception voltage. (See U.V. record 3A, 3B).

It was also observed that if a dielectric was connected in parallel with an air gap, little or no change occurred in the inception voltage or repetition rate. Only when a resistance of value less than the overall resistance of the gap was put in parallel with the gap was a drastic change observed. In any case none of the polymers connected across the gap had any measurable effect on the discharge characteristics of the air gap. (See figs. 29-31, also see chapter 9).

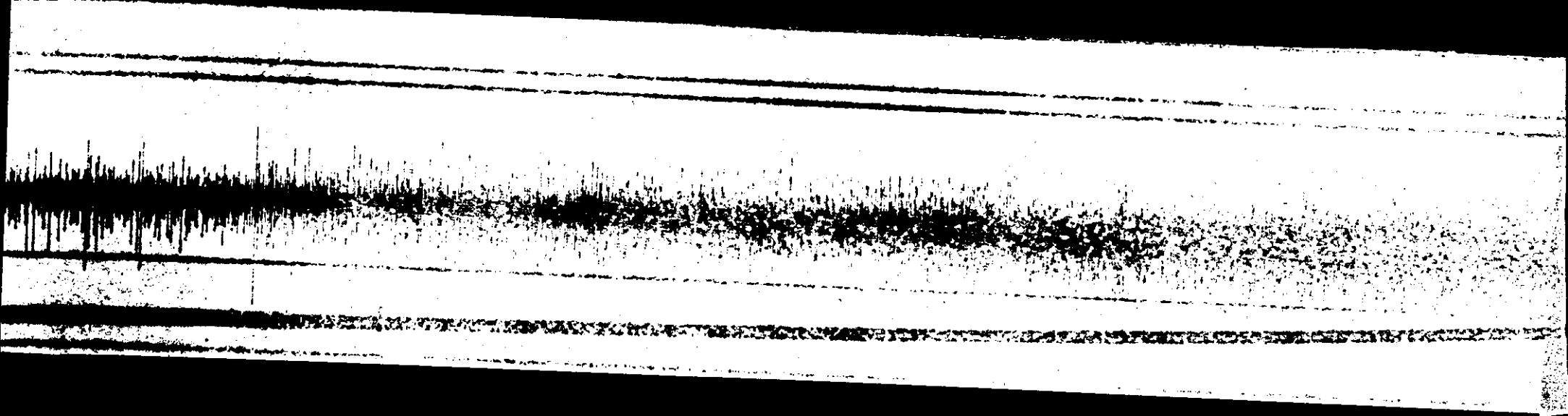

U.V. record 3A

(a) d.c. discharges - effect of void position on discharge characteristics, sample as in fig. 11b. void facing earth electrode. (compare with U.V. record 3B)

(b) Applied voltage trace
paper speed - 0.02 ins.sec^{-1}

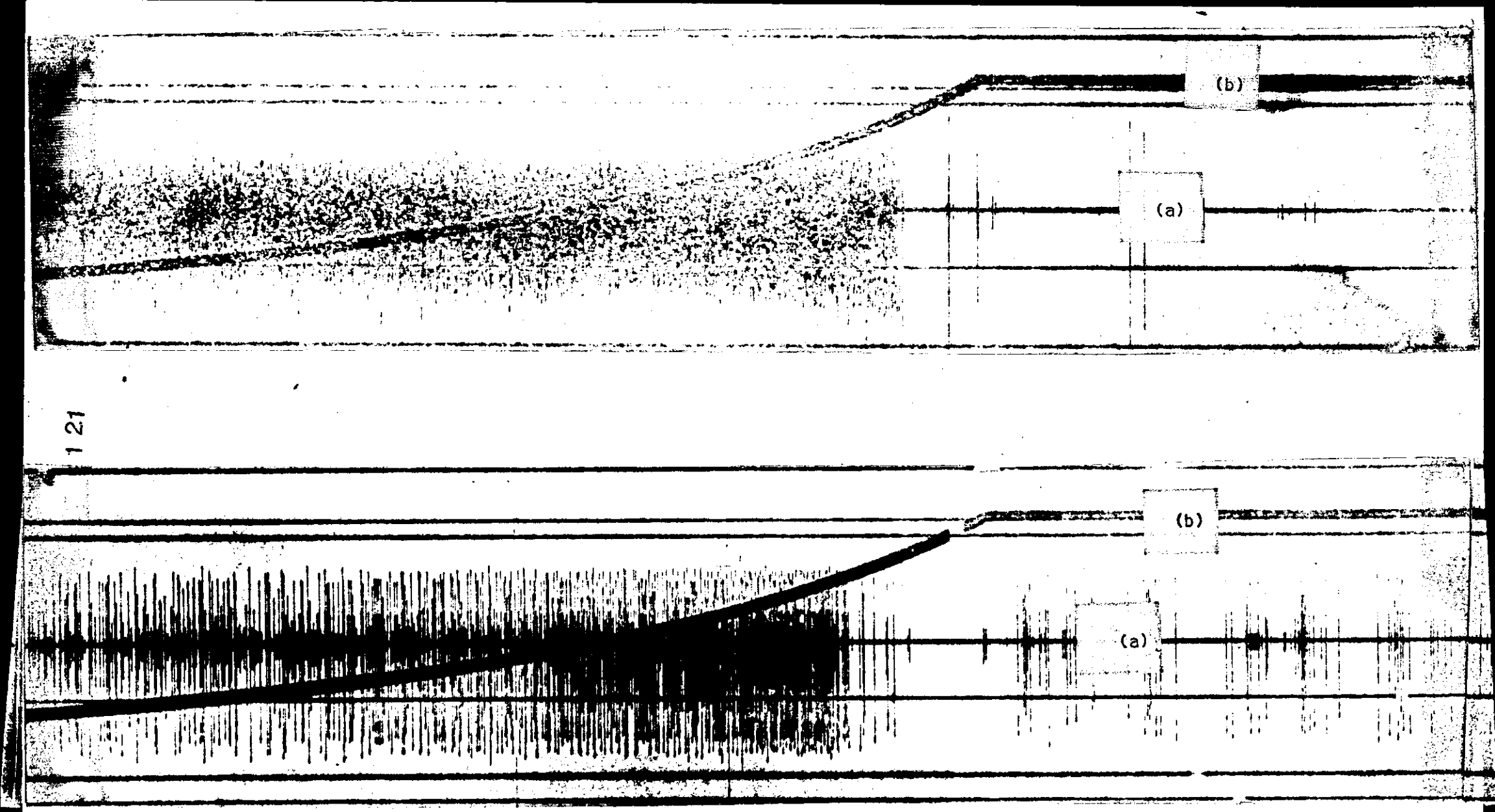
(b)
(a)
(b)
(a)

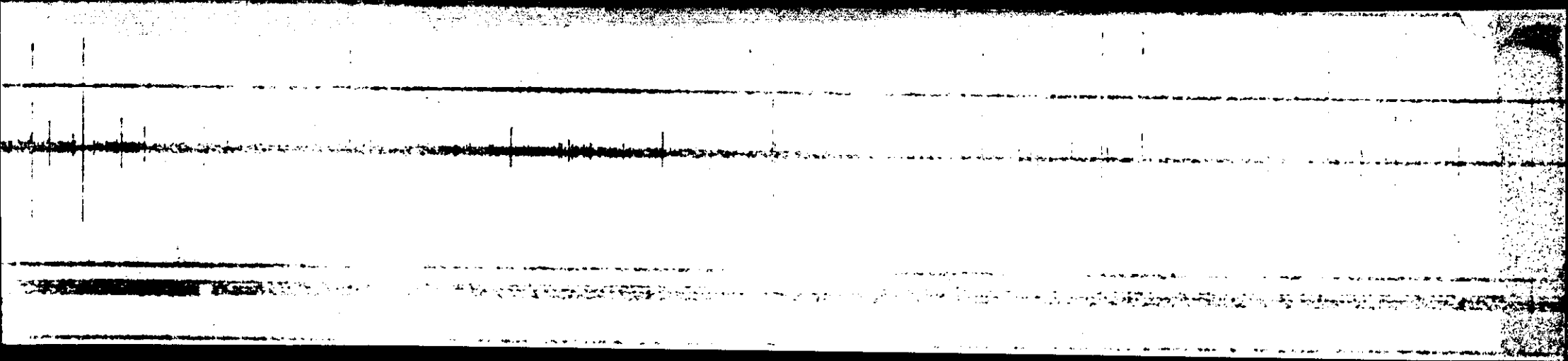

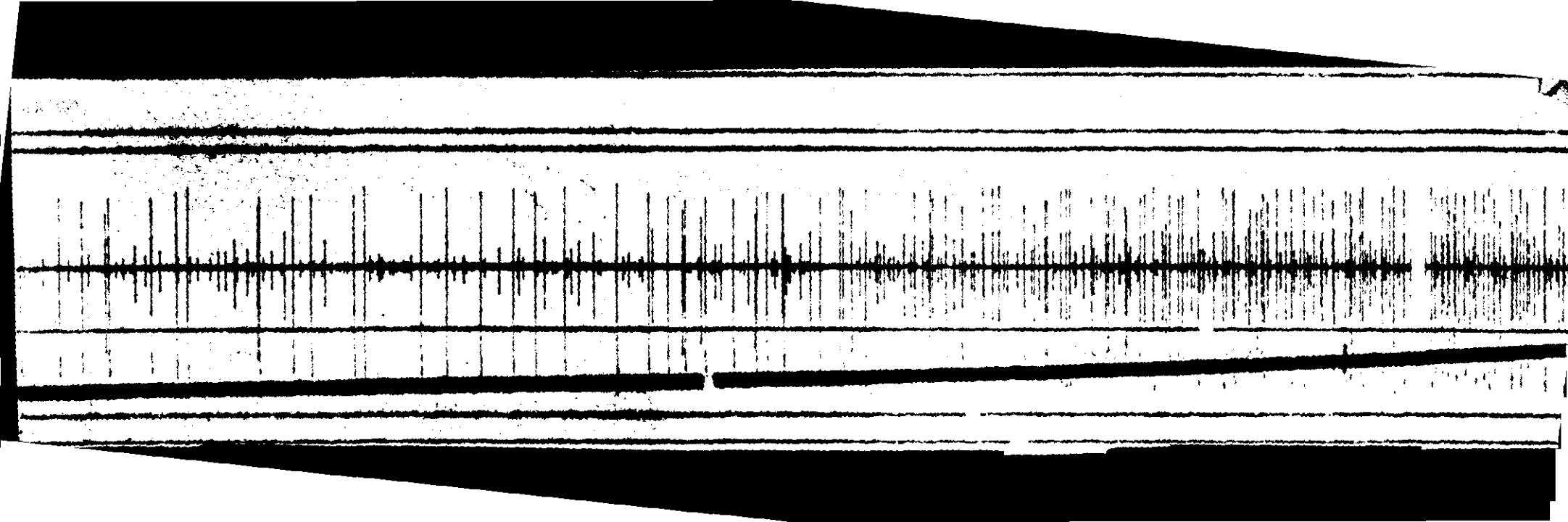

(a) U.V. record 3B
d.c. discharges - effect of void position on discharge characteristics, sample as in fig. void facing high voltage electrode.

(b) Applied voltage trace.
paper speed - 0.0 ins.sec^{-1}

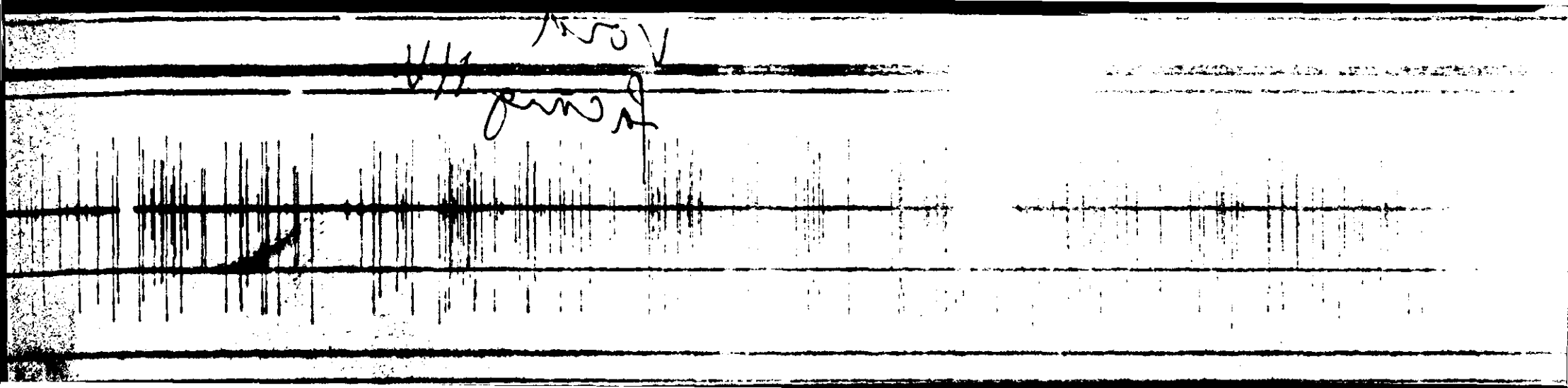

CHAPTER 8

Non-Ohmic and Anomalous Conductivity in Dielectrics

In order to analyse further and appreciate the results it is necessary to introduce a new dielectric equivalent circuit to replace the simple equivalent circuits, (Figs. 33a, 33b) which are normally used to represent the bulk properties of the dielectric such as its resistance capacitance and loss angle and also to explain the variation of current with voltage and time.

This new equivalent circuit and the ideas presented are intended to explain some of the anomalies such as the very long times for complete polarization, non-ohmic steady state conductivity, the possible increase of 'polarization' current with time and the thickness dependence of steady state conductivity. In order to achieve this it is assumed that there are at least two distinct charge carriers operative within the material for example, electrons and ions conducting simultaneously.

8.1 Theoretical considerations

Several workers[31,81,82], have stated that the current absorption formula for dielectrics is $I(t) = At^{-n}$ where $I(t)$ is current at any time t and A is a constant n being an index between o and 1. Objections to this formula have been raised on the basis that this is not a true representation of current response of a dielectric to a step function since this means that at $t = o$ $I(t) \to \infty$.

and at $t = \infty$, $I(t) \to o$.

Nevertheless this has been and is useful in explaining the complex time decaying phenomena in dielectrics at low stresses. At high stresses however this current response may be misleading to certain workers (notably high voltage engineers) since it has been observed that at high stresses $I(t)$ at $t \ggg o$ may be quite comparable to $I(t)$ for $t \to o$. Also the circuits mentioned above create the impression that initial 'charging' and eventual polarization time constants are equivalent.

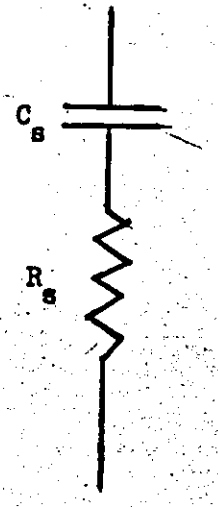

Fig. 33a

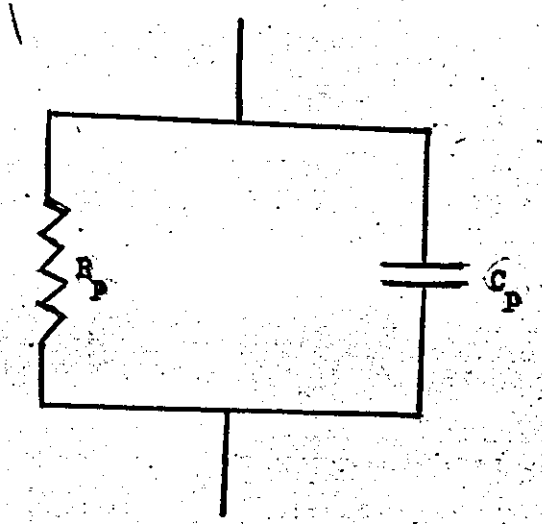

Fig. 33b

Simple Equivalent Circuits of a Dielectric

In order to deal with the phenomena of initial charging and eventual polarization, assume that initial charging and eventual polarization are different parts of the same time decaying processes. Then (from Figs. 34,) R_D' and C_D' will represent the time constant of the charging process and R_1, R_s C_s together with R_2, R_T, C_T the time constants of the polarization processes. (These parameters are stress dependent see Fig. 35). This type of concept is similar to the parallel series equivalent circuit employed as a Maxwell-Wagner two layer condenser (Fig. 36b) to explain interfacial polarization[43] at inhomogeneities within the dielectric or surface and bulk effects in heterogeneous dielectrics.

If the preferred equivalent circuit is to be consistent with the type of exponential decay functions observed by the author and others and also obtained by the irradiation of polythene[83], then there must be at least two time dependent exponential functions to explain the current response instead of the single exponential function yielded by the Maxwell-Wagner circuit (see section 8.3.1.) Also the time constants of the response are such that an equivalent circuit containing an inductance is inadmissible. (see appendix 2.5).

Hence this particular type of the two layer circuit was selected This circuit also covers the type shown in Fig. 36c as a star delta transformation will establish.

8.2 The new dielectric equivalent circuit

In the circuit in Fig. 36a assume that the components R_1, R_s and R_2, R_T are characterised by conductivities σ_1 and σ_2 or by charge carrier mobilities μ_1 and μ_2 and let the relative permitivites of C_S and C_T be ϵ_1 and ϵ_2 respectively. Then if a step voltage $v = o$, $t < o$, $v = V_A$ $t > o$ is applied, the current through the system can be shown by Laplace transformation and inversion to be (see appendix 2)

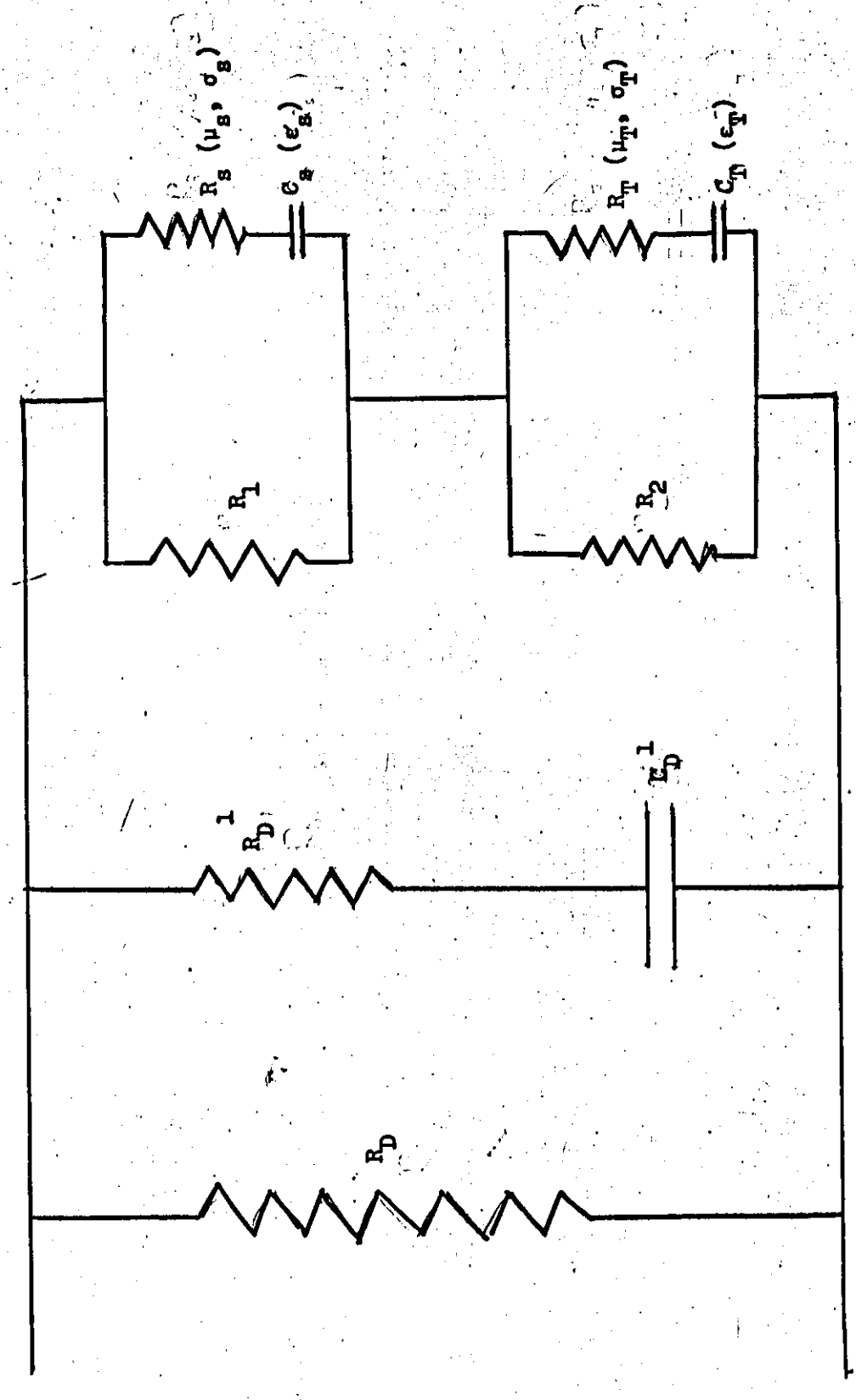

Fig. 34 A More Appropriate Equivalent of a Dielectric

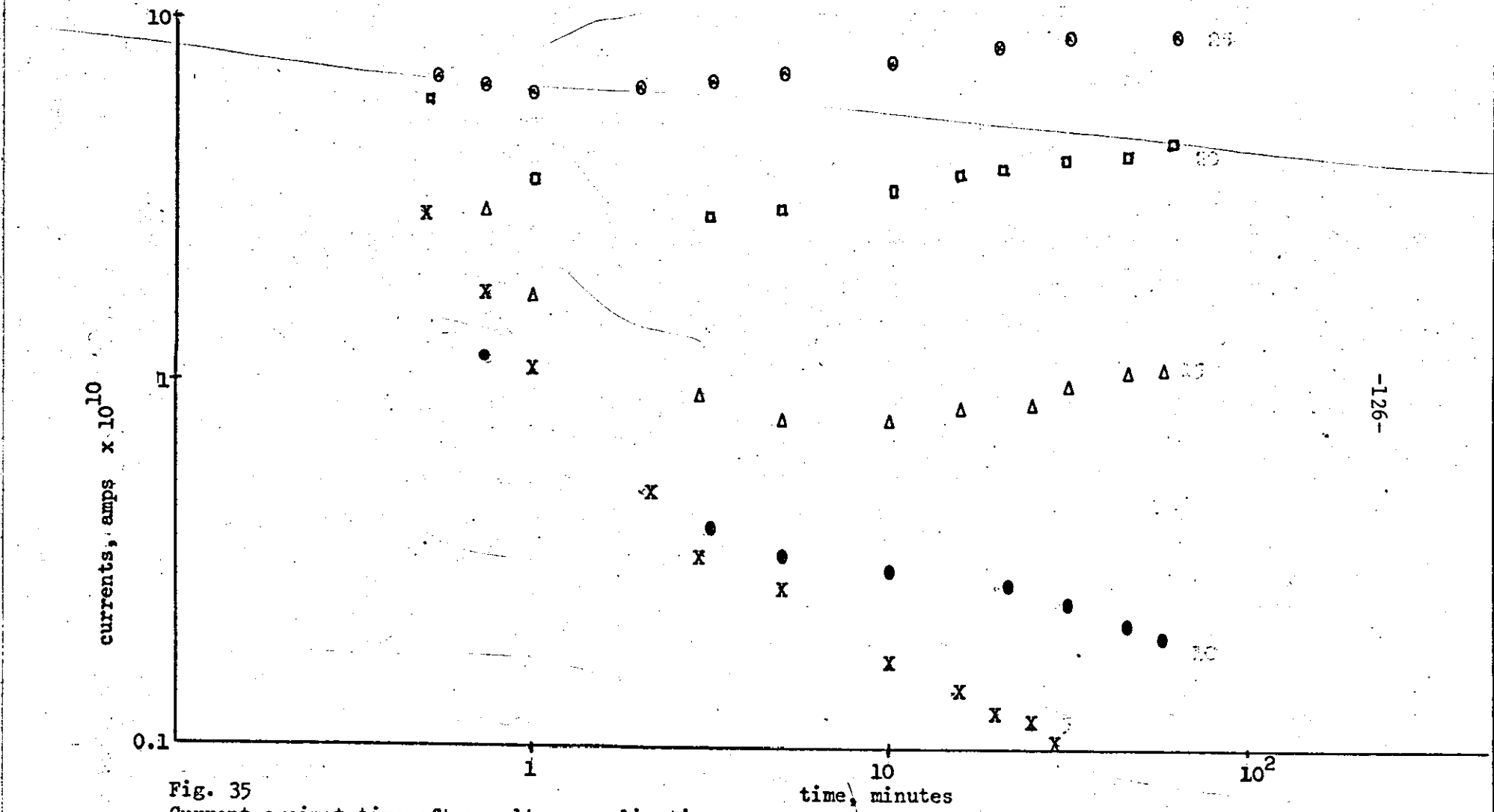

Fig. 35
Current against time after voltage application
Electrode diameter 1½ inches guarded
Dielectric thickness 0.02 inch
Sample X
X - applied voltage 5 kV
● - applied voltage 10 kV
Δ - applied voltage 15 kV
□ - applied voltage 20 kV
Θ - applied voltage 25 kV

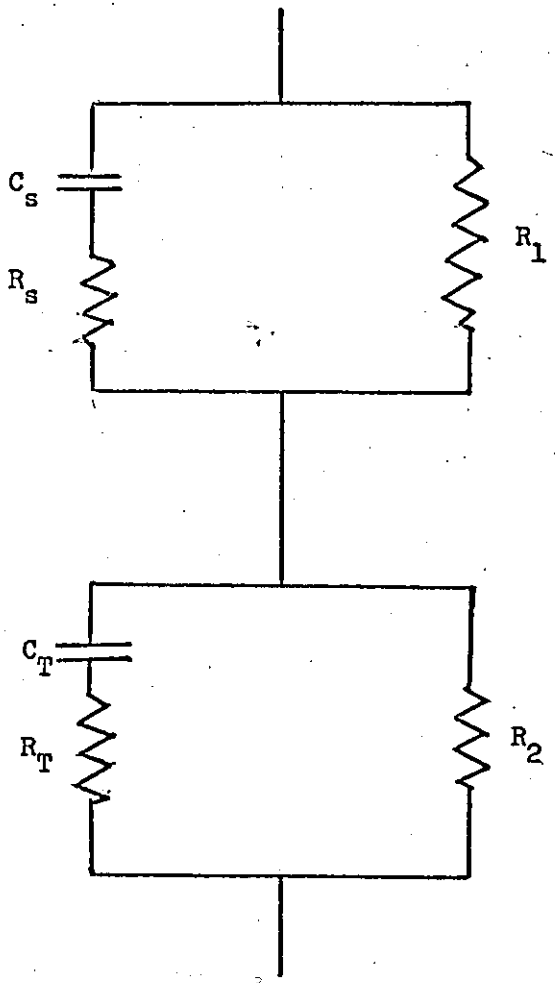

Fig. 36a

A Modified form of the 2 layer Condenser (I)

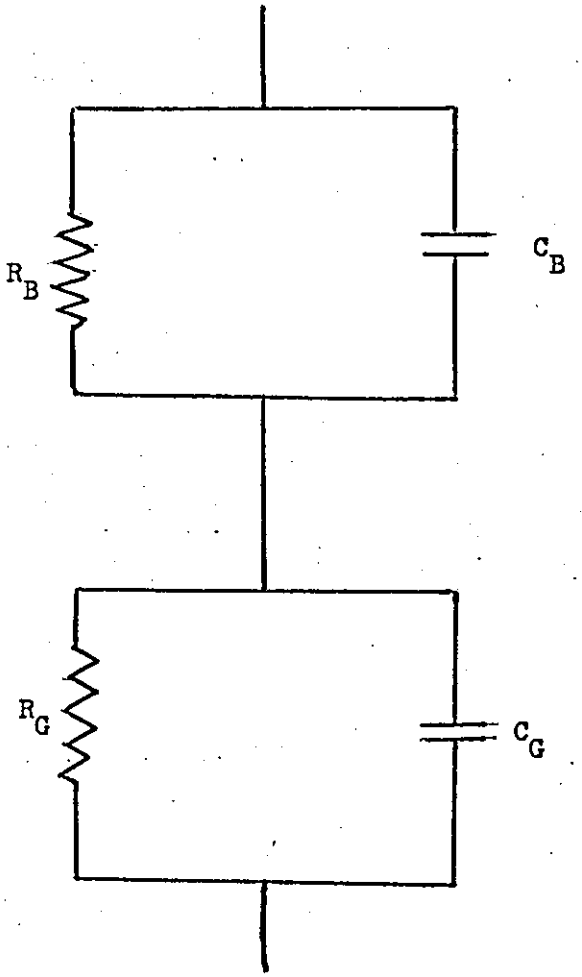

Fig. 36b

Wagner Two Layer Condenser

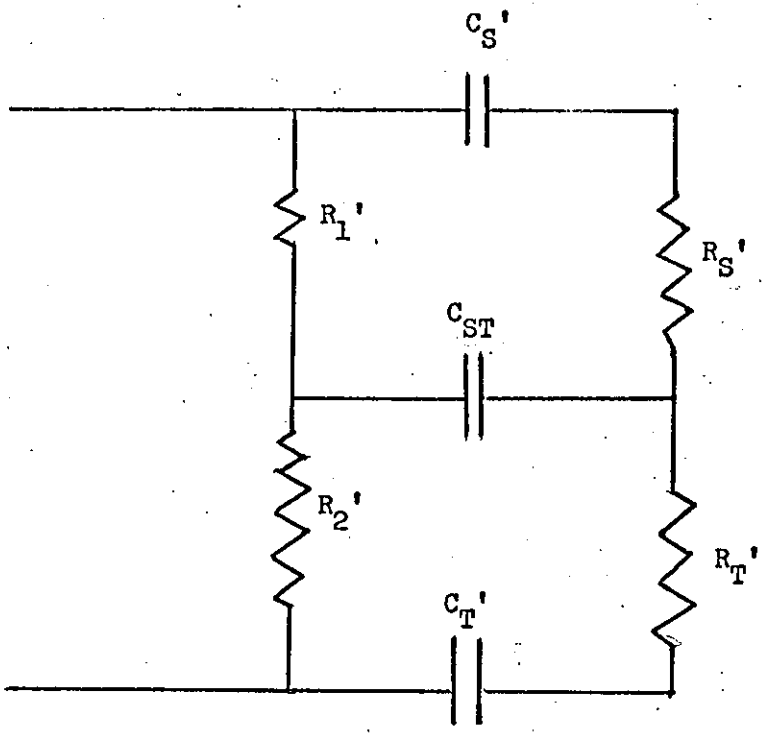

A Modified form of the 2 layer Condenser (II)

Fig. 36c

$$I_1 = \frac{V_A}{R_S + R_T}\left\{\frac{R_S + R_T}{R_1 + R_2} + \left[\frac{\beta C_S C_T R_2 R_S - C_T R_2 - C_S(R_2 + R_S)}{2\beta C_S C_T R_2 R_S}\right] \exp-(\alpha-\beta)t\right.$$

$$\left. + \left[\frac{\beta C_S C_T R_2 R_S + C_T R_2 + C_S(R_2 + R_S)}{2\beta C_S C_T R_2 R_S}\right] \exp-(\alpha+\beta)t \right\} \quad \ldots \quad 8.1$$

where 2α =

$$= \frac{C_T R_2(R_1 + R_T) + C_S R_1(R_2 + R_S)}{C_S C_T R_1 R_2(R_S + R_T)} \ldots \ldots \ldots \ldots \ldots$$

and $\beta^2 = \alpha - \frac{R_1 + R_2}{C_S C_T R_1 R_2(R_S + R_T)} \ldots \ldots \ldots \ldots \ldots \ldots$

assuming that $R_2 >> R_T$ and $R_1 >> R_S$.

It should be noted that the character of the exponential functions in equation 8.1 is very similar to that deduced for charge decay to explain reversal of charge in dielectrics[84] viz.

$$q(t) = \frac{\beta q_{fo}}{\beta-1} \exp(-t/\tau) + \left[q_o - \frac{\beta q_{fo}}{\beta-1}\right] \exp(-t/\tau_m)$$

where

τ = the relaxation time of the persistent polarization;

τ_m = the relaxation time of free charge with an allowance for short-circuiting (in a non-short-circuited electrect $\tau_M = \epsilon/4\pi\sigma$

$\beta = \tau_M/\tau$

q_{fo} = the initial hetero-charge density numerically equal to the persistent polarization.

The equation 8.1 also shows that for certain values of R_2, R_S, R_1, R_2, C_T, C_S the coefficient of the exponential expression $\exp-(\alpha-\beta)t$ may be negative, when this happens the type of response observed by Gershun and the author will be obtained.

Applying the principle of super-position and writing the admittances of R_D and R_D' with C_D' as $\frac{1}{R_D}$ and $\frac{pC_D'}{1 + pC_D'R_D'}$ (see Fig. 36a)

respectively where p is the Laplace operator p, the total current I will be given by multiplying this by the Laplace transform of V i.e. $\frac{V_A}{P}$, writing the Laplace inverse function and adding I_1.

i.e. $$I \text{ total} = \frac{V_A}{R_D} + \frac{V_A}{R_D'} \exp(-t/C_D R_D) + I_1$$

where R_2 and $R_1 >> R_D' >> R_D$, C_S and $C_T >> C_D'$

8.3 The Maxwell-Wagner equivalent circuit

8.3.1 The conventional analysis

When the same treatment is given to the Wagner-Maxwell two layer condenser one obtains a current of the form

$$i = \frac{V_A C_2 C_1}{C_1 + C_2} \left[\delta t + \frac{(R_1 C_1 - R_2 C_2)^2}{C_1 C_2 R_1 R_2 (C_1 + C_2)(R_1 + R_2)} \varepsilon^{-\psi t} + \frac{C_1 + C_2}{C_1 C_2 (R_1 + R_2)} \right]$$

... ... 8.2

where $\psi = \frac{R_1 + R_2}{R_1 R_2 (C_1 + C_2)}$

and δt is an impulse function.

It is obvious from equation 8.2 that since the coefficient of $\exp -\psi t$ is a perfect square the response mentioned earlier (Fig. 21) will never be obtained for all values of R_1 C_1 R_2 C_2, hence the equivalent circuit adopted by Adamec[83] is inadmissible.

8.3.2 A modified analysis I

A different expression for the current is however obtained for the circuit of Fig. 36b if one solves for this current by first solving for the voltage across one part say V_i and then writing the current as

$$I_1 = J_1 + \frac{\partial D_1}{\partial t} \quad \ldots \ldots \ldots \ldots \ldots \ldots \ldots \ldots \ldots \quad 8.3$$

in terms of a time changing voltage. In this case

$$V_1 = \frac{V_A C_2}{C_1 + C_2} \left[\frac{C_2R_2 - R_1C_1}{C_2(R_1 + R_2)} \varepsilon^{-\psi t} + \frac{R_1}{C_2} \left(\frac{C_1 + C_2}{R_1 + R_2} \right) \right] \ldots \quad \ldots \quad 8.4$$

Let $J_1 = \sigma_1 E_1$ (say) 8.5

and for simplicity

$D_1 = \epsilon_1 E_1$ 8.6

In general J may be defined as $J = \sigma_1 f(E)$ and $\frac{\partial D}{\partial x} (\epsilon E)$

where D is the normal electric charge displacement.

E_1 is the normal electric field intensity.

J_1 = current density

σ_1 = conductivity factor

ϵ_1 = permittivity factor

From equations 8.3, 8.5, 8.6

$$I_1 = \sigma_1 E_1 + \frac{\partial}{\partial t} (\epsilon_1 E_1)$$

$$= \sigma_1 \frac{\partial}{\partial x} V_1 + \epsilon_1 \frac{\partial}{\partial t} \cdot \frac{\partial}{\partial x} V_1$$

$$= \frac{\partial}{\partial x} \left\{ \sigma_1 V_1 + \epsilon_1 \frac{\partial}{\partial t} V_1 \right\} \quad \ldots \quad \ldots \quad \ldots \quad \ldots \quad \ldots \quad \ldots \quad 8.7$$

assume $\frac{\partial \epsilon}{\partial t} = o$

but from 8.4

$$\frac{\partial V_1}{\partial t} = \frac{V_A C_2 \psi}{C_1 + C_2} \quad \frac{(C_2R_2 - R_1C_1)}{C_2 (R_1 + R_2)} \quad \exp(-\psi t)$$

and $\psi = \frac{R_1 + R_2}{R_1R_2(C_1 + C_2)}$

therefore $\frac{\partial V_1}{\partial t} = \frac{-V_A}{R_1R_2(C_1 + C_2)^2} \quad (C_2R_2 - R_1C_1) \exp(-\psi t) \ldots \quad 8.8$

Therefore substituting equations 8.4 and 8.8 in equation 8.7

$$I_1 = \frac{\partial}{\partial x} \left\{ \frac{VC_2\,\sigma_1}{C_1 + C_2} \left[\frac{C_2R_2 - C_1R_1}{C_2(R_1 + R_2)} \exp(-\psi t) + \frac{R_1}{C_2} \left(\frac{C_1 + C_2}{R_1 + R_2} \right) \right] \right.$$

$$\left. \frac{\epsilon_1 V_A}{R_1R_2(C_1 + C_2)^2} (C_2R_2 - C_1R_1) \exp(-\psi t) \right\}$$

$$= \frac{\partial V_A}{\partial x} \left\{ \frac{R_1 \sigma_1}{R_1 + R_2} + (C_2R_2 - C_1R_1) \frac{\sigma R_1R_2(C_1 + C_2) - \epsilon(R_1 + R_2)}{R_1 R_2 (C_1 + C_2)^2 (R_1 + R_2)} \right\} \exp(-\psi t)$$

Once again this expression can have a response of the form shown in Fig. 21.

8.3.3 A modified analysis II

An expression whose response is similar to that in Fig. 21 can also be obtained if one solves for the current with an applied voltage of the form (see Appendix)

$$v = \frac{V_A}{K} \text{ from } t = o \text{ to } \tau \text{ and } V \text{ from } t = o \text{ to } \infty \; v = V$$

from $t = \tau$ to $t = \infty$

then for $t < \tau$

$$V_A \left[\frac{(t - T)}{K} + 1 \right] \quad \text{where } K >> 1$$

In this case the expression for current is given by applying the theorem of superposition.

i.e. $$i_c = \frac{V_A}{pZ_L} + \frac{V_A}{Kp^2Z_L} \quad \text{(from appendices 2.2 and 2.4)}$$

i.e. $$i_c(t) = \frac{V_AC_2C_1}{C_1 + C_2} \left\{ \delta t + \frac{(R_1C_1 - R_2C_2)^2}{C_1C_2R_1R_2(R_1 + R_2)(C_1 + C_2)} \exp(-\psi t) \right.$$

$$= \frac{C_1 + C_2}{C_1C_2(R_1 + R_2)} + \frac{1}{K} \left[\frac{t}{C_1C_2R_1R_2\psi} \right.$$

$$+\frac{C_2R_2 + C_1R_1}{C_1R_1C_2R_2\psi} - \frac{1}{C_1R_1C_2R_2\psi^2} - \frac{(R_1C_1 - R_2C_2)^2}{C_1C_2(R_1 + R_2)^2} \exp(-\psi t)\Big]\Big\}$$

But here again the solution can be eliminated from the possibilities by making k very small or $T \approx o$.

The foregoing analysis show that the conventional Maxwell-Wagner equivalent circuit as exists cannot produce the observed response, since it essentially contains a single exponential decaying function with a positive coefficient.

Bearing this in mind it is obvious that the circuits of Sillars[85] others[86,87] (Figs. 37a-38b), by inspection, cannot also give this anomalous current response.

8.4 Formation of an internal or space charge

8.4.1 Adaptation of Maxwell's analysis[88]

Now if the circuit in Fig.34 is the equivalent which gives the response in Fig.21 at these stresses, then R_1 must vary independently from R_2 hence there must be at least two possible types of mobility or conductivity within the dielectric. If this is so then Maxwell's theory of composite dielectric can be evoked.

Consider a parallel plate capacitor configuration with 'n' thicknesses of dielectrics with differing properties.

Then if we apply the theorem of superposition and consider isothermal conditions. The conduction and displacement currents can be separated into the following components

$$J^*_1 = \sigma_1 E_1 \quad \exp k_1 E_1 \quad \ldots \quad 8.9$$

$$\epsilon_1 E_1 = D_1 \quad \ldots \quad 8.10$$

Therefore the total current per unit area I_i is given by

$$I_1 = J_1 + \frac{\partial D}{\partial t} \quad \ldots \quad 8.11$$

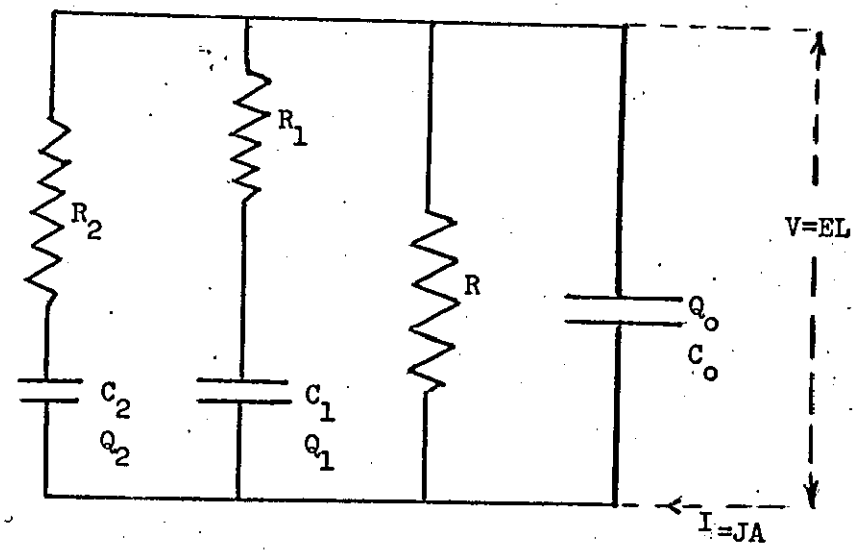

Tilley's Equivalent Circuit

Fig. 37a

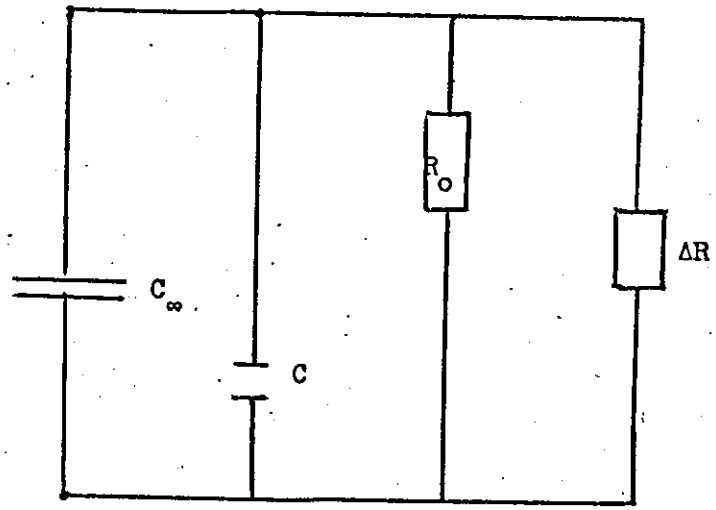

Kessler and Mariani's Equivalent Circuit
R_o - Ohmic Resistivity
C_∞ - Capacitance at Infinite Frequency
ΔC - Change in Capacitance
ΔR - Change in Resistivity

Fig. 37b

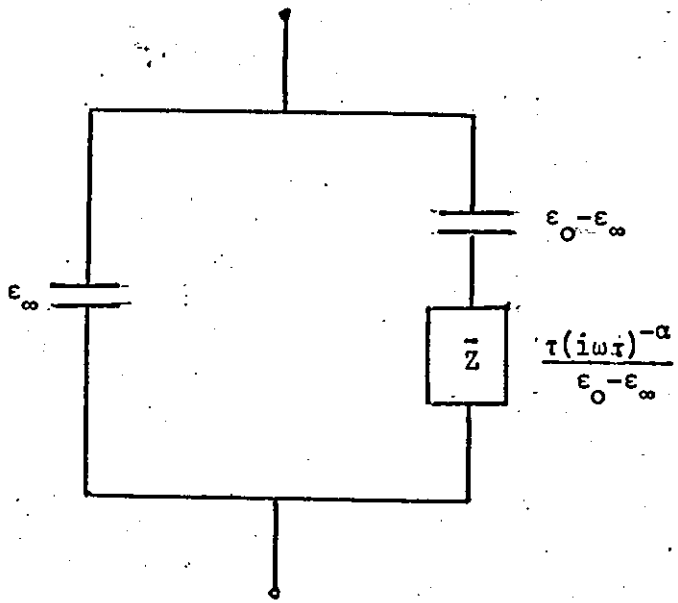

Fig 38a

Coles' Equivalent Circuit

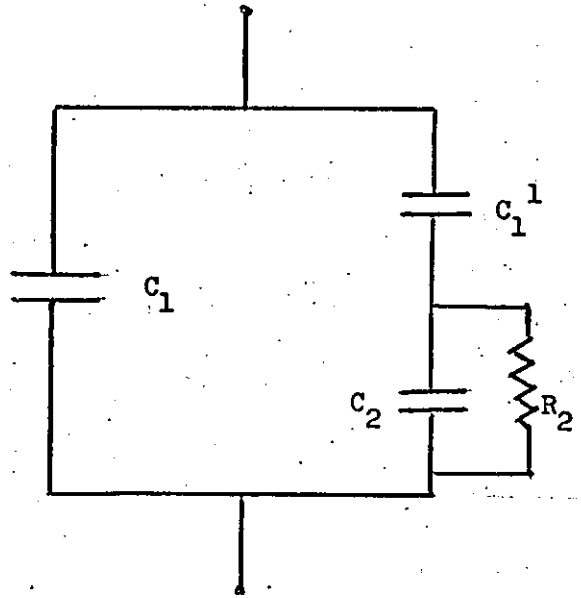

Fig 38b

Sillars' Equivalent Circuit

and $\rho_{12} = D_2 - D_1$ 8.12

$$\frac{\partial \rho_{12}}{\partial t} = J_1 - J_2 \text{ .. .. 8.13}$$

where σ_i and ϵ_i in the above case are defined as conductivity and permittivity functions respectively as against the conventional definitions.

Differentiating equation 8.12 with respect to t and equating to equation 8.13

$$J_1 + \frac{\partial D}{\partial t} = J_2 + \frac{\partial D_2}{\partial t} = I$$

also from 8.9, 8.10 and 8.11

$$I = \sigma_1 E_1 \ \text{expk}_1 E_1 + \epsilon_1 \frac{\partial E}{\partial t}$$

$$= E_1 (J_1 \ \text{expk}_1 E_1 + \epsilon_1 \frac{\partial}{\partial t})$$

*Under conditions where $\text{expk}_1 \epsilon_1 = 1$ i.e. kE = o the response in Fig. 21. has not been observed.

$$\therefore \quad E_1 = (\sigma_1 \ \text{expk}_1 E_1 + \epsilon_1 \frac{\partial}{\partial t})^{-1} I$$

If one assumes that E_1 across the elemental layer is linear then

$$V_A = E_1 d_1 + E_2 d_2 + \text{... ... ...} E_n d_n$$

$$\therefore V_A = I \left\{ d_1 (\sigma_1 \ \text{expk}_1 E_1 + \epsilon_1 \frac{\partial}{\partial t})^{-1} + d_2 (\sigma_2 E_2 \ \text{expk}_2 E_2 + \epsilon_2 \frac{\partial}{\partial t})^{-1} + \right.$$

$$\left. + \text{... ...} \ d_n (\sigma_n \ \text{expk}_n E_n + \epsilon_n \frac{\partial}{\partial t})^{-1} \right\}$$

$$= I \left\{ \frac{d_1}{\sigma_1 \ \text{expk}_1 E_1} (1 + \frac{\epsilon_1}{\sigma_1 \ \text{expk}_1 E_1} \frac{\partial}{\partial t})^{-1} + \frac{d_2}{\sigma_2 \ \text{expk}_2 E_2} (1 + \frac{\epsilon_2}{\sigma_2 \text{expk}_2 E_2} \right.$$

$$\left. \frac{\partial}{\partial t})^{-1} \right.$$

$$+ \frac{d_n}{\sigma_n \exp k_n E_n} \left(1 + \frac{\epsilon_n}{\sigma_n \exp k_n E_n} \frac{\partial}{\partial t}\right)^{-1} \Bigg\}$$

$$\text{If } \frac{\epsilon_1}{\sigma_1 \exp k_1 E_1} = \frac{\epsilon_2}{\sigma_2 \exp k_2 E_2} = \ldots \ldots = \frac{\epsilon_n}{\sigma_n \exp k_n E_n} = \frac{\epsilon}{\exp kE}$$

$$\text{Then } V_A \left(1 + \frac{\epsilon \partial}{\sigma \exp kE \, \partial t}\right) = I \left\{ \frac{d_1}{\sigma_1 \exp k_1 E_1} + \frac{d_2}{\sigma_2 \exp k_2 E_2} + \ldots + \frac{d_n}{\sigma_n \exp k_n E_n} \right\}$$

Now in the ideal case where $\epsilon_1 = \epsilon_2 = \ldots \ldots = \epsilon_n$ and $\sigma_1 \exp k_1 E_1 = \sigma_2 \exp k_2 E_2 = \ldots \ldots = \sigma_n \exp k_n E_n$ for $d_1 = d_2 = \ldots \ldots d_n$

and $kE \to o$.

(say in the charging of a capacitor at electronic voltages i.e. at very low stresses). This reduces to the familiar $I = \frac{V_A}{R} + C \frac{dv}{dt}$ where R is the charging resistance in series with a capacitor C. In this case kE is obviously zero.

At high stresses encountered in high voltage d.c. work however σ_1 and σ_2 may be different due to the possibility of more than one type of charge carrier.

Then under steady state conditions where

$$J_1 = J_2 = \ldots \ldots \ldots \ldots \ldots \ldots = J_n$$

we have $J_1 = \sigma_1 E_1 \exp k_1 E_1$

$$J_2 = \sigma_2 E_2 \exp k_2 E_2$$

$$J_n = \sigma_n E_n \exp k_n E_n$$

and assuming

$$D_1 = \epsilon_1 E_1 \text{ and } D_2 = \epsilon_2 E_2 \ \ldots \ \ldots \ \ldots \text{ and } D_n = \epsilon_n E_n$$

We may consider the following cases

(i) ohmic conditions

k_1E_1, k_2E_2, k_nE_n are approximately zero

$$D_1 = \frac{\epsilon_1}{\sigma_1} J_1$$

and $$D_2 = \frac{\epsilon_2}{\sigma_2} J_2$$

∴ Under steady state conditions

$$\rho_{12} = \left(\frac{\epsilon_2}{\sigma_2} - \frac{\epsilon_1}{\sigma_1}\right) J$$

and Total $\rho_1 \ \ldots \ \ldots \ n = \rho_{12} + \rho_{23} + \rho_{34} + \ldots \ \ldots \ \ldots + \rho_{(n-1)n}$

∴ $\Sigma\rho = \left(\frac{\epsilon_n}{\sigma_n} - \frac{\epsilon_1}{\sigma_1}\right) J$ For the simplest cases

but in general the total internal charge will be the sum of the separate interfacial charges.

(ii) Under non-ohmic conditions if $J = \sigma E \exp kE$

Then $\log J = \log \sigma E + kE$

In general $kE >> \log \sigma E$

∴ ρ_{12} is given by

$$\rho_{12} \doteq \log J \left(\frac{\epsilon_2}{k_2} - \frac{\epsilon_1}{k_1}\right)$$

In each case the total charge within dielectric equals $\Sigma\rho_{(r-1)r}$

Once again at electronic voltages this difference ρ_{12} is negligible or zero. At high direct voltages it may be significant and may well explain a lot of the anomalies[89,90] observed. (see figs. 39-42, U.V. records 4A, 4B.

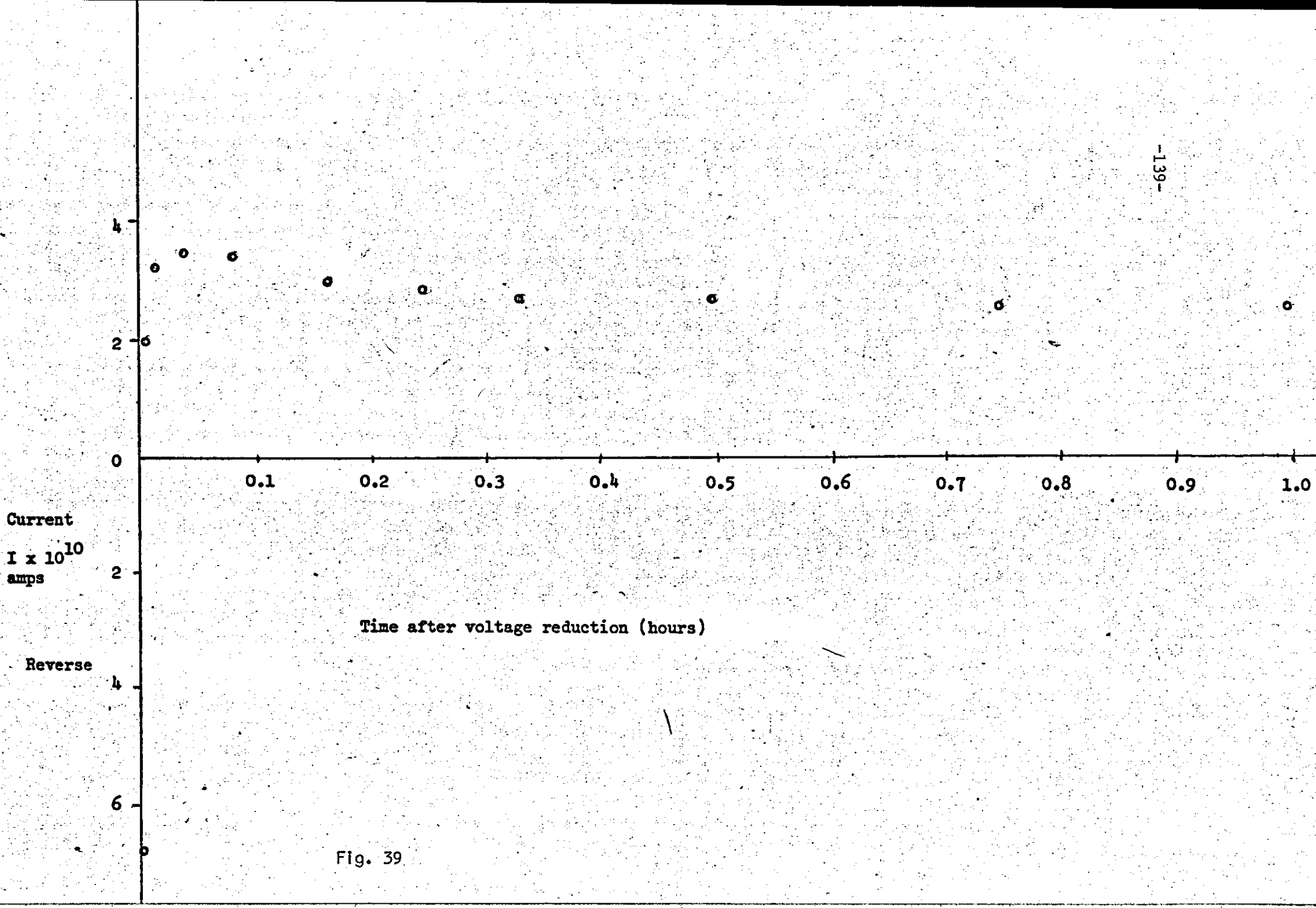
4
2
0
2
4
6
0.1
0.2
0.3
0.4
0.5
0.6
0.7
0.8
0.9
1.0
Current
I x 10^10
amps
Reverse
Time after voltage reduction (hours)

Fig. 39

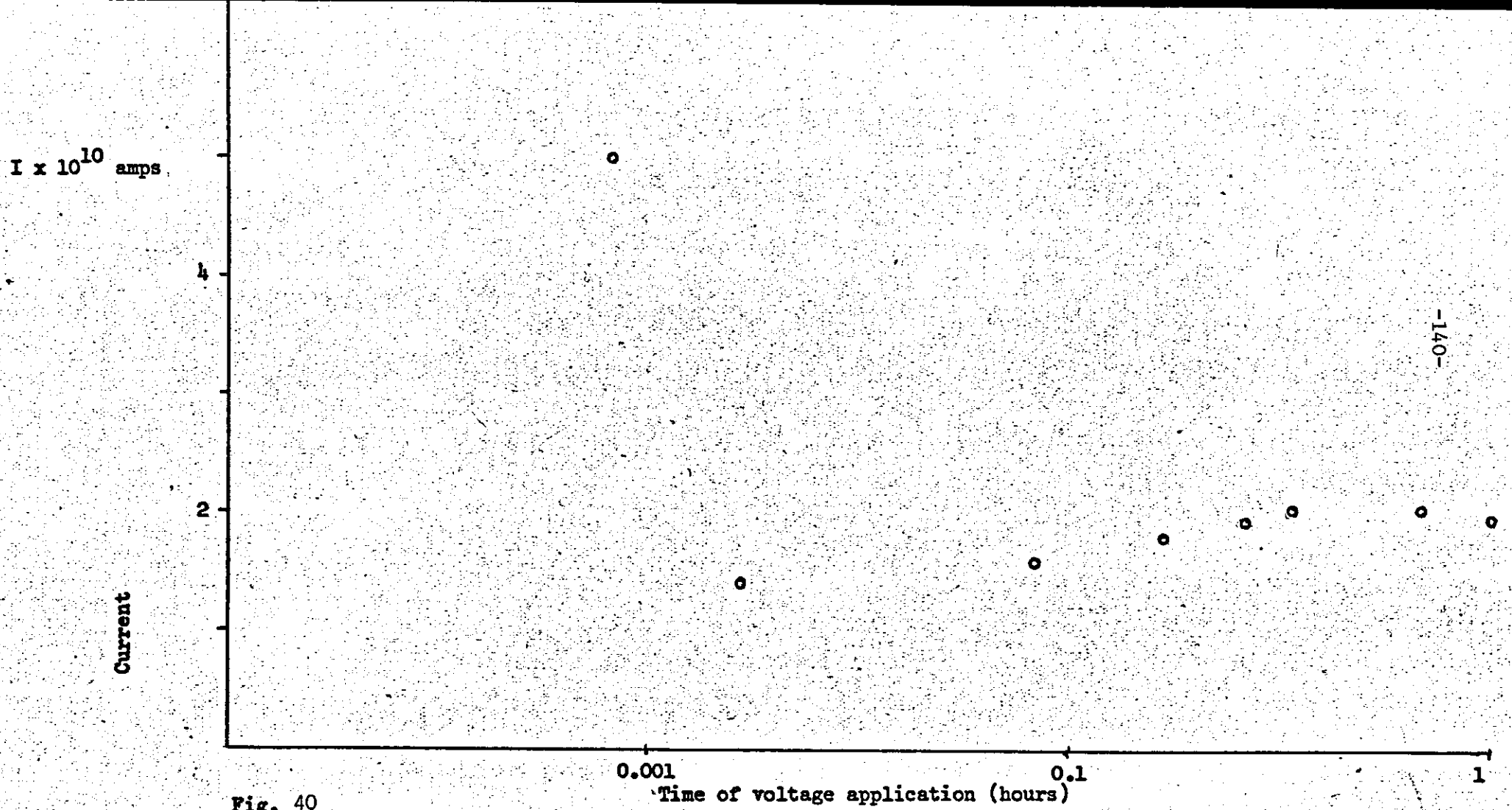

Fig. 40
Graph of current against time (hours)
AIR $\frac{1}{8}$" gap at 10kV - $1\frac{1}{2}$" electrodes

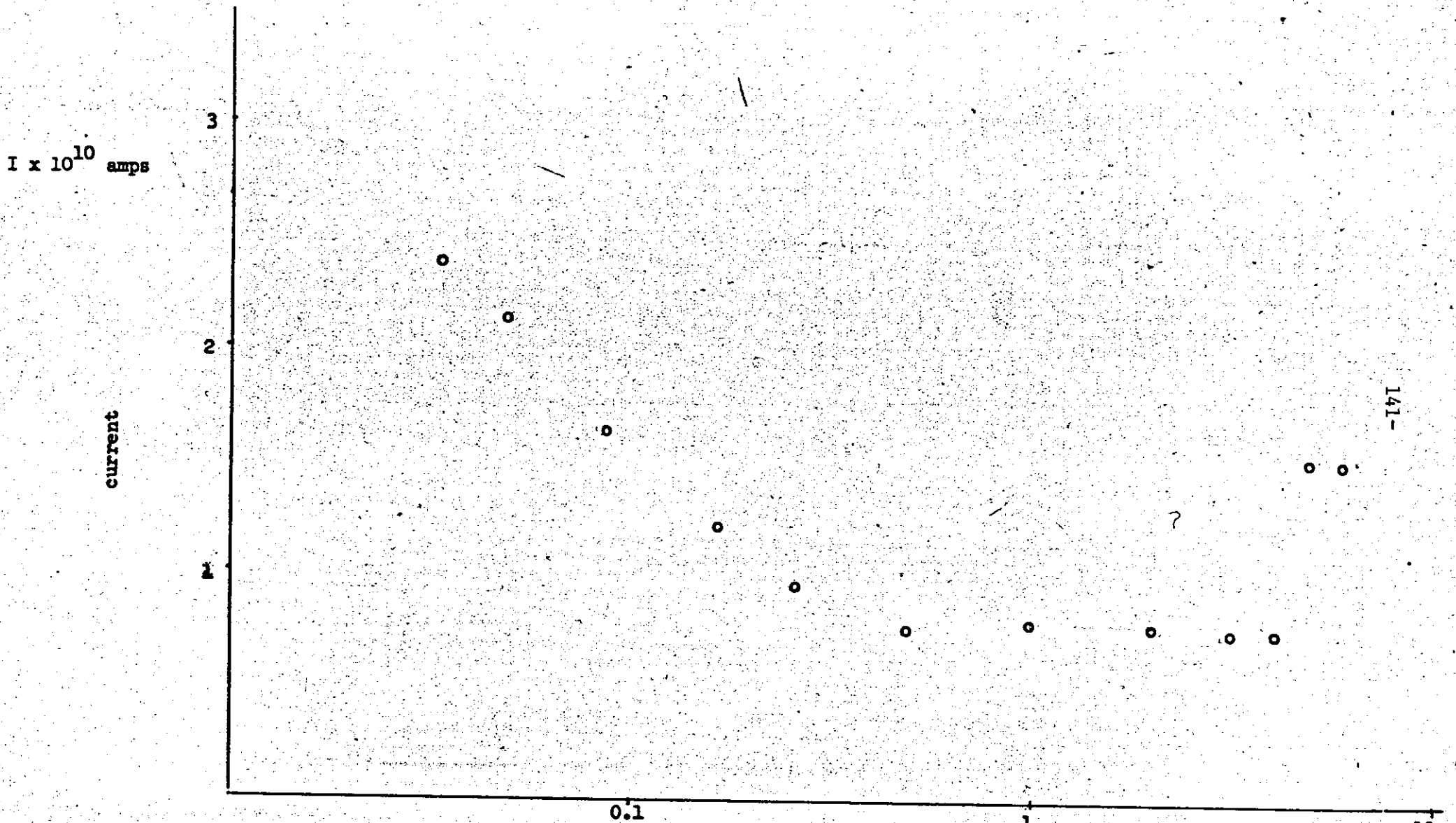

Fig. 41
Graph of current against time (hours)
20 mil Bloore Polythene at 15kV
1" Brass Electrodes (no guards)

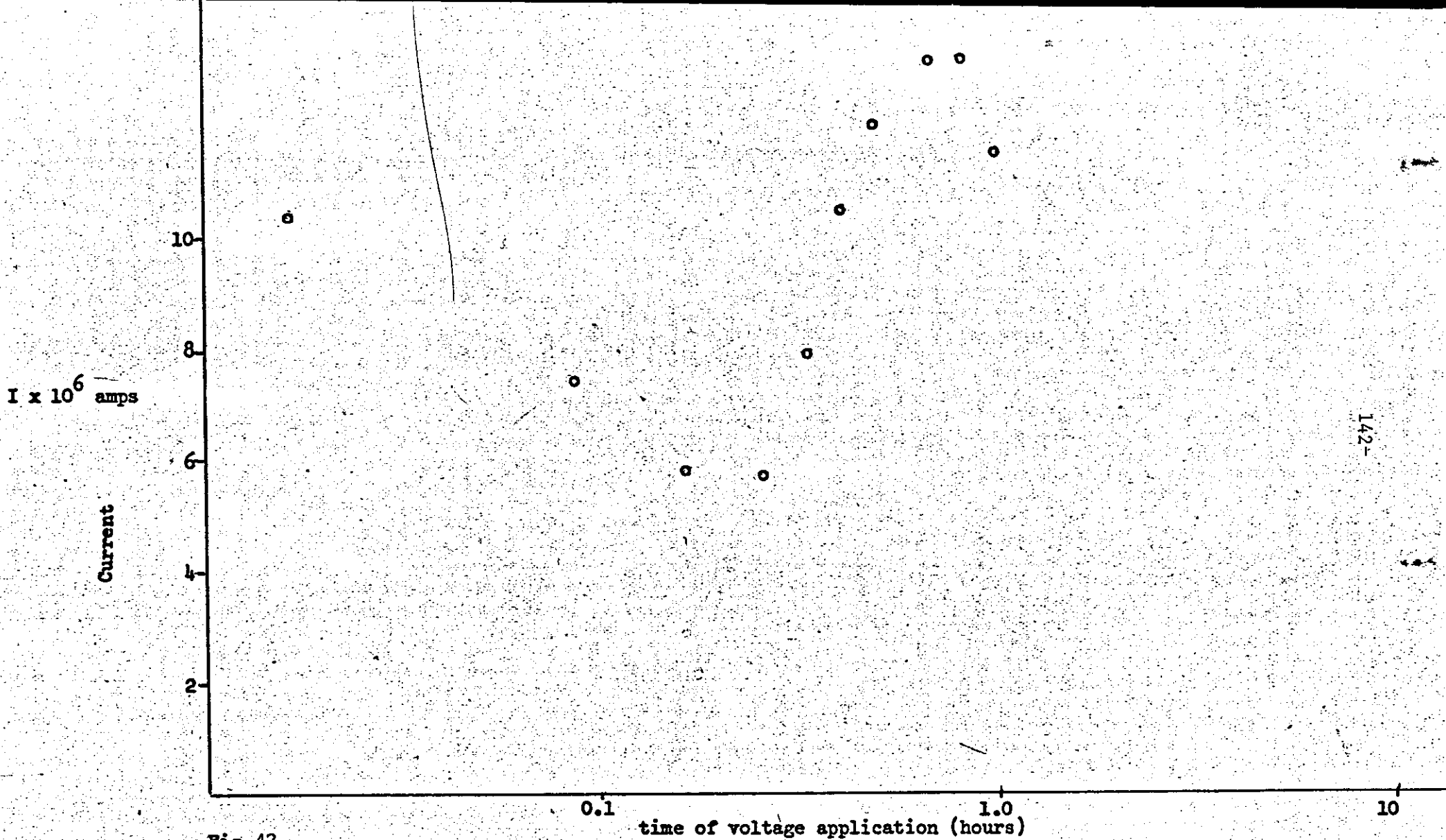

Fig. 42
Graph of Current against time of Voltage Application
5ml Oil-Impregnated Paper with 2¼" electrodes at 1.6kV

U.V. record 4A

Polarisation current - (i) Sudden decrease of current with decrease in stress (initial discharging phase)

(ii) Fast recovery to higher current value.

(iii) Gradual decay to steady state value (eventual polarisation phase). Illustrates decrease of built up internal charge (Compare with U.V. record 4B).

Sample X, applied stress - 500 $kVcm^{-1}$,
paper speed - 0.02 $ins.sec^{-1}$.

U.V. record 4A

Polarisation current - (i) Sudden decrease of current with decrease in stress (initial discharging phase)

(ii) Fast recovery to higher current value.

(iii) Gradual decay to steady state value (eventual polarisation phase). Illustrates decrease of built up internal charge (Compare with U.V. record 4B).

Sample X, applied stress - 500 $kVcm^{-1}$,
paper speed - 0.02 $ins.sec^{-1}$.

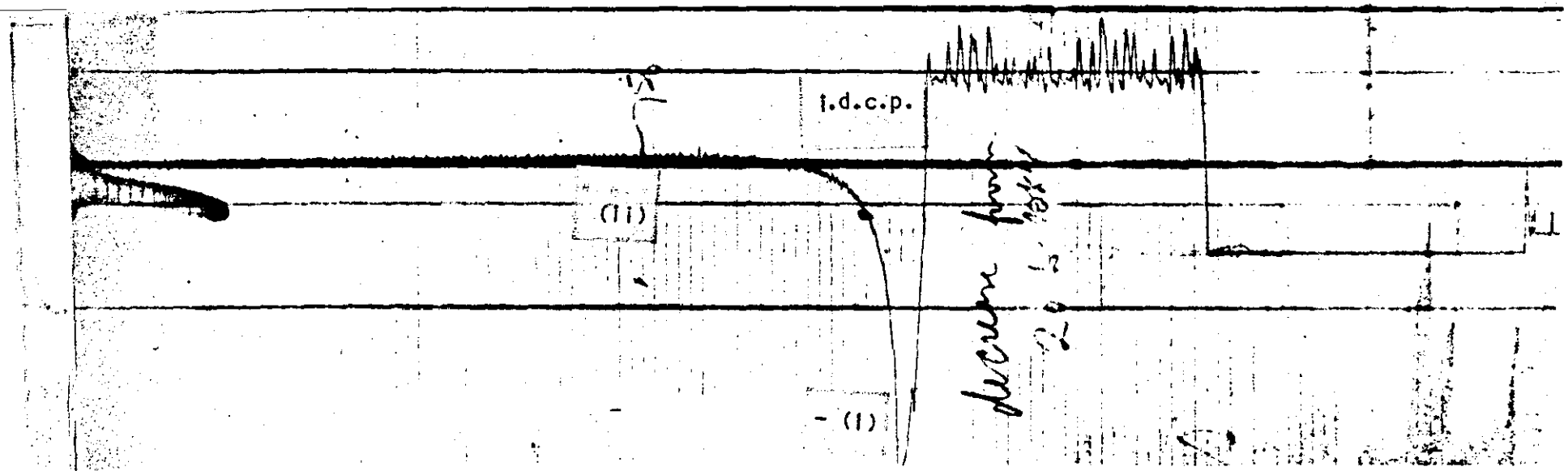

(a) U.V. record 4B
d.c. discharges - Comparison of number of discharges at constant voltage with reverse discharges with decrease of voltage.
Time lag before reverse discharges
(Compare with U.V. record) sample as in fig.11b.

(b) Applied voltage trace
paper speed - 0.05 ins.sec^{-1}

U.V. record 4A

Polarisation current - (i) Sudden decrease of current with decrease in stress (initial discharging phase)

(ii) Fast recovery to higher current value.

(iii) Gradual decay to steady state value (eventual polarisation phase). Illustrates decrease of built up internal charge (Compare with U.V. record 4B).

Sample X, applied stress - 500 $kVcm^{-1}$,
paper speed - 0.02 $ins.sec^{-1}$.

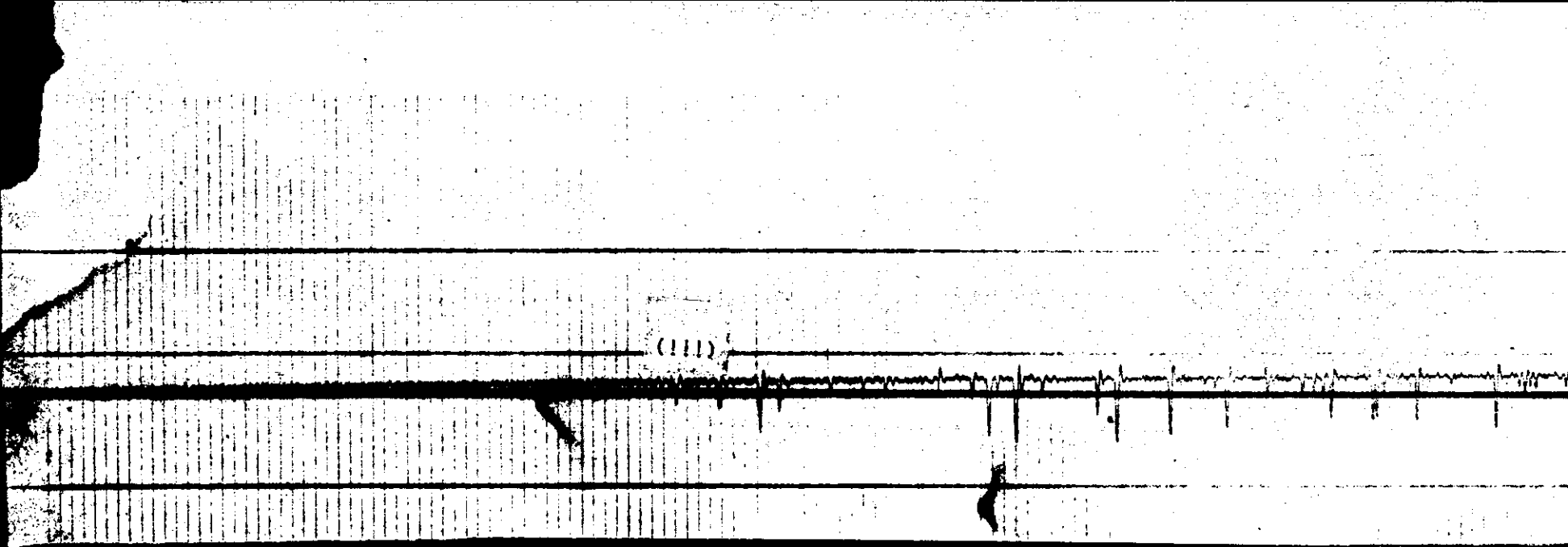
(III)

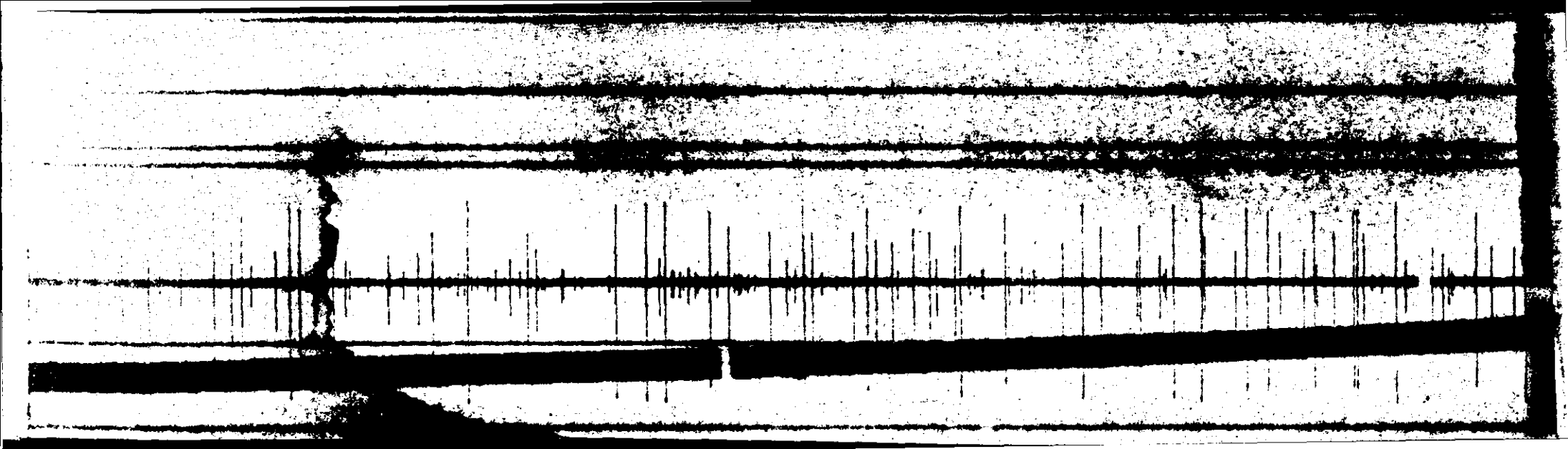

U.V. record 4B

(a) d.c. discharges - Comparison of number of discharges at constant voltage with reverse discharges with decrease of voltage.
Time lag before reverse discharges
(Compare with U.V. record) sample as in fig.11b.

(b) Applied voltage trace
paper speed - 0.05 ins.sec^{-1}

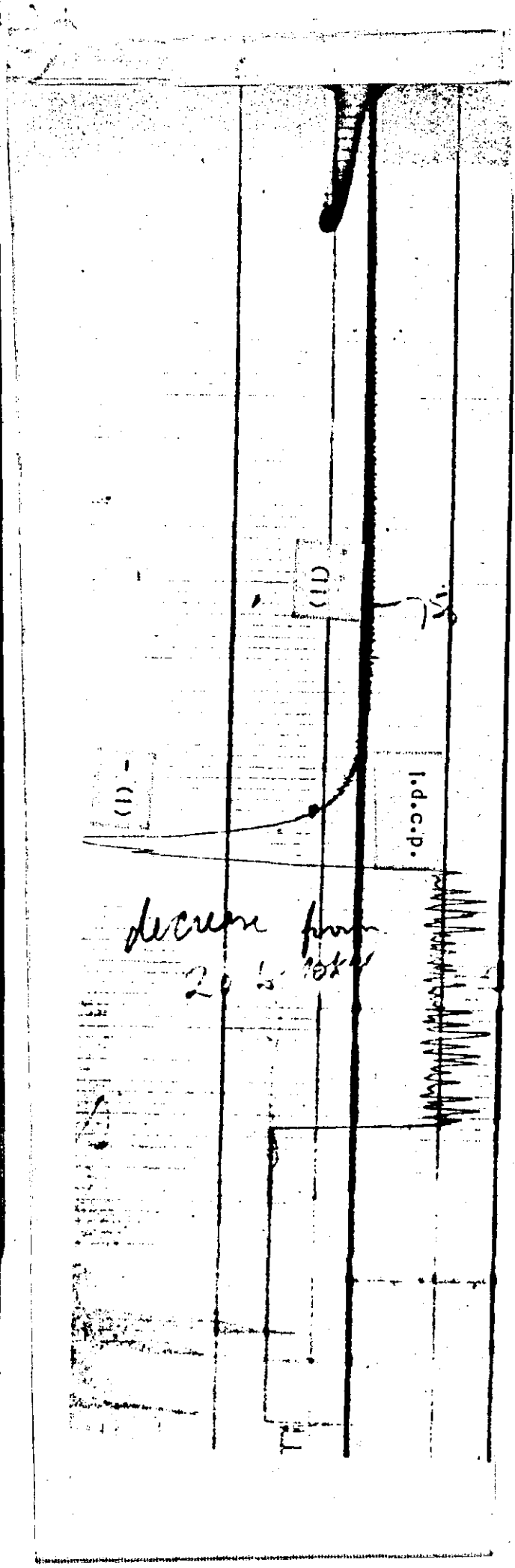
(II)
(I) -
l.d.c.p.
decrease from

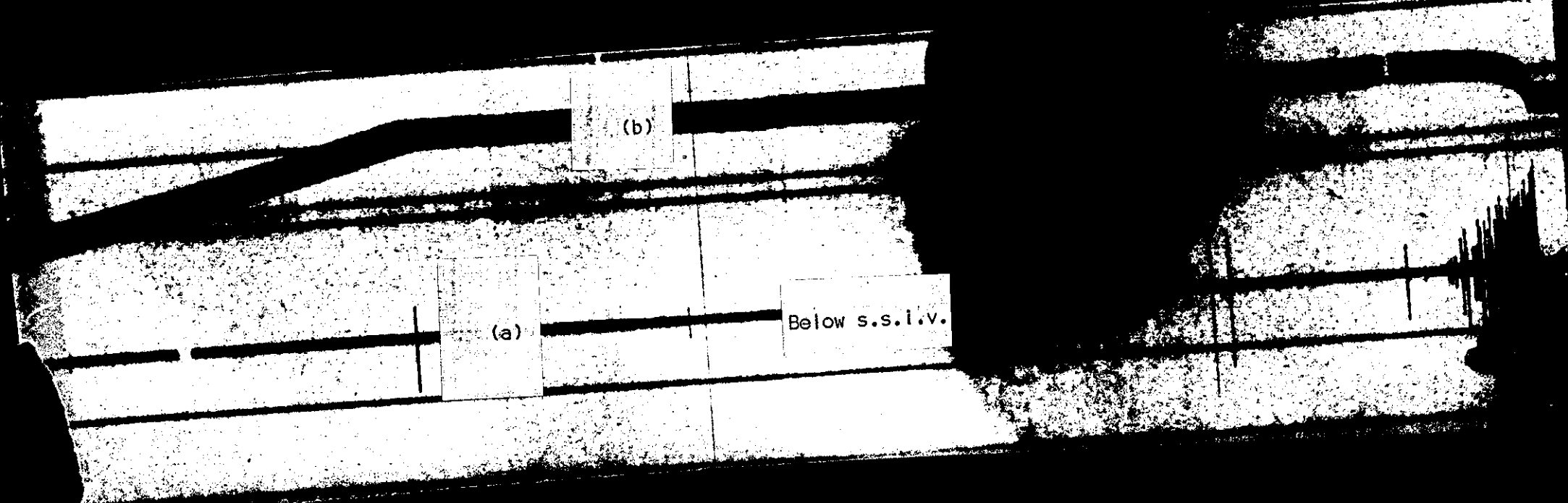
(b)
(a)
Below s.s.i.v.

8.4.2 Application of Poisson's equations

Now if $\Sigma\rho_{(r-1)r}$ is not zero Poisson's equation holds

i.e. Div D = $+\rho$

This means that unlike the case where $\Sigma\rho_{(r-1)r} = o$ $\quad \frac{\partial}{\partial x}\left(\epsilon \frac{\partial v}{\partial x}\right) = \rho$

Therefore $E_1 \neq E_2$

This means that for a parallel plate capacitor assuming it is possible to adopt a general dielectric constant ϵ for the system and that assuming ρ is uniformly distributed in the dielectric (i.e. applying the divergence theorem) hence writing Poisson's equation

$$\frac{d^2V}{dx^2} = +\frac{\rho}{\epsilon} \quad \ldots \quad \ldots \quad \ldots \quad \ldots \quad \ldots \quad \ldots \quad \ldots \quad \ldots \quad \ldots \quad \ldots \quad 8.14$$

In order to avoid making assumptions about boundary conditions for x = o with respect to the electric field, let us write a complementary function and a particular integral for equation 8.14. If this is done for

$$\frac{d^2V}{dx^2} = o$$

complementary function

$$\therefore \quad V_1 = A_1 + B_1x$$

and for $\frac{\partial^2V}{\partial x^2} = \frac{\rho}{\epsilon}$

Particular integral

$$V_2 = \frac{1}{\epsilon}\left(\frac{\rho x^2}{2} + Cx\right)$$

$$\therefore \quad V = V_1 + V_2 \quad \text{(General Solution)}$$

$$= A_1 + B_1 x + \frac{1}{\epsilon}\left(\frac{\rho x^2}{2} + Cx\right)$$

since ϵ is a constant, V can be expressed as

$$V = A + Bx + \frac{\rho x^2}{2\epsilon} \quad \ldots \quad \ldots \quad \ldots \quad \ldots \quad \ldots \quad \ldots \quad 8.15$$

The only boundary conditions which need to be used are the obvious ones viz

$$V = V_A \text{ at } x = o$$

$$V = 0 \text{ at } x = L$$

$$V = V_A - x\left(\frac{V_A}{L} + \frac{L}{2\epsilon}\right) + \frac{\rho x^2}{2\epsilon} \quad \ldots \quad 8.16$$

for an applied voltage of $-V_A$ since the direction of the steady state current J in the earlier analysis is reversed and ρ for positive V_A and ρ for negative V_A are opposite in phase but not necessarily equal.

Hence Div D = $-\rho_n$

and by a similar treatment to equation 8.14

$$V = A + Bx \quad \frac{-\rho_n x^2}{2\epsilon} \quad \ldots \quad 8.17$$

The boundary conditions this time are

$$V = -V_A \text{ at } x = o$$

and $V = o$ at $x = L$

$$\therefore \quad V = x\left(\frac{V}{L} + \frac{\rho_n L}{2\epsilon}\right) - V_A - \frac{\rho_n x^2}{2\epsilon} \quad \ldots \quad 8.18$$

By differentiating equations 8.16 and 8.18 it can be shown that the electric field density at x = o is not zero. The above treatment has been selected to avoid making this particular assumption which Jaffe[91,92] and others[93,94] make and which is very popular in semi-conductor theory. Discharge tests have established that the stress at the dielectric electrode interface cannot be zero. (see next chapter).

It must be borne in mind from equation 8.9 that ρ is a function of the current density, ($J/E = + F(V,L)$[95,96]) hence the effect of ρ is felt most at high current densities.

Thus the integration of equation 8.14 is not strictly correct but should only be considered as an approximate solution. Note that in this case relative permittivity is defined with respect to vacuum not

free space (as with electronic voltages) since the space charge carrier density in air at these stresses is quite considerable.

8.5 Space charge and polarization theories

It is claimed by some authors[97] that space charge theories are incompatible with conventional polarization analysis, thus before drawing any conclusions from the above analysis it will be informative to evaluate this controversial statement.

Thus for the microscopic inhomogeneity just outlined consider an analysis on the basis of conventional polarisation theories[98,99].

All capital letters are vectors. For a dipole of moment $M = qL$ the potential $d\phi$ due to the dipole per unit volume at a point within a dielectric of permittivity ϵ distance r from

the dipole is given by $d\phi = \frac{MI}{4\pi\epsilon r^2}$

where I is unit vector

$$d\phi = \frac{M.\ \nabla(\frac{1}{r})}{4\pi\epsilon} \quad \text{where } \nabla = \Sigma I\ \frac{\partial}{\partial n}$$

Now

$$\text{div } (aB) = a\ \nabla.\ B + B.\ \nabla a$$

$$\therefore \quad d\phi = \frac{1}{4\pi\epsilon} \left[\text{div } (\frac{M}{r}) - \frac{1}{r}\ \nabla.M \right]$$

$\therefore$ For the total volume, potential ϕ

$$\phi = \frac{1}{4\pi\epsilon} \int_v \left[\text{div } (\frac{M}{r}) - \frac{1}{r}\ \nabla.M \right] dv$$

applying the divergence theorem viz:

$$\oint E.\ N\ ds = \int_v \text{div } E\ dv$$

$$\phi = \frac{1}{4\pi\epsilon} \int_s \frac{M.N}{r}\ ds - \frac{1}{4\pi\epsilon} \int_v \frac{\nabla.M}{r}\ dv$$

Therefore interpreting the above equation in the light of the foregoing analysis, the surface charge $(\frac{M.N}{r})$ may be regarded as the basis for initial charging. The internal or ~~surface~~ space charge which in the general case includes all charges (both free and injected charge carriers) inside the volume (see appendix) may then be treated as a basis for eventual polarization. Above all the equation means that theories of space or internal charge within a dielectric can be consistent with and interpreted in terms of polarization phenomena.

CHAPTER 9

Behaviour and Equivalent Circuit of Gas/Solid Dielectric Systems

The implications of intrinsic non-ohmic conduction (discussed in the previous chapters) in connection with discharge processes and breakdown in gaseous and solid dielectrics are obvious but on a macroscopic scale non-ohmic effects caused by mixed dielectrics can be examined in more detail. Such a study can have two beneficial effects:
(i) It would help to clarify some non-ohmic behaviour at the microscopic level.
(ii) It could explain to some extent anomalies in results obtained with mixed systems such as air/solid dielectric, oil/paper, glasses etc. (Figs. 40-47 U.V. records 3A, 3B).

Unfortunately this has not always been done because of the need to simplify equations and experimental interpretations. In some cases such an approach is valid but in other cases this type of treatment is incomplete and renders inadequate and or misleading results.

This chapter treats this kind of problem (as it applies) to gas discharge processes in insulation and discusses its effect on discharge breakdown behaviour and equivalent circuits of imperfect insulation. It is hoped that the similarity of treatment between macroscopic and microscopic internal or space charge (treated in chapter 8) and their relationship to some of the unusual results obtained in this investigation will become apparent.

9.1 Theoretical considerations

Most papers on the breakdown of voids under direct voltage conditions in dielectrics represent the void as of infinite resistivity[39,40], i.e. zero conductivity, and hence calculate the equivalent stress in the void and its discharge characteristics neglecting the conductivity of the gas within the void. This has led

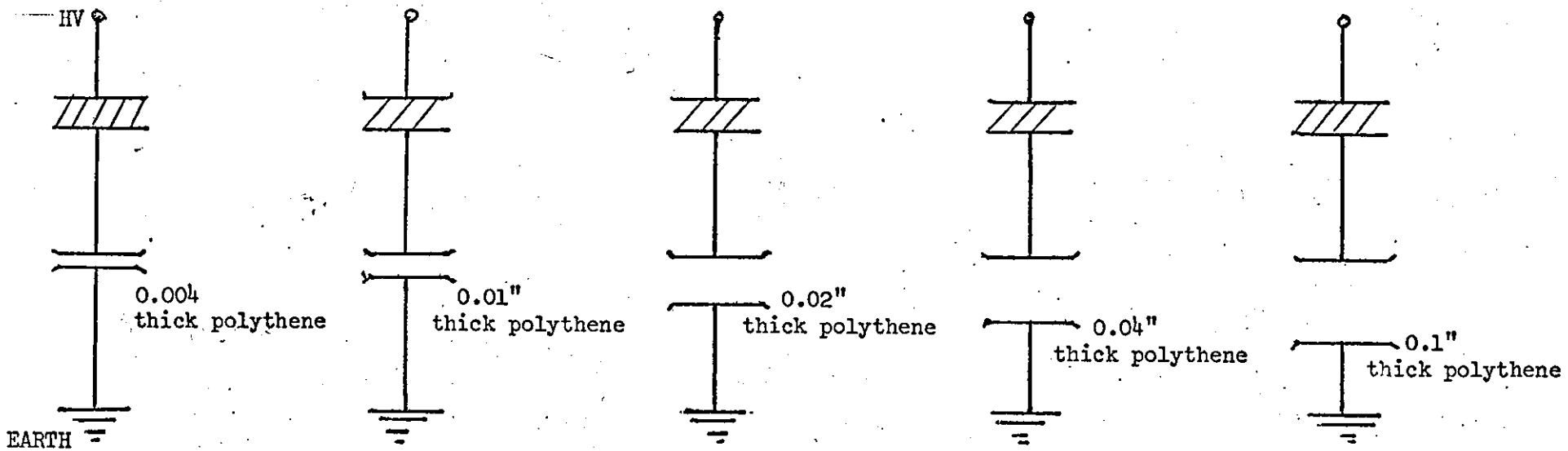

14Kv few discharges 20 kV Continuous Breakdown of air gap	15 kV - Sporadic discharges 30 kV - Continuous Breakdown	15kV - Sporadic discharges 32 - Continuous Breakdown of air gap	28 kV - Sporadic Discharges 32 kV - Continuous Breakdown of air	26 kV - Sporadic Discharges 32 kV - Continuous Breakdown of air

Fig. 43

Breakdown phenomena of air gaps in series with solid dielectrics (sample X)
air gap thickness - 0.08 inch
electrode dialmeter - 1½ inches
All electrode profiles in Figs. 43-47 are Rogowski

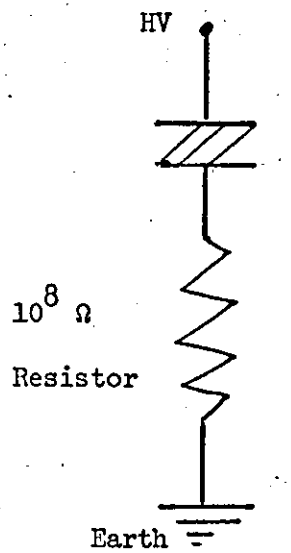

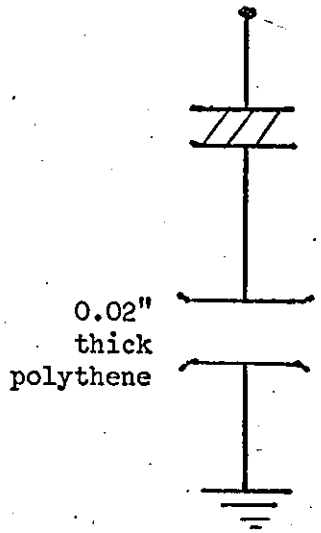

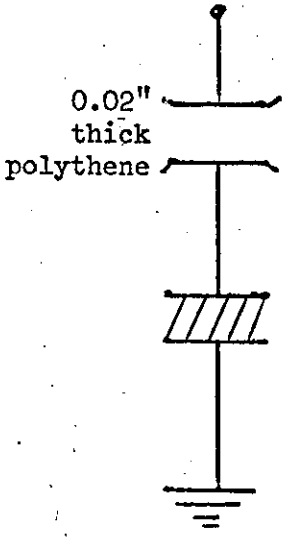

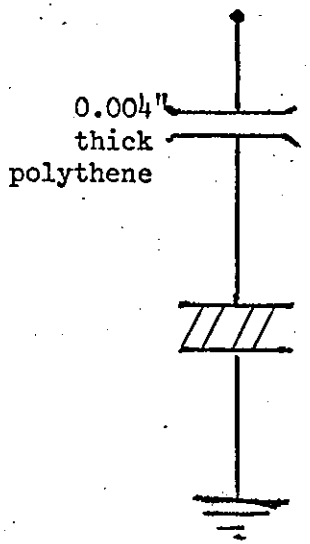

10 kV Continuous Breakdown of air gap nearing spark breakdown

11 kV - Inception
32-42 kV - Continuous Breakdown of air leading to spark breakdown

>45 - No continuous breakdown of air leading to spark breakdown of gap except a few extraneous discharges

14 kV - a few discharges
20 kV - No continuous breakdown of air leading to spark breakdown of gap.

Fig. 44 Breakdown voltage of air gap (isolated) - 10 kV
Breakdown phenomena of air gaps in series with solid dielectrics (sample X)
electrode diameter - 1½ inches

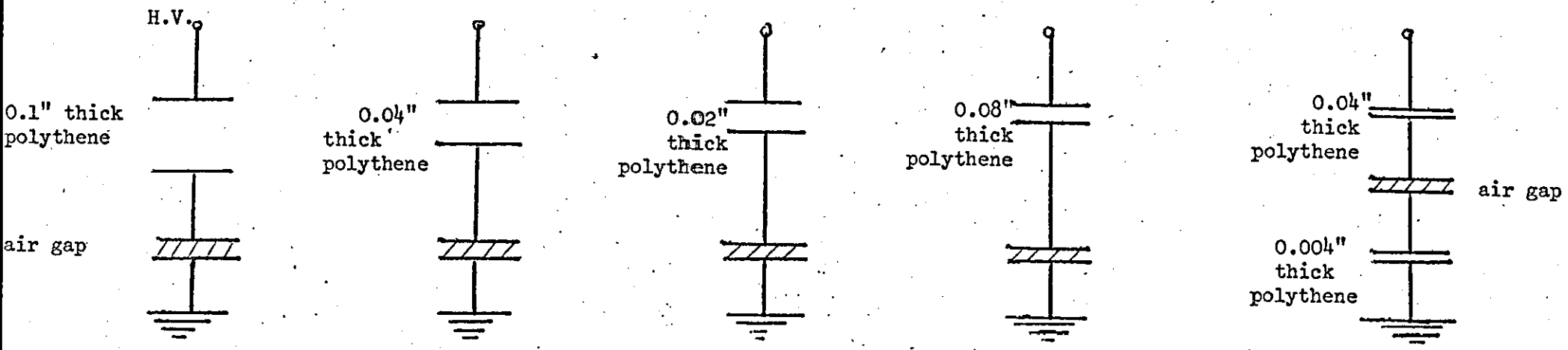

40 kV - No complete spark breakdown of air gap

40 kV - No complete spark breakdown of air gap

14 kV - few discharges
30 kV - a lot of discharges lending to spark breakdown at 40 kV

14 kV - Inception
25 kV - A lot of discharges

20 kV Inception
25 kV - few discharges

Fig. 45 Breakdown voltage of air gap (isolated) - 6 kV
Breakdown phenomena of air gaps in series with dielectrics
electrode diameter - 1½ inches

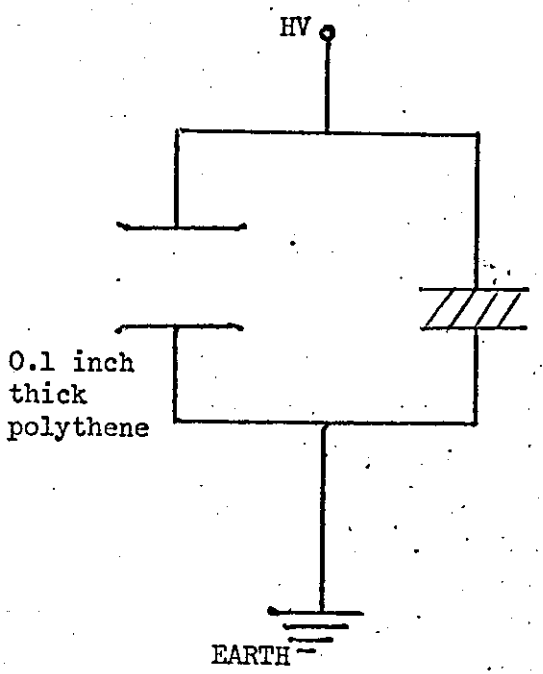

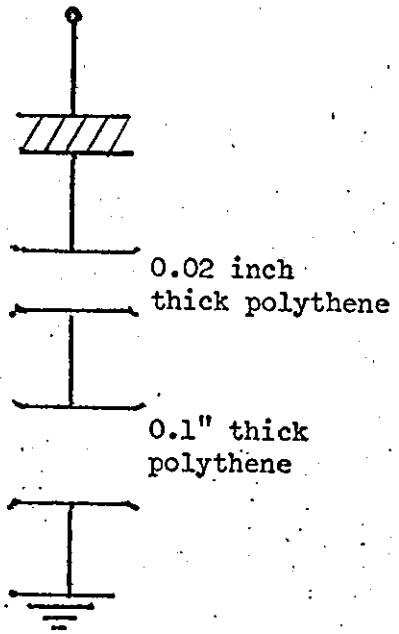

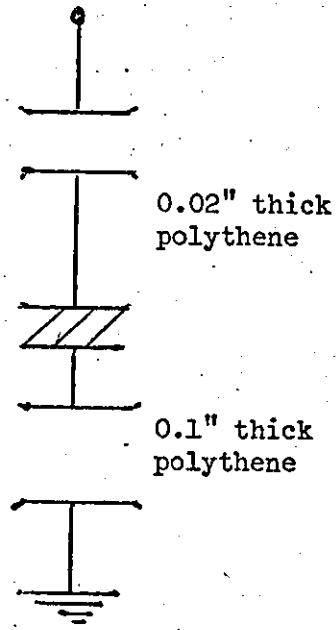

14 kV Continuous Breakdown of air gap

20 kV - Sporadic Breakdown of air gap
40-45 kV Continuous Breakdown of air gap

70 kV - No continuous Breakdown of air gap

Fig. 46
Breakdown phenomena of air gaps in conjunction with solid dielectrics (sample X)
electrode profile - Rogowski
electrode diameter - $2\frac{1}{4}$ inches

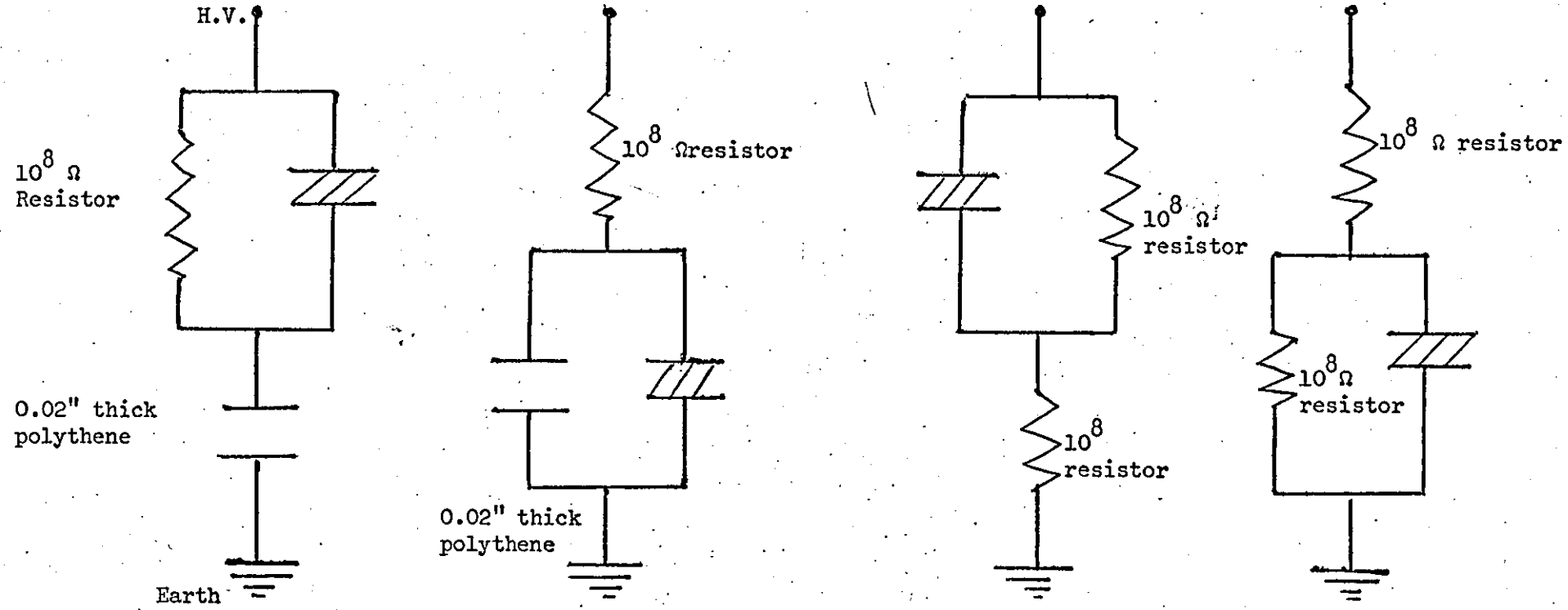

>50 kV - No spark breakdown of air gap

14 kV - Continuous breakdown of air gap

27 kV - Continuous break down of air gap

33 kV Continuous breakdown of air gap

Fig. 47
Breakdown phenomena of air gaps in conjunction with solid dielectrics (sample X)
breakdown voltage of air gap (isolated) - 12 kV
electrode diameter - 2¼ inches

to equivalent circuits[48] (see Fig. 48) which have neglected the influence of the conductivity of the gas within the void and hence misinterpreted information as to the discharge performance and in particular discharge extinction under direct voltage conditions.

In the past at fairly low stresses with dielectrics of relatively low resistivity this has been adequate but the experiments with air, polythene and epoxy resin dielectrics using a parallel plate configuration have shown that the conductivity of the gas is comparable and in some cases more than the dielectrics in parallel with it.

If the above factors are considered, the formation of a macroscopic internal or space charge at the air/solid dielectric interface is evident. This together with the very long times of complete polarization could account for much of the discharge behaviour[100,101] of voids within and at the interface of dielectrics when subjected to high d.c. design stresses. It could also explain in particular some aspects of discharge extinction[38,102,103] under high voltage conditions (the possibility of applying this theory to the alternating voltage case where necessary is outlined in appendix 6). The characteristics of this macroscopic internal charge should be fairly similar to that of the microscopic space charge outlined earlier. For simplicity however it will be assumed that the overall effect will be dominated by the macroscopic internal charge at the interface. The influence of the microscopic space charge for each dielectric will be evaluated in an equivalent circuit as a variation of conductivity with stress and its effect outlined.

In order to assess the effect of the macroscopic internal charge on discharge processes consider the following.

9.2 Equivalent stresses in voids

9.2.1 Maxwellian analysis

In the analysis of gas filled voids at high d.c. design stresses the conductivity of the air is finite, therefore the air and solid

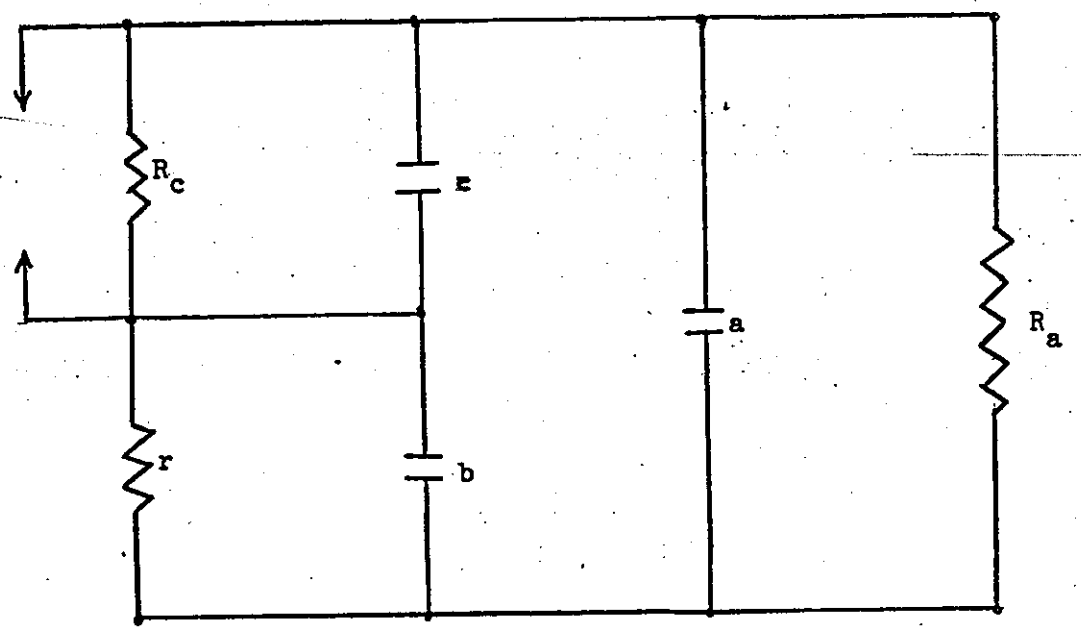

Fig. 48
Conventional equivalent circuit of a dielectric containing a cavity

c - capacitance of void
b - capacitance of sound insulation inseries with void
r - resistance of sound insulation in series with void
a - capacitance of the remaining sound dielectric
R_a - resistance of the remaining sound dielectric
R_c - resistance of void walls

dielectric system should be treated as a composite dielectric composed of two leaky dielectrics and Maxwell's theory of composite dielectric treated earlier (Chapter 8) used in the analysis).

Thus for a parallel plate configuration, considering elemental thicknesses L_a and L_i and assuming that the stress across each element is ohmic,

$$\text{then } V = E_i L_i + E_a L_a \quad \ldots \quad 9.1$$

$$\left.\begin{aligned} J_a &= \sigma_a E_a \\ J_i &= \sigma_i E_i \end{aligned}\right\} \quad \ldots \quad 9.2$$

$$\left.\begin{aligned} D_a &= \epsilon_a E_a \\ D_i &= \epsilon_i E_i \end{aligned}\right\} \quad \ldots \quad 9.3$$

and from the continuity equation

$$J_a + \frac{\partial D_a}{\partial t} = J_i + \frac{\partial D_i}{\partial t} \quad \ldots \quad 9.4$$

In the classical theories $\frac{\partial D_i}{\partial t}$ and $\frac{\partial D_a}{\partial t}$ are assumed to reduce to negigible proportions after a few seconds. In practice, at normal operating stresses for high resisitivity insulation $\frac{\partial D_i}{\partial t}$ may take much longer (e.g. $> 10^4$ secs) to decay to zero. (see Fig. 19). This means that there will be a long term build up of charge at the void dielectric interface.

The charge difference at the interface ρ_d can be expressed as

$$\rho = D_a - D_i \quad \ldots \quad 9.5$$

$$= \epsilon_a E_a - \epsilon_I E_I$$

Hence, under steady state conditions

$$\rho_d = J \left(\frac{\epsilon_a}{\sigma_a} - \frac{\epsilon_i}{\sigma_i}\right) \quad \ldots \quad 9.6$$

Again, at practical operating stresses,

$$J_a' = \sigma_a \bar{E}. \exp A_a E_a$$
$$\text{and } J_i' = \sigma_i E. \exp A_i E_i \quad \} \quad \ldots\ \ldots\ \ldots\ \ldots\ \ldots \quad 9.7$$

9.2.2 Application of Poisson's equations

The formation of ρ_d at the interface means that in the calculation of discharge inception stress, apart from the fact that one cannot use the straight forward charge equality relation as under alternating voltage conditions (see chapters 5, section 5.3), one cannot also use the straight forward resistive distribution formulae to calculate the stress.

viz: since $\sigma_a >> \sigma_i$ and $L_i < L_i$

$$V_a \doteqdot \frac{L_a}{\sigma_a} \Big/ \frac{L_i}{\sigma_i} \quad V$$

i.e. $$\frac{V_a}{L_a} \doteqdot \frac{\sigma_i}{\sigma_a} \cdot \frac{V}{L_i} \quad \ldots\ \ldots\ \ldots\ \ldots\ \ldots\ \ldots \quad 9.8$$

i.e. mean stress in void $\doteqdot \frac{\sigma_i}{\sigma_a}$ times mean stress in dielectric. (For if this were so the inception stress in the void will be virtually infinite irrespective of void position. However as a result of experimental evidence it has been found that this is not so and that the only analysis which suggests reasonable assessment is by the application of Poisson's equations. Thus let ρ_d be represented by a distributed charge density ρ_{ia} (i.e. invoking the divergence theorem where every surface charge can be represented by an equivalent volumetric charge).

Hence writing $\frac{\partial D}{\partial x} = -\rho_{ia}$ (for one dimensional case)

and considering a complementary function

$$F_1 = A + Bx$$

and a particular integral $F_2 = \frac{\rho_{ia} x^2}{2\epsilon_Q}$

This leads to a general solution of the form

$$V_x = A + Bx - \frac{\rho_{ia} x^2}{2\epsilon_Q} \quad \ldots \quad \ldots \quad \ldots \quad \ldots \quad \ldots \quad 9.9$$

where A and B are constants

The constants A and B can only be evaluated by applying the appropriate boundary conditions. This means that the position of the void within or without the dielectric should be taken into account in the assessment of discharge behaviour, that is, the fact that a void is bounded on only one side or only two sides by insulation or whether it is near or farther away from the high voltage electrode is relevant to its behaviour since the boundary and initial conditions alter significantly.

Hence for a laminar void bounded on one side by insulation, with the other side facing the h.v. electrode, the boundary conditions are: (see fig. 49)

$$v_x = V_A \text{ at } x = 0$$

$$v_x = v_1 \text{ at } x = L_a$$

$$\therefore A = 0$$

and $$v_1 = V_A + BL_a - \frac{\rho_{ia} L_a^2}{2\epsilon_Q}$$

hence $$v_x = V_A + \frac{1}{L_a}\left(v_1 - V_A + \frac{\rho_{ia} L_a^2}{2\epsilon_Q}\right) x - \frac{\rho_{ia} x^2}{2\epsilon_Q} \quad \ldots \quad \ldots \quad 9.10$$

Similarly, considering an identical void with one side adjacent to the low voltage (earth) electrode or void totally enclosed by

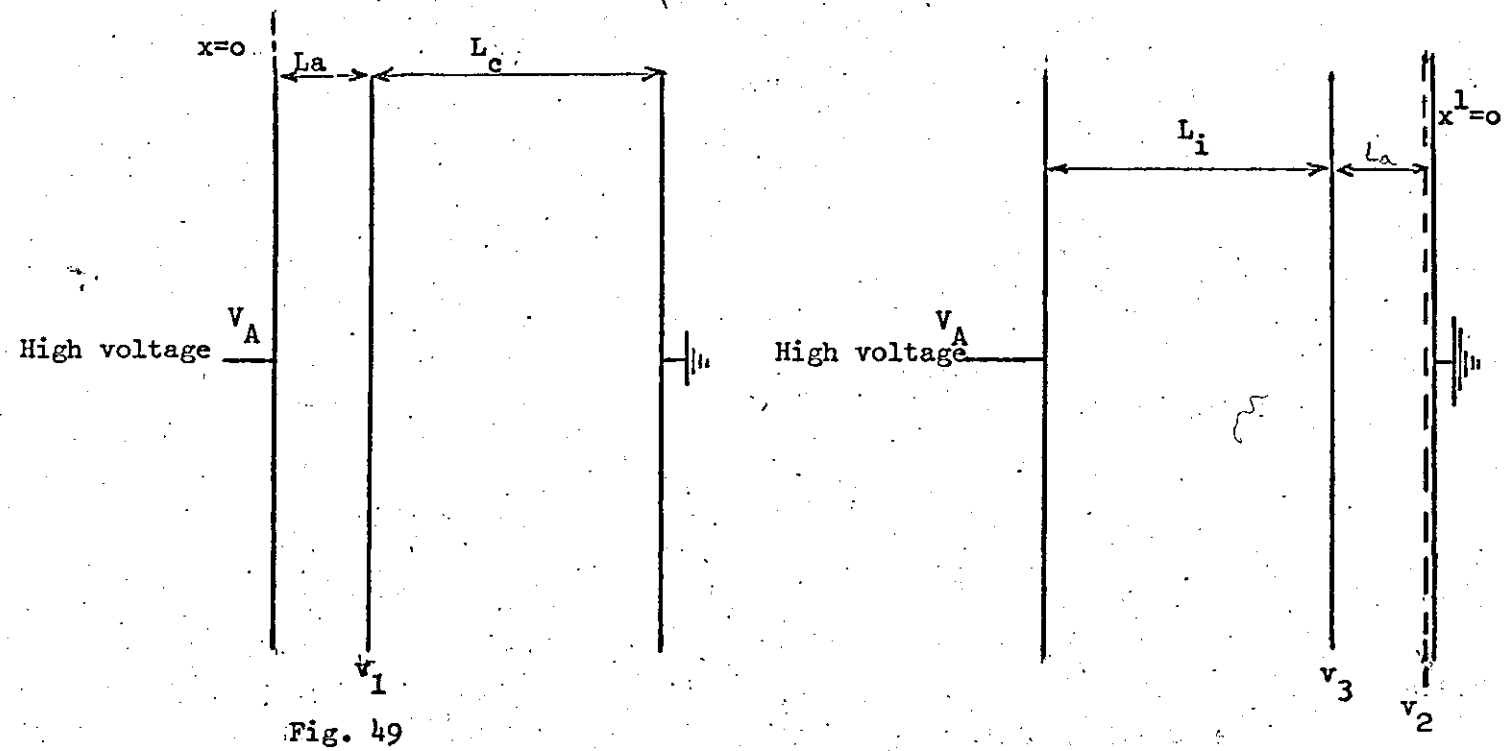

Fig. 49
The effect of void position on void stress assessment

insulation:

$$v^1_x = v_2 \text{ at } x^1 = 0 \quad \text{where } x^1 = -x$$

$$v^1_x = v_3 \text{ at } x^1 = L_a$$

$$\therefore A_1 = v_2$$

$$\text{hence } v_3 = v_2 + B_1 L_a - \frac{\rho_{ia} L_a^2}{2\epsilon_Q}$$

$$\text{and } v^1_x = v_2 + \frac{1}{L_a}\left(v_3 - v_2 + \frac{\rho_{ia} L_a^2}{2\epsilon_Q}\right) x^1 - \frac{\rho_{ia}(x^1)^2}{2\epsilon_Q} \quad \ldots \ldots \quad 9.11$$

In the case where one side of the cavity is earthed:

$$v_2 = 0$$

$$\text{and } v^1_x = v_2 + \frac{1}{L_a}\left(v_3 + \frac{\rho_{ia} L_a^2}{2\epsilon_Q}\right) x^1 - \frac{\rho_{ia}(x^1)^2}{2\epsilon_Q} \quad \ldots \ldots \quad 9.12$$

From (12)

$$\frac{\partial v^1_x}{\partial x^1} = \frac{1}{L_a}\left(\frac{\rho_{ia} L_a^2}{2\epsilon_Q} + v_3\right) - \frac{\rho_{ia} x^1}{\epsilon_Q}$$

$$= \frac{\rho_{ia} L_a}{2\epsilon_Q} + \left(\frac{v_3}{L_a} - \frac{\rho_{ia} x^1}{\epsilon_Q}\right) \ldots \ldots \ldots \ldots \ldots \ldots \quad 9.13$$

From (10) $$\frac{\partial v_x}{\partial x} = \frac{1}{L_a}\left(\frac{\rho_{ia} L_a^2}{2\epsilon_Q} + v_1 - V_A\right) - \frac{\rho_{ia} x}{\epsilon_Q}$$

$$= \frac{1}{L_a}\left(\frac{\rho_{ia} L_i^2}{2\epsilon_Q} + v_1\right) - \left(\frac{V_A}{L_a} + \frac{\rho_{ia} x}{\epsilon_Q}\right) \quad \ldots \ldots \quad 9.14$$

$$= \rho_{ia} \frac{L_a}{2\epsilon_Q} + \left(\frac{v_1 - V}{L_a} - \rho_{ia} \frac{x}{\epsilon_Q}\right)$$

In practice $V_A >> v_1$, $V_A >> v_2$, $V_A >> v_3$ also v_1, v_2 and v_3 are of the same order except in cases where $v_2 = 0$. Hence the stresses

in the two cases are different. The easiest verification of this theory is represented in the most obvious and simplest cases by Figs. 43-47; U.V. records 3A, 3B.

9.3. Equivalent circuit responses

9.3.1 Maxwell-Wagner response

The conventional equivalent circuit does not normally cater for the possible formation of ρ_{ia} at the interface since only the resistance of the dielectric in parallel with the void is considered. As pointed out earlier this resistance is shunted by the much lower resistance of the void gas.

Moreover an analysis of the conventional Maxwell-Wagner two layer equivalent circuit gives a voltage response of the form:

$$V_1 = \frac{VC_2}{C_1 + C_2} \left[\frac{C_2R_2 - C_1R_1}{C_2(R_1 + R_2)} e^{-\psi t} + \frac{R_1}{C_2} \left(\frac{C_1 + C_2}{R_1 + R_2} \right) \right] \ldots \quad \ldots \quad 9.15$$

where $\psi = \frac{R_1 + R_2}{R_1R_2(C_1 + C_2)}$

This is not a suitable response because of the fact that it shows a single exponential decay function, a response never obtained in practice and also the time constant means a fairly quick decay. It does not also cover the possible increase of conduction current with time.

Hence a new equivalent circuit was developed in order to simmulate more correctly discharge behaviour and in particular discharge extinction. This approach treats the system as a problem in inhomogeneity (just like the Maxwell-Wagner treatment) but the present equivalent circuit unlike the Maxwell-Wagner type includes an extra pair of resistive components termed the initial 'charging' resistances. This coupled with the pair termed the eventual 'polarization' resistances

would it is hoped represent the two distinct phases of complete polarization encoutered in practice and also present an extra exponential term to make the response more realistic.

9.3.2 A more appropriate response

Referring to the figure 50, r_a, r_i; R_a, R_i; C_a, C_i may be called the "charging" resistances, the "polarization" resistances and the capacitance for the air and dielectric in series with the void respectively.

Then if, in practice, $R_1 >> r_i$, $R_a >> r_a$ we have, for an applied direct voltage step function $V_A\,1(t)$.

$$v_a = \frac{V_A r_a}{r_a+r_i}\left\{\left(\frac{r_a+r_i}{R_a+R_i}\right)\frac{R_a}{r_a} + \frac{\beta C_a C_i (r_a R_i - R_a r_i)+C_i R_i - C_a R_a}{2\beta r_a C_a C_i (R_a+R_i)}\exp-(\alpha-\beta)t\right.$$

$$\left. + \frac{\beta C_a C_i (r_a R_i - R_a r_i)-C_i R_i + C_a R_a}{2\beta C_a C_i r_a (R_a+R_i)}\exp-(\alpha+\beta)t\right\} \ldots \quad \ldots \quad 9.16$$

where $$\alpha = \frac{C_a(R_i+r_a) + C_i R_i}{2(r_a+R_i)R_i C_i C_a}$$

$$\beta^2 = \alpha^2 - \frac{R_a+R_i}{C_a C_i R_a R_i (r_a+r_i)}$$

From the above analysis (equation 9.16) the initial "charging" and eventual polarization are identifiable. It follows that steady state conditions would have been achieved when the voltage drops represented by these terms have decayed to negligible values.

9.4 Practical considerations

In practice due to the possible values of the parameters C_a, r_a, R_a, C_i, r_i, R_i (a fair assessment of these may be obtained in

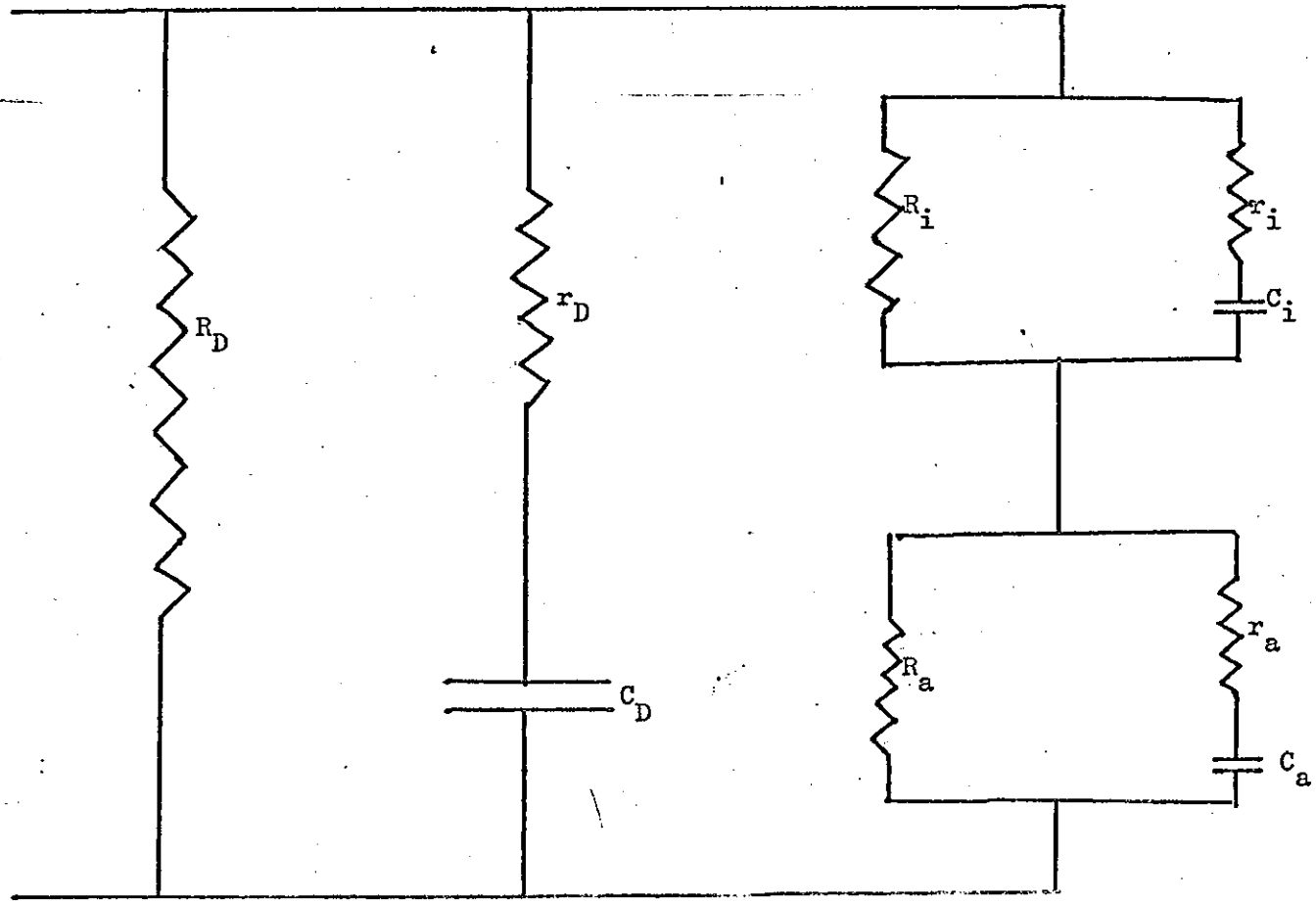

Fig.50
Equivalent circuit of an imperfect dielectric.
R_D- bulk resistance of dielectric.
r_d - 'charging resistance of dielectric.
C_d - Capacitance of dielectric. (bulk)

capacitance and polarization current tests) the constants α and β are very nearly equal. Hence the first exponential term in equation 9.16 will decay very slowly (the extended polarization effect) with a corresponding delay in discharge extinction (see U.V. records 1B, 2A, 3A, 3B, 4B). The second exponential term will give rise to a decay at a much more rapid rate (the charging effect), the discharges due to this will extinguish immediately after switch on.

Referring to equations 9.7, the incremental increase of relative conductivity with stress is very different for the air and the dielectric. In a few cases this may result in a sign change in the coefficient of the polarising term thus giving rise to an initial discharge extinction followed by subsequent reignition[6], this process may then be repeated to give an oscillatory sequence of discharges.

CHAPTER 10

Conclusions (and Suggestions for future work)

10.1 Conductivity in dielectrics.

Conductivity measurements in dielectrics under direct voltage conditions, lead to the following conclusions irrespective of polarity.

That oscillations in the steady state current response and other anomalies are independent of surface and internal discharges.

Also that in the absence of surfaces discharges samples with and without guard gaps give the same results under steady state conditions.

It has also been established that non-ohmic (exponential) conduction is a basic property of the dielectric. This non-ohmic conductivity and its variation with thickness elicits the conclusions that the operating bulk stress for all dielectrics and all thicknesses cannot be calculated simply as a function dependent only on the externally applied voltage V, and the thickness L, of the sample, since this would give a result which is independent of thickness in the case of a parallel plate capacitor.

The experiments so far conducted seem to suggest that the current variations shown in Fig. 28 are of the form:

$$J_{vol} = KE. \exp (\alpha_L + \beta_L E + \gamma_L E^2)$$

where α_L, β_L and γ_L are constants depending on the particular type of dielectric and such that $\alpha_L >> \beta_L >> \gamma_L$. J_{vol} is the bulk volumetric current density as opposed to the current density calculated on the basis of electrode area only and E is the ohmic stress defined by the voltage to thickness ratio of the dielectric.

Typical stress ranges over which α_L, β_L and γ_L predominate, for polythene, α_L for stresses up to about 30 kV cm^{-1}, β_L for stresses between about 30 kV cm^{-1} and about 2MV cm^{-1}, γ_L for stresses above 2 MV cm^{-1}. The above empirical conductivity relationship with stress and the anomalous nature of the polarization currents discussed earlier seem to

indicate that conduction in dielectrics is most probably by both electrons and ions and that the bulk 'volumetric' properties outlined above should be investigated in more detail in all aspects of dielectric properties[104].

Also if $\text{div } J = \frac{\partial \rho}{\partial t}$

and $\text{div } D = \rho$

then $\frac{\partial}{\partial x}(\epsilon E) = \rho$

hence $E_x = f(k\rho x)$

This means that constant stress conditions along the thickness of a dielectric in a parallel plate capacitor configuration can only be assumed if and when $\rho = o$ or is negligible. Thus if ρ is constant or is varying as is the case in a long polarization process then for all practical purposes div D has a definite value and the stress along the axis of a parallel plate capacitor is not a constant.

10.2 Space charge and anomalies

Attempts have been made in the preceding chapters to explain some of this anomolous behaviour in terms of some sort of internal or space charge.

Experiments with some crystals[14,29-31] have been claimed to show that in the presence of field omission a space charge exists within the crystal. Although the tests described in this paper have established that field emission from the electrodes is unlikely at these stresses, nevertheless the conductivity dependence on thickness points to a space charge explanation, the explanation probably resulting from inhomogeneities and trapping levels within the dielectric[105].

The above considerations leads to the conclusions that authors, who have observed similar anomalies, are interpreting $\Sigma\rho_{(r-1)r}$ as the

setting up of a reverse electro motive force in the material[106,107]. Obviously the setting up of $\Sigma\rho_{(r-1)r}$ within the material should explain the results of several authors with or without field emission, for example if the conventional capacitance is expressed as the surface charge per unit voltage the capacitance will vary[108,109] with a variation in stress or current density since $\Sigma\rho_{(r-1)r}$ is altered.

It was also observed that if an air gap was stressed from the very low stresses to the very high stresses a whole family of curves obtained for the solid dielectrics (including that of Fig 40) would be generated. This seemed to indicate that the behaviour of charge carriers in solid dielectrics above certain stresses might be very similar to that in air[110-112].

If this is the case then Jaffe and Joffe's theories[91,106] should be examined more closely especially that which appertains to the boundary conditions at the metal dielectric interface, that is the stress is zero. Objections have been raised to this because of the concept of carrier blocking[113] at the electrodes and the fact that the boundary conditions (strictly stated) reduces the steady state current to zero since J is proportional to KE. It should be noted from the analysis in chapter 8 that this assumption need not and should not be made as indeed the stress at the metal dielectric interface may not be zero. This is consistent with some of the most recent considerations[114-116]. In fact the present investigations of the current variations coupled with surface and internal discharge tests of air gaps, dielectrics and air gaps in series with dielectrics have led to the conclusion that the stress at the metal electrode interface is not zero but may be the maximum in most cases.

10.3 Discharge anomalies

The analysis in chapter 9 (see also ref 117) confirmed by experiment has indicated that for thick specimens the discharge

performance of a void particularly if partially enclosed, will depend upon its position relative to the earth electrode. (This was attributed to the existance of the macroscopic space charge ρ_{Ia} within the system).

The formation of ρ_{Ia} should not be confused with ρ_{12} which workers in gas breakdown theory have termed space charge distortion[2] to account for anomalies[118,119] in Townsend's theory for a stress to pressure ratio below 100 (where stress is measured in volts cm^{-1} and pressure is measured in millimetres of mercury). It is interesting to note that the breakdown of air at S.T.P. occurs at a stress to pressure ratio of around 39 - the value around and below which most anomalies of Townsend's theories occur.

The formation of ρ_{Ia} however will occur at stresses much smaller than those at which complete non-ohmicity (i.e. significant formation of ρ_{12}) occurs in either dielectric separately. Thus to some extent ρ_{12} can be considered as interfacial charge formation on a microscopic scale[19] and ρ_{Ia} as an interfacial charge formation on a macroscopic scale.

In this particular case ρ_{Ia} depends on the resistivities and permittivities of the gas in the void of the insulator hence the inception voltage will also depend on the relative resistivities and permittivities of the gas and the insulator.

In practice since the difference between the resistivities of the systems (especially in cases of high resistivity dielectrics - polythene etc) is far greater than the difference between the permittivities, the resistivity ratio becomes the most important determining factor. Hence it is misleading to neglect the conductivity of air in the discharge analysis or in the evaluation of cavity stresses at these high stresses.

The steady state d.c. inception level is orders higher than the equivalent a.c. value although once this latter is exceeded there are transitory discharges with every increase in voltage. Above a

particular value there are discharges with every change (both increase and decrease) of stress, after this point has been passed these discharges, which decay with time, occur even when the stress is reduced to a low value. Permanent (non-decaying) discharges occur once the steady state d.c. inception is exceeded.

It is felt that, in the majority of cases, discharge extinction (decay) in voids under direct voltage conditions can be explained by the extended polarization properties of the dielectrics involved and this is at least as significant as the formation of conducting paths in the voids due to discharge products.

10.4 Equivalent circuits

The equivalent circuits so far discussed for both sound dielectrics and for dielectrics containing voids incorporate as far as possible parameters to give a response nearer the actual one, an effect Cole tried to achieve by adding a time dependent impedance $\overline{Z} = a(1\omega\tau)^{-\alpha}/(\varepsilon_o - \varepsilon_\infty)$ to his equivalent circuit. This was in addition to the conventional capacitances and instead of a straight forward resistance.

Hence the equivalent circuits coupled with the awareness of the presence of a space or internal charge should present a better understanding of dielectrics especially macroscopically mixed dielectrics for it is obvious from the analysis on inhomogeneity discussed earlier that the anomalies should arise more easily at high stresses with macroscopically mixed systems like glasses[120,121], resins with fillers, highly ionic crystals, semi-conductors, oil paper systems and impure gases, impure liquids (Cole). On the other hand it might arise equally well where the dielectric (say polythene) has been treated with some sort of antioxidant. In general since it is virtually impossible to produce a homogeneous engineering material these anomalies should be looked for. In the final analysis it is not inconceivable that charged regions in the dielectric should oscillate as in gas plasma oscillations[78,79].

The influence of space/internal charge on design criteria

Finally it must be borne in mind that in spite of the fact that non of the existing laws of conduction provide adequate explanation for exponential conduction in dielectrics, the complexity of adequate space charge equations (see chapter 3) and the fact that different assumptions produce different results make their thorough application to practical design criteria difficult. Even now it is not very clear whether the use of exponential conductivity formulae alone are sufficient data to contain space charge effects.

In the above context two cases stand out in the present investigation, (i) exponential conduction alone cannot account for the boundary conditions effects encountered in the discharge experiments (and discussed in chapter 9). Moreover the analysis of stresses in a polythene cable (see appendix 8) assuming an exponential increase of conductivity with stress and employing constants used in previous practical calculations seemed to indicate that the stress at the core - screen cannot be as high as those obtained since if this were so a lot more core-screen discharges would have occured at the core-screen/air interface especially when compared to the discharge characteristics of the cable under alternating voltage conditions, thus once again indicating the necessity of the use of boundary conditions.
(ii) exponential conduction formula would have to take into account thickness and volume dependence, and the problem that different samples of material (e.g. X, Y_1, Y_3) with similar ohmic characteristics may have widely different non-ohmic characteristics and different log J/stress gradients.

Nevertheless it is probable that as more work is undertaken to evaluate the parameters affecting space changes, dielectrics could (in the future) be designed (for example in the resin range with fillers) which might possess the desired characteristics. Hence a lot more research is needed to assess more fully the stresses within and around dielectrics in the presence of this space or internal charge.

References:

1. WHITEHEAD, J.B., and MARVIN, R.H.: 'Anomalous conduction as a cause of dielectric absorption', Trans.Amer.Inst.Elect. Engrs., 1929, 48, pp.299-316.

2. MEEK, J.M., and CRAGGS, J.D.: 'Electrical breakdown of gases (Clarendon Press, Oxford 1953).

3. FROHLICH, H.: 'On the theory of dielectric breakdown in solids', Proc. Roy, Soc. 1947, 188(A), pp. 521-532.

4. WATSON, D.B., HEYES, W., and KAO, K.C.: 'Some aspects of dielectric breakdown of solids', IEEE Trans., 1965, EI-2(2), pp 30-37.

5. DAVIES, D.K.: 'Trapped charge on dielectric surface', ERA report 5170, 1966.

6. SAM, W.: 'A multi-stage high-voltage, direct-current generator for the detection and measurement of internal discharges in solid insulation', M.Phil. thesis, University of London, 1967.

7. SALVAGE, B and SAM, W.: 'Detection and measurement of discharges in solid insulation under direct voltage conditions', Proc. IEE., 1967, 114(9), pp. 1334-1336.

8. FRENKEL, J.: 'On pre-breakdown penomena in insulators and electronic semi-conductors', Phys. Rev., 1938, 54, pp. 647-649.

9. MOTT, N.F., and GURNEY, R.W.: 'Electronic processes in ionic crystals', (Dover, 1964).

10. FOWLER, R.H., and NORDHEIM, L.: 'Electron emission in intensive electric fields', Proc. R. Soc., 1928, 119 (A), pp 173-181.

11. POOLE, H.H.: 'On the dielectric and electrical conductivity of mica in intense fields', Phil. Mag. 1916, 32 (6) pp. 112-129.

12. OUDIN, J.M., and THEVENON, H.: 'Theory of d.c. cables calculation of gradient and its correlation with breakdown gradient', CIGRE, paper 208, 1966.

13. SIMMONS, J.G.: 'Poole-Frenkel effect and Schottky effect in metal-insulator-metal systems', Phys. Rev., 1967, 155 (3), pp 657-660.

14. KONOROVA, E.A.: 'Currents in alkali halide crystals due to the electric emission from the cathode in strong electric fields', Bull. Acad. Sci. USSR, Phys.Ser., 24 (1), pp 56-62.

15. WILLIS, C.H.: 'Space charge and current in alternating corona, Trans. Amer. Inst.Elec.Engrs., 1927, 46, pp 271-288.

16. PEEK, F.W.: 'Dielectric phenomena in high-voltage engineering' (McGraw-Hill, 1929).

17. TRICHEL, G.W.: 'The mechanism of the negative point to plane corona near onset', Phys. Rev., 1938, 54, pp 1078-1084.

18. BLEANEY, B.I. and BLEANEY, B.: 'Electricity and magnetism', (Oxford University Press, 1957, 1965).

19. HERZFIELD, K.F.: 'The influence of surface conditions and space charges on the conductivity of poor conductors', Phys.Rev., 1929, 34, pp 791-807.

20. TOWNSEND, J.S.: 'The conductivity produced in gases by the motion of negatively charged eons', Nature, 1900, 62, pp 340-341.

21. TOWNSEND, J.S.: 'The conductivity produced in gases by the aid of ultra-violet light, Phil. Mag., 1902, 3 (6), pp 557-576.

22. VARNEY, R.N., WHITE, H.J., LOEB, L.B. and POSIN, D.Q.: 'The role of space charge in the study of the Townsend ionization coefficients and the mechanism of static spark breakdown', Phys. Rev., 1935, 48, pp. 818-824.

23. OCCHINI, E., and MASCHIO, G.: 'Electrical characteristics of oil impregnated paper as insulation for HV DC cables', IEEE Trans., 1967, pas-86, 3, pp. 312-322.

24. KAGAYA, S., TAKOAKA, M. and INOHANA, S.: 'Potential field distribution throughout the insulation of solid-type paper-insulated direct-current cable', J.Instn.Elec.Engrs.,Japan, 1964, pp. 9-18.

25. BRONGULEEVA, M.N.: 'The electric field of a d.c. cable', Elektrichestvo, 3, 1959, pp 78-82.

26. ADAMEC, V.: 'Nature of anomalous conductivity of polymeric insulating materials', Proc. IEE, 1965, 112, (2) pp. 405-407.

27. KOJIMA, K., MICHIO, N., and MATSUURA, K.: 'Insulating properties of solid type high voltage direct current cable', Sumitomo Elec.Tech.Rev., 1965, 6, pp. 27-43.

28. LENGYEL, G., and MITRA, S.S.: 'Long-time d.c. conductivity of oil-impregnated paper capacitors under high field stresses', IEEE Trans.,1963, PAS-82, pp 951-957.

29. AFANASEVA, E.A., VINOGRADOV, V.S., and KONOROVA, E.A.: 'Temperature and voltage dependence of the current in KBr single crystals in the breakdown fields', Bull.Acad.Sci.USSR, Phys.Ser., 1960,. 24(1), pp 75-90.

30. VOROBEV, A.A. and VOROBEV, G.A.: 'Regularities of pulse breakdown of solid dielectrics', ibid.1960, 24(1), pp 75-90.

31. BOER, K.W.: 'Some theoretical considerations concerning inhomogeneous field distribution in electric breakdown', ibid. 1960, 24(1), pp 41-46.

32. 'H.V.D.C. transmission', IEE Conf. Publ.22, 1966.

33. GORODETZKY, S.S.: '220-400 kV direct current cables', CIGRE report 1958, paper 206.

34. LAWSON, W.G.: 'H.V.D.C. cable research', Elect.Times, August, 1967, pp. 303-305.

35. GEMANT, A., and PHILLIPOFF, W.: 'Die Funkenstrecke mit Vorkondensator', Z.Tech.Phys., 1932, 13, pp 425

36. LOEB, L.B.: 'Basic processes of gaseous electronics', (University of California Press, Berkeley, 1955).

37. RAETHER, H.: 'Electron avalanches and breakdown in gases', (Butterworth, London 1964).

38. MASON, J.H.: 'The deterioration and breakdown of dielectrics by internal discharges', Proc.IEE, 1951, 98(1), pp44-59.

39. ROGERS, E.C., and SKIPPER, D.J.: 'Gaseous discharge phenomena in high voltage d.c. cable dielectric', Proc.IEE, 1960, 107A (33) pp 241-254.

40. SALVAGE, B.: 'Electric stresses in gaseous cavities in solid dielectrics', Proc. IEE, 1964, 111 (6), pp 1162-1171.

41. KRAUS, J.D.: 'Electromagnetics', (McGraw-Hill, 1953).

42. McKELVEY, J.: 'Solid state and semiconductor physics', (Harper and Row, 1966).

43. ANDERSON, J.C.: 'Dielectrics', (Chapman and Hall, 1964).

44. BIRKS, J.B.: 'Progress in dielectrics', (Heywood, 1967).

45. DANIEL, V.: 'Dielectric relaxation', (Academic Press, 1967).

46. BUCCI, C., and FIESCHI, R.: 'Ionic thermoconductivity method for the investigation of polarisation in insulators', Phys. Rev. Letters, 1964, 12, (1) pp 16-19.

47. BUCCI, C., and FIESCHI, R.: 'Ionic thermocurrents in dielectrics, Phys.Rev., 1966, 148(2), pp 816-823.

48. KREUGER, F.H.: 'Discharge detection in high voltage equipment', (Heywood, Temple Press Books Ltd., London, 1964).

49. HULLS, L.R. and McKENZIE, K.A.: 'An electronic high voltage insulation tester', Electron.Engng.,1952, 24, pp. 500-503.

50. GOODLET, B.L.: 'The testing of porcelain insulators', IEEE Trans., 1929, 67, pp. 1177-1212.

51. MEMBRY, E.J.: 'An electronic instrument for high voltage testing', Electron.Engng., 1948, 20, pp. 390-391.

52. CAMERON, A.W.W., and SINCLAIR, A.M.: 'Experience and development in non-destructive d.c. testing for maintenance of high-voltage stators', Trans.Amer.Inst.Elec.Engrs., 1956, 75(3), pp. 201-210.

53. TAGG, G.F.: 'American practice in d.c. insulation testing', Proc. IEE, 1963, 110, pp 1243-1248.

54. AUSTEN, A.E.W., THOMAS, A.M. and WHITEHEAD, S.: 'H.V. service testing with particular reference to the use of d.c! ERA Report, 1959, L/T 102.

55. RUSHALL, R.T. and SIMONS, J.S.: 'An examination of high-voltage d.c. testing applied to large stator windings', Proc. IEE, 1955, 102(A), pp. 565-580.

56. BHIMANI, B.V.: 'Very low frequency high potential testing', Trans. Amer.Inst.Elect.Engrs., 1961, 80(3), pp. 148-155.

57. BHIMANI, B.V. and FOUST, C.M.: 'Predicting insulation failures with direct voltage', Trans.Amer.Inst.Elect.Engrs., 1957, 76(3), pp. 1120-1139.

58. AUSTEN, A.E.W. and HACKETT, Mrs. W.: 'Internal discharges in dielectrics, their observation and analysis', J.Inst.Elect. Engrs., 1944, 91(1), pp. 298-322.

59. ARMANN, A.N. and STARR, A.T.: 'The measurement of discharges in dielectrics', J. Inst.Elect.Engrs., 1936, 79, pp. 67-81.

60. QUINN, C.E.: 'A method for detecting the ionization point on electrical apparatus', Trans.Amer.Inst.Elect.Engrs., 1940, 59, pp. 680-682.

61. BASHARA, N.M.: 'The study of discharges in dieelectric voids by photomultiplier methods', ibid., 1961, 80(3), pp. 115-119.

62. BERG, D., and DAKIN, T.: 'Corona in discharges with a multiplier phototube', Rep.Ann.Con. on Elect.Insulation, National Academy of Sciences, National Research Council, Washington D.C., 1955, pp. 40.

63. MOLE, G.: 'Design and performance of a portable a.c. discharge detector', ERA Report, 1952, N/T115.

64. Vibron electrometer, model 330 and B33C-2 industrial converter unit, Electronic Instruments Limited, Richmond, Surrey, England.

65. ERA discharge detector, model 3, type 652, F.C. Robinson and Partners Limited, Cheadle, Cheshire, England.

66. EKCO automatic scaler, type N530G, EKCO Electronics Limited, Romford, Essex, England.

67. Direct recording ultraviolet oscillograph, type M1250, Southern Instruments Limited, Camberley, Surrey, England.

68. Brandenburg high voltage direct current generator, type MR30/R, Model 805, South Croydon, Surrey, England.

69. Keightley electrometer, model 602, Keightley Instruments, Incs., 28775 Aurora Road, Cleveland, Ohio 44139, U.S.A.

70. KING, A.: 'Ultraviolet light: Its effects on plastics', Plastics and Polymers, 1968, 23 (123) pp. 195-203.

71. RUDYAK, V.M.: and BOGOMOLOV, A.A.: 'Polarization discontinuities in ferroelectric SbSI caused by illuminations', Soviet Phys. Solid St., 1968, 9 (11), pp. 2624-2625.

72. TANAKA, T., and INUISHI, Y.: 'Photoconduction of high-density polyethylene', Jap.J.Appl.Phys., 1967, 6(12), pp. 1371-1380.

73. GERSHUN, A.S., SYSOEV, L.A. and TIMAN, B.L.: 'Some peculiarities of the volt-ampere characteristics of thin CdS single crystals with non-ohmic contacts', Soviet Phys.Solid St., 1966, 8(5), pp. 1302-1303.

74. GERSHUN, A.S., SYSOEV, L.A. and TIMAN, B.L.: 'Dependence of current on time in the system In-CdS-In under various voltages', Soviet Phys. Solid St., 1967, 8(10), pp. 2495-2496.

75. GERSHUN, A.S., SYSOEV, L.A. and TIMAN, B.L.: 'Investigation of the charge formed in cadmium sulphide crystals under the action of an applied electric field', Soviet Phys.Solid St., 1967, 8(12), pp. 2982-2983.

76. GERSHUN, A.S. and TIMAN, B.L.: 'Laws governing the non-stationary current in metal-dielectric-metal systems', Soviet Phys. Dokl., 1967, 12(3), pp 237-238.

77. GERSHUN, A.S. and TIMAN, B.L.: 'Formation of charged regions in CdS by the application of an electric field', Soviet Phys. Solid St., 1967, 9(3), pp 727-728.

78. PASTRNAK, J.: 'A thermodynamic investigation of the conditions for the generation of oscillations of an electric current flowing through a non-ohmic medium', Phys.Stat.Sol., 1967, 22, pp 407-413.

79. ISHIGURO, T. and TANAKA, T.: 'Non-ohmic and oscillatory behaviours at strong electric field in tellerium', Jap.J.Appl.Phys., 1967, 6(7), pp. 864-874.

80. CLARK, F.M.: 'Insulating materials for design and engineering practice', (John Wiley and Sons, New York and London, 1962).

81. COLE, K.S. and COLE, R.H.: 'Dispersion and absorption in dielectrics', (I A.C. Characteristics), J. Chem.Phys., 1941, 9, pp. 341-351, (II D.C. Characteristics), J.Chem.Phys., 1942, 10, pp. 98-105.

82. STARK, K.H.: 'Assessment of the insulation serviceability of turbo-generator stators and of high-voltage bushings', Proc.IEE, 1961, 109(A), pp. 71-88.

83. ADAMEC, V.: 'Temporary changes in electrical properties of polymer dielectrics due to ionizing radiation', J. Polym.Sci., 1968, 6(A-2), pp. 1241-1253.

84. GUBKIN, A.N., and MATSONASHVILI, B.N.: 'The physical nature of the electret effect in carnuaba wax', Soviet Phys.Solid St., 1962, 4(5), pp. 878-884.

85. SILLARS, R.W.: 'The properties of a dielectric containing semi-conducting particles of various shapes', J.Instn.Elect.Engrs.,1937, 80, pp. 378-394.

86. TILLEY, D.E.: 'A Phenomenological theory of dielectric response', J.Appl.Phys., 1967, 38(6), pp. 2543-2546.

87. KESSLER, A and MARIANI, E.: 'On the influence of the electrode performance on interfacial polarization of Nacl crystals', Physics Chem.Solids, 1968, 29(6), pp. 1079-1082.

88. MAXWELL, J.C.: 'A treatise on electricity and magnetism, Vol.1', (Oxford at the Clarendon Press, 1904).

89. KALLMAN, H. and ROSENBERG, B.: 'Persistent internal polarization', Phys.Rev., 1955, 97(6), pp. 1596-1610.

90. VON HIPPEL, A., GROSS, E.P., JELATIS, J.G. and GELLER, M.: 'Photocurrent, space-charge build up, and field emission in alkali halide crystals', Phys.Rev., 1953, 91(3) pp. 568-579.

91. JAFFE, G.: 'Theory of conductivity of semi conductors', Phys. Rev., 1952, 85(2), pp. 354-363.

92. JAFFE, G. and LEMAY, C.Z.: 'On polarization in liquid dielectrics', J.Chem.Phys., 1953, 21(5), pp. 920-927.

93. WEISS, S.Z., COBAS, A., TRESTER, S. and MANY, A.: 'Electrode limited and space-charge-limited transient currents in insulators', J.Appl.Phys., 1968, 39(5), pp. 2296-2302.

94. ROSE, A.: 'Space-charge-limited currents in solids', Phys.Rev., 1955, 97(6), pp. 1538-1544.

95. MIYOSHI, Y. and CHINO, K.: 'Electrical properties of polyethylene single crystals', Jap.J. Appl.Phys., 1967, 6(2), pp. 181-190.

96. LILLY, A.C. and McDOWALL, J.R.: 'High-field conduction in films of mylar and teflon', J. of Appl.Phys., 1966, 39(1), pp. 141-147.

97. SUTTER, D.H. and NOWICK, A.S.: 'Ionic conductivity and time-dependent polarization in Nacl crystals', J.Appl.Phys.,1963, 34(4) Part 1, pp. 734-736.

98. STRATTON, J.A.: 'Electromagnetic theory', (McGraw-Hill, 1941).

99. SEELY, S.: 'Introduction to electromagnetic fields',(McGraw-Hill,1958).

100. BHIMANI, B.V.: 'Some characteristics of ionization under direct voltage stress', IEEE Trans., 1960, paper 60-1196.

101. BAILEY, C.A.: 'A study of internal discharges in cable insulation', IEEE Summer Power Meeting, July 1966, Paper 31, pp. 66-363.

102. HALL, H.C. and RUSSEK, R.M.: 'Discharge inception and extinction in dielectric voids', Proc.IEE, 1954, 101 II, pp. 47-58.

103. ROGERS, E.C.: 'The self-extinction of gaseous discharges in dielectrics', Proc. IEE, 1958, 105A, pp. 621-630.

104. MORTON, V.M. and STANNETT, A.W.: 'Volume dependence of electric strength of polymers', Proc.IEE, 1968, 115(12) pp. 1857.

105. LAMPERT, M.A.: 'Simplified theory of space-charge-limited currents in an insulator with traps', Phys.Rev. 1956, 103(6), pp 1648-1656.

106. JOFFE, F.A.: 'The physics of crystals', (McGraw-Hill, 1928).

107. SMITH, R.W. and ROSE, A.: 'Space-charge-limited currents in single crystals of cadmium sulphide', Phys.Rev. 1955, 97(6), pp. 1531-1537.

108. MACFARLANE, J.C. and WEAVER, C.: 'Low frequency polarization effects in thin evaporated dielectric films', Phil.Mag.1968, 18 (151), pp. 27-39.

109. JACOBS, P.W. and MAYLOCK, J.N.: 'Polarization effects in the ionic conductivity of alkali halide crystals (1) a.c. capacity', J.Chem. Phys. 1963, 39(3), pp. 757-762.

110. HAYDEN, J.L.R. and STEINMETZ, C.P.: 'High-voltage insulation', Trans.Amer.Inst.Elect.Engrs.,1923, 42 pp. 1029-1041.

111. DEL MAR, W.A., DAVIDSON, W.F. and MARVIN, R.H.: 'Electric strength of solid and liquid dielectrics', Trans.Amer.Inst.Elec.Engrs. 1927, 46, pp. 1049-1063.

112. OKAZAKI, S. and HIRAMATSU, M.: 'Experimental investigation of double injection in P-type silicon', Jap.J.Appl.Phys.,1968, 7, pp. 557-558.

113. SEITZ, M.A. and WHITMORE, D.H.: 'Electronic drift mobilities and space-charge-limited currents in lithium-doped zinc oxide', J.Phys.Chem.Solids, 1968, 29(6), pp. 1033-1049.

114. GARTON, C.G.: 'Conduction in dielectrics part 1, potential distribution between conducting boundaries with zero current flow', ERA Report, 1968, No. 5256.

115. GARTON, C.G.: 'The contact potential distribution in a dielectric and IEE colloquium on charge movement and discharges in solid and liquid dielectrics, Colloquium digest No. 1968/17, pp. 1-3.

116. LAWSON, W.G. and MASON, J.H.: 'Conduction polarization and space charge phenomena in oil-impregnated paper insulation', ibid. pp. 5.

117. MARR, P.J.: 'The detection of discharges and a comparison between the behaviour of dielectrics under h.v.d.c. and a.c. voltages', Final year project report, Loughborough University of Technology, Dept. of Elect.Eng., March 1969.

118. SANDERS, F.H.: 'The value of the Townsend coefficient for ionization by collision at large plate distances and near atmospheric pressure', Phys.Rev.,1932, 41, pp. 667-677.

119. SANDERS, F.H.: 'Measurement of the Townsend coefficients for ionization by collision', Phys.Rev.,1933, 44, pp. 1020-1024.

120. HUGHES, K. and ISARD, J.O.: 'Measurement of ionic transport in glass, part 1 mixed alkali glasses', Physics and Chemistry of Glasses, 1968, 9(2), pp. 37-42.

121. HUGHES, K., ISARD, J.O. and MILNES, G.C.: 'Measurement of ionic transport in glass Part 2. soda-lead-silica glass', ibid, pp. 43-46.

122. JACKSON, J.D.: 'Classical electrodynamics', (John Wiley & Sons 1962).

123. SMYTHE, W.R.: 'Static and dynamic electricity', (McGraw-Hill, 1939).

124. ONSAGER, L.: 'Electric moments of molecules in liquids', J. Amer.Chem.Soc., 1936, 58, pp. 1486-1493.

125. BULLER, H.: 'Calculation of electrical stresses in d.c.cable insulation', IEEE Trans., 1967, PAS.86,(10), pp 1169-1178.

126. CHU, S.: 'Design stresses and current ratings of impregnated paper insulated cables for h.v.d.c.', IEEE Trans., PAS-86, (9), pp. 1029-1036.

APPENDIX 1.

Definition of Terms

1.1 Electrical discharge:

Movement of electrical charges through or across an insulating medium initiated by electron avalanches and maintained by various secondary processes that generate further avalanches.

1.2 Partial discharge:

An electrical discharge that only partially bridges the insulating medium between conductors i.e. internal surface discharges and corona.

1.3 Internal discharge:

Partial discharges in cavities or at the edges of conducting inclusion in non-gaseous insulation. The cavity may be entirely enclosed in insulation, or it may be covered on one side by a conductor.

1.4 Surface discharges:

Partial discharges from a conductor in a gaseous or liquid medium onto or across the surface of solid insulation that is not covered by the conductor.

1.5 Corona:

Partial discharges in gases or liquids around conductors that are remote from solid insulation or completely exposed.

1.6 Discharge inception voltage:

1.6.1 A.C.: The lowest voltage at which discharges of a special magnitude recur in successive cycles when an increasing alternating voltage is applied to the insulation.

1.6.2 Steady State d.c. The lowest voltage at which discharges occur under d.c. steady state conditions, i.e. number of discharges not decaying to zero (depending on the sensitivity of the circuit) with time of application of the voltage, at a fairly regular rate.

1.7 D.C. transient inception voltage:

The lowest voltage at which discharges occur upon further increasing the applied direct voltage then decaying with a time constant of seconds or less to zero. Below this voltage no discharges occur upon increasing the applied voltage. (It is the lowest voltage at which discharges occur upon suddenly decreasing the applied voltage.

1.8 Discharge extinction voltage:

A.C. - This is the lowest voltage at which discharges of a specified magnitude will reoccur when the applied voltage which has exceeded the discharge inception voltage is reduced.

1.9 Discharge magnitude Q:

Loss of charge, as measured at the terminals of a sample, caused by a single discharge.

1.10 Discharge detector:

A device for detecting and or measuring discharges.

1.11 Discharge detector sensitivity:

The magnitude of the smallest individual discharge that can be measured under particular test conditions.

1.12 Discharge resolution:

The time interval between two discharges that can be adequately distinguished and measured by a detector.

1.13 Calibrating pulse:

An artificially generated pulse or step wave voltage injected into a discharge detector circuit to provide a quantitative comparison with the magnitude of discharges in a test specimen.

1.14 Rogowski electrode profile:

An electrode with the edges of its contact faces shaped to follow a curved profile to reduce edge (and or discharge effects).

1.15 Steady state conduction:

The state reached at which there is no appreciable change of current with time.

1.16 Non-ohmic conduction:

Any steady state conductivity σ which does not obey Ohm's Law viz: $J = \sigma E$.

The following terms separate the conventional definition of charging/discharging which mean polarization/de-polarization, into two viz: initial charging/discharging and eventual polarization/de-polarization.

1.17 Initial charging/discharging process:

This is the initial burst of charge or current which has a very short time constant on the increasing/decreasing, of a step function. This process is the only type noticeable or measurable at low d.c. stresses and under normal a.c. conditions.

1.18 Eventual polarization/depolarization process:

This process is caused by the gradual 'polarization'/'depolarization' process within or across the medium. It is characterised by a very slow decay (or increase under special conditions) of charge or current to a steady state value. This process may take hours, days or even weeks and it is most noticeable at medium d.c. stresses. (*At high stresses with particular dielectrics the decay might turn into an increase).

APPENDIX 2 Current and Voltage response

Appendix 2.1

Current response for circuit in fig. 3a

For the circuit in fig. 3 the Laplace transform of the current is given by

$$i = \frac{V}{pZ_L}$$

where $Z_L = \dfrac{R_1R_S\left(p + \frac{1}{C_SR_S}\right)}{\left[R_1+R_S\right]\left[p + \frac{1}{C_S(R_S+R_1)}\right]} + \dfrac{R_2R_T\left(p + \frac{1}{C_TR_T}\right)}{\left[R_2+R_T\right]\left[p + \frac{1}{C_T(R_2+R_T)}\right]}$

Let $R_1 >> R_S$ and $R_2 >> R_T$

$$\therefore\ Z_L = \frac{R_1R_SR_2}{R_1R_2}\ \frac{\left[p + \frac{1}{C_SR_S}\right]\left[p + \frac{1}{C_TR_2}\right] + R_2R_TR_1\left[p + \frac{1}{C_TR_T}\right]\left[p + \frac{1}{C_SR_1}\right]}{\left[p + \frac{1}{C_SR_1}\right]\ \left[p + \frac{1}{C_TR_2}\right]}$$

$$= R_S\left[p^2 + p\ \left(\frac{1}{C_SR_S} + \frac{1}{C_TR_2}\right) + \frac{1}{C_SR_S}\ \frac{1}{C_TR_2}\right] + R_T\left[p^2 + p\left(\frac{1}{C_TR_T} + \frac{1}{C_SR_1}\right) + \frac{1}{C_TR_T}\cdot\frac{1}{C_SR_1}\right]$$

$$p^2 + p\left(\frac{1}{C_SR_1} + \frac{1}{C_TR_2}\right) + \frac{1}{C_SR_1}\cdot\frac{1}{C_TR_2}$$

$$i = \frac{V}{p}\cdot\frac{\left[p^2 + p\left(\frac{1}{C_SR_1} + \frac{1}{C_TR_2}\right) + \frac{1}{C_SR_1C_TR_2}\right]}{\left[R_S + R_T\right]\left[p^2 + \frac{C_TR_2R_1 + R_1R_SC_S + C_SR_2R_1 + C_TR_TR_2}{C_SC_TR_2R_1\ (R_S + R_T)}\ p + \frac{R_1 + R_2}{C_SR_1C_TR_2(R_S + R_T)}\right]}$$

writing this as

$$i = \frac{V}{p}\cdot\frac{\left[p^2 + p\ \left(\frac{1}{C_SR_1} + \frac{1}{C_TR_2}\right) + \frac{1}{C_SR_1\cdot C_TR_2}\right]}{(R_S + R_T)\ (p^2 + p\ C^1 + D^1)}$$

$$D^1 = \frac{R_1 + R_2}{R_S + R_T} \cdot \frac{1}{C_S R_1 C_T R_2} \quad \text{and} \quad C^1 = \frac{C_T R_2 (R_1 + R_T) + C_S R_1 (R_2 + R_S)}{C_S C_T R_2 R_1 (R_S + R_T)}$$

$$i = \frac{V_A}{R_S + R_T} \left\{ \frac{p}{p^2 + pC^1 + D^1} + \frac{\frac{1}{C_S R_1} + \frac{1}{C_T R_2}}{p^2 + pC^1 + D^1} + \frac{1}{C_S C_T R_1 R_2} \frac{1}{p(p^2 + pC^1 + D^1)} \right\}$$

$$= \frac{V_A}{R_S + R_T} \left\{ \frac{p}{p^2 + pC^1 + D^1} + \frac{\frac{1}{C_S R_1} + \frac{1}{C_T R_2}}{p^2 + pC^1 + D^1} + \frac{1}{D^1 C_S C_T R_1 R_2} \left[\frac{1}{p} - \frac{(p + C^1)}{p^2 + pC^1 + D^1} \right] \right\}$$

But $D^1 = \frac{R_1 + R_2}{R_S + R_T} \cdot \frac{1}{C_S C_T R_1 R_2}$

$$\therefore i = \frac{V_A}{R_S + R_T} \left\{ \frac{R_S + R_T}{R_1 + R_2} \cdot \frac{1}{p} + \left[\frac{(R_1 + R_2) - (R_S + R_T)}{R_1 + R_2} \right] \left[\frac{p}{p^2 (pC^1 + D^1)} \right] - \frac{C^1}{p^2 + pC^1 + D^1} \right\}$$

$\therefore$ Writing the inverse and substituting for C^1 and D^1

$$i = \frac{V_A}{R_S + R_T} \left\{ \frac{R_S + R_T}{R_1 + R_2} + \frac{\varepsilon^{-\alpha t}}{2} (\varepsilon^{\beta t} + \varepsilon^{-\beta t}) - \frac{C^1}{2\beta} \varepsilon^{-\alpha t} (\varepsilon^{\beta t} - \varepsilon^{-\beta t}) \right\}$$

if we assume that $R_1 >> R_T$

$$\text{Then } i = \frac{V_A}{R_S + R_T} \left\{ \frac{R_S + R_T}{R_1 + R_2} + \frac{\beta C_S C_T R_2 R_S - C_T R_2 - C_S (R_2 + R_S)}{2\beta C_S C_T R_2 R_S} \exp^{-(\alpha - \beta)t} + \frac{\beta C_S C_T R_2 R_S - C_T R_2 + C_S (R_2 + R_S)}{2\beta C_S C_T R_2 R_S} \exp^{-(\alpha + \beta)t} \right\}$$

$$\text{where } \alpha = \frac{C^1}{2} = \frac{C_T R_2 (R_1 + R_T) + C_S R_1 (R_S + R_2)}{2 C_S C_T R_2 R_1 (R_S + R_T)}$$

Let $R_1 > R_S > R_T$

$$\therefore \quad \alpha = \frac{C^1}{2} \doteq \frac{C_T R_2 R_1 + C_S R_1 (R_2 + R_S)}{2C_S C_T R_2 R_1 R_S}$$

$$\doteq \frac{C_T R_2 + C_S (R_2 + R_S)}{2C_S C_T R_2 R_S}$$

$$\beta^2 = \alpha^2 - D^1 = -\frac{R_1 + R_2}{R_S + R_T} \cdot \frac{1}{C_S R_1 C_T R_2} + \left[\frac{C_T R_2 (R_1 + R_T) + C_S R_1 (R_2 + R_S)}{2C_S C_T R_2 R_1 (R_S + R_T)}\right]^2$$

$$\doteq \left[\frac{C_T R_2 + C_S (R_2 + R_S)}{2C_S C_T R_2 R_S}\right]^2 - \frac{R_1 + R_2}{C_S C_T R_1 R_2 R_S}$$

$$\doteq \frac{\left\{R_1 \left[C_T R_2 + C_S (R_2 + R_S)\right]^2 - 4C_S C_T R_1 R_2 R_S (R_1 + R_2)\right\}}{4(C_S C_T R_1 R_S R_2)^2}$$

Let $R_1 >> R_2$

$$\beta^2 \doteq \frac{\left[C_T R_2 + C_S (R_2 + R_S)\right]^2 - 4C_S C_T R_2 R_S}{4(C_S C_T R_2 R_S)^2}$$

$$\beta \doteq \frac{\sqrt{\left[C_T R_2 + C_S (R_2 + R_S)\right]^2 - 4C_S C_T R_2 R_S}}{2C_S C_T R_2 R_S}$$

It should be noted in an extreme case where $D^1 > \alpha^2$ an oscillatory (sinusoidal) response might be obtained.

Let $C_T >> C_S$ and $R_2 \sim R_S$

$$\beta \doteq \frac{\sqrt{C_T^2 R_2^2 - 4C_S C_T R_2 R_S}}{2C_S C_T R_2 R_S}$$

Appendix 2.2 Current response for circuit in Fig. 36b

For a parallel R-C circuit

$$\frac{R \cdot \frac{1}{pC}}{R + \frac{1}{pC}} = \frac{R}{1+pCR}$$

$\therefore$ For maxwellian, equivalent as shown in Fig. 36b

$$Z_T = \frac{R_1}{1 + pC_1R_1} + \frac{R_2}{1 + pC_2R_2}$$

$$= \frac{R_1(1 + pC_2R_2) + R_2\ (1 + pC_1R_1)}{(1 + pC_1R_1)\ (1 + pC_2R_2)}$$

$$= \frac{R_1C_2R_2\ (p + \frac{1}{C_2R_2}) + C_1R_1R_2\ (p + \frac{1}{C_1R_1})}{C_1R_1C_2R_2\ (p + \frac{1}{C_1R_1})\ (p + \frac{1}{C_2R_2})}$$

$$= \frac{p\ (C_2R_2R_1 + C_1R_1R_2) + R_1 + R_2}{C_1R_1C_2R_2\ \left[p^2 + p(\frac{1}{C_1R_1} + \frac{1}{C_2R_2}) + \frac{1}{C_1R_1C_2R_2}\right]}$$

$\therefore$ $$i_A = \frac{V_s}{p} \cdot \frac{C_1R_1C_2R_2\ \left[p^2 + p\ (\frac{1}{C_1R_1} + \frac{1}{C_2R_2}) + \frac{1}{C_1R_1C_2R_2}\right]}{R_1R_2\ (C_2 + C_1)\ \left[p + \frac{R_1 + R_2}{R_1R_2(C_1 + C_2)}\right]}$$

$$= \frac{V_s}{\frac{C_2 + C_1}{C_2C_1}} \left\{ \frac{p}{p + \frac{R_1 + R_2}{R_1R_2(C_1 + C_2)}} \cdot \frac{\frac{1}{C_1R_1} + \frac{1}{C_2R_2}}{p + \frac{R_1 + R_2}{R_1R_2(C_1 + C_2)}} \right.$$

$$\left. + \frac{\frac{1}{C_1R_1C_2R_2}}{p\left[p + \frac{R_1 + R_2}{R_1R_2(C_1 + C_2)}\right]} \right\}$$

$$= \frac{VC_2C_1}{C_1+C_2}\left\{ p + \frac{R_1 + R_2}{R_1 R_2(C_1 + C_2)} - \frac{R_1 + R_2}{R_1R_2(C_1 + C_2)} + \frac{\frac{1}{C_1R_1} + \frac{1}{C_2R_2}}{p + \frac{R_1 + R_2}{R_1R_2(C_1 + C_2)}} \right.$$

$$\left. + \frac{\frac{1}{C_1R_1C_2R_2}}{p\left[p + \frac{R_1 + R_2}{R_1R_2(C_1 + C_2)}\right]} \right\}$$

$$i_A(t) = \frac{VC_2C_1}{C_1+C_2}\left\{ (\delta t) - \exp^{-\psi t}\ \frac{R_1 + R_2}{R_1R_2(C_1 + C_2} + \left(\frac{1}{C_1R_1} + \frac{1}{C_2R_2}\right) \right.$$

$$\left. \exp^{-\psi t} + \frac{R_1R_2(C_1 + C_2)}{C_1R_1C_2R_2(R_1+R_2)}\left[1-\epsilon^{-\psi t}\right] \right\}$$

where $\psi = \dfrac{R_1 + R_2}{R_1R_2(C_1 + C_2)}$

$$= \frac{VC_2C_1}{C_1+C_2}\left\{ \delta t + \left[\frac{1}{C_1R_1} + \frac{1}{C_2R_2} - \frac{R_1 + R_2}{R_1R_2(C_1 + C_2)} - \frac{C_1 + C_2}{C_1C_2(R_1 + R_2)}\right] \epsilon^{-\psi t} \right.$$

$$\left. + \frac{C_1 + C_2}{C_1C_2(R_1 + R_2)} \right\}$$

$$= \frac{VC_2C_1}{C_1+C_2}\left\{ \delta t + \frac{(R_1C_1 - R_2C_2)^2}{C_1C_2R_1R_2(R_1 + R_2)(C_1 + C_2)} \exp^{-\psi t} + \frac{C_1 + C_2}{C_1C_2(R_1 + R_2)} \right\}$$

$$= \frac{VC_2C_1}{C_1+C_2}\left\{ \delta t + \frac{(R_1C_1 - R_2C_2)^2}{C_1C_2R_1R_2(R_1 + R_2)(C_1 + C_2)} \exp^{-\psi t} + \frac{C_1 + C_2}{C_1C_2(R_1 + R_2)} \right\}$$

where (δt) is an impulse function

For n layers the coefficient of the exponential term equals

$$\frac{\left[R_1C_1 - (R_3 + \ldots \ldots R_n)\ \dfrac{1}{\frac{1}{C_3} + \ldots \ldots \frac{1}{C_n}}\right]^2}{C_1 \Sigma\dfrac{1}{\frac{1}{C_3} + \ldots \ldots \frac{1}{C_n}}\ R_1\ (R_3 + \ldots + R_{n-1} + R_n)\ (C_1 + \Sigma \dfrac{1}{\frac{1}{C_3} + \ldots \frac{1}{C_n}}}$$

Appendix 2.3

Voltage across one layer for the circuit in fig. 4a

$$Z_1 = \frac{R_1}{1 + pC_1R_1}$$

$$Z_T = \frac{R_1}{1 + pC_1R_1} + \frac{R_2}{1 + pC_2R_2}$$

Therefore for a step function V = o and V = V, t>0

$$\therefore\ V_1 = \frac{V_A}{p} \cdot \frac{\frac{R_1}{1 + pC_1R_1}}{\frac{R_1}{1 + pC_1R_1} + \frac{R_2}{1 + pC_2R_2}}$$

$$= \frac{V_A}{p}\ \frac{1}{1 + \frac{R_2(1 + pC_1R_1)}{R_1(1 + pC_2R_2)}}$$

$$= \frac{V_A}{p}\ \frac{1}{1 + \frac{C_1\ (p + \frac{1}{C_1R_1})}{C_2\ (p + \frac{1}{C_2R_2})}}$$

$$= \frac{V_A}{p}\ \frac{p + \frac{1}{C_2R_2}}{p + \frac{1}{C_2R_2} + \frac{C_1}{C_2}\ (p + \frac{1}{C_1R_1})}$$

$$= \frac{V_A}{p} \frac{p + \frac{1}{C_2R_2}}{(\frac{C_1}{C_2} + 1)\, p + \frac{1}{C_2R_2} + \frac{1}{C_2R_1}}$$

$$= \frac{V_A}{\frac{C_1 + C_2}{C_2}\, p} \left[\frac{p + \frac{1}{C_2R_2}}{p + \frac{\frac{1}{C_2R_2} + \frac{1}{C_2R_1}}{\frac{C_1 + C_2}{C_2}}} \right]$$

$$= \frac{VC_2}{C_1 + C_2} \left[\varepsilon^{-(\frac{1}{R_2} + \frac{1}{R_1})\frac{1}{C_1 + C_2}} + \frac{1}{C_2R_2} (1 - \varepsilon^{-\psi t}) \frac{C_1 + C_2}{(\frac{1}{R_2} + \frac{1}{R_1})} \right]$$

$$= \frac{VC_2}{C_1+C_2} \left\{ \exp \frac{(R_1 + R_2)t}{R_1R_2(C_1 + C_2)} \left[1 - \frac{R_1R_2(C_1 + C_2)}{R_2C_2(R_1 + R_2)} \right] + \frac{R_1R_2(C_1 + C_2)}{C_2R_2(R_1 + R_2)} \right\}$$

$$= \frac{VC_2}{C_1+C_2} \left\{ \left[\frac{C_2 (R_1 + R_2) - R_1 (C_1 + C_2)}{C_2 (R_1 + R_2)} \right] \varepsilon^{-\psi t} \frac{R_1R_2}{C_2R_2} \left[\frac{(C_1 + C_2)}{R_1 + R_2} \right] \right\}$$

$$= \frac{VC_2}{C_1+C_2} \left\{ \left[\frac{C_2R_1 + C_2R_2 - R_1C_1 - R_1C_2}{C_2 (R_1 + R_2)} \right] \varepsilon^{-\psi t} + \frac{R_1}{C_2} \left[(\frac{C_1 + C_2}{R_1 + R_2}) \right] \right\}$$

$$= \frac{VC_2}{C_1+C_2} \left\{ \frac{C_2R_2 - R_1C_1}{C_2(R_1 + R_2)} \varepsilon^{-\psi t} + \frac{R_1}{C_2} \left[(\frac{C_1 + C_2}{R_1 + R_2}) \right] \right\}$$

where $\psi = \frac{R_1 + R_2}{R_1R_2(C_1 + C_2)}$

2.4. Current response for waveform $v = \frac{V_A}{K} t$ for $t = o$ to $t = \tau$ and $v = V_A$ for $t > \tau$

For the circuit in fig.36b assume that the applied waveform is as shown. in Fig. 51a

$$i_c = \frac{V_A}{pZ_L} + \frac{-V_A}{Kp^2Z_L}$$

from appendix 2.2, $i_A = \frac{V}{pZ_L}$

By superposition and by applying Laplace as in the previous cases.

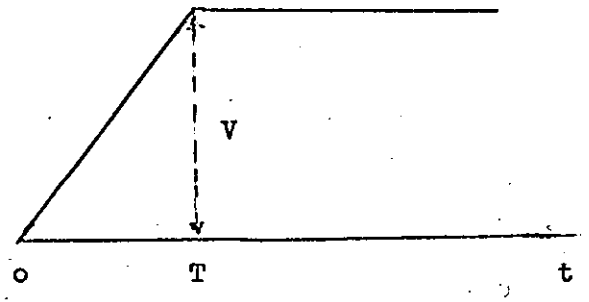

Fig. 51a

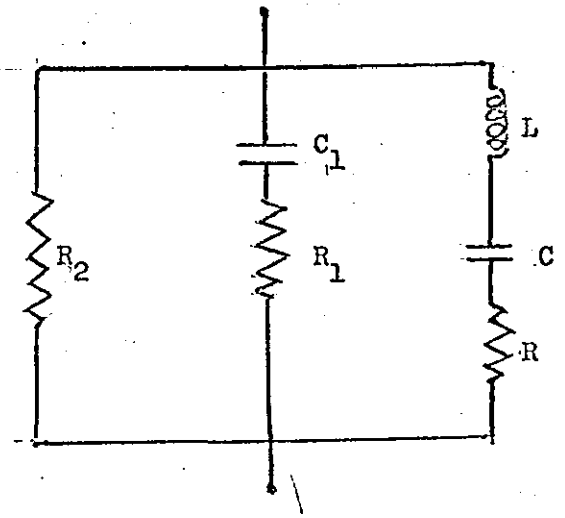

Fig. 51b

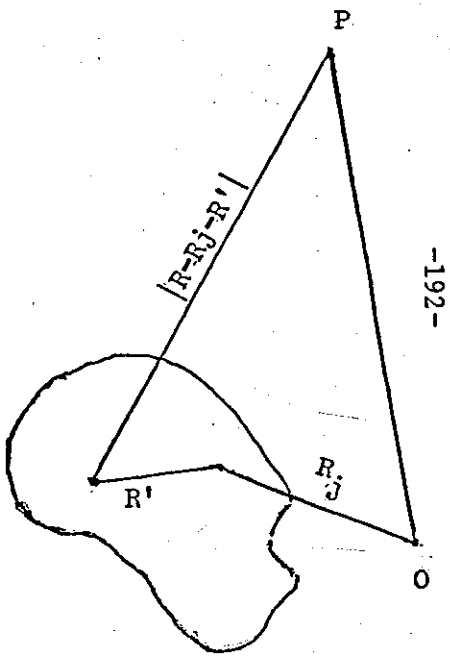

Fig. 51c

$$i_C = i_A + \frac{V_A}{Kp^2} \frac{C_2C_1}{C_1+C_2} \left\{ \frac{p^2 + p\left(\frac{1}{C_1R_1} + \frac{1}{C_2R_2}\right) + \frac{1}{C_1R_1C_2R_2}}{p + \frac{R_1+R_2}{R_1R_2(C_1+C_2)}} \right\}$$

$$= i_A + \frac{VC_2C_1}{K(C_1+C_2)} \left\{ \frac{1}{p+\psi} + \frac{\frac{1}{C_1R_1} + \frac{1}{C_2R_2}}{p(p+\psi)} + \frac{\frac{1}{C_1R_1C_2R_2}}{p^2(p+\psi)} \right\}$$

where $\psi = \frac{R_1+R_2}{R_1R_2(C_1+C_2)}$

$$= i_A + \frac{VC_2C_1}{K(C_1+C_2)} \left\{ \frac{1}{p+\psi} + \left(\frac{1}{C_1R_1} + \frac{1}{C_2R_2}\right)\frac{1}{p(p+\psi)} + \frac{1}{\psi^2 C_1R_1C_2R_2} \left(\frac{1}{p+\psi} + \frac{\psi-p}{p^2}\right) \right\}$$

Taking the inverse

$$i_c(t) = i(t) + \frac{V_A}{K} \frac{C_2C_1}{C_1+C_2} \left\{ \varepsilon^{-\psi t} + \frac{1}{\psi}\left(\frac{1}{C_1R_1} + \frac{1}{C_2R_2}\right)(1-\varepsilon^{-\psi t}) + \frac{1}{C_1R_1C_2R_2\psi 2} (\varepsilon^{-\psi t} + \psi t - 1) \right\}$$

$$= i_A(t) + \frac{V_A}{K} \frac{C_2C_1}{C_1+C_2} \left\{ \frac{1}{\psi}\left(\frac{1}{C_1R_1} + \frac{1}{C_2R_2}\right) + \frac{1}{C_1R_1C_2R_2\psi 2}(\psi t - 1) + \left[1 - \frac{1}{\psi}\left(\frac{1}{C_1R_1} + \frac{1}{C_2R_2}\right) + \frac{1}{C_1R_1C_2R_2\ 2}\right]\varepsilon^{-\psi t} \right\}$$

substituting for ψ in the exponential expression and simplifying

$$= i_A(t) + \frac{V_A}{K} \frac{C_2C_1}{C_1+C_2} \left\{ \frac{1}{\psi}\left(\frac{1}{C_1R_1} + \frac{1}{C_2R_2}\right) + \frac{1}{C_1R_1C_2R_2\psi 2}(\psi t - 1) - \frac{(C_1R_1 - C_2R_2)^2}{C_1C_2(R_1+R_2)^2} \varepsilon^{-\psi t} \right\}$$

Hence the full solution can be obtained by substituting for $i_A(t)$ from Appendix 2.2.

Appendix 2.5 Inductive response

Consider the circuit in Fig. 51b

$$\bar{Y} = \frac{1}{R_2} + \frac{1}{R_1} + \frac{1}{pC_1} + \frac{1}{pL + R + \frac{1}{pC}}$$

for an applied voltage, V, $\bar{i} = \bar{Y}\ \frac{V}{p}$

Let L^{-1} = Laplace inverse function

$$\therefore I(t) = \frac{V}{R_2} + \frac{V}{R_1} \exp -t/C_1R_1 + \mathcal{L}^{-1} \frac{V_A}{pL + R + \frac{1}{pC}}$$

Now consider $\mathcal{L}^{-1}$ of $\frac{1}{pL + R + \frac{1}{pC}} = \mathcal{L}^{-1} \left(\frac{1}{Lp^2 + Rp + \frac{1}{C}}\right)$

$$= \frac{1}{L} \frac{1}{(p + \frac{R}{2L})^2 - (\frac{R^2}{4L^2} - \frac{1}{LC})}$$

$$\therefore \quad I(t) = K(\exp -R/2L)\sinh at$$

$$= K^1(\exp -R/2L)(\exp at - \exp -at)$$

$$= K^1 \exp (a-R/2)t - (\exp -(at\ R/2L)t \quad \ldots \ldots \ldots (2)$$

Now $a = \sqrt{\frac{R^2}{4L^2} - \frac{1}{LC}} = \sqrt{\frac{R^2C - 4L}{4L^2C}}$

Therefore for a to be positive

$$RC > 4L$$

simplifying $a = \frac{R}{2L} \left(1 - \frac{4L}{R^2C}\right)^{\frac{1}{2}} \quad \ldots \ldots \ldots \ldots \ldots \ldots \ldots (3)$

Now from (2) and from U.V. recorder observations for (2) to correspond to observations

$$a + \frac{R}{2L} >> \frac{R}{2L} - a$$

$$a >> 0$$

If L should be of the order of microhenries (since it is not normally measurable and R ~ 10" Ω C ~ pFs

then $\frac{4L}{R^2C} << 1$

From (3) $a = \frac{R}{2L}\left(1 - \frac{1}{2}\frac{4L}{R^2C}\right) \doteq \frac{R}{2L} - \frac{2L}{R^2C}$

By Binomial expansion

Therefore substituting in (2)

since $I(+) = K^1\left[\exp -(R/2L-a)t - \exp-(a+R/2L)t\right]$

$$I(t) = K^1\left[\exp -(2L/RC)t - \exp -(R/L - 2L/R^2C)t\right]$$

once again considering possible values of L, R and C

$$I(t) = K^1\left[1 - \exp-Rt/L\right]$$

$\therefore$ time constant of anomaly $\simeq \frac{L}{R}$

If L is of the order of μH and R of the order of 10^{Ω}

Time constant is of the order of 10^{-16} secs.

Now since the 'time constant' of anomaly observed is of the order of minutes and decreases with apparent measured decrease in R, the Fig 5b circuit cannot be the equivalent circuit.

Appendix 3

Polarization microscopic analysis

From Coulomb's law the force F between two charges can be written as

$$F = kq_1 q_2 \frac{(R_1 - R_2)}{|R_1 - R_2|^3}$$

where q is located at R_1

and q_2^1 is located at R_2

Therefore the electric field at a point R due to a point q_1 at the point R is

$$E(R) = kq_1 \frac{(R - R_1)}{|R - R_1|^3}$$

This means that assuming superposition is applicable the electric field due to a system of point charges q_2 located at R_j, j = 1, 2 ... ... n

$$E(R) = k \sum_{j=1}^{n} q_1 \frac{(R - R_j)}{|R - R_j|^3}$$

If the charges are so small and so numerous that they can be described as a charge density $\rho(R^1)$.

and if Δq is the charge in a small volume $\Delta x\ \Delta y\ \Delta z$ at a point R^1 then

$\Delta q = \rho(R^1)\ \Delta x\ \Delta y\ \Delta z$

Thus the sum above is replaced by the integral below

$$E(R) = k \int \rho(R^1) \frac{(R - R^1)}{|R - R^1|^3} d^3R^1$$

where $d^3R^1 = dx^1\ dy^1\ dz^1$

See fig. 51c, page 192

Consider the microscopic field due to one molecule with centre of mass at point Rj while the observation point is at R. The molecular charge density is $\rho^1(R^1)$, where R^1 is measured from the centre of mass of the molecule. It should be noted that ρ_j^1 generally depends on the position of R_j of the molecule, since the distortion of the charge depends on the local field present.

The microscopic electric field due to the jth molecule is

$$E_j(R) = - \nabla k \int_{mol} \rho j(R^1) \frac{1}{|R - R_j - R^1|} d^3R^1$$

Expanding the above expression in multipoles around the centre of mass of the molecule by Taylor's theorem.

$$E_j(R) = - \nabla k \left[\frac{e_j}{R - R_j} + \nabla j \frac{1}{R - R_j} \cdot P_j + \dots \dots + \right]$$

where $e_j = \int_{mol} \rho j \ (R^1) \ d^3R^1$

$$P_j = \int_{mol} R^1 \rho_j^1 \ (R^1) \ d^3R^1$$

are the molecular charge and dipole moment respectively.

The above expansion neglects higher terms; (quadruple terms). Since microscopic variations of field occur over distances large compared to molecular dimensions the quadruple term contributes negligibly to the averaged field relative to the dipole term.

∴ Summing for all the molecules over j.

$$E(R) = - \nabla k \sum_j \left[\frac{e_j}{R - R_j} + P_j \nabla_j \left(\frac{1}{R - R_j} \right) \right]$$

For the average the discrete sum is replaced by an integral, introducing apparaently continuous charge and polarization densities.

$$\rho \text{ mol } (R) = \sum_j e_j \delta(R - R_j)$$

$$\rho \text{ mol } (R) = \sum_j \rho_j \delta(R - R_j)$$

$$\text{Thus } E(R) = - \nabla k \int d^3R^{11} \left[\frac{\rho \text{ mol } (R^{11})}{\left| R - R^{11} \right|} + P \text{ mol } (R^{11}) \cdot \nabla^{11} \left(\frac{1}{\left| R - R^{11} \right|} \right) \right]$$

Assuming that R^{11} is replaced by $R^{11} = R^1 + \lambda$

Then it can be shown[48] that the average of E(R) i.e.

$$E(R) = - \nabla k \int N(R^1) \left[\frac{\overline{\rho \text{ mol } (R^1)}}{R - R^1} + \overline{P \text{ mol } (R^1)} \cdot \nabla^1 \left(\frac{1}{R - R^1} \right) \right] d^3R^1$$

Where the lines above the values signify average values.

On the microscopic level P mol etc. consfitutes the surface charge on polarization.

$$\int N(R^1) \frac{\rho \text{ mol } (R^1)}{R - R^1}$$

The above expression represents volumetric charge and in the general case includes both injected and free carriers. It can be deduced from the properties of delta functions that the above equations for the electric field are similar to the ones discussed earlier (Chapter 8).

Appendix 4

Voltage nalysis: double layer dielectric

Convert the circuit in Fig.36ainto a Laplace equivalent circuit, when a waveform of the type $E e^{\alpha(wt+kx)}$ is applied if one writes for jw, the Laplace operator p then the total impedance for all t is given

$$\frac{R_1\left(R_S + \frac{1}{pC_S}\right)}{R_1 + R_S + \frac{1}{pC_S}} + \frac{R_2\left(R_T + \frac{1}{pC_T}\right)}{R_2 + R_T + \frac{1}{pC_T}}$$

Therefore the Laplace transform of a voltage V_2 across R_2 for a step function V = o, t < o: V = V for t > 0 is given by

$$V_2 = \frac{V}{p}\left[\frac{1}{\left[1 + \frac{R_S R_1}{R_S+R_2}\,\frac{\left(p + \frac{1}{C_S R_S}\right)}{p + \frac{1}{C_S(R_1+R_S)}}\right]\left[\frac{p + \frac{1}{C_T(R_2+R_T)}}{p + \frac{1}{C_T R_T}}\,\frac{R_2+R_T}{R_2 R_T}\right]}\right]$$

$$= \frac{V}{P}\cdot\left(\frac{p^2 + p\left[\frac{1}{C_S(R_1+R_S)} + \frac{1}{C_T R_T}\right] + \frac{1}{C_S C_T R_T(R_1+R_S)}}{p^2\left[1 + \frac{R_S R_1(R_2+R_T)}{R_2 R_T(R_S+R_1)}\right] + p\left\{\left[\frac{1}{C_S(R_1+R_S)} + \frac{1}{C_T R_T} + \frac{R_S R_1(R_2+R_T)}{R_2 R_T(R_S+R_1)}\right] + \frac{1}{C_T(R_2+R_T)} + \frac{1}{C_S R_S}\right\}}\right.$$

$$\left. + \frac{1}{C_S C_T R_T(R_1+R_S)} + \frac{R_1}{C_T C_S R_2 R_T(R_S+R_1)}\right)$$

Assuming that $R_1 >> R_S$ and $R_2 >> R_T$ and simplifying

$$V_2 = \frac{V}{p}\cdot\frac{\left\{p^2 + p\left(\frac{1}{C_S R_1} + \frac{1}{C_T R_T}\right) + \frac{1}{C_S C_T R_1 R_T}\right\}}{\left(p^2\left[1 + \frac{R_S}{R_T}\right] + p\left\{\frac{1}{C_S R_1} + \frac{1}{C_T R_T} + \frac{R_S}{R_T}\left(\frac{1}{C_T R_2} + \frac{1}{C_S R_S}\right)\right\} + \frac{1}{C_S C_T R_1 R_T} + \frac{1}{R_2 R_T C_T C_S}\right)}$$

$$V_2 = \frac{V}{p} \cdot \frac{\left\{ p^2 + p\,\frac{C_TR_T+C_SR_1}{C_SR_1C_TR_T} + \frac{1}{C_SC_TR_1R_T} \right\}}{\frac{R_S+R_T}{R_T}\left\{ p^2 + \frac{R_T}{R_S+R_T}\left[\frac{C_TR_T+C_SR_1}{C_SR_1C_TR_T} + \frac{C_SR_S+C_TR_2}{R_2R_TC_SC_T} \right] p + \frac{R_1+R_2}{(R_S+R_T)C_TC_SR_1R_2} \right\}}$$

since $R_1 >> R_S$, $R_2 >> R_T$

$$V_2 = \frac{VR_T}{R_S+R_T}\ \frac{1}{p}\ \frac{\left[p^2 + p\,\frac{(C_TR_T+C_SR_1)}{C_SR_1C_TR_T} + \frac{1}{C_SC_TR_TR_1} \right]}{p^2 + \frac{C_T(R_1+R_T)+C_SR_1}{(R_S+R_T)R_1C_SC_T} + \frac{R_1+R_2}{C_SC_TR_1R_2}}$$

If this is written as

$$v_2 = \frac{VR_T}{R_S+R_T}\ \frac{1}{p} \cdot \left[\frac{p^2 + Ap + B}{p^2 + 2\alpha p + D} \right]$$

Then $$v_2 = \frac{VR_T}{R_S+R_T} \left[\frac{p}{p^2+2\alpha p+D} + \frac{A}{p^2+2\alpha p+D} + \frac{B}{D} \left(\frac{1}{p} - \frac{p+2\alpha}{p^2+2\alpha p+D} \right) \right]$$

$$= \frac{VR_T}{R_S+R_T} \left[\left(1 - \frac{B}{D}\right) \frac{p}{p^2+2\alpha p+D} + \frac{B}{D} \cdot \frac{1}{p} + \left(A - \frac{2\alpha B}{D}\right) \frac{1}{p^2+2\alpha p+D} \right]$$

Thus the inverse, substituting for A, B, C and D, simplifying and assuming $R_1 >> R_S$, $R_2 >> R_T$ is given by

$$V_2(t) = \frac{VR_T}{R_S+R_T} \left[\left(\frac{R_S+R_T}{R_1+R_2}\right) \frac{R_2}{R_T} + \frac{R_1R_T-R_SR_2}{R_T(R_1+R_2)}\ \frac{\varepsilon^{-\alpha t}}{2} \left(\varepsilon^{\beta t} + e^{\varepsilon-\beta t}\right) \right.$$

$$\left. + \frac{C_SR_1-C_TR_2}{C_SC_TR_T(R_1+R_2)}\ \frac{\varepsilon^{-\alpha t}}{2\beta} \left(\varepsilon^{\beta t} - \varepsilon^{-\beta t}\right) \right]$$

where $\alpha = \dfrac{C_T(R_1+R_T)+C_SR_1}{2(R_S+R_T)R_1C_SC_T}$

and $\beta^2 = \alpha^2 - \dfrac{R_1+R_2}{(R_S+R_T)(C_SC_TR_1R_2)}$

$$\therefore \quad v_2 = \frac{VR_T}{R_S+R_T} \left\{ \left(\frac{R_S+R_T}{R_1+R_2}\right) \frac{R_2}{R_T} + \left[\frac{\beta C_S C_T(R_1R_T-R_SR_2)+C_SR_1-C_TR_2}{2\beta R_T C_S C_T(R_1+R_2)}\right] \right.$$

$$\exp^{-(\alpha-\beta)t}$$

$$\left. \left[+\frac{\beta C_S C_T(R_1R_T-R_SR_2)-C_SR_1+C_TR_2}{2\beta C_S C_T R_T(R_1+R_2)}\right] \exp^{-(\alpha+\beta)t} \right\}$$

Modification of the enclosed spherical cavity analysis

In order to appreciate fully the significance of ρ_{12} at the air and solid insulation interface consider the two classical solutions of (1) an earthed hollow conducting sphere and (11) a hollow dielectric sphere in an infinite dielectric medium. Let the radius of the sphere be 'a'.

(1) If one assumes Laplace's equation for the potential in the medium remote from the sphere even though there is charge accumulation on the sphere then from Laplace's and Legendre functions[18,123]

$$\phi = - Er \cos \theta$$

where the origin of the coordinates is taken at the centre of the sphere. Now at infinity the potential superimposed on this due to the induced charges on the sphere must vanish so that no terms of the form r^n can occur in it. Since this potential must be symmetrical about the x-axis no terms involving Sin θ can occur. The final potential outside must therefore be of the form

$$\phi = - E\, r\text{Cos}\ \theta + \sum_{n=1}^{\infty} A_n r^{-n} \text{Cos}\ n\theta \quad \ldots \quad \ldots \quad \ldots \quad \ldots \quad \ldots \quad (1)$$

Also in order to make V = o at r = a for the earthed conducting sphere for all values of θ, only Cos n θ with n=1 can be added to Er Cos θ

$$\therefore \quad \phi_2 = -Er\text{Cos}\theta + Ar^{-2} \text{Cos}\ \theta \quad \ldots \quad \ldots \quad \ldots \quad \ldots \quad \ldots \quad \ldots \quad \ldots \quad (2)$$

where ϕ_2 is the potential outside the sphere.

Inside the sphere a solution of the type in (2) is not acceptable

hence by inspection a term ErCosθ is added which will cancel the potential of the external field so that O=o everywhere inside the sphere.

(11) For the case of the dielectric sphere two separate potential functions must be taken into accout. Hence by inspection of the previous case let the potential ϕ_i inside the sphere be

$$\phi_i = (Cr^{-2} + Br) \text{ Cos } \theta$$

$$\text{and } \phi_i = (Ar^{-2} - Er) \text{ Cos}\theta$$

since ϕ_i is finite as r→a, C = o

The constants B and A may be evaluated by assuming that the radial Dielectric displacement is continuous at r=a

i.e. $\epsilon_i E_{2r} = \epsilon_1 E_{1r}$

where ϵ_i and ϵ_o are the respective permittivities, also that the tangential components of the electric field should be equal at r=a.

i.e. $E_{2t} = E_{1t}$

also since $\phi_2 = \phi_1$ at r=a this leads to a third boundary condition Applying the above boundary conditions following results are obtained

$$\phi_1 = - \left(\frac{3\epsilon_2}{\epsilon_1+\epsilon_2}\right) \text{ Er Cos } \theta$$

$$\phi_2 = - \left(1 - \frac{a^3}{r^3} \frac{\epsilon_1-\epsilon_2}{\epsilon_1+2\epsilon_2}\right) \text{ Er Cos}\theta$$

(111) In the case where the conductivities of both the dielectric sphere and the medium in which it is immersed are finite there will be a charge accumulation ρ_{12} on the surface of the sphere (just like the case of the earthed conducting sphere) but in this case since the potential inside the sphere is not zero, the treatment is similar to Case II with different boundary conditions.

Here if $\phi_2 = Ar^{-2} \text{ Cos } \theta - Er \text{ Cos } \theta$

and $\phi_1 = Cr^{-2} \text{ Cos } \theta + Br \text{ Cos } \theta$

Now as ϕ_1 is finite at r=o, $\therefore$ C=o

then $\epsilon_1 \left(\frac{\partial \phi_1}{\partial r}\right)_{r=a} - \epsilon_2 \left(\frac{\partial \phi_2}{\partial r}\right)_{r=a} = -\rho'_{12}$

Now $\frac{\partial \phi_2}{\partial r} = -\left(\frac{2A}{r^3} + E\right) \text{Cos}\,\theta$

$\frac{\partial \phi_1}{\partial r} = D\text{Cos}\,\theta$

$\therefore \quad \rho_{12} = -(2Ar^{-3} + E)\,\epsilon_2\,\text{Cos}\theta - \epsilon_1 D\text{Cos}\theta$

Also the tangential components are equal

$\therefore \quad E_{1t} = E_{2t}$

i.e. $-\frac{1}{r}\left(\frac{\partial \phi_1}{\partial \theta}\right)_{r=a} = -\frac{1}{r}\left(\frac{\partial \phi_2}{\partial \theta}\right)_{r=a}$

Now $\therefore \quad B = Aa^{-3} - E$

$\therefore \quad -\rho_{12} = -\text{Cos}\theta \left[\frac{2A}{a^3}\,\epsilon_2 + \epsilon_2 E + \epsilon_1 (Aa^{-3} - E_o)\right]$

$+\rho_{12}\,\text{sec}\theta = Aa^{-3}(2\epsilon_2 + \epsilon_1) + E(\epsilon_2 - \epsilon_1)$

$\therefore \quad A = a^3 \left[\frac{E(\epsilon_1 - \epsilon_2) + \rho_{12}\,\text{sec}\theta}{2\epsilon_2 + \epsilon_1}\right]$

$D = \frac{1}{2\epsilon_2 + \epsilon_2}\left[E(\epsilon_1 - \epsilon_2) + \rho_{12}\,\text{sec}\theta\right] - E$

$= -\frac{1}{2\epsilon_2 + \epsilon_1}\left[3\epsilon_2 E - \rho_{12}\,\text{sec}\theta\right]$

$\therefore \quad \phi_1 = -\frac{1}{2\epsilon_2 + \epsilon_1}\left[3\epsilon_2 E - \rho_{12}\,\text{sec}\theta\right] r\,\text{cos}\theta$

i.e. $\phi_1 = -\frac{1}{2\epsilon_2 + \epsilon_1}\left[3\epsilon_2 - \frac{\rho_{12}}{E}\,\text{sec}\theta\right] Er\text{Cos}\theta$

$\therefore$ Substituting for A

$$\phi_2 = -\left\{1 - \frac{a^3}{r^3(2\epsilon_2+\epsilon_1)}\left[\epsilon_1-\epsilon_2 + \frac{\rho_{12}}{E}\sec\theta\right]\right\} E r\cos\theta$$

(Compare the above analysis with Onsager's theories)[124]

Appendix 6

Maxwellian Polarization under a.c. conditions

Assume that two media A and I meet at a surface S and that a unit normal N is drawn from medium A into medium I such that A lies on the negative side of S, with I on the positive side.

Then from boundary conditions[122,123]

$$N \times (E_L - E_A) = 0, \ldots (1) \quad N.(D_I - D_A) = \rho \ldots (2)$$

$$\times = \text{vector multiplication}$$

where E_I, D_I and E_A, D_A are the stresses and displacements in the media where e is the density of any surface charge distributed over S.

The flow of charge across or to the boundary must also satisfy the equation of continuity:

$$\text{i.e. } N.(J_I - J_A) = -\frac{\partial\rho}{\partial t} \ldots \ldots \ldots \ldots \ldots \ldots \ldots (3)$$

Suppose that a waveform of type (constant $\epsilon^{-j\omega t}$) is applied

Then (1), (2) and (3) give

$$\epsilon_I E_{IN} - \epsilon_A E_{AN} = \rho \ldots \ldots \ldots \ldots \ldots \ldots \ldots (4)$$

$$\sigma_I E_{IN} - \sigma_A E_{AN} = j\omega\rho \ldots \ldots \ldots \ldots \ldots \ldots \ldots (5)$$

(assuming Ohm's law)

where E_I and ϵ_A are the bulk permittivities, σ_I and σ_A are the bulk resistivities. ρ is only zero when

$$\rho_I \epsilon_A - \rho_A \epsilon_I = 0$$

In the general case the above equality is not satisfied and hence from (4) and (5)

$$E_{AN} = \frac{j\omega\epsilon_I - \sigma_I}{\epsilon_A\sigma_I - \epsilon_I\sigma_A}\rho$$

and $E_{IN} = \dfrac{j\omega\epsilon_A - \sigma_A}{\epsilon_A\sigma_I - \epsilon_I\sigma_A}\ \rho$

Hence even for the A.C. case Maxwellian polarization is applicable

Appendix 7

Modification of Rogers and Skipper analysis to include the finite Conductivity of the air inclusion.

When one considers the earlier stages of the analysis of Rogers and Skipper[39]

$$\frac{1}{\lambda} = 1 - \left[\alpha \frac{\text{arc cot } \alpha - 1}{\sigma_2}\right]\left[\frac{\alpha_{SO}\alpha}{c} + (\sigma_1 - \sigma_2)(1 + \alpha^2)\right]$$

$$\text{and } \tau = \epsilon_o \frac{\left\{\epsilon_1(1+\alpha^2)(\alpha \text{ arc cot } \alpha - 1) - \epsilon_2\left[(1+\alpha^2)(\alpha \text{ arc cot } \alpha - 1) + 1\right]\right\}}{(1+\alpha^2)\left(\sigma_{SO}\frac{\alpha}{c} + \sigma_1\right)(\alpha \text{ arc cct } \alpha - 1) - \sigma_2\left[(1+\alpha^2)(\alpha \text{ arc cot } \alpha - 1) + 1\right]}$$

$$\text{where } \alpha = a/c = \left[(b/a)^2 - 1\right]^{\frac{1}{2}}$$

and a, b and c are parameters of an oblate spheroidal cavity described in the paper

a, b = semi-axis and radius of the oblate spheroidal cavity

c = Radius of the focal circle of the cavity

$\sigma_1\sigma_2$ = conductivities of the media inside and outside the cavity

τ = is the time constant for stress response in the cavity expressible as $E_1(t) = E^1\lambda\ (1-\exp t/\tau)$.

σ_{SO} = surface conductivity of the cavity boundary at the poles.

If an air/polythene interface is considered then clearly

$\sigma_1 >> \sigma_2$

$$\text{Then } \frac{1}{\lambda} \doteq 1 - \left[\frac{\alpha \text{ arc cot } \alpha - 1}{\sigma_2}\right]\left[\frac{\sigma_{SO}\alpha}{c} + \sigma_1(1 + \alpha^2)\right]$$

and

$$\tau = \epsilon_a \frac{\left\{\epsilon_1(1+\alpha^2)(\alpha \text{ arc cot } \alpha - 1) - \epsilon_2\left[(1+\alpha^2)(\alpha \text{ arc cot } \alpha - 1) + 1\right]\right\}}{\left(\sigma_{SO}\frac{\alpha/c}{1+\alpha^2} + \sigma_1\right)(1 + \alpha^2)(\alpha \text{ arc cot } \alpha - 1)}$$

The time τ_o required for the stress to rise from zero to the discharge inception value E_i is given as

$$\tau_o = - \tau \log_\varepsilon \left(1 - \frac{E_i}{\lambda E^1}\right)$$

where E^1 = Uniform stress applied to dielectric

For the minimum time σ_{SO} is assumed to be zero.

If this is assumed for the above analysis then

$$\frac{1}{\lambda a} = 1 - \frac{\sigma_1}{\sigma_2} (1 + \alpha^2) (\alpha \text{ arc cot } \alpha - 1)$$

$$\text{and } \tau_a = \frac{\epsilon_o}{\sigma_1} \left\{ \epsilon_1 - \epsilon_2 \left[1 - \frac{1}{(1 + \alpha^2) (\alpha \text{ arc cot } \alpha - 1)} \right] \right\}$$

From the analysis of Rogers and Skipper

$$\lambda^{1-} = \frac{1}{(\alpha \text{ arc cot } \alpha - 1) (1 + \alpha^2) + 1} > 1.5$$

Also $(\alpha \text{ arc cot } \alpha - 1) (1 + \alpha^2) + 1 < 1$

$\therefore$ From the two inequalities

$$- 1 < (\alpha \text{ arc cot } \alpha - 1) (1 + \alpha^2) < 0$$

hence λ^1 lies between 1 and ∞

Putting $K = 1 - \frac{1}{(1 + \alpha^2) (\alpha \text{ arc cot } \alpha - 1)}$

$$\tau_a = \frac{\epsilon_o}{\sigma_1} (\epsilon_1 - K \epsilon_2)$$

k lies between 2 and $- \infty$

Hence for minimum τ_o

$$T_m = - \tau_a \log_\varepsilon \left(1 - \frac{E_i}{\lambda_a E^1}\right)$$

$$= - \frac{\epsilon_o}{\sigma_1} (\epsilon_1 - K\epsilon_2) \log_\varepsilon \left(1 - \frac{E_i}{\lambda_a E^1}\right)$$

For a laminar cavity

$$(1 + \alpha^2)\ (\alpha \text{ arc cot } \alpha - 1) \rightarrow -1$$

$$\therefore \quad K = 2$$

and $\frac{1}{\lambda a} = 1 + \frac{\sigma_1}{\sigma_2} \doteqdot \frac{\sigma_1}{\sigma_2}$ Since $\sigma_1 >> \sigma_2$

$$\therefore \quad \tau_m \doteqdot \frac{\epsilon_o}{\sigma_1} \quad (\epsilon_1 - 2\epsilon_2) \log_\varepsilon \quad (1 - \frac{\sigma_1 E_i}{\sigma_2 E^1})$$

The above expression is finite only when $\frac{\sigma_1 E_i}{\sigma_2 E^1} << 1$

and reduces to $\tau_m = \frac{\epsilon_o}{\sigma_1} \quad (\epsilon_1 - K\epsilon_2) \quad \frac{\sigma_1 E_i}{\sigma_2 E^1}$

$$= \epsilon_o \quad (\epsilon_1 - K\epsilon_2) \frac{E_i}{\sigma_2 E^1}$$

When $\frac{\sigma_1 E_i}{\sigma_2 E^1} >> 1$ the expression for τ_m becomes infinite,

In practice the performance is much more likely to involve a few more powers of the expansion of

$$\log_\varepsilon \quad (1 - \frac{\sigma_1 E_i}{\sigma_2 E^1})$$

Thus neglecting powers greater than the second order just as an example.

$$\tau_m = \frac{\epsilon_o}{\epsilon_1} \quad \left\{ \epsilon_1 - K\epsilon_2 \right\} \left\{ \frac{\sigma_1}{\sigma_2} \quad \frac{E_i}{E^1} \quad + \quad (\frac{\sigma_1 E_i}{\sigma_2 E^1})^2 \right\}$$

It should be noted that convergency of the expression

$$\log_\varepsilon \quad (1 - \frac{E_i}{\lambda_a E^1})$$

can be a <u>certainty</u> only when

$$(1 + \alpha^2)\ (\alpha \text{ arc cot } \alpha - 1) \simeq 0$$

In which case

$$\tau_m = \frac{\epsilon_o E_i}{\sigma_1 E^1} \quad (\epsilon_1 - K\epsilon_2)$$

where $t \to \infty$

The above analysis should give an idea of the influence the finite conductivity of the included gases has on the discharge rate etc. The analysis however is not complete since it ignores completely the effect of interfacial charges and space charges which prevents the voltage immediately after discharge decaying to zero and hence an implied increase in the discharge repetition rate.

The effect of the portion of the void on the discharge characteristics is also neglected in this analysis. This is very significant.

Appendix 8

Some considerations on the design and performance of high voltage d.c. cables.

It is the practice to design most d.c. cables on the basis that the conduction current is an exponential function of the stress. With small orders of thicknesses and at relatively low stresses this might suffice but recent breakdown tests*with cables have indicated that the influence of space charge or some consideration might influence the performance to a great extent. In order to check this for a given cable, radial stresses were computed using IBM 1905 computer and ICL subroutines (to plot the graphs).

(* see refs. 12, 23, 24, 25, 27, 32, 33).

*

Theory I.I:

In order to establish an expression for the D.C. stress distribution in cable insulation it is assumed that the exponential conductivity [125,126] variation with temperature and stress is applicable and that there is no space charge within the insulation.

Hence

$$\text{Let } \sigma_1 = \sigma_E e^{+kE} \quad \ldots \quad (1)$$

$$\text{and } \sigma_2 = \sigma_T e^{+\alpha\Delta T} \quad \ldots \quad (2)$$

describe the stress and temperature variations respectively

where σ_E, σ_T, k and α are special constants;*

Now at $E = \Delta T = o$ $\sigma_1 = \sigma_2 = \sigma_o$ say

$\therefore$ Combining (1) and (2)

$$\sigma = \sigma_o \exp(\alpha\Delta T + kE) \quad \ldots \quad (3)$$

Thus at any point within the cable

$$\sigma_x = \sigma_o \exp(\alpha\Delta T_x + kE_x) \quad \ldots \quad (4)$$

In order to assess the effect of cable loading in terms of known

constants, consider the temperature difference across the insulation.

Treating this as a thermal-electrical analogue and considering the section shown

(fig.52a) If $\delta R = \frac{\delta V}{I}$ ... ... (5)

and W (Heat loss/cm) ≡ I (current/cm)

K (Thermal Conductivity) ≡ σ (electrical conductivity)

δT (Temperature drop) ≡ δV (voltage drop)

Now for the electrical case for an elemental strip

$$R = \frac{\text{length}}{\sigma \text{ Area}} \quad \text{which from the section in Fig. 52a gives}$$

$$\delta \frac{V}{I} = \delta R = \frac{dx}{\sigma 2\pi x} \quad \ldots \ldots \ldots \ldots \ldots \ldots \ldots \ldots \quad (6)$$

Thus substituting from the thermal analogue for the electrical analogue

$$\frac{\delta V}{I} = \frac{\delta T}{W} \quad \ldots \ldots \ldots \ldots \ldots \ldots \ldots \ldots \quad (7)$$

$$\therefore \quad \frac{\delta T}{W} = \frac{1}{K} \frac{dx}{2\pi x} \quad \ldots \ldots \ldots \ldots \ldots \ldots \ldots \ldots \quad (8)$$

Hence remembering the direction of heat flow in a cable and integrating between limits r, R for the cable (where r is the conductor radius, and R is the radius over the insulation).

∴ Total temperature drop

$$\Delta T = \int_r^R \delta T$$

$$= \int_r^R \frac{W}{K} \frac{dx}{2\pi x}$$

$$\therefore \quad \Delta T = \frac{W}{2\pi K} \log_e \frac{R}{r} \quad \ldots \ldots \ldots \ldots \ldots \ldots \ldots \ldots \quad (9)$$

Hence at radius x temperature T_x is given by $T_x = T_c - \frac{W}{2\pi K} \log_e \frac{r}{x}$ (10)

where T_c is the conductor temperature

Thus writing equation (9) in the form

$$\frac{W}{2\pi K} = \Delta T / \log_e \frac{R}{r} \quad \ldots \ldots \ldots \ldots \ldots \ldots \ldots \ldots \quad (11)$$

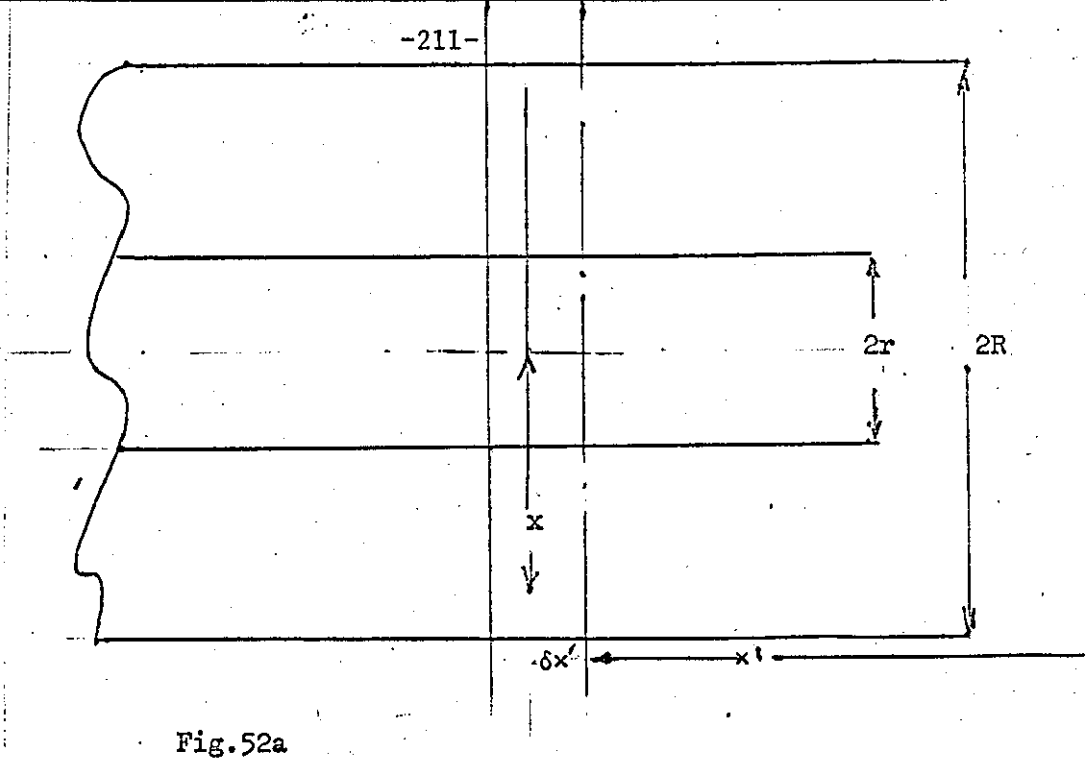

Fig.52a

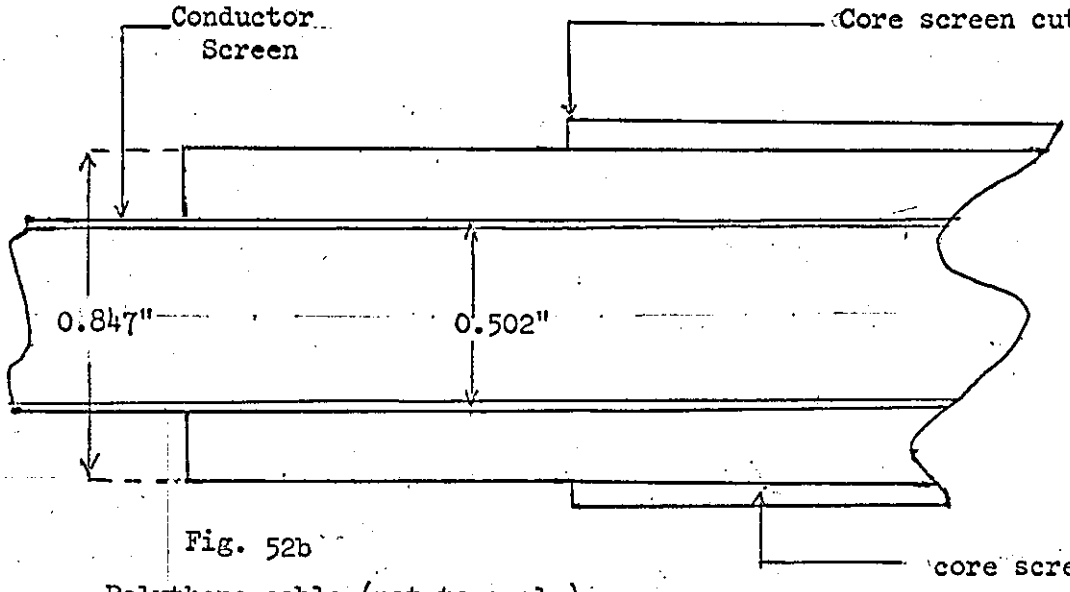

Fig. 52b

Polythene cable (not to scale)

above (i) core screen/polythene interface in air
below (ii) core screen/polythene interface in oil

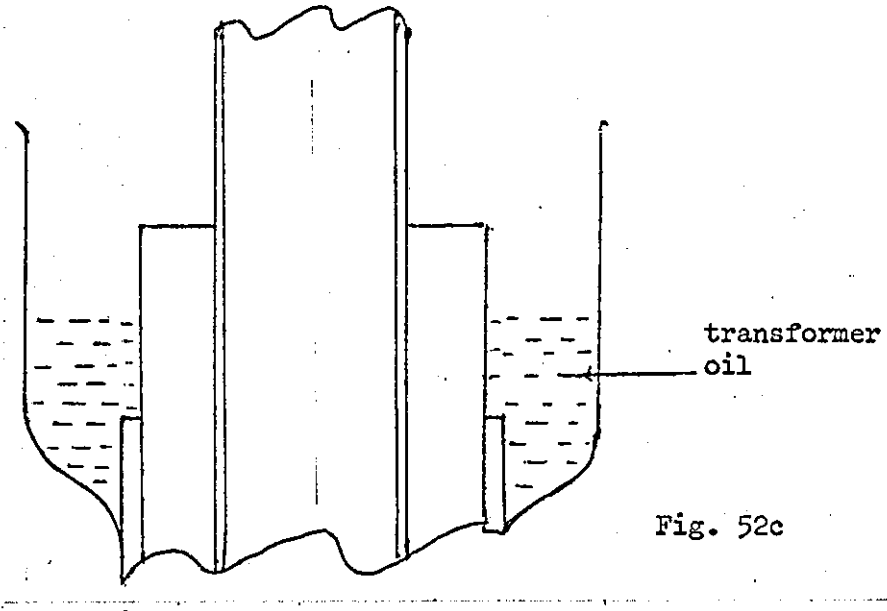

Fig. 52c

$\therefore$ Hence from (10) and (11)

$$T_c - T_x = \frac{\Delta T . \log_e \frac{r}{x}}{\log_e \frac{R}{r}} \quad \ldots \quad (12)$$

In order to simplify expression (12) define β such that

$$\frac{\beta}{\alpha} = \frac{\Delta T}{\log_e \frac{R}{r}}$$

$$\therefore \quad T_c - T_x = \frac{\beta}{\alpha} \log_e \frac{r}{x}$$

$$\therefore \quad \frac{r}{x} = \exp \frac{\alpha}{\beta} (T_c - T_x) \quad \ldots \quad (13)$$

Effect of stress:

Consider an insulation current of I per unit length.

Then stress at any point x in the section shown E_x is given by

$$E_x = \frac{I}{\sigma 2\pi x \exp (kE_x + \alpha T_x)} \quad \ldots \quad (14)$$

Let the stress at an arbitary position r_m be E_m

$$E_m = \frac{I}{\sigma 2\pi r_m \exp (kE_m + \alpha T_m)} \quad \ldots \quad (15)$$

Therefore from (14) and (15)

$$\frac{E_x}{E_m} = \frac{r_m}{x} \frac{\exp (kE_m + \alpha T_m)}{\exp (kE_x + \alpha T_x)}$$

$$\frac{E_x}{E_m} = \frac{r_m}{x} \exp k(E_m - E_x) . \exp \alpha(T_m - T_x) \quad \ldots \quad (16)$$

Hence from (13) since

$$\exp \alpha(T_m - T_x) = \left(\frac{x}{r_m}\right)^{\beta} \quad \ldots \quad (17)$$

and substituting (17) in (16)

$$\therefore \quad \frac{E_x}{E_m} \exp k (E_x - E_m) = \left(\frac{r_m}{x}\right) \left(\frac{x}{r_m}\right)^{\beta}$$

$$\therefore \quad \frac{E_x}{E_m} \exp k (E_x - E_m) = \left(\frac{x}{r_m}\right)^{\beta-1} \quad \ldots \quad (18)$$

when there is no loading on the cable the conditions are assumed to be

isothermal that is $\Delta T = 0$ hence from the definition of β, $\beta = o$.

Therefore equation (18) becomes

$$\frac{E_x}{E_m} \exp k (E_x - E_m) = \frac{r_m}{x} \quad \ldots \quad \ldots \quad \ldots \quad \ldots \quad \ldots \quad \ldots \quad (19)$$

This is the simplest form of equation (18) but even this cannot be integrated by normal integration procedure to obtain V, one of the best means of obtaining V is to employ iterative or step by step method and this is efficiently done by a computer when a value for k is known for the particular dielectric.

b. Loaded Condition:

In order to analyse the stress for this case β together with k has to be known for the operating conditions.

The quantity β is obtained by first evaluating $\frac{W}{2\pi K}$ from data and multiplying this by α to obtain β. The process for calculating the stress is then similar to the unloaded case, only slightly more complicated.

1.2: Alternating voltage conditions

The radial stress for alternating operation of the cable is a far simpler case as Ohm's law is obeyed for the capacitive stress distribution and the stress is obtained in the familiar form

$$E_m = \frac{V}{r_m \log_e \frac{R}{r}}$$

where the symbols have the same meanings as before.

The above formula applies in the d.c. case for ohmic operation i.e. at the very low voltages (below stresses of about 30 kV/per cm.

Space charge theory

In order to consider the case of a cable in which there is space charge formation. Consider the very approximate solution (with certain assumptions) below.

If space charge acts then Poisson's equation holds i.e.

$$\frac{\partial^2 V}{\partial r^2} + \frac{1}{r}\frac{\partial V}{\partial r} = \frac{-\rho_r}{\epsilon} \quad \ldots \quad (1)$$

In order to solve the above equation in a less complicated way assume that superposition is applicable and obtain a Laplace form of equation (1) by obtaining two separate solutions (a complementary function (F) and a particular integral P.I.).

This is done by defining V and a function F(r)

where $V = \phi + F(r)$ ... ... (2)

such that

$$\nabla^2 \phi = o \quad \ldots \quad (3)$$

If equation (1) and (2) are to be maintained then

$\frac{\partial^2 F(r)}{\partial r^2}$ should equal $\frac{-\rho_r}{\epsilon}$

Hence equation (3) is written as

$$\frac{\partial \phi}{\partial r}\left(r \frac{\partial \phi}{\partial r}\right) = o$$

$$\phi = A \log Br - (C.F.)$$

Also assuming that $\rho_r = \rho$ (const) ie independent of radius r the particular Integral is simply $F(r) = \frac{-\rho r^2}{2\epsilon}$ and the full solution is

$$V = A \log Br - \frac{\rho r^2}{2\epsilon}$$

The above solution is one very special case but it demonstrates the effect of ρ. Other possible forms of variation will be given by $\rho_r = f\left(\frac{\rho}{r}\right)$ or $\rho_r = f(\rho.r)$

These will be more complicated and will lead to other solutions.

Theory 3 (Maxwell's consideration)

Consider the cable and circuit representation in Figs. 52a Let v be the potential at any point in the conductor.

Let Q be the total quantity of electricity which has passed through a section δx since the beginning of current flow.

Let C be the capacitance of the cable per unit length where $C = \frac{2\pi\epsilon}{\log_e \frac{R}{r}}$ assume Ohm's law and let λ be the resistance per unit length where $\lambda = \frac{1}{2\sigma\pi} \log_e \frac{R}{r}$ assume Ohm's law where σ is the conductivity of the dielectric. Then the quantity which at the time t exists between sections x and x + δx is

$$Q - (Q + \frac{dQ}{dx'} \delta x') = - \frac{dQ}{dx} \quad \delta x'$$

$$\text{But } c\ v\ \delta x' = - \frac{dQ}{dx'} \cdot \delta x'$$

$$\text{Therefore } - \frac{dQ}{dx'} = c\ v \quad \ldots \quad (1)$$

But if the resistivity of the dielectric is finite

$$\frac{d^2Q}{dx'\,dt} = \frac{c\ dv}{dt} + i \quad \ldots \quad (2)$$

where $i = \frac{v}{\lambda}$

$$= 2\ v\sigma\pi / \log_e \frac{R}{r}$$

Now let γ be the conductivity of the cable conductor

then since $J = \gamma E$

$$\therefore \quad \frac{-dv}{dx'} = \frac{1}{\gamma} \frac{dQ}{dt} \quad \ldots \quad (3)$$

Therefore differentiating (3) with respect to x and eliminating $\frac{d^2Q}{dx'\,dt}$

$$\frac{d^2v}{dx^2} = \frac{C}{\gamma} \frac{dv}{dt} + \frac{v}{\gamma\lambda} \quad \ldots \quad (4)$$

The above equation is established in order to show the need for extra factors such as λ and γ to be taken into account in the assessment of d.c. transmission voltages.

This assessment of the variation of voltage with time could include the initial charging and eventual polarization processes outlined in earlier chapters.

Method (a) Program structure

The program structure presented in the following pages is for the cable in a cold state with no temperature gradient across its section, as this involves fewer assumptions. A comparative one for the hot state was analysed but not presented here since this involves only a change of constants.

For this analysis a fixed value of stress is assumed. In this case it is assumed that this stress is the conductor screen stress (SA) under ohmic conditions. The radial position (RADX) of this value of stress is varied from the conductor screen to the core screen for the d.c. computation. At each setting of radius and stress, corresponding radii (X2) can be evaluated for various stress values (SX). Thus a whole series fo stresses {S(K)} at known radii X(K) is obtained.

For each set of values of SA and RADX a stress/radius graph is plotted and the resulting voltage (Y) is obtained as an integral of this curve by application of Simpson's rule. But comparing this resulting voltage (Y) with the actual applied voltage (V) the relevant stress/radius curve can be selected.

The example shown in Fortran serves to compute the stress/radius curve under ohmic conditions and a similar curve for one setting of RADX determined previously as described above. (see page 224, also table 1).

Method (b) Tests

A cable of dimensions as shown in Fig. 52b was used. (see plate 8)

First of all the cable core screen was cut back several inches from the polythene surface.

The cable with the exposed ends (see fig.52c) was first tested for discharges in air (i.e. without any stress relief at the core-screen/air interface) then with the ends surrounded by oil under both a.c. then subsequently under d.c. conditions, but then cold.

From the discharge tests it was possible to assess the discharge

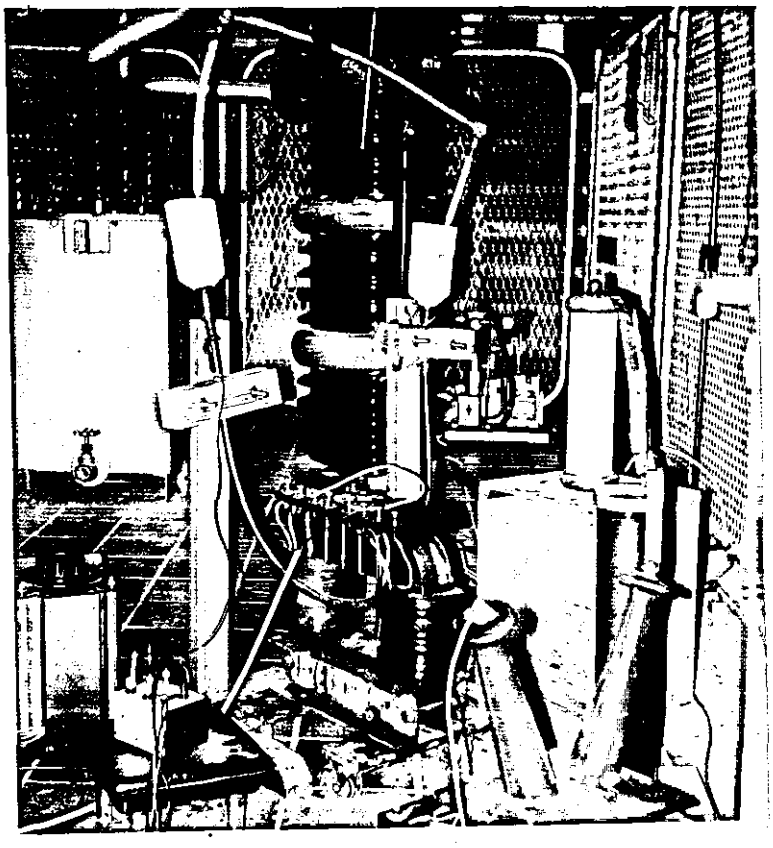

PLATE 8.
Equipment for cable tests.
top - current measuring coil.
middle - cable threaded through a heating transformer.
bottom left - heating transformer regulator.
bottom right - a.c. high voltage transformer.
middle right - measuring resistor.
rear ground - Cockcroft-Walton d.c. generator.

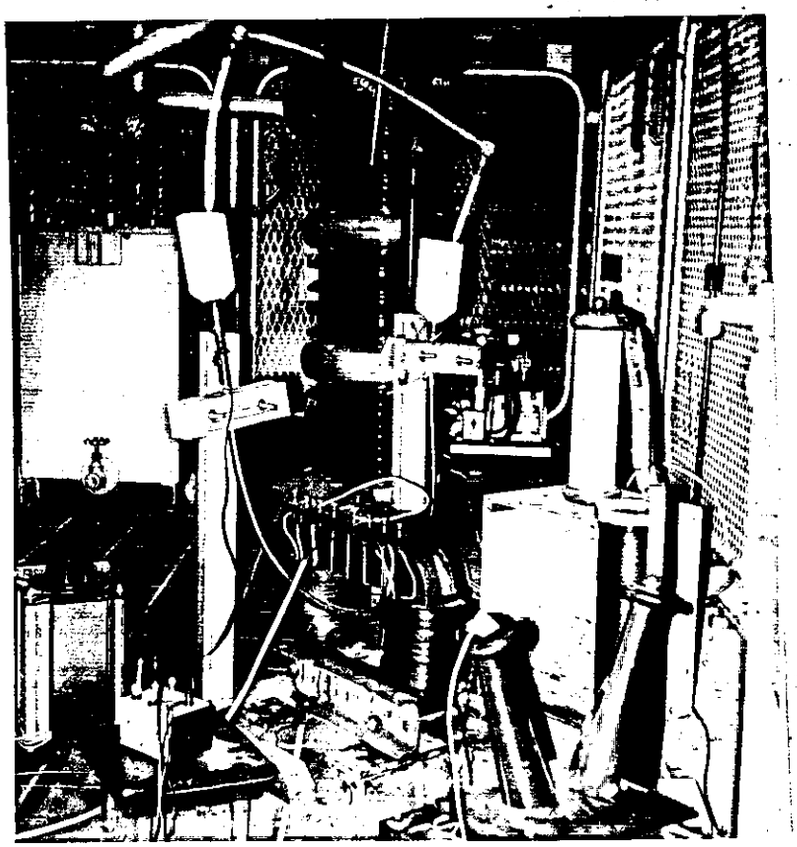

PLATE 8.
Equipment for cable tests.
top - current measuring coil.
middle - cable threaded through a heating transformer.
bottom left - heating transformer regulator.
bottom right - a.c. high voltage transformer.
middle right - measuring resistor.
rear ground - Cockcroft-Walton d.c. generator.

due to the core-screen cut, that is, discharges at the core screen/air interface under various conditions. See table 2 and U.V. Records 5A-5F.

Observations and conclusions

It was noted that as the position of SA was varied towards the core screen, the resulting computed increased in value for the whole cable at uniform (room) temperature. For the cable with a temperature gradient across it the situation was reversed.

The results of the discharge test indicated that the stress at the core screen might be well below the expected computed stress in the d.c. case (contrast the a.c. graph in Fig. 53). This shows that the straight forward logarithmic relation without any boundary conditions being imposed) may not fully cover the stress assessment over the entire section of the cable.

It is obvious that only when these other factors are taken into account will a comprehensive design be produced.

Table 1

U = 20 kV		
SA	RADX	Y
kV cm^{-1}	inches	kV
76.162	0.502	16.780
76.162	0.602	18.785
76.162	0.675	20.057
76.162	0.702	20.589
76.162	0.725	20.831
76.162	0.775	21.629
76.162	0.825	22.523
76.162	0.847	22.788
SA = conductor screen stress under ohmic conditions		
69.264	0.552	16.512
69.264	0.652	18.256
69.264	0.752	19.97
50.842	0.752	15.60
50.843	0.852	17.02
CABLE (with temperature gradient)		
76.162	0.675	27.142
76.162	0.847	22.318

V = 30 kV		
SA	RADX	Y
kV cm^{-1}	inches	kV
114.244	0.675	26.761
	0.725	27.581
	0.775	28.633
	0.825	29.416
	0.847	29.799

Type of test	voltage setting kV	Count above 3 pc per 300 seconds	
		No stress relief at core screen	stress relief with oil
AC (COLD)	7	300018	1389
AC (COLD)	6	86021	1122
DC (COLD)	20 (steady state)	nil	nil
DC (COLD)	30 " "	16	10
DC (COLD)	40 " "	50	
AC (HOT)	7	46491	190
DC (HOT)	20	25	nil
DC (HOT)	30	105	
DC (HOT)	40	310	

Table 2

U.V. record 5A
a.c. discharges -cold cable @ 6 kV, terminations in air.

U.V. record 5B
a.c. discharges - cold cable @ 7 kV, terminations in air.

U.V. records 5A, 5B, 5C, 5D, 5E, 5F.

Graphs from computer, cable-cold

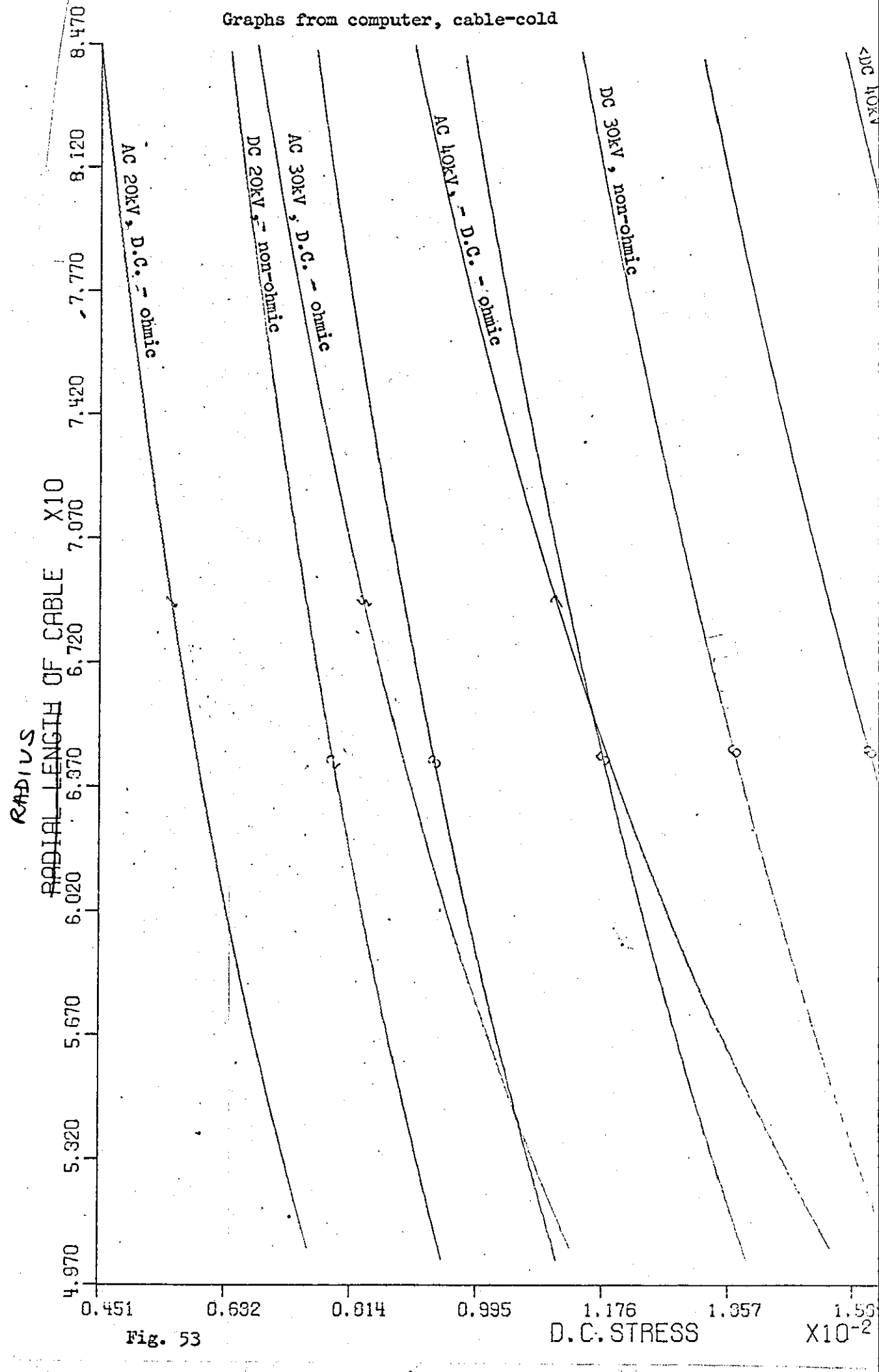

Fig. 53

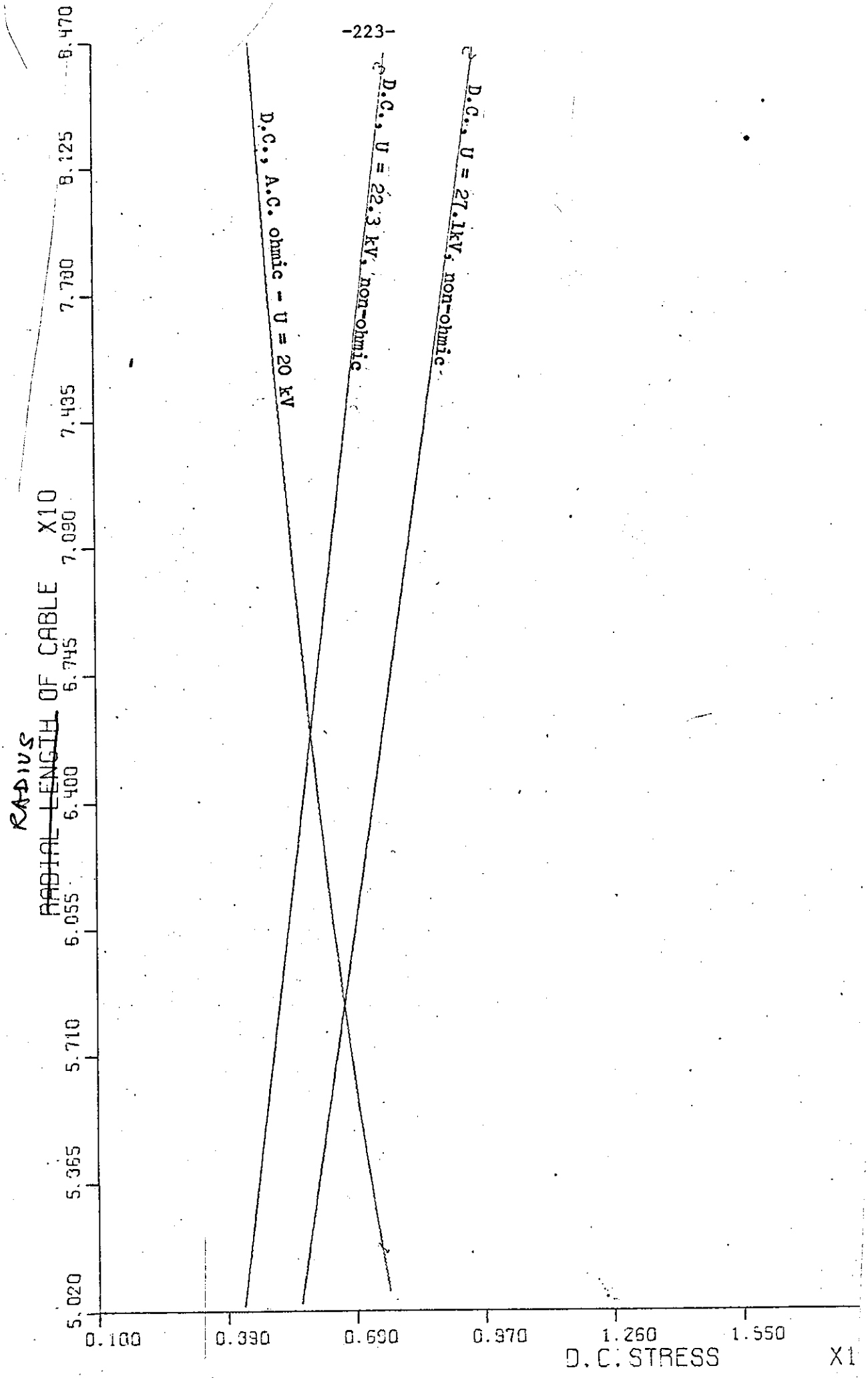

Fig. 54
Graphs from computer, cable hot

Program Structure for IBM 1905

```
      DIMENSION S(2000), X(2000)
      DIMENSION XTITLE (3), STITLE(2)
      DATA STITLE (1)/10HD.C.STRESS/,XTITLE(1)/22HRADIAL LENGTH OF CABLE/
      READ(1,150)RAD1,RAD2,CONST
  120 READ(1,160)U
  150 FORMAT(3F5.0)
  160 FORMAT (F5.0)
      CALL UTPOP
      IF (U-1) 90,90,29
   29 RADX=RAD2
      K=0
   32 IF(RAD1-RADX-1.E-3)33,33,68
   33 SA=U/(RADX*ALOG(RAD2/RAD1))
      K=K+1
      X(K)=RADX
      S(K)=SA
      RADX=RADX-0.01
      GO TO 32
   68 XLAST=RADX
      SLAST=SA*3.
      IF (U-20.)70,69,70
   69 CALL UTP4A (S(1),SLAST,XLAST, X(1), 10.0,10.0, STITLE,2,XTITLE,3)
   70 CALL UTP4B(S,X,K,2)
      RADX=RAD1
      J=0
   30 SA=U/(RADX*ALOG(RAD2/RAD1))
   54 RADX=RADX+(RAD2-RAD1)/2
   50 K=0
      J=J+1
      SX=SA/2.
   55 X2=RADX*(SA/SX)*EXP(CONST*(SA-SX))
```

```
275   IF(RAD2-X2-1.E-3)25,105,105
105   IF(X2-RAD1-1.E-3)95,85,85
 85   K=K+1
      S(K)=SX
      X(K)=X2
      WRITE(2,35)S(K),X(K)
 35   FORMAT(2F10.3)
 25   SX=SX+0.01*U
      GO TO 55
 95   XLAST=X(K)
      SLAST=S(K)
      WRITE(2,65)K,J,SA,RADX
 65   FORMAT(16H PART OF SET K=,I4,4H J=,I4,2F10.3)
      CALL UTP4B(S,X,K,2)
      ZZ=K
      MM=K
      AA=ZZ/2.
      NN=MM/2
      BB=NN
      LL=MM-2
      JJ=MM-1
      ODD=0
      EVEN=0
      IF(2.*(BB-AA)) 221, 331, 441
441   STOP
221   DO 551 MMM=3,LL,2
551   ODD=ODD+X(MMM)
      DO 661 MMM=2,JJ,2
661   EVEN=EVEN+X(MMM)
      GOTO 711
331   DO 99 MMM=3,JJ,2
 99   ODD=ODD+X(MMM)
```

```
      DO 42 MMM=2,LL,2
   42 EVEN=EVEN+X(MMM)
  711 Y=(S(2)-S(1))/3.*(X(1)+4.*EVEN+2.*ODD+XLAST)
      WRITE(2,171) Y
  171 FORMAT(7H Y =,F10.3)
   39 IF(RAD2-RADX-1.E-3)120,120,40
   40 RADX=RADX+0.3
   10 IF(RADX-RAD2-1.E-3)50,50,88
   88 RADX=RAD2
      GO TO 50
   90 CALL UTPCL
      STOP
      END
```

Data

where U = Applied Voltage

RAD1 = Radius over Conductor

RAD2 = Radius over Insulation

CONST = Empirical Constant

SA = Stress at RAD X

CALL UTPOP = Opens graph plotting facilities

UTP 4A = sub-routine for drawing axes for graphs

UTP 4B = sub-routine for plotting points and curve

CALL UTPCL = closes graph plotting facilities.